Modelling the Neuropathology of *Ehmt1* Haploinsufficiency

By

Brittany Davis

A thesis submitted in partial fulfillment of the requirements for the degree of Doctor of Philosophy in Neuroscience

Cardiff University

2014

Abstract:

EHMT1 is a gene that encodes an epigenetic regulator important for normal brain development. Disruption in *EHMT1* is associated with a number of neurodevelopment and psychiatric conditions, like schizophrenia, Autism Spectrum Disorders, developmental delays and intellectual disabilities. In order to help elucidate the role of *Ehmt1* in cortical development two models are examined: the differentiation of mouse pyramidal neurons lacking one copy of the gene and a forebrain-specific *Ehmt1*-haploinsufficient mouse model. *Ehmt1*$^{+/-}$ cells demonstrated changes in cell cycle, with significant differences in proliferation rates at embryonic stem cell and neural progenitor stages. *Ehmt1*$^{+/-}$ cells demonstrated significantly different transcriptional profiles in early and late stages of progenitor development, which suggested these cells, underwent precocious differentiation. In addition, the dysregulation of mRNA expression in a number of the *Nrsf/Rest* repressor complex members and *Rest* target genes was found; and *Ehmt1*$^{+/-}$ cells did not survive as post-mitotic neurons. The forebrain-specific *Ehmt1*-haploinsufficient mouse model, *Ehmt1*$^{D6Cre/+}$, importantly showed normal Mendelian birth ratios, survival, motor coordination and function and no gross morphological changes in brain structure. However, these mice demonstrated differences in activity levels and anxiety-related measurements; deficits in sensorimotor gating and object recognition; and significant differences in a number of electrophysiological measurements, including abnormal event-related neural responses in the cortex and high frequency oscillatory patterns. Taken together, these data suggest that *Ehmt1* expression is important for normal pyramidal development and *Ehmt1* haploinsufficiency throughout development manifests cortical dysfunction, which leads to marked behavioural and electrophysiological abnormalities.

List of Abbreviations:

24P—24th pulses in Mismatch Negativity

5-HT2—5-hydroxytryptamine

5hmC—5-hydroxymethylcytosine

5mC—5-methylcytosine

Acinus—Apoptotic Chromatin Condensation Inducer 1 gene

ADHD—Attention Deficit Hyperactivity Disorder

AEP—Auditory vent-related potential

AP—Alkaline Phosphatase

Ascl1—Achated-scute family bHLH transcription factor 1 gene

ASD—Autism Spectrum Disorder

ASR—Auditory Startle Response

ATP-dependent—Adenosine triphosphate dependent

B2m—Beta-2-microglobulin gene

Blimp1/Prdm1—PR domain containing 1 gene

Blk—B lymphoid tyrosine kinase gene

Bmp5—Bone morphogenetic protein 5 gene

Bmper—BMP binding epithelial regulator gene

Bpil—Bactericidal permeability increasing gene

BSA—Bovine serum albumin

B-Tublin—Beta Tubulin gene

CA1 & CA3--Cornu Ammonis 1, 2, 3

Camk2a—Calcium/calmodulin-dependent protein kinase II alpha 2

CAs—Cellular aggregates

Casp1-Caspase 1 gene

Cdkn1c—Cyclin-dependent kinase inhibitor 1C gene

CDP/cut—Homeobox protein Cux-1 protein

Cydl1—Chromo-domain protein, Y Chromosome-Like gene

cm—Centimetre

CNS—Central Nervous System

Cntnap2—Contactin-associated protein like 2 gene

CP—Cortical plate

CpG—C and G dinucleotides

CT values—Cycle threshold

CTCF—CCCTC-binding factor (zinc finger protein)

Ctnnd2—catenin, cadherin-associated protein, delta 2 gene

Cux1—Cut-like homeobox 1 gene

Dach1—Dachshund 1 gene

Dach2—Dachshund 2 gene

ΔΔCT—Delta-delta CT

DG—Dentate gyrus

Dlg3—Disc large homolog 3 (Drosophila) gene

Dlg4-- Disc large homolog 3 (Drosophila) gene

DNA—Deoxyribonucleic acid

Dnmt1—DNA methyltransferase 1 gene

Dnmt3a—DNA methyltransferase 3a gene

Dnmt3b—DNA methyltransferase 3b gene

Dnmt3I-- DNA methyltransferase 3I gene

Dpall—Dorsal pallium

Dppa5a—Developmental pluripotency associated 5 gene

DvP—Deviant pulse

E12.5-E14.5, E18.5—Embryonic stage 12.5, 14.5, 18.5

Ebbr4—Epidermal growth factor receptor family gene

EC—Entorhinal cortex

EdU—5-Ethynyl-2'-deoxyuridine

EEG—Electroencephalography

Ehmt1—Euchromatic histone methyltransferase 1 gene

Ehmt2—Euchromatic histone methyltransferase 2 gene

Eif4ebp1—Eukaryotic translation initiation factor 4E-binding protein 1 gene

EPM—Elevated Pulse Maze

ERP—Event Related Potential

ESCs/mESCs—Embryonic stem cell/mouse embryonic stem cells

EtOH--Ethanol

FACS—Florescence-activated cell sorting

FBS—Fetal bovine serum

Fez1—Fasciculation and elongation protein zeta 1 gene

FFC-A—Forward scatter

Fmr1—Fragile X mental retardation 1 gene

Fmr2—Fragile X mental retardation 2 gene

Foxg1—Forkhead box G1 gene

G1 phase—Growth 1/Gap 1 phase

G9a—Protein encoded by EHMT2

GABA—Gamma-aminobutryic acid

Gabrb3—Gamma-aminobutryic acid A receptor, beta 3 gene

Gdi1—GDP dissociation inhibitor 1 gene

Gfap—Glial fibrillary acidic protein gene

GLP—G9a-like protein

Gpr54—G protein-coupled receptor 54 gene

Grin1—Glutamate receptor, ionotropic, N-metnyl D-aspartate 1 gene

Grm8—Glutamate receptor, metabotropic 8 gene

GSK-3—Glycogen synthase kinase 3 inhibitor

H2A, H2B, H3, H4—Histone 2A, 2B, 3 and 4

H3K9me1—Histone 3 Lysine 9 monomethyltransferase

H3K9me2—Histone 3 Lysine 9 dimethyltransferase

H3K9me3—Histone 3 Lysine 9 trimethyltransferase

Hdac1—Histone deacetelyase 1 gene

HKMT—Histone lysine methylatransferase

HP1—Heterochromatin protein 1

HPF—Hippocampal formation

Hprt—Hypoxanthine phosphoribosyltransferase gene

hrs—Hours

Hz—Herz

iPSC—Induced pluripotent stem cells

IPCs—Intermediate progenitor cells

IZ—Intermediate zone

Jmjd1a—Jumonji C domain-containing histone demethylase 1A gene

Jmjd2c—Jumonji C domain-containing histone demethylase 2C gene

KMT—Lysine methyltransferase

Kmt1d—Lysine methyltransferase 1D gene

KO—Knockout

KS—Kolmongolov Smirnov test

L1cam—L1 cell adhesion molecule/L1-like gene

LFP—Local field potential

LG—Lateral geniculate complex

LIF—Leukaemia inhibitory factor

LMA—Locomotor activity

Map2—Microtubule-Associated Protein 2 gene

Mapk7—Mitogen-activated protein kinase 7 gene

MB—Midbrain

Mbd5—Methyl-CpG binding domain protein 5 gene

Mecp2—Methyl CpG binding protein 2 (Rett syndrome associated) gene

MEFs—Murine embryonic fibroblasts

MEG—Megnetoenchephalography

MEK1/2—Mitogen-activated protein kinase protein inhibitor

MH—Hedial habenula

Mll3—Mixed-lineage leukaemia 3 gene

MMN—Mismatch Negativity Paradigm

Mpal—Medial pallium

mV—Millivolts

N100—First negative-going inflection in electrical signal of the human event related potential components

Nanog—Homeobox transcription factor gene

Nefh—Neurofilament, heavy polypeptide gene

Nes—Nestin gene

Neurod1—Neuronal differentiation 1 gene

Nf1—Neurofibromin 1 gene

Ngn2—Neurogenin 2 gene

NMDA—N-Methyl-D-aspartate; an amino acid derivative

Nog—Noggin gene

NOR—Novel object recognition

NPCs—Neural progenitor cells

NPP—Novel Place Preference

Nr1i3—Nuclear receptor subfamily 1, group 1, member 3 gene

Nrg1—Neuregulin 1 gene

Nrsf/Rest—Neuron-restrictive silence factor/RE1-silencing transcription factor gene

Nrxn1—Neurexin-1 gene

Nrxn3—Neurexin-3 gene

Ntrk3—Neurotrophic tyrosine kinase, receptor, type 3 gene

OCD—Obsessive Compulsive Disorder

Oct4—Octamer-binding transcription factor 4 gene

OFT—Open Field test

P1 & P7—Postnatal day 1 and 7

P300—Second positive-going inflection in electrical signal of the human event related potential components, peaking around 300ms post-stimulus

P50—First positive-going inflection in electrical signal of the human event related potential components, peaking around 50ms post-stimulus

P53—Tumor protein, referring to the molecular mass 53-kilodalton gene

Pal—Pallium

Pax6—Paired box 6 gene

PBS—Phosphate buffered saline solution

PBST—Phosphate buffered saline solution with Tween-20

PCR—Polymerase chain reaction

PDD-NOS—Pervasive Developmental Disorder Not Otherwise Specified

PDD—Pervasive Developmental Disorders

PFA—Paraformaldehyde

PFC—Prefrontal cortex

PGC7/Stella/Dppa3—Developmental pluripotency-associated protein 3 gene

PPI—Prepulse Inhibition

Pten—Phosphatase and tensin homolog gene

PTM—Post-translation modification

qRT-PCR—quantitative Real-time polymerase chain reaction

RA—Retinoic acid

RC2—Radial glial cell antibody that recognize and isoform of Nestin

Rcor1—Rest corepressor gene

RGCs—Radial glial cells

RI—Recognition Index

RM-ANOVA—Repeated-Measures Analysis of Variance

RNA—Ribonucleic acid

Rpm—Rotations per minute

RSPC—Retroplenial cortex

RT—Reaction time

S1—Stimulus 1 in Paired Pulse experiment

S2—Stimulus 1 in Paired Pulse experiment

SAM S-Adenosyl-Methionine

SCZ—Schizophrenia

SEM—Standard error of mean

Sfrp2—Secreted frizzled-related protein 2 gene

Shank3—SH3 and multiple ankyrin repeat domain 3 gene

SI—Sociability Index

Slc6a7—Solute carrier family 6 (neurotransmitter transporter), member 7 gene

Smad2—SMAD family member 2 gene

Smarca2—SWI/SNF related, matrix associated, actin dependent regulator of chromatin, subfamily a, member 2 gene

Smarcd3-- SWI/SNF-related matrix-associated actin-dependent regulator of chromatin subfamily d, member 3 gene

Smarce1-- SWI/SNF-related matrix-associated actin-dependent regulator of chromatin subfamily e, member 1

Snap25—Synaptosomal-associated protein, 25kDa

Spall—Subpallium

Srr—Serine racemace gene

SSC-A—Side scatter

SSEA-1—Stage specific embryonic antigen 1

Stk10—Serine/threonine kinase 0

Stmn3/Scg10—Stathmin-like 3 gene

SV—Subventricular zone

SWI/SNF—SWItch/Sucrose or NonFermentable chromatin remodelers

Syn1—Synapsin 1 gene

Syp—Synaptophysin gene

Tbr1—T-brain 1 gene

Tbr2—T-brain 2 gene

TBS—Tris-buffered saline

TelR—Telencephalon roof plate

TF—Transcription factor

TFs—Transcription factor

TH—thalamus

Tnfrsf8—Tumor necrosis factor receptor superfamily, member 8 gene

Ts65Dn—A mouse model of Downs Syndrome; trisomic for the region of mouse chromosome 16 homologous to human chromosome 21

Vgat—Vesicular GABA transporter

Vglut1—Vesicular Glutamate transporter 1

Vglut2—Vesicular Glutamate transporter 2

VP—Ventral pallium

VZ—Ventricular zone

Wiz—Widely-interspaced zinc finger-containing protein gene

Wnt2—wingless-type MMTV integration site family member 2

Acknowledgements

Firstly, I would like to thank my supervisor Professor Adrian Harwood for his support. Ultimately, your supervisorial approach has made me a better scientist and for that, I am grateful. I would like to thank my supervisor Dr. Anthony Isles who has remained incredibly patient and helpful throughout the four years. Thank you especially for initiating the project. And thank you for offering the opportunity to write a review and weathering my demonstrative approach so coolly. I would like to thank Professor Vincenzo Crunelli who has been a great support throughout both personal and professional challenges. Thank you for welcoming me into your epilepsy lab where you not only allowed me to design and experiment with a whole new set of tools, but on a completely different model of disease. I will forever be in debt to you. I would also like to thank Professor Yves Barde for welcoming me into his lab, for allowing me to visit Basil and gain direct instructions on how to differentiate pyramidal neurons. I will certainly be as welcoming and helpful throughout my career as a result of your example.

Secondly, I have a tremendous amount of gratitude for those individuals that directly helped or supported my research. I am very grateful to the research fellow Francois David, whom aided in the design and implementation of the AEP experiments, and also spent countless hours programming the data. Without his help Chapter 6 would not have been possible. Thank you also to the research fellow Cian McCafferty who trained me in surgical and electrode implantation techniques, your patients are more than commendable. I would like to thank Ciara O'Reagan for her time and effort with running mouse behaviour. I also owe a huge thank you to Anika, Ken, Liz, Mark, Kez, Mela, and Gui jie who were all a constant source of help for developing skills and protocols in the lab. Without your guidance, I'm not sure I would be a scientist still today. Thank you to Dr. Pete Watson for his help with the microscope. Thank you also to Professor Ming Li for advice and guidance.

Thirdly, I would like to thank those individuals that were generally supportive over the last four years. Thank you to my wonderfully supportive family—it's been a long journey. Thank you to all the wonderful friends and fellow scientists I've met in the last four years. I would especially like to thank Grainne—for all of the things. In addition, thank you to Cath, Vanessa and Emma for making PhD life easier. Finally, I am incredibly grateful to the Wellcome Trust for the funding and for making these last four years possible.

Table of Contents

Chapter I. General Introduction

1.1 Summary

Post-translational modifications of histone proteins, like the methylation at lysine residues, greatly influence chromatin dynamics and transcriptional regulation (Akbarian & Huang, 2009; Wen et al., 2009; Zhou et al., 2011). Such modifications are essential for the highly choreographed processes of lineage commitment and differentiation of the cell during development; and for on-going somatic maintenance and survival throughout the lifetime of the organism (for review, Hirabayashi & Gotoh, 2010; Tyssowski & Gotoh, 2014). Perhaps unsurprisingly, the genetic disruption of a number of post-translational modifying enzymes is found to lead to significant increases in the risk of inheriting a neurodevelopmental disorder (Bokhoven & Kramer, 2010; Parkel et al., 2013; Peter & Akbarian 2011; Tsankova et al., 2007; Vogel-Ciern & Wood 2013; Wilczynski, 2014). One example is the histone methyltransferase gene *EHMT1*. Mutations or deletions of *EHMT1* are associated with increased risks for inheriting a number of neurodevelopmental disorders (Cooper et al., 2011; Kirov et al., 2011; Kleefstra et al., 2012; O'Roak et al., 2011;); while the majority of the patients with known *EHMT1* disruptions present severe cognitive deficits (Kleefstra et al., 2005; 2009).

One question that remains is how much of the adult phenotype may be accounted for by epigenetic dysregulation during development versus the ongoing epigenetic dysregulation of cellular responses to transient environmental change, or cellular memory. What makes *EHMT1* a particularly fascinating gene is that it provides an opportunity to explore the parallels that exist in the epigenetic regulation of the cell (Sweatt & Day, 2011; Cavalli, 2006). Disruption in the gene allow us to investigate the molecular homology between the role of an epigenetic regulator in cellular

development and the role as an active place-holder for metastable responses to the environment, processes essential for learning and memory (Marcus et al., 1994; Atkins et al., 1998; English and Sweatt, 1996, Sweatt, 2001).

Epigenetic regulation of cellular development and memory are not isolated process, and indeed they share many of the same signaling cascades (Sweatt & Day, 2011). However, while neuropathology that occurs in response to aberrant development is not easily ameliorated, on-going disruptions of epigenetic regulation important for cellular memory just might be. Recent work has shown that modifying certain epigenetic regulators can have cognitive enhancing effects (see for example, Graff & Tsai, 2013; Fass et al., 2013). So even without a complete dissociation between the two types of epigenetic regulation, we can potentially identify and target dysfunction associate with on-going cellular memory and somatic maintenance.

Despite the fact *EHMT1* is associated with neurodevelopmental disorders, very little is known about its actual role in development and whether patients with *EHMT1* show irreversible neuropathology. And surprisingly little evidence has been found for there being substantial morphological or structural changes in previous studies of *Ehmt1*-haploinsufficiency in model species (Schaefer et al., 2009; Balemans et al., 2010). Thus the first goal of my research is to establish whether change in *EHMT1* dosage is associated with changes in cellular development and differentiation. I investigate *Ehmt1*-haploinsufficiency using a model of pyramidal differentiation beginning with mouse embryonic stem cells.

In order to potentially target the often-severe cognitive deficits that are associate with *EHMT1* disruptions—a model where cognitive deficits can be addressed independent from gross changes in motor function, weight, and motivation is necessary. At the outset of my research, such a model did not exist. Thus the second goal of my research was to design a model of *Ehmt1*-haploinsufficiency that allows us to assess discrete changes in cognition and to focus specifically on cortical circuits. Such a model provides not only a greater understanding of the functional role of *Ehmt1* in intellectual disabilities and cognitive deficits, but also provides a

platform for the molecular characterization and eventual mechanistic explanations of such deficits. In the long term, such a model may also provide a rubric for assessing pharmacological interventions in the epigenetic dysregulation of cellular memory. And, the third goal of my research is to draw a connection between the potential disruptions we find in pyramidal differentiation and the deficits we find in an animal model of forebrain *Ehmt1*-haploinsufficiency.

1.2 The *EHMT1* gene and neurodevelopmental disorder risk

Mutations in numerous lysine methylatransferases (KMTs) and demethylases genes are associated with neurodevelopmental and psychiatric disease (for general reviews see Peter & Akbarian, 2011; Kleefstra et al., 2014). Evidence for the important role these molecules play in normative brain function have been collected from their disrupted expression in post-mortem analysis of individuals with psychiatric illness (Akbarian et al., 2005; Huang & Akbarian, 2007; Huang et al., 2007), genetic association and risk studies (O'Roak et al., 2012; Talkowski et al., 2012; Kirov et al., 2012; Kleefstra et al. 2012) and animal models (for review see, Peter & Akbarian, 2011). The G9a-like (GLP) enzyme, encoded by Euchromatic histone methyltransferase 1 (*EHMT1*) is one such KMT, which has been identified as a psychiatric risk gene.

1.2.1 EHMT1 mutations and intellectual disabilities

Between 7-10% of individuals with severe intellectual disorders have subtelomere rearrangements (Dawson et al, 2002). This may be due, in part to telomeres being gene-rich. The human *EHMT1* gene is located on the subtelomeric region of chromosome 9 (see Figure 1). Disruptions in *EHMT1* expression are associated with a 9q34 subtelomeric-deletion syndrome, also known as Kleefstra Syndrome. These individuals often display intellectual disability, childhood hypotonia, facial dysmorphism, delays in reaching developmental milestones and behavioural problems such as aggressive outbursts and hypoactivity (Kleefstra et al., 2002; 2005; 2006). Approximately half of those diagnosed with Kleefstra syndrome also have congenital heart defects; ~20% have comorbidities with epilepsy and sleep disturbances (Kleefstra et al., 2009). In one study,

23% of Kleefstra patients reportedly display autism spectrum disorders (ASD) (Kleefstra et al., 2005) or autistic-like features (Iwakoshi et al., 2004). While the vast majority of the known cases with *EHMT1* mutations develop severe psychiatric pathology later in life (Kleefstra et al., 2005).

A quarter of individuals diagnosed with Kleefstra syndrome have loss-of-function mutations in *EHMT1* while the majority of the remainder appear to have deletions in the entire chromosome region surrounding the *EHMT1* (Kleefstra et al., 2012). Only a small percentage of individuals with Kleefstra do not have disruptions in *EHMT1*; instead these patients were found to have *de novo* mutations in one of four functionally related genes, *MLL3, SMARCB1, MBD5,* and *NR1I3* (Kleefstra et al., 2012). Functional relation was determined in Drosophila by modulating expression of each gene in an *EHMT*-induced wing phenotype. Strong interactions occurred in each of these genes and led to a striking enhancement in the wing phenotypes (Kramer et al., 2011).

Most Kleefstra syndrome cases occur either *de novo* or as a result of complex chromosomal rearrangements or translocations. Recently however two patients were found to have inherited interstitial deletions in *EHMT1*. Further investigation of these cases identified milder forms of the syndrome and somatic mosaicism in the mothers (Rump et al., 2013). Thus, even within the association of a highly specific deletion syndrome, a large degree of variability in clinic presentation is associated with disruptions in EHMT1 expression. In addition, cases of duplication have also been reported. In one instance, 145 kb duplication spanning exons 2 to 10 of the EHMT1, which led to a frame shift with a premature stop codon in the gene (Schawaibold et al., 2014).

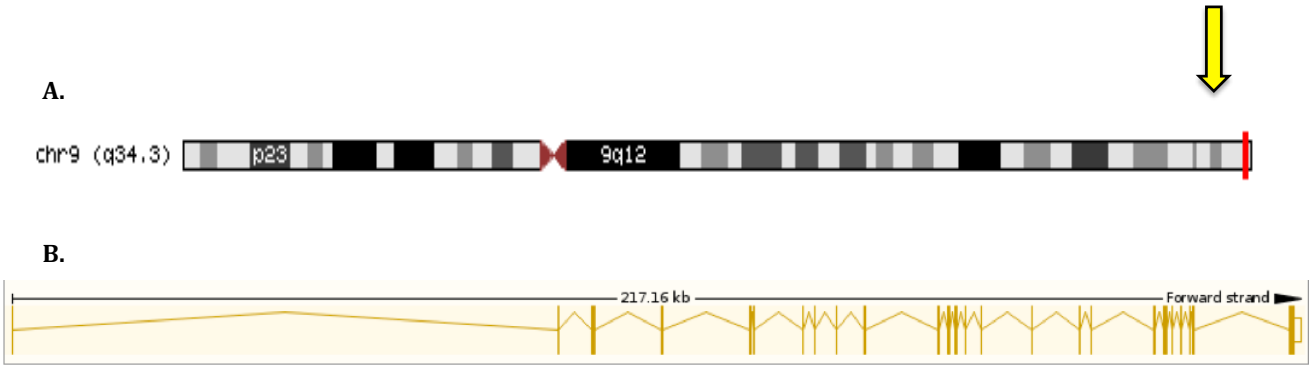

Figure 1. Chromosome 9 & EHMT1 structure
A.) On Chromosome 9 *EHMT1* start: at 140,513,444; End: 140,764,468; Size: 251,025; **B.)** *EHMT1* transcript has 27 exons and is associated with 543 variations. There are four known isoforms; however, only one expresses the full length protein. The transcript length is 5,137bps and the translation length is 1,298 residues (ENST00000460843; borrowed from Ensembl) .

1.2.2 EHMT1 mutations in schizophrenia

Schizophrenia is a serious psychiatric disorder affecting approximately 1% of the population. It is believed to be a neurodevelopmental disorder, with initial neurophysiological changes occurring in earlier postnatal stages and fully culminating into the adult disorder nearly two decades later (Jaaro-Peled et al., 2009). Like ASD, Schizophrenia is associated with heterogonous symptoms. Symptoms are typically classed into positive symptoms (e.g. hallucinations and delusions); negative symptoms (e.g. blunting affect, anhedonia, social deficits and avolition); as well as cognitive deficits (e.g. working memory, executive function, and attention deficits) (Eack et al., 2013; Harrison & Weinberger, 2005). While genetic factors are consistently found to account for a large percentage of the risks in developing the disease (Kendler, 1983; Shih et al., 2004), while known

environmental risks have also been identified (Brown, 2006; Brown & Susser, 2008; Mittal et al., 2008; Murphy et al., 2011; Chen et al., 2006).

Progress in understanding the aetiology and molecular underpinnings of schizophrenia has been slow. However, considerable advancements have been made in identifying the genetic architecture of the disorder in the last few years, this is especially promising, as heritability estimates are around 81% for the disorder (Sullivan et al., 2003). Progress has come with the combination of advancements in sequencing technology and significant increases in the sample sizes, necessary to generate significant statistical power and identify risk alleles of small effect (Kavanagh et al., 2015).

Both common genetic variance, which have small effect sizes and confer only small individual risk, but are more commonly found; and rare genetic variance, which have large effect sizes but are found extremely rarely contribute to the genetic risk of schizophrenia (Sullivan, Daly & O'Donovan, 2012). For common genetic variance genome-wide association studies (GWAS) are used. In the largest genome-wide association studies (GWAS) schizophrenia study to date, which considered 34241 cases, 45604 controls and 1235 parents of affected offspring trios, 108 distinct genomic loci were identified, 25 of which confirmed previous GWAS studies in the population and 83 were novel loci (Schizophrenia Working Group of the Psychiatric Genomics Consortium, 2014). Prior to this, only 30 loci had been reported at the genome-wide significance level (for review see, Sullivan, Daly & O'Donovan, 2012). The large increase in associated loci is the direct result of the large increase in sample sizes.

Advancements in sequencing technology have also enabled the screening of the coding exome, and the identification of rare single nucleotides variants (SNVs) or small insertions or deletions (indels) (Fromer et al., 2014; Purcell et al., 2014). What these and other reports find is evidence that increased polygenetic burden, arising from rare disruptive mutations, were especially enriched in genes relating to voltage-gated calcium channel function, the ARC-complex and scaffolding proteins

of the postsynaptic density complex (PSD)—similar to the genesets which have also been implicated by GWAS and CNV studies (Hall et al., 2014; Purcell et al., 2014; Gilman et al., 2012).

Another form of rare variance is copy number variants (CNVs), which are submicroscopic variations in the genome around <500kb in size. CNVs account for .1% of the genetic difference, similar to the .1% that exists at the single nucleotide level (Malhotra & Sebat, 2012). Such rare variance may have very low frequency of occurring (<. 5%) (Sullivan et al, 2012); however, they are extremely penetrant. One of the first identified instance of rare variance were deletions at chromosome 22q11.2, which confirms substantial risks for a range of psychiatric and neurodevelopmental disorders and in fact, 25% of 22q11.2 microdeletion cases manifest symptoms of psychosis (Malhotra & Sebat, 2012). Interestingly, duplications in this locus also provide the first evidence of what may be the first putative protective mutation for schizophrenia (Rees et al., 2014). Meanwhile, the enrichment of large (>100kv) CNVs has been reported in a number of psychiatric conditions, including schizophrenia, autism and bipolar disorder (for review see, Malhotra & Sebat, 2012); in the case of schizophrenia a 3-fold enrichment of such rare variance have been reported (Walsh et al., 2008; Kirov et al., 2012).

In a report of one of the largest analysis of *de novo* copy number variations (CNVs) in schizophrenia to date, Kirov et al. (2012) identified two *de novo* and three additional exonic CNVs in the *EHMT1* gene. In their analysis, *EHMT1* was one of the highest risk genes of those identified. Highly penetrant risk alleles like *EHMT1* are especially useful for understanding the aetiology of a complicated disease like schizophrenia. As an important regulator of gene expression throughout development, investigation of *EHMT1* disruption may allow insight into forms of inheritance that continues to elude classic genomics. As an epigenetic modification with a role in transcriptional regulation, it may also provide a tool for understanding the mediation of environmental and genetic factors risks in psychiatric populations.

1.2.3 *EHMT1* mutations in Autism Spectrum Disorders and developmental delays

Autism spectrum disorders (ASDs) is a spectra of neurodevelopmental disorders inclusive of autism, Asperger syndrome and pervasive developmental disorder not otherwise specified (PDD-NOS) (Betancur, 2011). ASD is a heterogeneous disorder associated with a range of symptoms. However, ASDs are typically classified by three primary phenotypes—abnormal social interactions, impaired communication and restricted interests or repetitive behaviours (Belmonte et al., 2004). A large percentage, up to ~70%, also display intellectual disabilities and ~25% have epilepsy (as reviewed in Betancur, 2011). In a recent scan of Autism Spectrum Disorder probands with either *de novo* CNVs or rare inherited CNVs, *EHMT1* was identified as a *de novo* mutation (O'Roak et al., 2012). Meanwhile, in an examination of copy number variations in 15,767 children, CNVs effecting *EHMT1* were the second most significant cause of developmental delay (Cooper et al, 2011).

1.3 Introduction to epigenetics

Epigenetics is a term originally coined by C.H. Waddington in the 1940s. Waddington's inspiration came from 'genetics' and 'epigenesis' and his intentions were to study the genetic control of development (Slack, 2002). Today epigenetics is a burgeoning field which aims to understand the complex regulatory mechanism involved in gene expression. The two central focuses in the field of epigenetics are: first, how such vast temporal and spatial cellular diversity arises from the invariable genomic sequences; and second, how these patterns of regulation may be inherited and maintained without lasting change to the underlying DNA (Shin, Ming & Song, 2014).

Epigenetic states are often thought of as forms of cellular memory. Patterns of gene expression in dividing cells may be passed onto daughter cells; or in the post-mitotic cell, patterns of gene expression may be encoded as metastable responses to the environment (Day & Sweatt., 2011). These states are established through complex interactions between transcription factors, noncoding RNAs, ATP-dependent chromatin remodeling, DNA methylation, the inclusion of different histone variants, or histone modifications

and occur at the level of chromatin (Tsankova et al., 2007). Epigenetic modifications of DNA and/or chromatin can be dynamic, undergoing very precise and coordinated changes throughout development and the lifespan of the organism (Feil & Fraga, 2012).

1.3.1. Nucleosome particle

The most basic unit of chromatin is the nucleosome, which consists of a DNA strand wrapped around a histone octamer composed of two copies of each of the histones H2A, H2B, H3 and H4 (Qureshi & Mehler 2014; Shin, Ming & Song 2014). The multidimensional structure of nucleosomes allow for the DNA to be tightly packaged within the nucleus of the cell. Inactive areas of the genome, or regions where little transcriptional activity takes place are often found in closed or more compact chromatin states, referred to as heterochromatin. Heterochromatic regions are generally found in areas that are gene poor (Horvath et al., 2001). The relationship between chromatin compaction and gene inactivation is evidenced in X-chromosome silencing or X-inactivation in females and the parent-of-origin-specific silencing of the imprinting genes (Pauler et al., 2007). In both instances large regions of the genome—the entire X chromosome in the case of X-inactivation are transcriptionally silenced. The silenced state is not only more compact than areas with active gene transcription, but is also found to correspond with very low levels of activating posttranslational modifications, like histone acetylation; but high levels of silencing modifications, like DNA methylation and histone H3 lysine-9 methylation (Kouzarides, 2007).

The rate of DNA methylation and histone H3 lysine-9 methylation in compact heterochromatin regions can be contrasted with the largely unmethylated state of the promoter regions in active genes and regions of the genome referred to as euchromatin (Shin, Ming & Song, 2014). These transcriptionally active areas of the genome are often found in more open confirmations. About 93% of the human genome is found in the euchromatic state (International Human Genome Consortium, 2004). Chromatin is thus a platform for which the actual conformational structure may indirectly effect transcriptional regulation. In addition and as discussed below, it also acts as a platform

for the reception of a diverse range of post-translational modifications, which directly effect transcriptional regulation.

1.3.2 DNA methylation

The transfer of a methyl group from S-Adenosyl-Methionine (SAM) to cytosine residues at CpG dinucleotides in the genome, results in 5-methylcytosine (5-mC), a modification which when found at promotor regions of a gene corresponds with transcriptional repression. The mode of repression can be the general presence of 5-mC DNA methylation (Iguchi-Ariga & Schaffner, 1989); or DNA methylation may recruit methly-binding domain proteins, which act as transcriptional repressors (Nan et al., 1998; Fuks et al., 2000).

Recently, the oxidative products of 5-mC, or 5-hydroxymethylcytosine, (5-hmC), 5-formylcytosine (5-fC) and 5-carboxylcytosine (5-caC) were discovered (for review, Shin, Ming & Song, 2014). Research demonstrating the dynamic nature of these modifications has resulted in the upheaval of the classic dogma—that DNA methylation is robust and stable modification. These markings are believed to represent stages in the DNA demethylation pathway, which repairs DNA back to unmethylated C, corresponding to the de-repression of the locus. Furthermore, recent research on the 5-hmC, has been suggestive of both tissue specific and gene activating roles of the modification, especially in the brain (Khare et al., 2012).

DNA methylation is catalysed by one of three methylatransferases—Dnmt1, Dnmt3a or Dnmt3b. Dnmt1 is by far the most abundant methylatransferases in humans, account for 80-90% of methylation sites. It is predominantly found to methylate hemimethylated CpG dinucleotides (Rhee et al., 2002); while Dnmt3a and Dnmt3b are found to predominantly methylate *de novo* CpGs (Shin, Ming & Song, 2014). Despite the differences in function, these methylatransferases are also found to act cooperatively (Rhee et al., 2002). The constitutive knockouts of any one of the Dnmt genes are lethal in mice, although there is some variation in the age of lethality (Li, Bestor & Jaenisch, 1992; Okano et al., 1999).

1.3.3 Histone Methylation

Histone modifications contribute to the functional architecture of the genome. This class of modifiers are probably the best studied in the brain and are those that involve the post-translational modification (PTM) of histones (Tsankova et al, 2007.). More than 70 known sites undergo PTM. These modifications occur at distinct amino acid residues on the amino (N)-terminal of the histone tail and include histone methylation, acetylation, ubiquitylation, SUMOylation or ADP-ribosylation at lysine residues (K), methylation at arginine residues (R), and phosphorylation at serine (S) threonine (T), tyrosine (Y), and histidine (H) residues and ADP-ribosylation at glutamate (E) residues (Tsankova et al, 2007). The complex combination of PTMs on the tails of histones composes what is often referred to as the histone code. The dynamics of the histone code is further complicated by classes of enzymes that catalyse the removal of many of these PTMs modification, for example deacetylases and demethylases (Fierz & Muir, 2012).

Histone methyltransferases catalyse the transfer of a methyl group from S-Adenosyl-Methionine (SAM) to amino acid tails of histone proteins. In vertebrates, there are an estimated 70 genes containing the Su(var)3-9, Enhancer of Zeste, Trithorax (SET) catalytic domain and which are K-specific, alone (Black & Whestine, 2011). Histone methyltransferases are also highly specific in the number of methyl groups they transfer to the site-specific substrate as well, and may catalyse between 1 and 3 methyl groups (Black & Whestine, 2011).

1.4 Biochemistry of the *EHMT1* encoded GLP protein

1.4.1 GLP activity

EHMT1 encodes the G9a-like protein (GLP), also known as Eu-HMTase1 or KMT1D. GLP is a member of the Suv39h subgroup of SET domain-containing molecules. GLP is involved in a diverse number of processes from heterchromatin formation, gene silencing, DNA methylation to gene activation and transcriptional elogation (Rea et al.,

2000; Sims et al., 2003). However, GLP is recognized primary for its role as a histone 3 lysine 9 monomethyltransferase (H3K9me1) and dimethyltransferase (H3K9me2) (Ogawa et al., 2002; Tachibana et al., 2005).

1.4.2 G9a/GLP heteromeric complex

GLP is most often found in a heteromeric complex with its mammalian paralog G9a or KMT1C, encoded by the EHMT2 gene—another member of the Suv39h subgroup of SET domain containing molecules. In fact, the G9a/GLP heteromeric complex is the most stable form for both enzymes (Tachibana et al., 2005). While they retain partial HKMT activity when found in a homomeric complex, genetic ablation of either gene leads to a significant reduction in the levels of H3K9me2, specifically (Peters et al., 2003; Rice et al., 2003; Tachibana, 2001).

Interestingly, a GLP/G9a double knockout (KO) does not further reduce H3K9me1 or H3K9me2. Tachibana et al., found that GLP deficient mice and embryonic stem cells showed almost identical phenotypes with that of the G9a KOs, which suggests little compensation with the loss of function in either enzyme and instead potential interdependence (2005). Furthermore, GLP and G9a do not appear to have redundant functions. The cooperative function of these enzymes is important for future consideration, as much of the work that focuses on H3K9me2 is biased towards G9a. This bias persists despite the consistent and severe phenotypes associated with *EHMT1* disruption in psychiatric genetics (van Bokhoven & Kramer 2010). Nevertheless, research on G9a is informative for work on GLP.

1.4.3 Dual role of H3K9me2 repression

1.4.3.1 Global effects: Heterochromatinisation

Patterns of H3K9me2 are fairly highly conserved across mouse and human. Unlike other epigenetic modifications, H3K9me2 coverage shows a longer, continuous distribution, across megabase-long stretches of genomic DNA (Wen et al., 2009). The modification also appears to be both differentiation-enriched, covering 4% of the genome in embryonic stem cells (ESCs) and 31% in terminally differentiated cells; and tissue-specific, with 10% of the genomic coverage in the adult brain and over 40% in the adult

liver (Wen et al., 2009). Furthermore, the pattern of increase in H3K9me2 appears to be G9a/GLP specific. In the differentiation of a G9a-/- cell line there is a reduction of over 90% in H3K9me2, as compared to the wild type cells. Wen and colleagues suggests H3K9me2 plays an important role in chromatin organization during cellular differentiation, in a process of marked heterochromatinisation (2009). In their study, Wen et al., identified huge increases in genomic coverage of H3K9me2 as cells differentiated—suggesting H3K9me2 may be regulating the switch from euchromatic to heterchromatic regions (2009). However, these findings remain somewhat controversial. As Lienert et al., reported H3K9me2 coverage of ~50% of the genome in mESCs (2011).

1.4.3.2 Local effects: Targeted gene repression

Although H3K9me2 often spans long stretches of the genome, G9a/GLP regulation at specific gene targets has also been reported. For example, the role of H3K9me2 repression during neuronal and glial fate restriction was reviewed in Hirabayashi & Gotoh (2010). While in a *Ehmt1* postnatal knockout mouse, GLP deficiency resulted in a significant reduction in H3K9me2 modification and the subsequent up-regulation of a large number of genes across several brain structures—84 genes in the hippocampus, 116 genes in the hypothalamus and 127 genes in the striatum. Of those identified, some 60 genes comprised a genetic "signature" of dysregulated expression in both the G9a and GLP postnatal deficiency (Schaefer et al., 2009). A majority of the up-regulated genes were those not normally expressed in the adult brain. In fact, a significant proportion of these genes are normally expressed in the development and function of skeletal, muscular, cardiovascular, hematological and immune systems. Schaefer and colleagues suggested GLP haploinsufficiency leads to global transcriptional dysregulation in a region specific manner; and GLP-mediated activity may act to regulate brain function through the maintenance of transcriptional homeostasis (2009).

In drosophila, EHMT-specific H3K9me2 was found at more than 350 gene loci within the brain. Unlike the conditional mouse model above, a significant proportion of these genes play critical roles in nervous system development and function (Kramer et al., 2011). Furthermore, after discovering a reversal of the cognitive defects identified in haploinsufficient flies with the re-expression of EHMT protein, these researchers argued,

EHMT orchestrates an epigenetic program that directly regulates a battery of important neuronal genes, key to normal cognitive processes. However, such differences in neuronal-specific gene regulation and in restoration of cognitive function with EHMT re-expression may be the result of there being only one homolog, as opposed to the two found in mammals. Thus the functional conservation in between drosophila EHMT and mouse *Ehmt1* and *Ehmt2* is a relevant question to consider before assuming homology.

1.4.4 H3K9me transcriptional activation

A disproportionate number of reports on H3K9me2 focuses on its role as a transcriptional repressor. However, this modification is also found at euchromatic regions of chromatin, or areas consistently associated with active transcription. In fact in one report, H3K9me2 modifications occur in active genes and were further associated with transcriptional elongation (Vakoc et al., 2005). These changes were G9a-specific (though GLP was not examined). Of note, the H3K9me2 target sites existed outside of the promoter regions of the genes and instead in the transcribed regions. It was also found that the levels of methylation at the transcribed regions declined after the cessation of transcription, which suggests the G9a/GLP cascade, might act rapidly and transiently during active gene transcription (Vakoc et al., 2005).

The involvement of GLP in gene activation may be inferred by a handful of reports that identify transcriptional changes in *Ehmt1*-haploinsufficiency. As reviewed above, the de-repression of GLP or G9a-specific H3K9me2 predicts the up-regulation in the expression of a large number of genes (Kramer et al., 2011; Lienert et al., 2011; Schaefer et al., 2009; Wen et al., 2009). However, along side those genes found to be transcriptionally up-regulated, a group of genes are consistently found to be significant down-regulated as well. While direct involvement of GLP or G9a cannot be assumed, what these findings suggest is that H3K9me2 and H3K9me1 histone methyltransferases are at least indirectly involved in active gene transcription (Wen et al., 2009; Yokochi et al., 2009; Schaefer et al., 2009).

The rapid deposition and removal of H3K9me at active regions of the genome reported by Vakoc and colleagues are especially interesting in terms of its potential biological function (2005). This suggests that while GLP is continually found to be important for more long-term cellular memory and setting-up transcriptional profiles inherent to cell fate specification (as reported by Schaefer et al., 2009 and Wen et al., 2009); it may also be important for other forms of cellular memory—for encoding and storing rapid environmental changes essential for learning and memory. Indeed, G9a/GLP activity has been found to differentially regulate gene transcription in two different areas of the brain, the entorhinal cortex and hippocampus, during memory consolidation. Such findings may suggest GLP is essential for regional communication in a process of long-term memory formation (Gupta-Argarwal et al., 2012). In another study, G9a repression in mice led to enhanced cocaine preference and subsequent increases in dendritic spine plasticity (Maze et al., 2010). Furthermore, cognitive phenotypes associated with EHMT-mediated transcriptional dysregulation may be reversible, as the work in drosophila suggest (Kramer et al., 2011).

1.4.5 Non-histone related activity

1.4.5.1 De novo DNA Methylation.

In addition to histone-related activities, the G9a/GLP complex is found to interact with DNA methyltransferases, what can be a more stable form of transcriptional repression. For example, G9a/GLP complex catalyses *de novo* DNA methylation by recruitment of DNA methyltransferases Dnmt3a and Dnmt3b via its ankryin domain (Ikegami et al., 2007; Xin et al., 2003; Epsztejn-Litman et al., 2008); inasmuch, G9a and GLP knockout mouse embryonic stem cells (mESCs) have dysregulated DNA methylation (Dong et al., 2008; Epsztejn-Litman et al., 2008; Tachibana et al., 2008). However G9a/GLP related DNA methylation in this instance appears to be independent of its HMT activity and the SET domain. Whereas DNA methylation in G9a null cells is dysregulated, catalytically inactive G9a cells are found to have partially restored DNA methylation patterns (Dong et al., 2008; Epsztejn-Litman et al., 2008). In addition to the recruitment of Dnmt3a and Dnmt3b, G9a is found to bind with Dnmt1—this complex leads to enhanced DNA and histone methylation, at least during an *in vitro* essay (Esteve et al., 2006).

1.4.5.2 PGC7-binding in early embryogenesis.

In early embryogenesis, conserved H3K9me2 sites are believed to act like a protective buffer from the conversion of the DNA modification 5-methylcytosine (5mC) to 5-hydroxymethylcytosine (5hmC), by tet methylcytosine dioxygenase (Tet) family of enzymes (Koh et al., 2011). The balance between 5hmC and 5mC is linked with cellular differentiation processes such as pluripotency and lineage commitment (Koh et al., 2011). In mice, H3K9me2 acts as a binding site for the maternal factor PGC7, on genes important during early embryonic development and the imprinting regions in the maternal genome (Nakamura et al., 2012). In turn, PGC7 also known as *Dppa3 or Stella*, is necessary for the maintenance of DNA methylation by protecting it from the Tet3-mediated conversion. Thus the G9a/GLP complex through PGC7 binding supports essential DNA 5mC maintenance in early mouse embryogenesis (Nakamura et al., 2012).

In addition to its role as a histone methyltransferase and its interaction with DNA methyltransferase, GLP is found to self-methylate at its catalytic site. GLP also catalyses the methylation of non-histone proteins, like p53, Wiz, CDYL1, ACINUS, and Reptin (Sampath et al., 2007; Rathert et al., 2008; Huang et al., 2010; Lee et al., 2010).

1.4.5.3 Repressor complexes and interacting molecules

A number of molecules are found to interact with G9a (for review see Shinkai & Tachibana, 2011); unfortunately very few comparable studies focus explicitly on GLP interacting molecules. With exception, in the process of heterochromatinisation, G9a and GLP are found to bind with the Heterochromatin Protein 1 (HP1) (Nozawa et al., 2010). In addition, G9a-mediated activity is essential for the silencing of developmental genes through interaction with CDP/cut (Nishio & Walsh, 2004) the plasma cell transcription-factor Blimp-1 (Gyory et al., 2004) and the NRSF/REST transcriptional repressors/complex (Roopra et al., 2004). Research considering the neuronal specific NRSF/REST transcriptional repressor complex is reviewed in more detail, in Chapter 2.

1.5 Modelling Ehmt1 haploinsufficiency in the mouse forebrain

1.5.1 Crossing diagnostic boundaries

As discussed, *EHMT1* confers risk across diagnostic boundaries in psychiatric populations, from neurodevelopmental disorders—developmental delays and ASD; the adolescent and adult-onset neuropsychiatric disorder—schizophrenia; and the genetic disorder—Kleefstra syndrome (Talkowski et al., 2012). The variation of symptoms associated with *EHMT1* haploinsufficiency suggests perturbations in the gene leads to variation in the severity of neuropathology and the life stage at which symptoms manifest. There are numerous possible explanations for why this may be. The variation of symptoms may be due to differences in mutational mechanisms or there may be a range of effects due to differences in genetic background and epistasis ((Burmeister et al., 2008). Similarly variation in environmental influences and the natural stochasticity of epigenetic processes during development could play a huge role (Feinberg & Irizarry, 2010). Finally, as evidenced in two patients, there could be differences in mosaic expression patterns of the gene (Rump et al., 2013).

Regardless of the large degree of variation in clinical presentations, there are several important commonalities found in *EHMT1*-risk populations. First, from what is known about ASD, schizophrenia and intellectual disabilities, disorder manifests during development (Jaaro-Peled et al., 2009; Kleefstra et al., 2014; Marie du bois et al., 2007; Owen et al., 2011). This may suggest *EHMT1* plays an important role in neurodevelopment. Second, forebrain-dependent cognitive functions are disrupted in these populations, pointing to the importance of forebrain-specific *EHMT1* expression (Butler et al., 2012; Di Cristo et al., 2007; Gogtay et al., 2004; Talamini et al., 1999). Finally, the high rate of comorbidity with epilepsy and disruption in excitatory/inhibitory balance in these clinical populations may point to an overlap in the mechanistic disruptions of the relevant amino acid neurotransmitter pathways in

individuals with *EHMT1*-specific mutations (Amiet et al., 2008; Cascella et al., 2009; Clarke et al., 2012; Wotton & Goldacre, 2012).

Despite the evidence of the importance of *EHMT1* for normal brain function, very little is known about its role in neurodevelopment. Similarly, the molecular pathways involved in GLP-specific activity and important to normal cognitive function are not well understood. In this thesis, I aim to explore the functional outcome of *Ehmt1*-haploinsufficiency during mouse brain development. Focus is placed on the concordant phenotypes shared by *EHMT1*-associated psychiatric risk populations. The data herein reported is that from mouse models of *Ehmt1* haploinsufficiency in neuronal differentiation, in forebrain-specific activity, and in *in vivo* electrophysiology.

1.5.1.1 Modelling the role of GLP in neuronal differentiation and development

As discussed above, the epigenome is involved in the cascade of temporally and spatially specific gene regulation, throughout lineage commitment and cellular development. Epigenetic programs take their regulatory cues for the unfolding of these processes from the environment, both extrinsically and intrinsically. Thus, there are fairly robust differences between gestational and postnatal epigenetic effects; differences in susceptibility to epigenetic alterations during development may be tied to the degree of pluripotency (Feil & Fraga, 2012). For example, there is an abundance of highly expressed epigenetic regulators from DNA methyltransferases to chromatin modifiers in pluripotent embryonic stem cells. The rate of gene expression and enzyme activity of these regulators drastically decreases throughout cellular differentiation and in the post-mitotic cell (Hirabayashi & Gotoh, 2010). Following this pattern, the GLP enzyme in the mouse has greater and broader expression pattern in early developing tissues, with tissue-specificity and lower expression occurring in adulthood (Kleefstra et al., 2005).

One very likely cause for *EHMT1*-associated dysfunction is the global epigenetic disruption of H3K9me2 repression during early stages of cellular differentiation and lineage commitment. If such alterations occur during prenatal development, they would be amplified by further cell divisions and somatic maintenance (Feil & Fraga, 2012). Thus

any deficits we find in adult behaviour and function could in fact have origins in very early stages of cellular development. Therefore, the first questions I address are how *Ehmt1*-haploinsufficiency effects the differentiation of mouse pyramidal neurons. Pyramidal projection neurons are excitatory cells of the brain, which are most abundant in the cerebral cortex—and in structures, which are typically associated with advanced cognition (Spruston, 2008)

In Chapter 2, I begin with a thorough discussion of the previous work on *Ehmt1* and He3K9me2 in cell development. I report data where the expression of pluripotency markers and proliferation rates of mouse embryonic stem cells (mESCs) lacking one copy of the *Ehmt1* gene and their isogenic controls are examined. The mESCs are differentiated into pyramidal neurons. I then examine the rate of proliferation and differentiation in the progenitor populations at two stages of development. I examine the transcriptional profile of *Ehmt1*$^{+/-}$ mutant progenitors, looking for changes in the expression of lineage markers and cell signalling molecules. Finally, I consider cell fate and the neuronal phenotypes of these cells.

1.5.1.2 Modelling EHMT1 haploinsufficiency in the forebrain

Cognitive impairments—which include deficits in behavioural domains such as attention, learning, memory, or processing speed occur in a large percentage of individuals with schizophrenia, ASD and intellectual disabilities (Parkel et al., 2013; Kleefstra et al., 2014; Morgan et al., 2012; van Bohoven & Kramer, 2010)—are arguably the most devastating phenotypes shared by these disorders. Currently such phenotypes remain untreatable. Meanwhile, the degree of cognitive impairment is often the best predictor of long-term functional outcomes for some of these patients (Green, 1996). In addition, at least in the case of schizophrenia, often mild cognitive impairments are identifiable in first degree relatives, which suggests such deficits are indeed a result of underlying genetic risk (Egan et al., 2001).

Impairments in cognition reflect abnormalities in cortical circuits. Thus, limiting the scope of genetic disruption to the forebrain allows focus to be placed on the functional outcome of *Ehmt1*-haploinsufficiency in these circuits. I generated an *Ehmt1* conditional

knockout mouse line that has only one copy of the *Ehmt1* gene in the forebrain, throughout development; the deletion is limited primarily to the pyramidal cells of the forebrain. Conditional mouse models reduce anatomical complexity, and in the case of forebrain-specificity, they allow more precise focus on learning, memory, and executive functions. In fact, many of the mouse models found to be the most representative of human psychiatric illness have been those that involve remarkable cellular and tissue specificity (for review, Marin, 2012). By focusing only on forebrain *Ehmt1* haploinsufficiency, forebrain-specific deficits associated with psychiatric populations can be identified. In addition, this model provides an opportunity to compare the range of behavioural impairments previously reported on the global knockout mouse (Balemans et al., 2010; 2013; 2014). Corroboration of cognitive impairment between models allows more precise validation of the role of *Ehmt1* in cortical function

In Chapter 3, I begin with an overview of the previous models of *Ehmt1* haploinsufficiency. The development of the mouse model used throughout the remainder of my thesis is then described in detail. Basic descriptions of the breeding conditions, physicality, motoric functions and gross anatomical measurements are then assessed. In Chapter 4, I begin with an overview of anxiety in psychiatric illness and mouse correlatives of anxiety-related behaviours. I then investigate three measurements of anxiety in these mice. In Chapter 5, I begin with a discussion about translational human endophenotypes in mouse models of psychiatric illness. Three endophenotypes shared by the *EHMT1*-neurodevelopmental risk populations are then examined: sociality, sensorimotor gating and working memory.

1.5.1.3 Modelling Electrophysiological dynamics of EHMT1 haploinsufficiency

As reviewed above there is a significantly comorbity with epilepsy in individuals diagnosed with schizophrenia, ASDs and intellectual disabilities. However this statistic underestimates the general and more-subtle rate of perturbations in the excitatory/inhibitory activity that likely exists in these populations. Such imbalances are consistently reported across numerous mouse models of Schizophrenia risk genes (e.g. *Nrg1*—Chen et al., 2008; *Erbb4*—Fisahn et al., 2009; *Grin1*—Belforte et al., 2010); models of ASD risk genes (e.g. *Shank3*—Peca et al.,

2011; *Nrxn1*—Etherton et al., 2009); as well as in the *Ts65Dn* model of Down's syndrome (Kleschevnikov et al., 2004); the *Fmr1* model of Fragile X syndrome (Olmos-Serrano et al., 2010; Gibson et al., 2008); the *Gabrb3* model of Angelman's syndrome (Jiang et al., 2010); and the GABAergic-specific deletion of *Mecp2* gene, a model of Rett's syndrome (Chao et al., 2010).

The brain is comprised of complex hierarchical networks of excitatory and inhibitory neurons (Ward, 2003). The balance of excitation and inhibition is essential to all cortical function (Basar & Guntekin, 2008; Uhlhaas & Singer, 2010; Hermann & Demiralp, 2005). Therefore disruptions in in either circuit have serious implications for a range of cognitive functions and behaviours. In Chapter 6, I review electrophysiological endophenotypes commonly found in the relevant neurodevelopmental risk populations. I discuss types of measurements in both time and frequency domains. I report evidence of disruptions in auditory event related potential measurements using paired pulse and mismatch negativity paradigms; I then report evidence of changes in the patterns of global oscillations at different frequency bands.

Finally, in Chapter 7, I summarise the main findings of this work. I provide preliminary hypotheses regarding the potential mechanistic causes for the disruptions reported. I discuss the specific limitations of the experiments. I discuss where improvements might be made in the future and what pressing questions might be answered next. I attempt to place my findings in the broader context of our progress in understanding psychiatric illness.

1.6 Aims

- Characterise *Ehmt1*$^{+/-}$ mESC, and their ability to produce neuronal precursors and pyramidal neurons *in vitro* (Chapter 2).
- Generate, characterise and behaviourally profile a forebrain-specific *Ehmt1* haploinsufficient mouse model (Chapters 3-5).
- Model the electrophysiological dynamics in a forebrain specific *Ehmt1* haploinsufficient mouse model (Chapter 6).

Chapter II. GLP in pyramidal neuronal differentiation

2.1 General Introduction

The loss of function of a single copy of the *EHMT1* gene in humans leads to variation in the severity and time course of pathology. However, that all disorders associated with gene disruption are neurodevelopmental is a strong indicator that GLP activity is especially important during development. In this chapter, haploinsufficiency at the embryonic stem cell stage is examined using two hemizygous *Ehmt1* mouse embryonic stem cell lines and compared with isogenic controls. These cells are then differentiated into pyramidal neurons. Differences in neuronal progenitor proliferation and rate of differentiation are then examined using S-phase characterisation, growth curves, western blot, immunohistochemistry and RT-PCR expression and finally, images of end stage neurons are presented.

2.1.1 Introduction to embryonic stem cells

Embryonic stem cells (ESCs) are defined by their transcriptional profile, pluripotency and ability to self-renew. Pluripotency refers to the power of the cell to divide and produce cells from all three germ layers—the endoderm, ectoderm or mesoderm (Evans, 2011); while self-renewal refers to their ability to eliminate differentiation-inducing signalling from different kinase pathways, like the mitogen-activated protein kinases and glycogen synthase kinase 3 (Ying et al., 2008). In mice, ESCs (mESCs) exist until the early post-implantation stage and were first identified over three decades ago (Evans & Kaufman; 1981). Today research that considers the derivation, propagation and maintenance of pluripotency in ESCs provides an important niche in developmental biology. Stem cell technologies provide useful *in vitro* tools for manipulating cellular differentiation and lineage commitment processes. And allow precise control of fate restriction and opportunities to closely monitor temporal resolution of the differentiation process.

2.1.1.1 GLP-mediated repression and pluripotency

Among the most recognised and potentially important G9a/GLP-specific histone methylation targets are the pluripotency transcription factor genes *Oct4* and *Nanog.* Both transcription factors (TFs) are required for the maintenance of pluripotency and self-renewal in embryonic stem cells (Loh et al., 2006). In addition to its role as a TF, Oct4 is also found to play an important role in higher-order chromatin structure, perhaps via the binding of CTCF—a binding factor that mediates long distance regulatory elements (Donohoe et al., 2009). The G9a/GLP complex binds directly to the promoter of *Oct4*, mitigating its repression via H3K9me2 (Fritsch et al., 2010; Epsztejn-Litman et al., 2008). H3K9me2 repression is directly followed by the G9a/GLP-specific recruitment of DNA methylatransferases, DNMT3a and DNMT3b—which leads to more stable transcriptional repression. $G9a^{-/-}$ knockout mice showed prolonged expression of Nanog and Oct4 until embryonic day 7.5; an equivalent examination in Nanog and Oct4 expression in $GLP^{-/-}$ is lacking. Prolonged expression of these pluripotent transcription factors led to delayed development (Yamamizu et al., 2012). In addition to *Oct4* and *Nanog*, pluripotency associated genes *Stk10, Dnmt3l, Tnfrsf8, Gpr54, Cdkn1c* have also been identified as targets of G9a-specific repression, and thus presumably GLP. This finding suggests a prominent role for the G9a/GLP complex in the direct epigenetic silencing of a relatively large embryonic gene network (Epsztein-Litman et al., 2008).

Adding further to the complexity, the H3K9 demethylases jumonji domain-containing 1A (JMJD1A) and 2C (JMJD2C) are positively regulated by Oct4 (Gaspare-Maia et al., 2011). JMJD1A and JMJD2C are histone demethylases that remove the methylation marks on H3K9me2 and H3K9me3, respectively. Therefore, Oct4 and Nanog expression levels are involved in a JMJD1a and JMJD2 histone demethylase-mediated positive feedback-loop, which is important for the maintenance of pluripotency. Thus, H3K9 methylation may act as an important trigger in the initial stages of differentiation and lineage commitment.

2.1.1.2 Histone demethylases & reprogramming pluripotency

Further evidence of the role of H3K9me-related repression in stem cell biology

comes from work demonstrating fibroblast-induced pluripotent cells (iPSCs) reprogramming involves an up-regulation in both JMJD1A and JMJD2C (Takahasi and Yamanaka, 2006). This work suggests the removal of the H3K9me-specific repression sites is essential for cell fate reversal and the renewal to a pluripotent state. Furthermore, the significant depletion of JMJD1A and JMJD2C enzymes in ESCs leads to early differentiation (Loh et al., 2007). Without the expression of the demethylase enzymes to balance H3K9me, the rapid and premature increase in H3K9me led to the repression of essential pluripotency transcription factors and early differentiation (2007).

2.1.1.3 Chromatin structure and the role of GLP in early differentiation

There are several lines of evidence that suggest G9a/GLP-specific H3K9me2 is important for chromatin organization during ESC differentiation. Once methylated, these sites bind a set of heterchromatin proteins HP1a or HP1ɣ. The binding of HP1 corresponds with chromatin compaction or heterchromatisation, which in turn leads to a more transcriptional restrictive state (Fierz & Muir, 2012). One ChIP-chip study found a 6-27% increase in genomic coverage of H3K9me2 between the embryonic stem cell state and lineage committed progenitor states (Wen et al., 2009). Meanwhile, in another study, G9a was found to be significantly up regulated in very early stages of differentiation, from differentiation day 0.5-2.5, which immediately preceded the increases in H3K9me2 (Yamamizu et al., 2012). Further support comes from immunofluorescent imaging, which has demonstrated increased staining of heterochromatin in the nucleus of differentiated cells (Meshorer & Misteli, 2006).

The chromatin of embryonic stem cells is also unique in the large number of bivalent sites present, or the co-expression of H3K4me3 and H3K27me3 (Vastenhouw & Schier, 2012). Bivalent sites are rarely found in terminally differentiated cells, further suggesting that chromatin may undergo radical changes during differentiation. The bivalent modifications mark promoters of developmental and lineage-regulating genes. The co-expression of both repressor and activator

modifications is believed to keep genes poised for transcriptional activation or repression in later stages of fate restriction (Efroni et al., 2008).

Not all evidence supports a process of marked heterchromatinisation during differentiation however. In one study, H3K9me2 coverage was reportedly present on 50% of the ESC genome (Lienert et al., 2009). While Lienert et al. did find discrete changes of H3K9me2 in a cell-specific manner and altered gene expression, which mirrored cell fate; they did not find the same global increase during neuronal differentiation. Thus, it may be premature to assume a significant increase of H3K9me2 occurs during ESC differentiation; however, there is evidence to support a global reorganisation of heterochromatic sites (for review see, Li, Liu & Belmonte 2012). Regardless of whether there are such increases in heterochromatisation or just a mass reorganisation, the G9a/GLP complex is involved in chromatin structuring during cellular differentiation. In addition, G9a/GLP is also found to be essential for the regulation of several pluripotency markers and for early fate restriction in mESCs.

2.1.2 Development of the cerebral cortex

The mammal cerebral cortex represents perhaps the most profound evolution of anatomical complexity evidenced in the animal kingdom (Finlay & Darlington, 1995). It is a layered structure with 100s of diverse cell types; all together these cells generate incredibly powerful and complex computational circuitry (Greig et al., 2013). Meanwhile, the cortex is responsible for a diverse range of cognitive processes, from mediating sensory information to coordinating motor output and employing higher order cognitive processes. It is made up of two major groups of neurons, the interneurons—which are largely inhibitory, and the projection neurons—which are excitatory (Greig et al., 2013). Interneurons are connected more locally and primarily contribute to local neural circuitry assemblages, whereas projection neurons project to more distal regions and transmit information across cortical areas and different brain regions (Marin, 2012). Meanwhile pyramidal projection neurogenesis originates in the cortical germinal zone in the dorsolateral

wall of the telencephalon, while inhibitory interneurons in mice originate in subcortical regions like the ganglionic eminence (Anderson et al., 2002).

2.1.2.1 Pyramidal-projection neurons

Projection neurons or pyramidal neurons are morphologically characterized by the pyramidal shape of their soma and their large apical and basal dendritic trees (Spruston, 2008) (See Figure 2.1). However they may be classified based on regional identity or based on individual characteristics like dendritic morphology, electrophysiological properties, projection patterns, transcriptional profile or epigenetic profile (Molyneaux et al., 2007). In the mammalian brain, pyramidal neurons are found in forebrain structures like the neocortex, hippocampus, and amygdala (Spruston, 2008). All pyramidal neurons receive synaptic input from their soma, dendrites and axons. However, only the soma and axon receive inhibitory GABAergic inputs, while most excitatory input comes through dendritic synapses from multiple sources (Spruston, 2008).

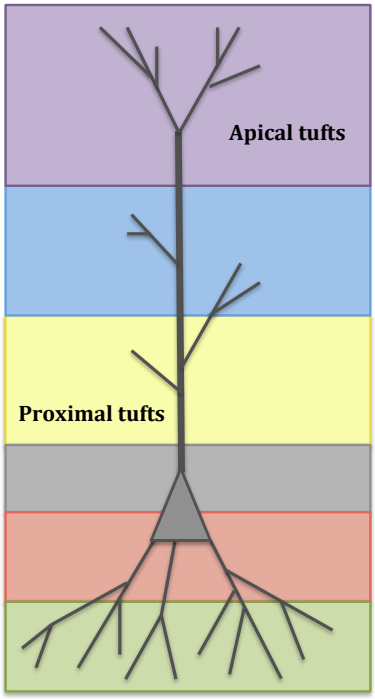

Figure 2.1 Pyramidal Neuron Structure
The structures of the different types of pyramidal neurons all demonstrate apical dendrites and apical tuft. Cells of the V layer for example, may receive synaptic input from any one of multiple layers of the 6 layers of the cortex. (images based on that reported in Spruston et al., 2008)

2.1.2.2 Pyramidal neurogenesis

Neurogenesis is a series of developmental events characterized by a sequential order; these events are transitional and typically involve progressive fate restriction; and similar patterns are found in both embryogenesis and adulthood (Eposito et al., 2005). The cortex develops from the inside out, with the earliest born cells occupying deeper layers and the later born cells migrating towards superficial layers (Angevine & Sidman, 1961). The developing cortex is subdivided into four

areas, each developing sequentially—the ventricular zone (VZ), the subventricular zone (SV) intermediate zone (IZ) and the cortical plate (CP).

Cell proliferation and fate specification take place in the VZ and the SVZ (Hevner et al., 2006). These layers drive cortical expansion throughout corticogenesis (Sessa et al., 2008). The VZ or the ventricular surface of the telencephalon consists of the radially oriented cells or radial glia cells (RGCs) (Kriegstein & Gotz, 2003). RGC populations derive from neuroepithelial cells and are often considered apical progenitors. They are capable of both symmetrically and asymmetrically dividing into postmitotic neurons and intermediate progenitor cells (IPCs) (Gotz and Barde, 2005; Kowalczyk et al., 2009).

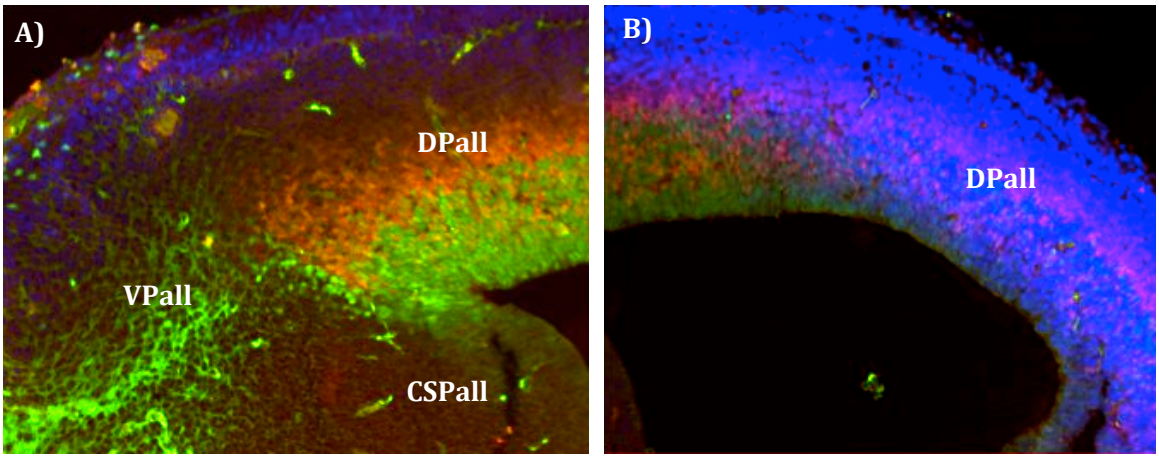

Figure 2.2 E14.5 TF expression in developing telencephalon (forebrain structures).
A. More anterior regions of dorsolateral pallium: Dpall—Dorsal pallium (isocortex); VP—ventral pallium (isocortex); Spall—subpallium (isocortex); **B.** Posterior regions of the dorsolateral pallium (isocortex). Green—Pax6; Red—Tbr2; Blue—dapi nuclear stain.

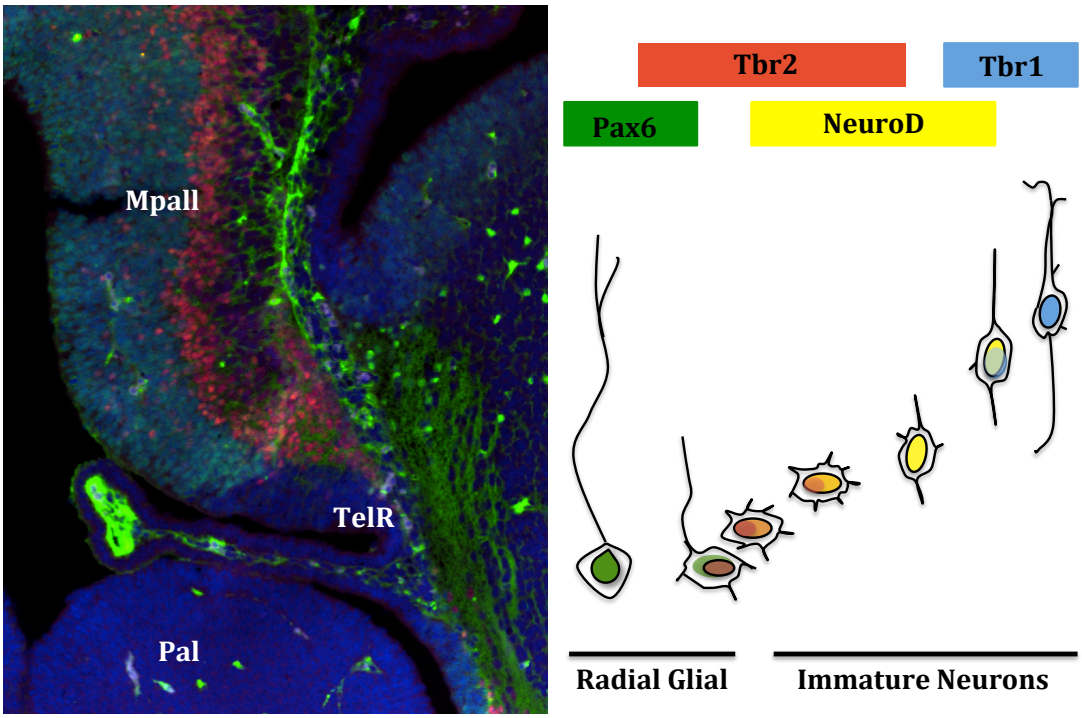

Figure 2.3 E14.5 TF expression in developing telencephalon (forebrain structures)
A. Posterior region of the vetrolateral pallium; Mpall—medial pallium (hippocampus allocortex) ; TelR—roof plate of evaginated telencephalic vesicle; Pal—pallidum (extrapyramidal motor system). Green—Pax6; Red—Tbr2; Blue—dapi nuclear stain. **B.** Schematic depiction of the sequential transcription factor profile as cortical progenitors migrate during prenatal development(image based on Hevner et al., 2006)

2.1.3 GLP regulation in neural development

There are several system level analyses of *Ehmt1* haploinsufficiency in mice and drosophila which show differences in behaviour. However, only two transcriptional profiles of *Ehmt1* mutants have been reported (Schaefer et al., 2009; Kramer et al., 2011). Both reports were in adult tissue. Outside of these investigations, not much is known about GLP function during brain development and neuronal differentiation. While there is evidence of significant transcriptional dysregulation in the profiles of *Ehmt1* haploinsufficiency models reported by Schaefer et al., (2009) and Kramer et

al., (2011); this line of evidence only reflects the continual regulation of GLP in the adult brain, or the time at which tissue was taken. Unfortunately, very little information can be gathered about the consequences of having significantly reduced expression of GLP throughout development from such data. In other words, gene expression levels in the adult brain may provide information about ongoing activity; but they may not necessarily even reflect gross histological changes in structure, changes in the number of specific cell types and cell morphology or differences in the number of neurotransmitter receptors. Regardless of such limitations, these data are a starting point and do exemplify the importance of GLP expression for continual transcriptional regulation in the brain.

In addition to the transcription data, the important interaction between the *RE*1-*s*ilencing *t*ranscription factor repressor complex (REST) and G9a/GLP-specific repression in the brain is reviewed. The functional overlap between these two repressor complexes is informative. Research that looks at REST-specific disruption allows for some speculation about how the disruption of GLP may also effect brain development. In addition, the introduction helps inform experiments that consider REST-complex gene expression and REST-regulate target gene expression in the *Ehmt1*$^{+/-}$ neural progenitor cells.

2.1.3.1 GLP-related transcriptional dysregulation

Changes in the transcriptional profile of G9a or GLP $^{+/-}$ mouse and fly brains are significant. However, both models present fairly different profiles. In the mouse model, of the 56 genes mis-regulated across different brain areas, 18 were non-neuronal genes (Schaefer et al., 2009). In flies, the GLP ortholog targets over 350 genomic loci on neuronal genes (Kramer et al., 2011). While a considerable difference might be expected between fruit fly and the mouse transcriptional profiles; one additional explanation for the discrepancy is the difference in the developmental stage at which the histone methylatransferase is ablated. The fly model lacked a copy of Ehmt throughout development, while in the conditional mouse model *Ehmt1* knockout was postnatal. The mouse model therefore did not capture disruptions that may have occurred during prenatal development.

Despite the disparity in findings, 20 genes between these two publications overlap, suggesting a reasonably high level of conservation in GLP-specific H3K9me2 targets (Kramer et al., 2011). Of particular interest, Neuroligin 1, a gene that encodes a post-synaptic adhesion protein essential to the maintenance of postsynaptic membrane and for the presynaptic connection with B-Neurexins, was dysregulated in both animals. Dach2, another gene highly expressed in the developing forebrain, was also identified. Meanwhile, *Nf1*, *Fmr1*, *Fmr2*, *Cntnap2*, *Gdi, Dlg3* orthologs were among those found to be altered in the fly, and are also known to be associated with syndromic and non-syndromic intellectual disabilities (Kramer, 2013).

2.1.3.2 REST-repression and G9a/GLP recruitment

With the exception of the reports above, where GLP-deficiency led to changes in transcription profiles, very little research has focused on the function of the G9a/GLP heteromeric complex during neuronal differentiation. Research on the transcription repressor neuron restrictive silencing factor (NRSF), also known as the RE1-silencing transcription factor (REST), is one area that may provide hints of its role in neurodevelopment. REST-regulated repression targets mostly neuronal genes, some of which contain the 23-bp RE1 elements, some of which do not (Abrahabo et al., 2009). REST-repression targets include a long list of neurotransmitter and neurotrophic receptor genes, ion channel and transporter genes, as well as those, which encode vesicular trafficking and fusion proteins and are important to axonal guidance (Bruce et al., 2004). Initially, work in REST focused on its function in repressing neuronal genes outside of the CNS. More recently REST is found to be extremely important in brain development as well, by acting as a repressor that directly regulates the orderly expression of genes during neuronal differentiation (Ballas et al., 2005). REST repression involves modular scaffolding for recruitment of specific epigenetic regulators (Abrahabo et al., 2009). Importantly, a primary mechanism of REST repression is its recruitment of the G9a/GLP complex onto its C-terminus: the recruitment of G9a creates a highly localized domain of H3K9me2, which acts to silence REST-target genes (Roopra et al., 2004).

The repressive activity of REST is essential for radial migration and the timing of neural progenitor differentiation during neocortical development (Mandel et al., 2011). The finely coordinated spatio-temporal development of this region is highly dependent on differential levels of REST expression. The sustained presence of REST blocks radial migration and greatly delays differentiation. Thus, the targeted down-regulation of REST and its subsequent disappearance is critical for the transition of NPC into neurons (2011).

Meanwhile, the deletion of *Rest* results in the loss of coordination between pluripotency and neural induction. Soldati et al. (2012) found in $Rest^{-/-}$ cells had a delayed repression of pluripotent transcription factor genes—*Sox2*, *Nanog* and *Oct4*—coupled with the simultaneous and precocious activation of both neural progenitor genes and genes expressed in mature neuronal and glial cells. Furthermore, while REST was not found to be essential for the development of the radial glial progenitors, it was found to be essential for the subsequent maintenance and differentiation of these cells (Soldati et al. 2012).

REST regulation and repression has a highly specific role in neuronal cell fate specification as well (Greenway et al., 2007; Abrahabo et al., 2009; Rodenas-Ruano et al., 2012). In one study the differences in REST-specific targets were compared between cholinergic, GABAergic, glutamatergic and medium spiny projection neurons (Abrahabo et al., 2009). An overlapping profile of gene targets across these cell types was found; however, a disproportionate number of REST-target genes were cells specific. Profoundly, the single gene that was found to be a REST-specific target across all four cell types was *Ehmt1*.

To summarize, REST may act as a regulatory hub that coordinates the repression of pluripotent transcription factors and induction of neural differentiation. In addition it appears to be involved in the coordination of cell-specific gene expression as well as the switch in receptor subtypes of mature neurons in the postnatal neocortex. One mechanism for REST-directed repression is its recruitment of G9a. GLP-specific REST recruitment has not been directly investigated. However, as reviewed in

Chapter 1, a majority of G9a-related activity corresponds with GLP-related activity, and these two enzymes are most stable in a heteromeric complex (Tachibana et al., 2005).

Further evidence of the complicated REST-G9a/GLP interaction is found with data suggesting the REST complex is involved in the repression of *Ehmt1* in the four neuronal cell types examined (Abrahabo et al., 2009). In fact, *Ehmt1* was the only target that overlapped in all cell-types examined. While the REST-specific mechanism of *Ehmt1* repression is unknown, GLP could potentially be involved in its own negative feedback loop. Meanwhile, REST appears to control the expression of an enzyme important for its own mechanism of repression, which may suggestion a tightly regulated second feedback loop.

2.1.4 Chapter aims

The general goal of this chapter is to investigate the basic cell biology of an *Ehmt1* haploinsufficieny during pyramidal differentiation. The first aim is to identify whether there are differences between *Ehmt1*$^{+/-}$ mutant mESCs and *Ehmt1*$^{+/Flped}$ control mESCs in pluripotency markers and proliferation rate. The second aim is to differentiate mESCs down a pyramidal lineage and demonstrate positive expression of classic radial glial marker, Pax6 and intermediate progenitor marker, Tbr2 in these cells. The goal is then to identify whether differences in the NPC cell populations exist by looking at a range of progenitor markers and the proliferation rates of the NPCs. In addition, the transcriptional profiles of the NPCs is examined at two distinct stages of differentiation—genes important for NPC developmental and lineage specificity, the REST complex and REST target genes and developmental signalling pathways are examined. Examination of the transcription profile provides evidence about the rate of differentiation in the cells. The final aim is to characterise any differences that arise from *Ehmt1* haploinsufficiency throughout development, in the end state pyramidal cell, in the cell type and morphology.

2.2 Methods

2.2.1 'Knockout first': Ehmt1+/- cell line

All mESCs were purchased from EUCOMM and the European Mouse Mutant Cell Repository center (EuMMCR). Both mutant and wild type cells were of JM8A3.N1 cell type. There were 2 clonal populations of the *Ehmt1* mutant cells, which had a single copy of the *Ehmt1*$^{tm1a(EUcOMM)Hmgu}$ allele, which is a 'knockout first' conditional allele (Skarnes et al., 2011). The allele has a lacZ trapping cassette and floxed promoter-driven neo cassette inserted at the intron of the gene—disrupting gene activity. After transfection with a pCAGGS-Flp recombinase E vector, Flp recombinase results in the deletion of the frt-flanked sites surrounding the LacZ trapping cassette and promoter-driven neo cassette, which restores gene activity. Thus this cell line provides a hemizygous *Ehmt1* knockout and an isomorphic control lines upon transfection with the flp cassette.

2.2.2 Generation of isogenic control: mESC flp transfection

The pCAGGS-Flp recombinase E vector was a gift from the Trevor Dale lab, at Cardiff University. For transfection, 4800 cells/cm^2 were plated on 12-well plate in 1ml medium and grown overnight. 4hrs before transfection cells were washed with DMEM and antibiotic-free medium was added to the cells. 3µg of plasmid DNA was added to 400ul of OPTIMEM (Gibco). 10ul of Lipofectamin (Gibco) was added to 400ul of OPTIMEM. The two mixtures were then incubated for 5mins separately and then added together and incubated for a further 20mins. 65ul of the solution was then added to 10/12 wells. Cells were incubated with the DNA/Lipofectamin mixture for 4hrs. After incubation the mixture was replaced with an antibiotic-free medium. The next day cells were dissociated until a single cell suspension was observed and then seeded at a low density on a 10cm dish. Cells were grown on a 10cm dish with 1µl/ml of puromycin for two days. After two days individual mESCs colonies were handpicked under the microscope and expanded in a flat-bottom 96-well plate. Once confluent cells were passaged onto 24-well plates. Finally 12 wells from a 24-well plate were split a second time, half of the cells in each well were extracted for PCR verification (see Apendex Chart 3 for PCR conditions) and half

were expanded further. 7 cell lines were successful transfected, 3 of which were used for used for the experiments reported here.

2.2.3 mESC culture

ES cells were maintained on gelatin-coated plates in Knockout DMEM (Gibco); supplemented with ESC certified FBS (Invitrogen; cat # 16141079), 2mM L-Glutamin (Gibco), 50uM 2-mercaptoethanol (Sigma), and ESGRO leukemia inhibitory factor (LIF) (Chemicon, ESG1107). Cells were grown at 37°C in a humidified 5% $C0^2$ incubator. The mESC medium was changed daily and cells were split every other day. Cells were always split at a 1:4 to 1:5 ratio and were tossed if >90% confluence was reached. Cells were split by first washing in pre-warmed PBS (Gibco) and disassociated by introducing TrypLE (Gibco) to cells for 3mins. The enzyme was stopped with pre-warmed media. Cells were then pelleted by spinning for 3m at 200g in a centrifuge, re-suspended in fresh media and plated at a 1:4 dilution.

Cell morphology was continually analysed and cells were discarded if the morphological characteristics of stem cell colonies was not maintain or if routine AP staining was negative (see Figure 2.5 for mESC colony morphology). In addition cells were regularly tested for mycoplasma using the MycoAlert mycoplasma detection kit (Lonza). Kit protocol was followed when carrying out routine lab tests. All analysis on the mESCs was carried out on cells at passage number 12 or less.

2.2.4 Cortical pyramidal neuronal differentiation

The differentiation of pyramidal neurons from mouse embryonic stem cells involved five stages (see Figure 2.4). The protocol has been explained in detail previously, for medium conditions see (Bibel et al., 2004; 2007). Briefly, ES cells were expanded on a population of mouse embryonic fibroblast cells (MEFs) for two or three passages; they were then expanded without MEFs, on gelatin-coated plates for three to four passages. Afterward cells at a $3X10^6$ density were then plated without gelatin and on non-adhesive bacteriological plates in media lacking LIF (Chemicon, ESG1107) and the small molecules, GSK-3 (Stemgent, CHIR99021) and MEK1/2 (Stemgent,

PD0325901) inhibitors for 4 days. Cells in this condition form Cellular aggregates (CAs).

After 2 days medium was replaced by allowing aggregates to settle to the bottom of a 25ml flask. Retinoic acid (Sigma) at a 5uM concentration was added after 4 days grown as CAs. 8 day-old CAs were then dissociated with .05% trypsin (Sigma). The trypsin reaction was stopped using the .05% trypsin inhibitor (Sigma). Cells were spun down at 200g for 3mins. Medium was removed and replaced with N2 medium and filtered using a 40um nylon cell strainer (BD Falcon). Cells were then counted and medium was added in order to establish a seeding density of $1.5X10^5$ per cm^2. Cells were then plated on substrates coated with laminin (Roche) (coated at 5mg/ml, at 37° overnight and washed 3 x with TC safe H_2O) and Poly-D-ornithine (Sigma) (coated at .5mg/ml at 37° for >2hrs) at a density of $1.5X10^5$ per cm^2. Medium changes took place 2hrs after initial plating and 24hrs later. After 48hrs Complete medium was added (See Bibel et al., 2007). From this stage onward only half the medium was ever replaced.

2.2.5 Growth Curve

Cells were plated at a 1:5 density on 24-well plates. Cells were counted every 6-10 hours and 8-time points were taken. Three 24-wells were counted fore each time point and all cell line. Cells were first washed with 100ul of PBS. Cells were then incubated with 50ul of trypsin (Sigma) for 2mins; trypsin reaction was stopped with 200ul of medium. Cells were pipetted until a single cell suspension was established. After dissociation, 10ul of cell solution was combined with 10ul of trypan blue (Bio-Rad), a vitality stain used to detect dead cells. Immediately 10ul of the cell solution was added to each side of a hemocytometer and three measurements per side were averaged for each well. Medium was replaced on the remaining wells every 24hrs.

2.2.6 Flow Cytometry

Nonspecific IgG controls were used for compensation and to set sort gates (See Appendix Figures 2.1A & B). To discriminate cells from debris the side scatter (SSC-A, log) and forward scatter (FCC-A, log) were plotted. Higher SSC-A signals indicate

granularity and were likely unviable cells at fixation or cellular debris. Thus we defined the population by lower SSC-A signals (see Appendix Figure 2.1A for example of cell population gating). To gate for florescent cells, we plotted the signal from the 660-nm laser (APC-A, log) for the EdU experiment and the 488-nm laser (FITC-A, log) for the Pax6 experiment against the SSC-A signal (see Appendix Figure 2.1B or example of the control gating for florescent staining and 2.2A&B for control and mutant NPC).

2.2.6.1 EdU Click-it G1 proliferation assay in mESCs

For the EdU staining, the Click-iT EdU Flow Cytometry Assay kit was used (Invitrogen, C10418) on cells at a density of 10^6 cells/ml. The provided protocol was followed with one exception. Prior to EdU introduction, cells were not removed from the surface or suspended, as to avoid the effects of temperature changes or any disruption that may slow the growth rate of the cells. Briefly cells were incubated with 12uM of EdU for 1h, washed and fixed. Prior to adding the Click-it labelling, a saponin-based permeabilization reagent was used to wash the cells and then cells were incubated with the Click-it reaction cocktail according to the number of samples and quantity of cells. Cells were spun down and washed before FACs sorting was carried out.

2.2.6.2 EdU Click-it G1 proliferation assay in NPCs

EdU incorporation was determined using the Click-iT EdU Flow Cytometry Assay kit (Invitrogen, C10418). Prior to incubation with EdU total cell numbers were calculated by removing 1:10 of the volume of media with CAs. The 8day CAs were dissociated and counted. The number of cells in the remaining volume was estimated. A volume of 10^6 cells/ml was used in three technical repeats and across three independent biological tests. The proliferation rate of the NPCs was determined by counting the number of cells that incorporated EdU, using the flow cytometer.

The EdU Click-it G1 protocol provided was followed with a few exceptions. CAs were incubated with 15uM of EdU for 1.5hrs. Afterwards CAs were washed with PBS 2Xs.

Cells were then trypsinized using .05% (Sigma) for 5mins at 37°. The reaction was stopped using .05%of trypsin inhibitor (Sigma), and the cells pipetted several times up and down in order to establish a single cell suspension. Cells were then spun at 300g for 5mins and suspended in PBS before filtering using 40um nylon cell strainer (BD Falcon). At this stage cells were fixed using the provided fixative and the manufacturer protocol was followed.

2.2.6.3 Pax6 populations in NPCs

In order to determine the rate of radial glial cells in the 8d day CAs an additional fluorescent associated cell sorting (FACs) experiment was also run on cells labeled with anti-Pax6. For this experiment cells were first dissociate and fixed as described in the EdU experiment (using same fixative). After fixation, cells were washed twice with cold PBS. Cells were permeabilized by incubating for 10min in PBS containing .25% Triton X-100 (or PBST). The cells were then blocked for 30 mins with 1% BSA in PBST and .3M glycine. Afterwards, they spun and resuspended in the primary antibody diluted in 1% BSA, 10% anti-goat in PBST. Cells were incubated in a humidified chamber overnight at 4°C. After primary antibody incubation, cells were spun and washed in PBS 1X then incubated in the secondary antibody diluted in 1% BSA in PBS for 1h at room temperature in the dark. Finally before FACs experiment was begin, cells were washed 2X in PBS and filtered using a cell strainer in order to remove any clumps from repeat spinning and washing.

2.2.7 qPCR

RNA was extracted using the RNeasy micro kit (Quiagen) following the product protocol. Afterwards RNA was converted into cDNA using the ImProm-II Reverse Transcription System (Promega). Three controls for the reverse transcription (RT) were used: a positive control to test the RT reaction, a no template control to reveal any contamination, and a negative no-reverse transcriptase control to confirm the absence of DNA template contamination. RT-PCR was performed with RT^2 SYBR PCR Master Mix (Qiagen). Standard melt curves were generated for each primer pair to confirm single amplicons. Average expression of B-actin and Gapdh were used as endogenous controls in the experiment. The ΔΔ CT values were calculated by first

normalising the data, or subtracting the average endogenous control Ct values from the *Ehmt1*$^{+/-}$ mutant 'sample' Ct values and the *Ehmt1*$^{+/Flped}$ 'reference' Ct values. The ΔΔCt value is then extracted: ΔΔCt = ΔCt 'sample' – ΔCt 'reference'. This calculation generates values, which represent the relative fold-change in gene expression. Primers for *Wnt2, Bpil* and *Grm8* were used (see Appendix Chart 2.4 for primers).

For the NPC q-RT-PCR array, a 96 well RT^2 Custom Profiler PCR Array (CAPM12608, Qiagen) for mice was used. The arrays were run on NPCs from day 6 and day 8 of the differentiation protocol. There were three biological replicates for the two *Ehmt1*$^{+/-}$ clonal populations and one replicate for 3 separate *Ehmt1*$^{+/Flped}$ clones (see Chart 6.1) for the 2 *Ehmt1*$^{+/-}$ clonal populations were Due to time and space constraints the results of all 88 RT-PCR tests are not reported. The custom genes list was generated based on GLP targets identified in the literature, tissue-specific relevance and the hypothesis outlined in the results section. For the array 1µg of total RNA was used and manufacture's instructions were followed, for RNA extraction—RNeasy Mini Kit (Qiagen) for cDNA synthesis—RT^2 First Strand Kit (Qiagen) and for the RT-PCR reaction—RT^2 SYBR Green ROX qPCR Matermix (Qiagen) . The average Ct values across the three housekeeping genes *B2m, Hprt* and *Mapk7* were used as endogenous controls.

Chart 2.1 RT-PCR experimental design in NPC samples.

Sample	Day 6	Day 8
E01 (3) (*Ehmt1*$^{+/-}$ clone)	3 Bio-Reps	3 Bio-Reps
E02 (3) (*Ehmt1*$^{+/-}$ clone)	3 Bio-Reps	3 Bio-Reps
FLP1, FLP2, FLP3	3 Samples	3 Samples
Total:	9	9

2.2.8 Western blot analysis

For western blot analysis NuPage 4-12% Bis-tris gels (Invitrogen) were ran with a MES running buffer. Electrophoresis was run at 150V for 40mins or until the gel marker reached the bottom of the gel. Gels were then transferred using the Easy Blot Gel Transfer System (Invitrogen). The membrane blot was washed 3 times for 5mins each in TBS with 0.025% Triton X-100 (Sigma-Adrich) (or TBST) and blocked overnight a 4°C using 5% milk powder in TBST. The next day the blot was washed 3 times for 5mins each in TBST and blocked with the primary antibody diluted in 5% milk powder and PBST for 2+ hours at room temperature or overnight at 4°C. After the primary antibody blots were washed 3 times for 5mins each in PBST and incubated for 1h in the secondary antibody diluted by PBST only. Next blots were washed 3 times for 5mins each in PBST and incubated for 5mins in 5-10ml equal parts lumino enhancer and peroxide solution of the Supersignal West Pico system (Thermo Scientifica). Finally blots were imaged using the GeneGnome (Syngene Bio Imagining).

2.2.9 Immunohistochemistry

2.2.9.1 Immunocytochemistry in mESCs

Cells were grown on gelatin coated glass cover slips prior to conducting immunocytochemistry. Cells were first washed once with PBS and fixed with 4% PFA for 10mins. After fixation, cells were washed twice with cold PBS. Cells were permeabilized by incubating for 10min in PBS containing .25% Triton X-100 (or PBST). The cells were then blocked for 30mins with 1% BSA in PBST and .3M glycine. Afterwards, they were incubated with the primary antibody diluted in 1% BSA in PBST, in a humidified chamber overnight at 4°C. After primary antibody incubation cells were washed in PBS 3X for 5mins each and then incubated in the secondary antibody diluted in 1% BSA in PBS for 1h at room temperature in the dark. The following commercial antibodies were used at manufacturer suggested concentrations: for primaries anti-SSEA-1, anti-Oct4 anti-Nanog (for all primary antibodies see Appendix Chart 2.2); for secondaries DyLight 488 goat anti-rabbit polyclonal; Alexa Fluor 568 goat anti-rabbit polyclonal; Cy 3 goat anti-mouse polyclonal (for all secondary antibodies see Appendix Chart 2.3). Dapi stain was used as a nuclear stain. For AP staining, the Akaline Phosphatase staining kit (Stemgent) was used; manufacturers protocol was followed.

2.2.9.2 Immonhistochemistry in E14.5 brain

For Pax6 and Tbr2 expression, sagattal sections of embryonic day 14.5 were used to assess endogenous antigen expression patterns (Figures 2.2 & 2.3). The staining patterns in developing cortex at 10x and 20x were verified using Allen's Brian atlas for the developing mouse brain.

For staining, E14.5 timed mating litters of wild type pups were used. Whole brains were extracted from pups and incubated in 4% PFA overnight at 4°. Brains were washed 3X in PBS and then wax embedded (by the histology lab at Cardiff University) and sectioned into 4um sections before mounting on slides. Sections were then de-paraffined after incubating in 100% xylene 2X for 3mins each and then taking sections through 100%, 95%, 70% and 50% EtOH gradient each for 3mins. Sections were then washed 3X for 5mins in TBS, 5% BSA, 10% anti-goat and

.05% Triton before blocking in primary antibodies overnight at 4° using manufacturer guidelines for antibody concentrations. Afterwards sections were washed 3X for 3mins TBS and incubated in the appropriate species of a fluorophore-conjugated secondary antibody (for all antibodies for primary see Appendix Chart 2.2; secondary see Appendix Chart 2.3).

2.2.9.3 Immocytochemistry in CAs

The CAs proved to be difficult for imagining experiments. Therefore multiple methods were attempted for antigenic labeling and imaging. First cells were washed once with PBS and fixed with 4% PFA, in the dark, at RT, for 10mins. After fixation, cells were washed twice with cold PBS and then permeabilized by incubating for 10min in PBS containing .025% Triton X-100 (or PBST). All staining then took place in suspended CAs. After staining (using the same staining methods as that for the adherent mESCs and neurons), CAs were then imaged in a PBS, 5% BSA suspension. Both confocal microscopy and classic fluorescent microscopy methods were tested for image quality (only images from inverted fluorescent microscope are reported).

A second method involved fixing CAs in 4% PFA, wax embedding and sectioning the CAs in 4um sections, before mounting on slides. The same histology protocol as that used on E14.5 above was then used. A combination of experiments using both the suspension staining and section staining methods is reported, depending on the quality of the images for each antigen. The following commercial antibodies were used at manufacturer suggested concentrations: for primaries anti-Pax6, anti-Tbr2 anti-Ngn2, anti-Nrg1, anti-RC2 (for all primary antibodies see Appendix Chart 2.2); for secondaries Alexa Four 488 both monoclonal and polyclonal, and Alexa Fluor 568 (for all secondary antibodies see Appendix Chart 2.3). Dapi stain was used as a nuclear stain.

2.2.9.4 Immocytochemistry in Neurons

Neurons were grown in 6cm plastic dishes, after fixation and staining the plastic walls of the dishes were removed and glass cover slides were fixed to the cell surface to enable better optical quality. This method eliminated complications that

arose with generating a consistent substrate on glass coverslips for which the neurons would consistently adhere. Prior to staining, cells were first washed once with PBS and fixed with 4% PFA, in the dark, at RT, for 10mins. After fixation, cells were washed twice with cold PBS. Cells were permeabilized by incubating for 10min in PBS containing .025% Triton X-100 (or PBST). The cells were then blocked for 30mins with 1% BSA in PBST and .3M glycine. Afterwards, they were incubated with the primary antibody diluted in 1% BSA, 10% goat serum in PBST in a humidified chamber overnight at 4°C. After primary antibody incubation cells were washed in PBS 3X for 5mins each and then incubated in the secondary antibody diluted in 1% BSA in PBS for 1h at room temperature in the dark. The following commercial antibodies were used at manufacturer suggested concentrations: for primaries anti-Vgat, anti-Vglut1, anti-Vglut2; anti-MAP2, and anti-βTubulin; for secondaries: Northern Lights557; Northern Lights 637; Alexa Fluor 488; Alexa Fluor 568 (for product details see Appendix Chart 2.2 & 2.3). Dapi stain was used as a nuclear stain.

2.2.9.5 Florescent Microscopy

Cell images were captured on an Olympus IX-71 inverted wide field fluorescent microscope with an Exfo X-cite 120 light source using the SimplePCI (Hamamatsu) software package. Blue, green and red fluorescence was detected using the Chroma excitation filters ET402/15x, ET490/20 and ET 572/35x, respectively. Fluorescence emission was separated by a multiband dichroic emission filter set #69002 (Chroma) and captured using an Orca ER CCD camera from Hamamatsu. GFPR8 emission was separated using a single GFP T495LP dichroic and an ET525/50m emission filter. Cells were imaged at 10X and 20X magnification.

2.2.10 Statistical Analysis

For data with small samples sizes and a non-normal distribution, non-parametric statistics were run: the Mann-Whitney U test (a rank-sum test similar to the parametric t-test) was used to examine the differences between protein expression from western blot analysis; the Kruskal-Wallis test (a non-parametric equivalent to the one-way analysis of variance) was run to test differences in the FACs count for

the two EdU proliferation experiments. For all RT-PCR statistical tests the ΔCt values for samples (mutants) and references (controls) were compared. In the mESC RT-PCR, Repeated Measures Analysis of variance (RM-ANOVA) were run to compare inhibitor concentration and genotype, for each of the three genes. In the NPC R-PCR array, RM-ANOVAs were run to compare differentiation day (whether day 6 or day 8) and genotype. To maintain familywise error rates in the RT-PCR arrays Bonferroni corrections were used. In other words, the alpha value .05 was adjusted for the number of tests ran in a geneset. Finally all error bars reported represent the standard error of the mean (SEM).

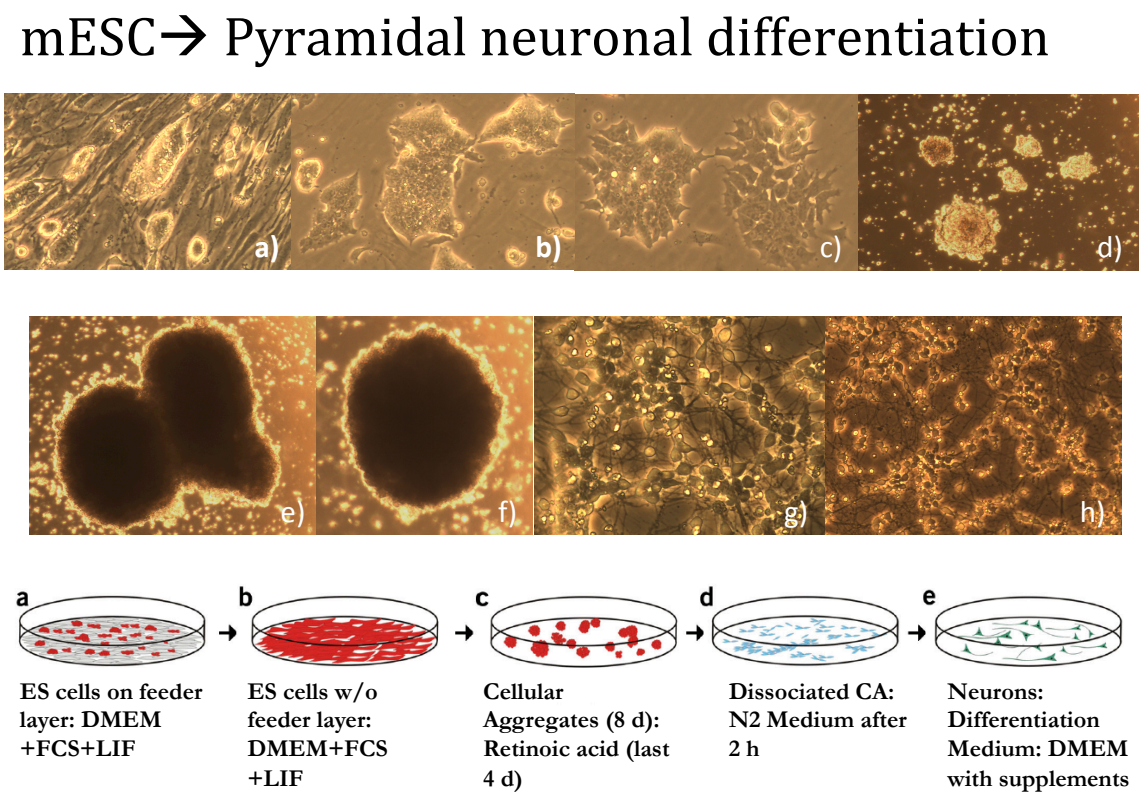

Figure 2.4 In vitro pyramidal differentiation.
Top images. **a.** mESC first grown on feeder cells; **b.** & **c.** passaged on gelatin; **c.** mESC grown in suspension & forming cellular aggregates; **e.** & **f.** RA-induction after 4 days grown as cellular aggregates; **g**. Dissociated and plated onto N2 medium; e. N2 medium replaced with complete medium. Bottom images. Schematic depiction of the differentiation work-flow (Borrowed from Bebel et al., 2004).

2.3 mESC Results

2.3.1 mESC characterization

Two independent clonal populations of *Ehmt1*$^{+/-}$ mESC (clones E01 and E02) were compared to controls for the characterization of mESC-like properties. Cells were stained for akaline phosphatase (AP), as undifferentiated pluripotent cells have elevated levels of AP on the cell membrane, which allows for easy detection. No differences were detected in the level of AP staining (Figures 2.5b & g). A panel of

ESC-specific markers, including transcription factors Oct4 (also known as Pou5f1) (Figures 5c & h), Nanog (Figures 2.5d & i), and the cytoskeletal protein Stage-Specific Embryonic Antigen-1 (SSEA-1) (Figures 2.5e & j) were compared. There was no observable difference in the antigenic expression of these markers.

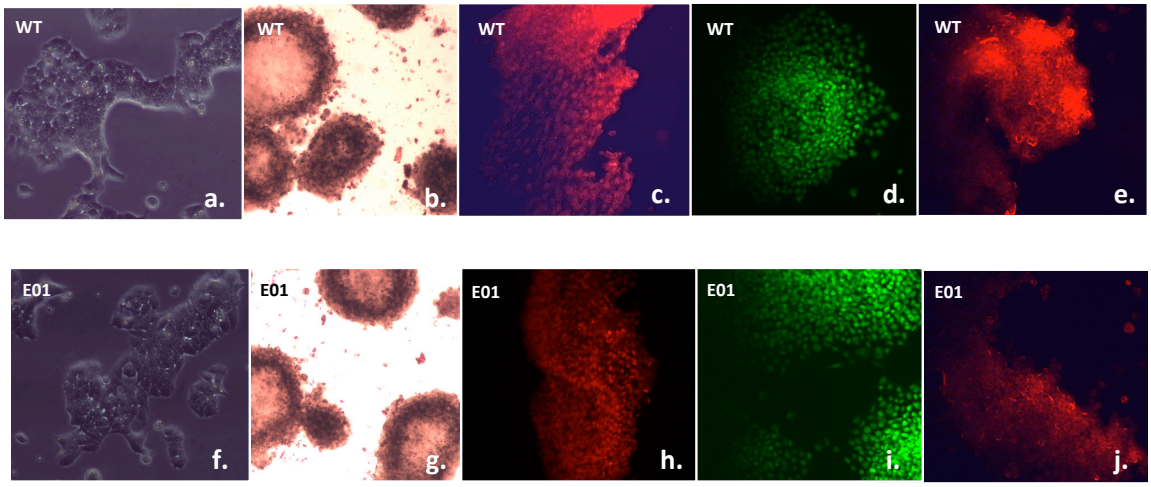

Figure 2.5 mESC characterization
a. & f. Phase contrast images of WT and Ehmt1$^{+/-}$ mESC colonies; **b. & g.** AP staining; **c. & h.** Oct4; **d. & i.** Nanog; **e. & j.** SSEA-1.

2.3.2 mESC protein analysis

GLP protein expression was analysed in *Ehmt1*$^{+/-}$ and control mESCs using Western blot analysis (Figure 2.6). *Ehmt1*$^{+/-}$ mutant mESCs expressed between 50-60% of the control GLP protein expression levels, this value was significantly less than controls, $\boldsymbol{t = -8.546, p < .001}$. In order to quantify H3K9m2 the highly selective GLP/G9a inhibitor UNCO638 (Vedadi et al., 2011) was titrated into both *Ehmt1*$^{+/-}$ and control cells (Figure 2.8). The inhibitor allows the comparison of both chronic and acute down regulation in the GLP expression and subsequent H3K9me2 changes. Three concentrations of UNCO638 were determined based on the half maximal inhibition (IC50) after 24hrs of 250nM (Vivadi et al., 2011), the 125nM and 500nM

concentrations were also used. The *Ehmt1*$^{+/-}$ mESC showed significantly less H3K9me2 than the control cells ***p* =.029** (*Mann-Whitney U test*). The relative expression of H3K9me2 was found to be the same as the control cells exposed to the IC50 value of 250uM concentration of UNC0638. This experiment establishes that there is a dose dependent, linear response between GLP/G9a expression and the levels of H3K9me2 in mESCs.

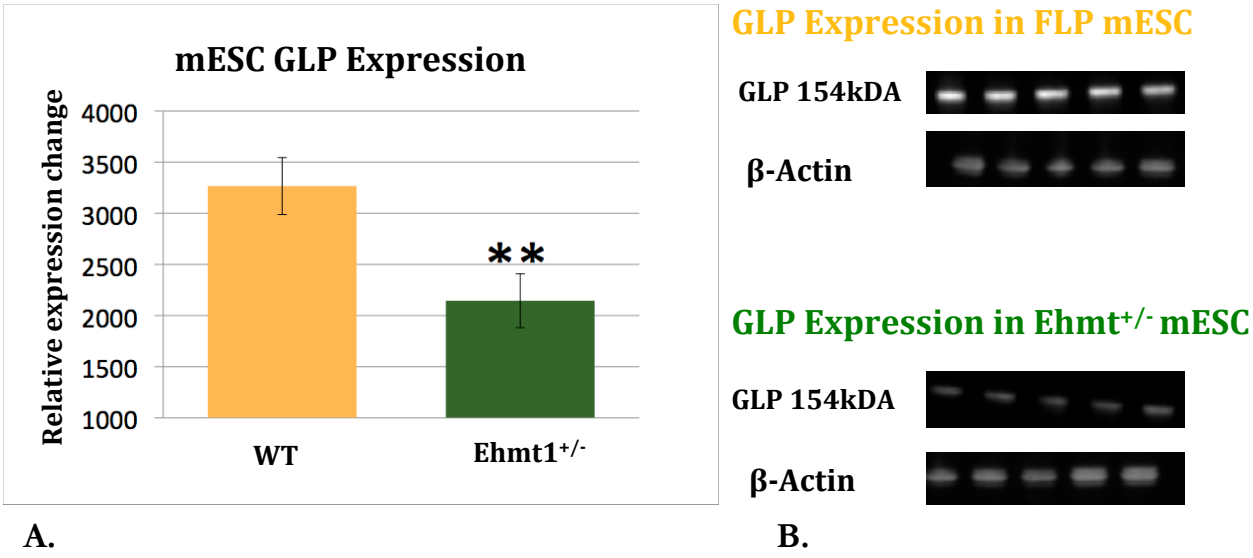

Figure 2.6 GLP expression in mESC
A. GLP quantification of Western Blot analysis. *Ehmt1+/-* mESCs is reduced to 50-60% of WT. **B.** Western blot of 5 independent lysed samples.

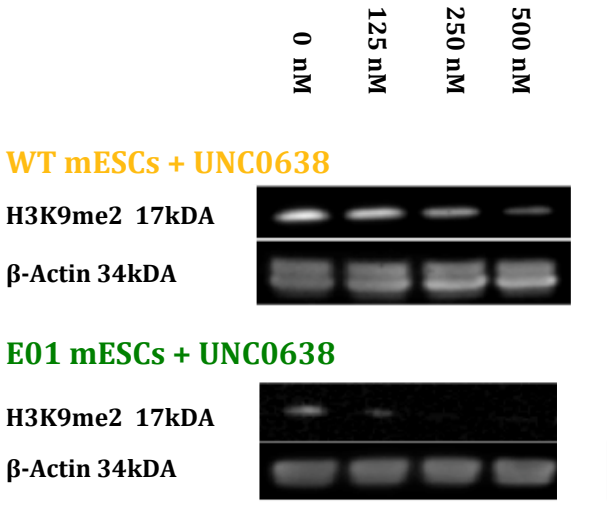

Figure 2.7 H3K9me2 expression in mESC
Western blot analysis of WT and Ehmt1+/- mESCs expression of H3K9me2. Three concentrations of UNCO638 were titrated in to the cells 24h before extraction to determine G9a/GLP mediated change to H3K9me2. Mutant cells demonstrate ~50% or the IC50 equivalent of 250nM in WT cells.

2.3.3 mESC growth and proliferation

Growth curves were calculated for the two *Ehmt1*$^{+/-}$ clonal populations, two control lines were used, two *Ehmt1*$^{+/Flped}$ lines and a wild type line (Figure 2.8). There appeared to be differences in the cell-doubling rate across the lines. Both *Ehmt1*$^{+/-}$ mESCs had doubling rates faster than the controls. *Ehmt1*$^{+/-}$ clone E01 doubled after 19.25h and clone E02 doubled after 18h; the control cells only doubled after 25.7h. However the overall pattern in growth remained fairly consistent, E01 increased from a 5.2% growth rate per hour to 7.84% after initial doubling, while E02 growth rate increased from 5.6% to 6.45% and controls increased from 3.9% to 5.6% per hour—suggesting there may be differences in the shift from the lag growth phase to log occurring. In order to substantiate these findings, an EdU proliferation assay was run.

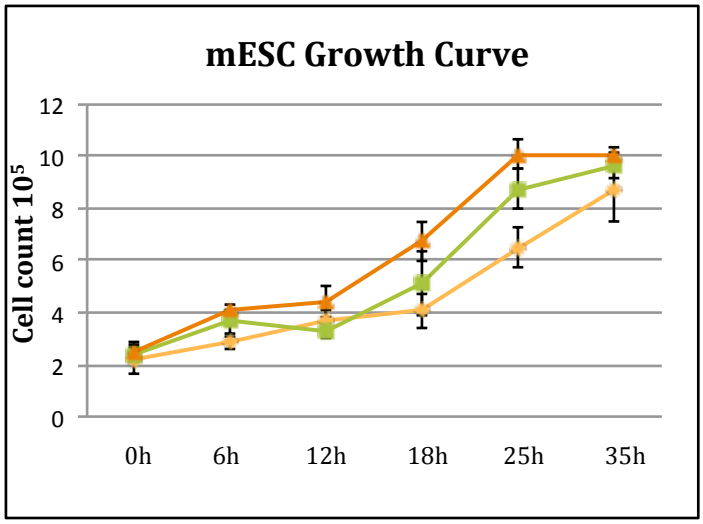

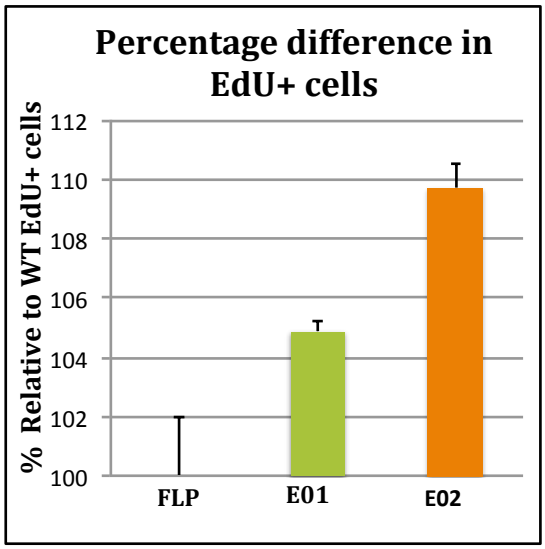

2.8 mESC Proliferation

EdU labelled cells were counted using flow cytometry. Ehmt1$^{-/+}$ cells were found to have significantly more cells in S-phase $H(2) = 7.28$; $P < .05$ (Kruskal-Wallis test)

In addition to a growth curve, the incorporation of 5-ethynyl-2'-deoxyuridine (EdU) in active DNA synthesis was analysed. EdU was detecting using a copper ethynyl moiety of EdU. EdU is a nucleoside analog to thymidine, which is incorporated during S-phase of the cell cycle. EdU detection determines the percentage of cells going through S-phase cells using flow cytometry. *Ehmt1*+/- mESC populations had significantly more cells in S-phase after 1h of EdU incorporation, $\boldsymbol{H(2) = 7.28, p < .05}$ (*Kruskal-Wallis test)* (Figure 2.8). These findings corrobotate the quicker doubling rate found in the *Ehmt1*$^{+/-}$ mESCs.

2.3.4 Gene expression

To validate decreased GLP activity and the reciprocal reductions in H3K9me2, GLP was further inhibited using inhibition of GLP three published G9a-specific genomic targets were used: *Grm8*, *Bpil* and *Wnt2* (Wen et al., 2009). Using real time polymerase chain reaction (RT-PCR). *Wnt2* was found to be significantly up-regulated in the *Ehmt1*$^{+/-}$ mutant cells $\boldsymbol{F(1,29) = 18.792, p = .012}$, which increased fold-change after further GLP inhibition $\boldsymbol{F(1,29) = 9.034, p = .031}$ (Figure 2.9). However, the other markers were not (by genotype, *Bpil* $F(1,29) = 1.321$ p = .361; *Grm8* $F(1,29) = .372$, p = .594).

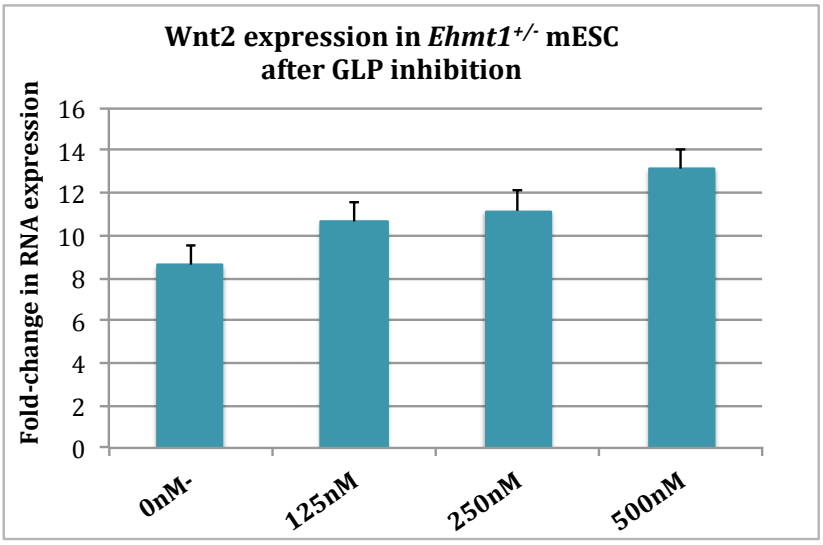

Figure 2.9. Wnt2 expression in Ehmt1+/- mESCs .
Ehmt1+/- mESCs demonstrated an over 8 fold-increase in Wnt2 compared to wild type. There was a linear increase in expression in response to further GLP inhibition using UNCO638.

2.4 NPC Results

2.4.1 Neuronal progenitor populations

Previous work has identified the sequential expression of *Pax6→Ngn2→Neurod1→ Tbr2 →Tbr1* for glutamatergic neurogenesis (for example see Figure 2.3) (Hevner et al., 2006). Thus protein expression of the NPC markers Pax6, Ngn2 and Tbr2 were analysed in the cellular aggregates (CAs) after 4 days of RA-induction (on day 8 of differentiation). The CNS developmental markers Nrg1, and RC2 were also analysed at the same stages.

In addition, CAs were dissociated before fixation and labeled with the a Pax6 antibody and a Florescent Associated Cell sorting experiment was ran in order to gain a more accurate measure of the percentage of cells expressioning a transcription factor in radial glial cells. The EdU proliferation assay was also used to examine differences in S-phase in the NPC populations.

2.4.1.1 Pax6 protein expression

Pax6 protein expression was used to determine the percentage of RGCs in the population 8 days after RA-induction. Endogenous expression in an embryonic 14.5 brain was used as a positive control for antigenic expression (Figure 2.1). Antibody staining matched previously reported patterns of expression in the E14.5 brain. Pax6 protein was expressed in 60-88% of the cells across three separate experiments (e.g. variation appeared to be based on the methods of quantification, as opposed to an overall difference in population levels across the experiments). The lower number of Pax6+ cells came from manually counted positive expression in 3000+ cells, in three independent samples for each experiment (Figure 2.10A; 2.11), while the higher averages are based on the number of cells that were FACs tested. Despite absolute quantification differences between experimental methods, there were no differences in Pax6 protein levels between control and the *Ehmt1*$^{+/-}$ mutant NPC population F (2,29) = .352, p = .708 (Figure 2.10).

2.4.1.2 Tbr2 protein expression

Cells were stained for Tbr2 and manually counted for positive expression in 3000+ cells, in three independent samples for each experiment counted (Figure 2.10B; 2.11). There was an average of 22-26% of Tbr2+ cells in the same populations of Pax+ manually counted cells. No differences were found across the cell lines $F(2,29) = .310$, $p = .737$.

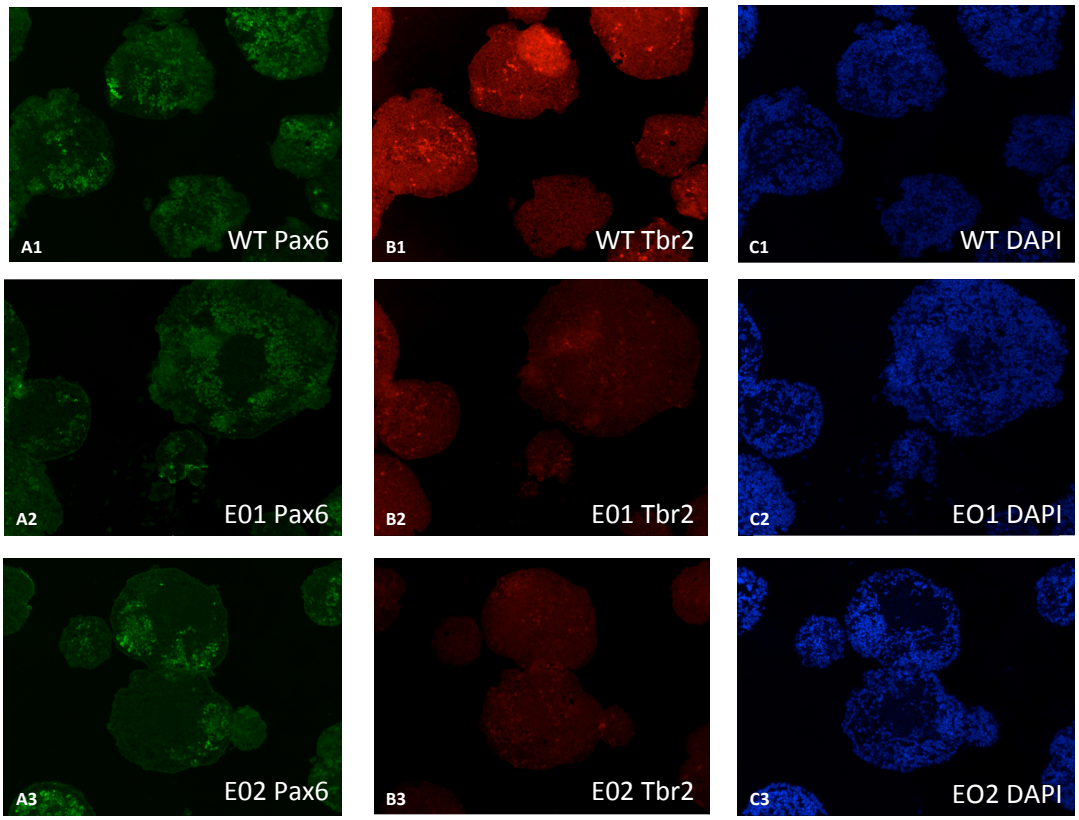

Figure 2.11 Pax6+ & Tbr2+ 4-days post-RA induction.
3000+ cells per antigen were counted using DAPI, those co-labeled with Pax6 or Tbr2 were determined. No differences in the number of cells expressing either marker.

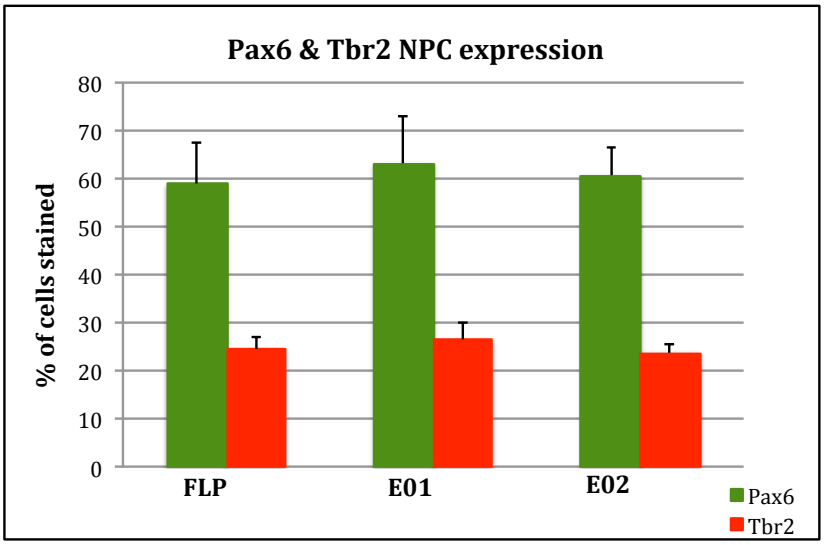

Figure 2.11 Pax6+ & Tbr2+ 4 days post-RA induction quantification .
Cell counts for Pax6+ and Tbr2+ cells. No differences were identified across experiments.

2.4.1.3 Nrg1 protein expression

Neuregulin-1 (*Nrg1*) member of the NRG family is expressed in early migrating neurons of the cortex. This marker is found to be important for the establishment and maintenance of radial glial cells in the cerebral cortex (Hevner et al., 2006). There was little staining in the nucleus of the cell, thus limiting quantification. Although no formal testing was performed on these data (due to difficulty in detecting cell boundaries with antigen labelling), there were no apparent differences in the staining patterns of Nrg1 between *Ehmt1*$^{+/-}$ and control cells (Figure 2.12D).

2.4.1.4 RC2 protein expression

In addition to the sequential expression of the above markers, Radial glial cell marker-2 (*RC2*) was also examined. *RC2* is a label for mouse radial glial cells in the developing CNS; the antigen recognizes a 295-kDA intermediate filament protein that is encoded by the C-terminal of a Nestin domain (Park et al., 2009). *RC2* is an

intermediate filament and expressed outside of the nucleus. RC2 was expressed throughout the CAs. Although no formal testing was performed on these data (due to difficulty in detecting cell boundaries with the antigen labeling), there were no apparent differences in the staining patterns of RC2 between *Ehmt1*$^{+/-}$ and control cells (Figure 2.12E).

2.4.1.5 Ngn2 protein expression

Cells were stained for Ngn2 protein. The staining pattern in both E14.5 brains and in the CAs did not appear strictly in the nucleus of the cell, limiting the quantification of independent cells. However, a majority of the CAs appeared to stain for Ngn2. Although no formal testing was performed on these data (due to difficulty in detecting cell boundaries with the antigen labelling), there were no apparent differences in the staining patterns of Ngn2 between *Ehmt1*$^{+/-}$ and control cells. (Figure 2.12F).

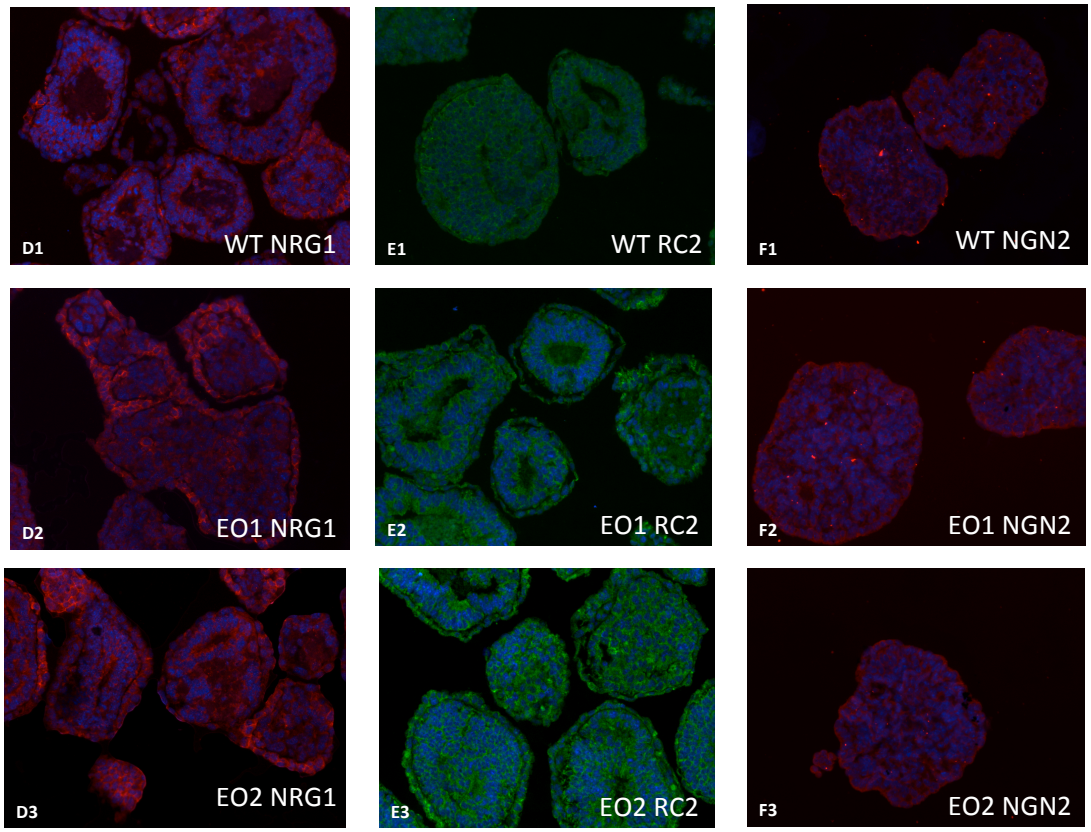

Figure 2.12 Nrg1+ RC2+ & Ngn2+ CA staining 4 days post-RA induction.
No differences were identified in the staining patterns of these three antigens. Although the lack of nuclear localization limited quantification.

2.4.2 NPC proliferation

The percentage of cells with EdU incorporation after 1 hr incubation was determined using flow cytometry. Nonspecific IgG controls were used for compensation and to set sort gates. The histogram for the three cell lines shows a distinct bimodal distribution suggesting two populations of cells were counted, those with EdU incorporation and those without (Appendix Figure 2.2). *Ehmt1*$^{+/-}$ cells had significantly fewer cells in S-phase than control cells after 1h of EdU incubation $\boldsymbol{H(2) = 18.86; p = .003}$ (Figure 2.13).

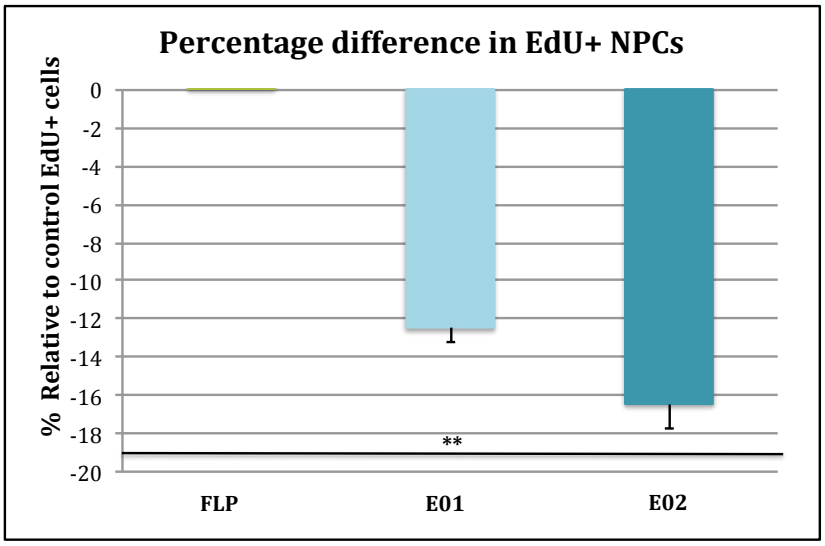

Figure 2.13 EdU-positive NPCs.
Percentage of EdU-positive NPCs across 2 independent FACs experiments, using 1h incubations $H(2) = 18.86$; $P = .003$ (Kruskal- Wallis)

2.4.2.1 Rate of differentiation and NPC gene expression

In order to determine whether there were differences in the rate of differentiation and in fact the mutant cells demonstrate a successful pattern of sequential gene expression for proper RGCs and IPCs development, an RT-PCR experiment was designed to examine 42 genes after the 2nd and 4th days of neural induction or day 6 and 8 of the differentiation protocol, respectively (for a gene list with delta delta Ct values, and test statistics see Appendix Chart 2.5). First, delta Ct values for the 42 genes were compared between *Ehmt1*$^{+/-}$ E01 and E02 clonal populations, across the two days using a repeated measure ANOVA. No differences were found between day 6 or day 8 $F(1, 2) = .662$, $p = .416$; clonal populations $F(5, 430) = .193$, $p = .942$; or as an interaction between the day and clonal population $F(5, 430) = .228$, $p = .923$. Similarly for the three populations of control NPCs, no differences were found between the day $F(1, 2) = 2.610$, $p = .107$; populations $F(2, 264) = .085$, $p = .919$ or

as an interaction between the day and clonal population $F(5, 430) = .049$, $p = .952$ Thus the RT-PCR values from *Ehmt1*$^{+/-}$ NPCs clones were considered the same population and the *Ehmt1*$^{+/fl ded}$ controls were considered the population.

The Bonferroni adjusted alpha value for the number of genes in this array is $p = .001$. At the adjusted value, four genes were found to have significantly higher expression in the *Ehmt1*$^{+/-}$ NPCs: *Fez1, Neurod1, Smarce1,* and *Srr* (Appendix Chart 2.5). The highly conservative *p*-value may however exclude, what may be biologically relevant differences between these populations of progenitor cells. Therefore, in order to evaluate additional trends towards significance, differences in gene expression that reach a *p*-value of <.01 are reported.

Despite there being no detectable difference in the protein expression levels of the sequential expression markers *Pax6*→*Ngn2*→ *Tbr2*→ *Neurod1* →*Tbr1* we found large differences in mRNA levels of these markers. The *Ehmt1*$^{+/-}$ NPCs had significantly higher expression in 3 out of 5 of these genes: *Pax6, Neurod1* and *Tbr1*, with a very large fold-change increase in *Ngn2*, but too much variation in expression across samples and experiments to reach significance. In addition to the main effect of genotype for the *Pax6*, the earliest RGC marker, there was also a trend for decreased expression from day 6 to day 8. *Pax6* went from a 19 fold-difference to a 10.7 fold-difference from day 6 to day 8 compared to control, although this difference did not reach significance. Meanwhile, there was a significant interaction of genotype and time in the later IPC markers *Neurod1* and *Tbr1.* Both had significant increases in expression from day 6 to day 8 (Appendix Chart 2.5).

Ehmt1$^{+/-}$ NPCs had significantly higher expression in mRNA levels of 11 genes, which are found to have peak expression in the prenatal period of the telencephalic development. There were seven genes that had E11.5 peaks (Figure 2.14): of those, 2 were significantly down-regulated from day 6 to day 8 (*Nr2f1 & Bmp4*), 2 had a trend of being down-regulation, though did not reach significance (*Emx2 & Pax6*), and 2 were found to have bimodal peaks, with the second peak in the postnatal period (*Ascl1 & Smarce1*). The final gene, *Dlx2*, was significantly up regulated from

day 6 to day 8 in mutants. However this gene is found to have fairly high expression levels at E18.5 and into postnatal periods in the developing telencephalon. Therefore, while several earlier markers have significantly greater expression in *Ehmt1*$^{+/-}$ NPCs a majority of these were found to be down regulated between days 6 and 8 of differentiation (Figure 2.14).

Ehmt1$^{+/-}$ NPCs had significantly higher expression in 11 genes, which are found to have peak expression in the postnatal period of telencephalic development (Figure 2.14). Eight of these genes also had a significant interaction between genotype and time, 7/8 of the genes were up-regulation between days 6 and 8 (*Ascl1, Nrtk3, Dlg4, Syn1, Nrxn3, Fez1, L1cam*) with a non-significant trend for 2 of the other genes (*Ctnnd2 & Grin2a*). One gene, *Bmp4*, was significantly down regulated from day 6 to day 8. Thus, mutant cells had a significant up-regulation of those genes, which are most highly expressed in postnatal stages of development.

Only three genes had significantly less expression in our mutant population. Such a low number may suggest these cells have greater global gene transcription in general, which might be expected with the de-repression of a global epigenetic regulator. A previously published GLP-specific target for H3K9me2 repression, *Grm8,* was significantly down-regulated, while also demonstrating and an interaction between genotype and time, with a greater reduction from day 6 to day 8. In addition, *Foxg1* and *Gfap* were also significantly less expressed in the mutant NPCs (for overall picture of relative changes see Figure 2.14).

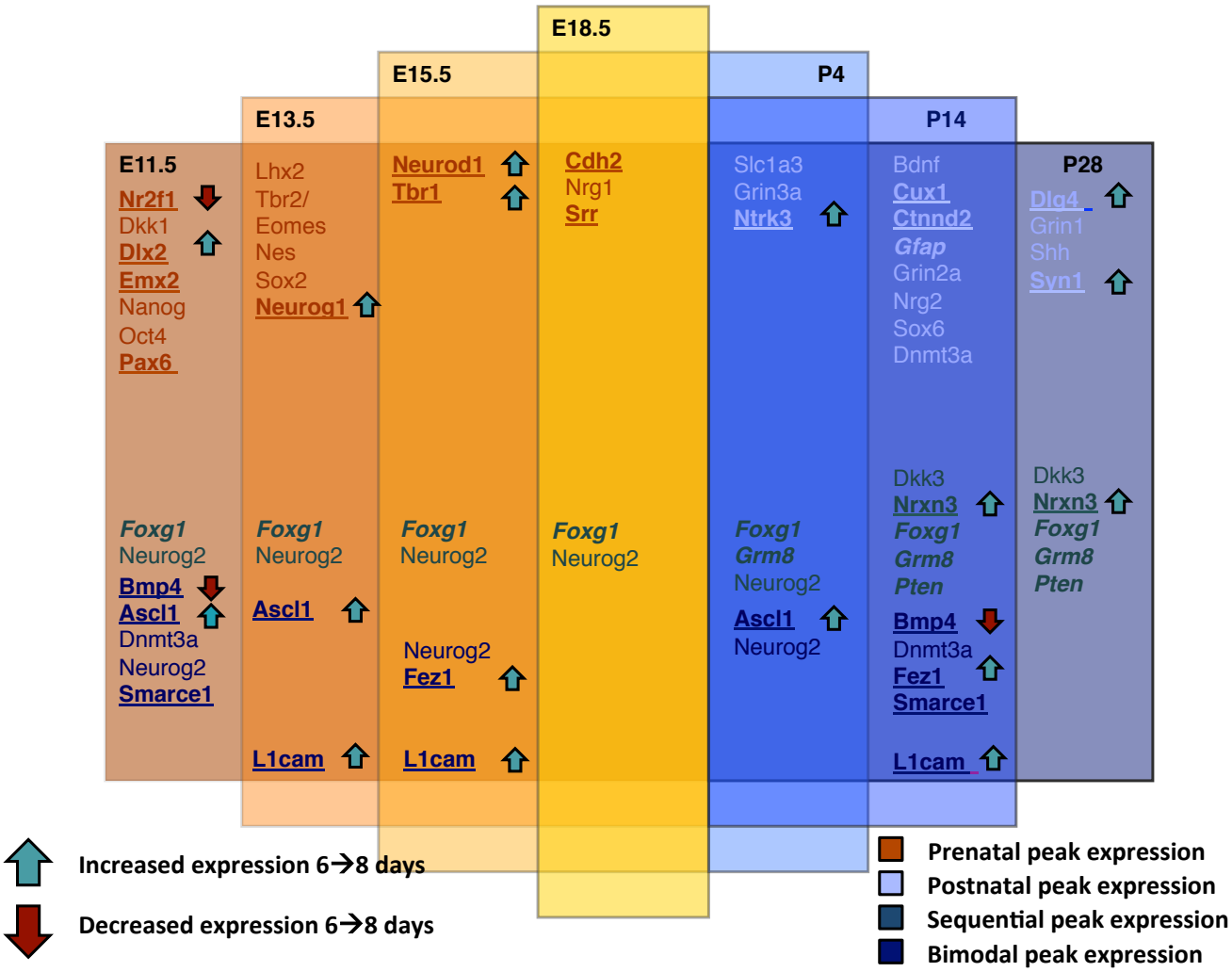

Figure 2.14 Peak gene expression patterns in mouse telencephalon.
Orange columns include genes with prenatal peaks; blue columns include genes with postnatal peaks. Peak expression was based on the published expression profiles on the developing mouse brain on Allen's Brain Atlas. The green labelled genes are those that have sequential peaks, while dark blue are those with bimodal peaks. Bold underlined genes indicate those that are found to be significantly higher expressed in mutant cells (p<.01), while bold italicized are significantly lower expressed in mutant cells (p<.01). Green arrows indicate those genes that have an interaction between genotype and time and are found to have a significant up-regulation from day 6 to day 8; while red arrows indicate a significant down-regulation from day 6 to day 8.

2.4.2.2 REST regulation in NPCs

The expression levels of eight primary components of the REST/Nrsf-complex were analysed: *Ehmt2, Hdac1, Mecp2, Rcor1, Smarca2, Smarcd3, Smarce1* and *Nrsf* (Figure 2.15). At the Bonferroni corrected p-value of .006 (.05/8 genes), two genes in this complex were significantly mis-regulated in the mutant population. The chromatin remodeler *Smarce1* had significantly higher expression in the mutant cells, while *Nrsf* or REST was found to have significantly less expression. At a less stringent *p*-value of >.01 we find two addition REST complex chromatin remodelers were up-regulated, *Smarca2* and *Smarcd3* (Appendix Chart 2.6).

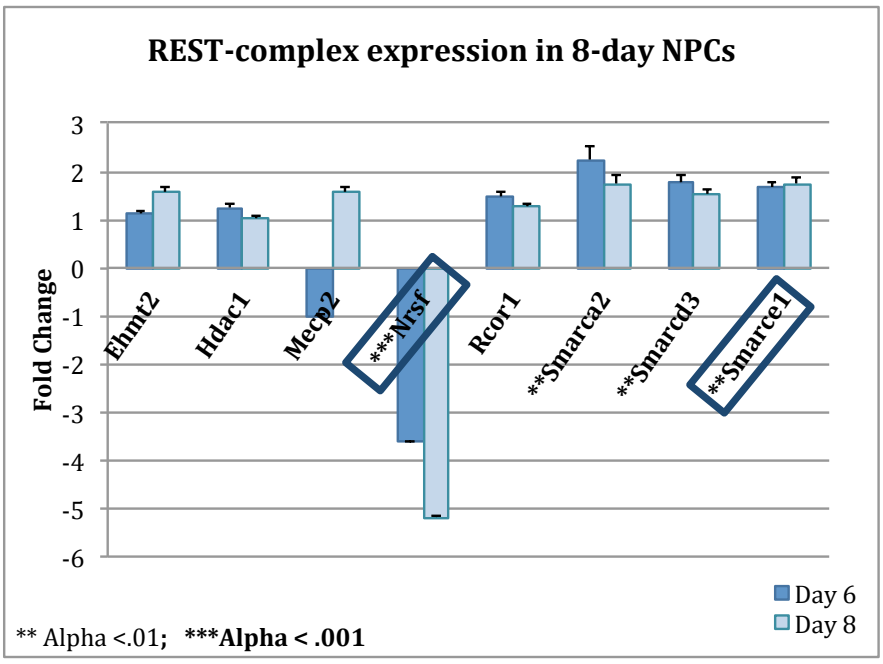

Figure 2.15 REST-Complex component gene expression.
Nrsf is significantly down-regulated *Ehmt1+/-* NPCs, while SWI/SNF members Smarca2, Smarcd3, and Smarce1 are all significantly up-regulated.

In addition to the REST complex, the expression levels of 14 published targets of REST-repression were also examined. At the Bonferroni corrected *p*-value of >.004, 5 of the 14 genes were significantly up-regulated in the *Ehmt1+/-* NPCs: *Ntrk3, Snap25, Syn1, Syp,* and *Stmn2*. At the less stringent *p*-value of >.01, three additional genes were found to be up-regulated *Ctnnd1, L1cam*, and *Nrx3* (Appendix Chart 2.7). In totally 8 out of 14 of these targets were found to have significantly increased expression levels which corresponds with the significant down-regulation of the repressor, REST/Nrsf (Figure 2.16; Figure 2.17).

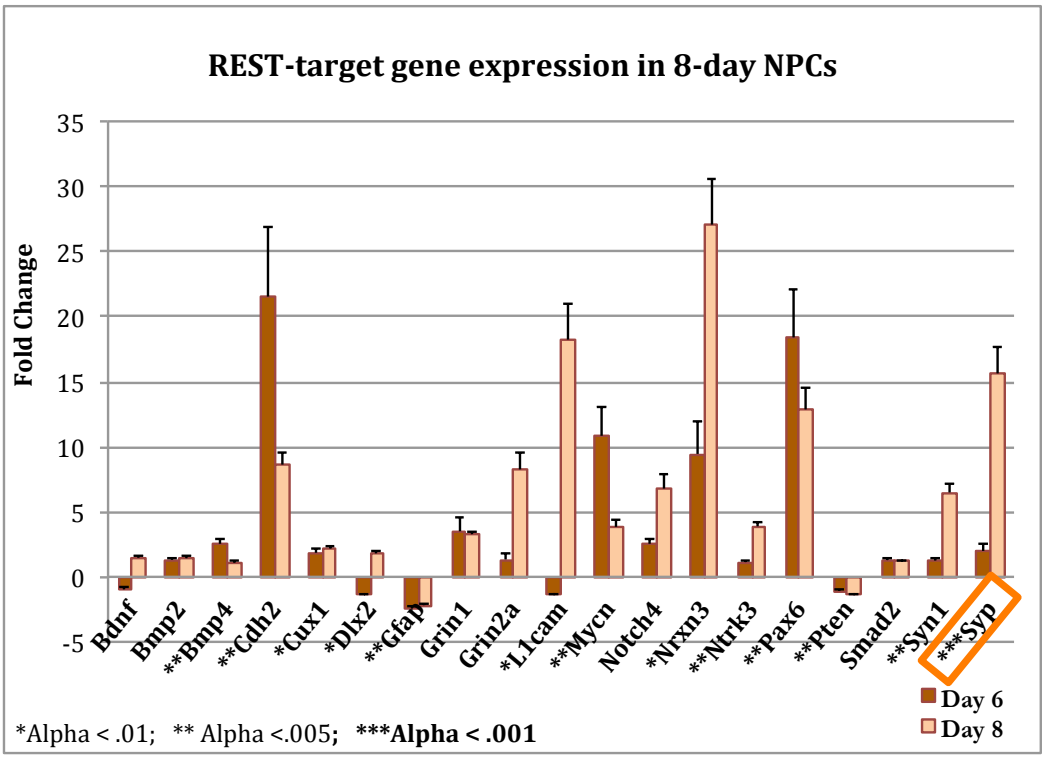

Figure 2.16 REST-regulated neuronal developmental gene expression.
8/14 genes analysed were found to have significant increases in gene expression compared to controls. Three different alpha values are considered here <.01, <.005 and <.001.

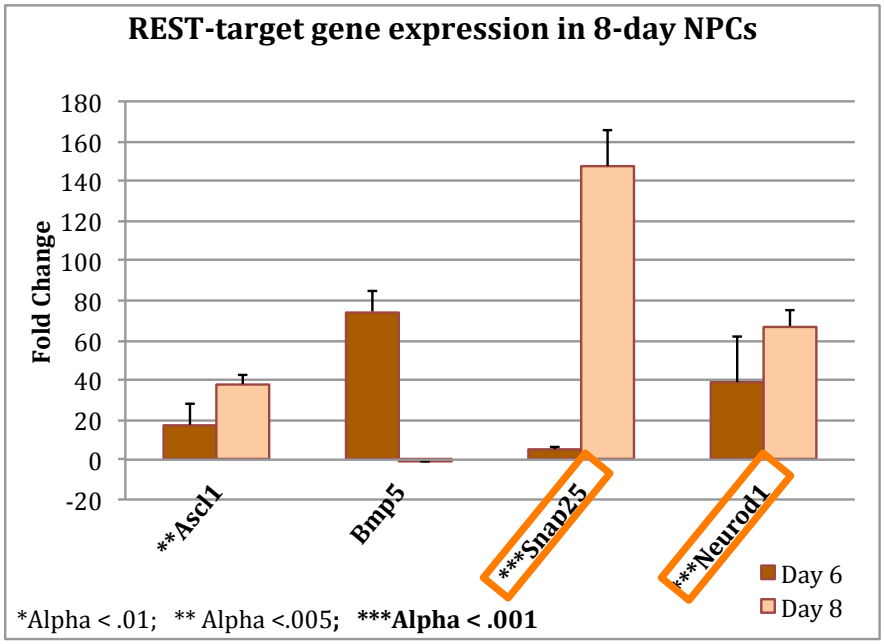

Figure 2.17 REST-regulated neuronal developmental gene expression CONTINUED. Snap25 and Neurod1 had the largest fold increase and interaction between time and genotype. Three different alpha values are considered here <.01, <.005 and <.001.

2.4.2.3 H3K9me2 target controls

In a third RT-PCR experiment H3K9me2 targets of repression and genes previously found to be dysregulated in *Ehmt1*$^{+/-}$ mESC were examined. Of the six genes examined, *Slc6a7, Bmp5, Bmper, Casp1, Dppa5a* and *Eif4ebp1* which are all up-regulated in both fly and mouse models, only one reached significance at the Bonferroni correct *p*-value thresholdof .083. However, *Eif4ebp1* had significantly less expression in the *Ehmt1*$^{+/-}$ NPCs, not more. Three other genes, *Bmp5, Bmper* and *Casp1* did have trends for large fold-increases, however these changes were not significant (Appendix Chart 2.8). The remaining six genes were all found to be up-regulated in a pilot study of mESC expression, *Sfrp2, Nes, Nog, Pten, Wnt2,* and *Blk.* Only one of these genes reached significance at the Bonferroni correct *p*-value of

.004. *Pten* demonstrated a significant interaction between genotype and time, with a decrease in expression from day 6 to day 8 of differentiation. Again three of the other genes, *Sfrp2, Nes* and *Nog* all showed a trend for greater fold-change in the mutant NPCs, but these differences were not significant (Appendix Chart 2.9).

2.5.1 Neuronal population

The NPCs were dissociated and plated after 8 days grown as CA. Both *Ehmt1*$^{+/Flped}$ controls and *Ehmt1*$^{+/-}$ mutant NPCs successfully adhered, and little difference was found in initial survival and seeding density within 4 hours plating. However, within the first two days of plating less cell survival and growth was observed in *Ehmt1*$^{+/-}$ NPCs compared to control NPCs. By day 6 there was significantly less survival and reduced neurite outgrowth demonstrated in the mutant population (Figure 2.18). After 8 days, there were no visible living cells with a clear neural morphology in the *Ehmt1*$^{+/-}$ population.

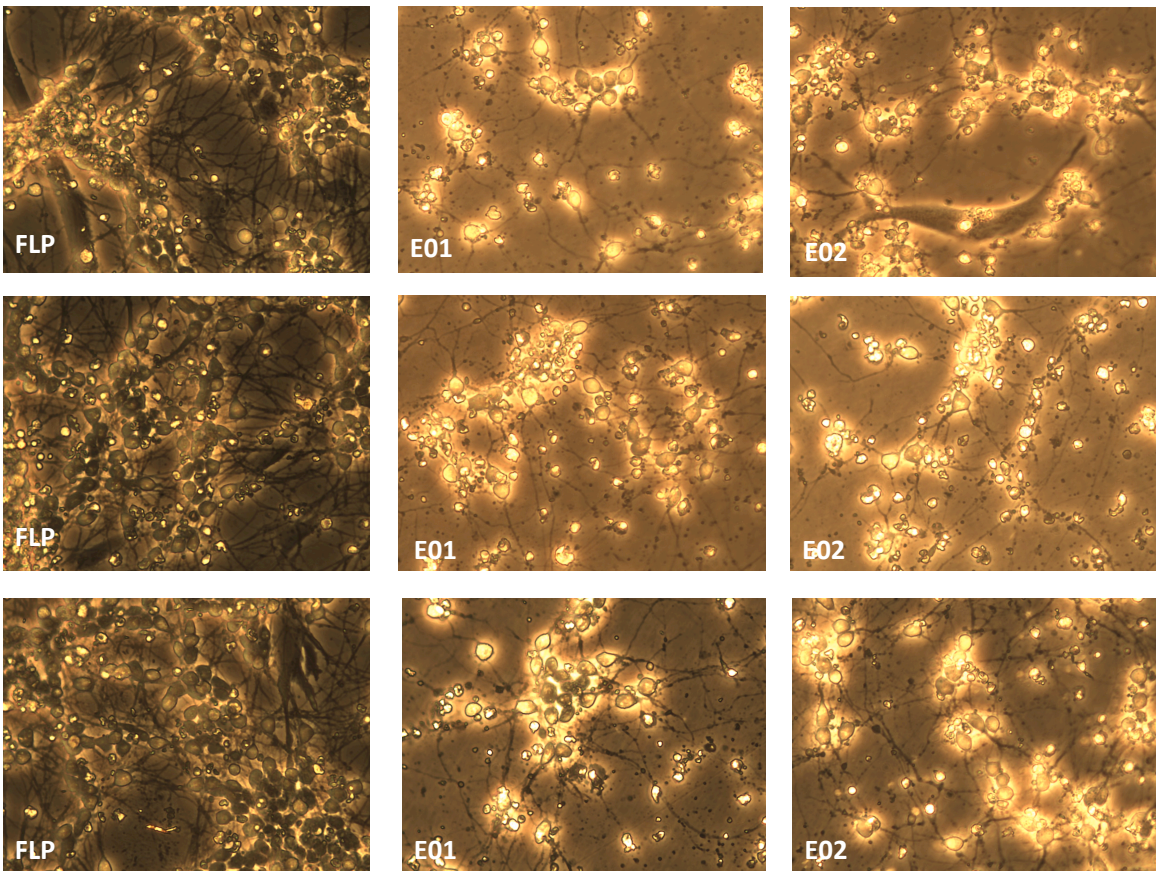

Figure 2.18 Pyramidal neurons 6 days after plating
Substantial cell death and decreases in neurite outgrowth is observed in both populations of Ehmt1+/- pyramidal neurons 6 days after plating. Neither E01 or E02 clones survive 8 days after plating.

Ehmt1$^{+/Flped}$ control neurons demonstrated global Vglut1 expression with much more localized and specific expression of Vglut2, as might be expected in pyramidal neurons. In addition we found high levels of both *ß*-tubulin and Map2 expression. However, very little Vgat expression was identified. A few potential Vgat synapses could be found close to the cell bodies and axons, like those found in pyramidal neurons. The drastic decrease in cell survival at this stage of development prevented examination of the same markers in *Ehmt1*$^{+/-}$ mutant neurons.

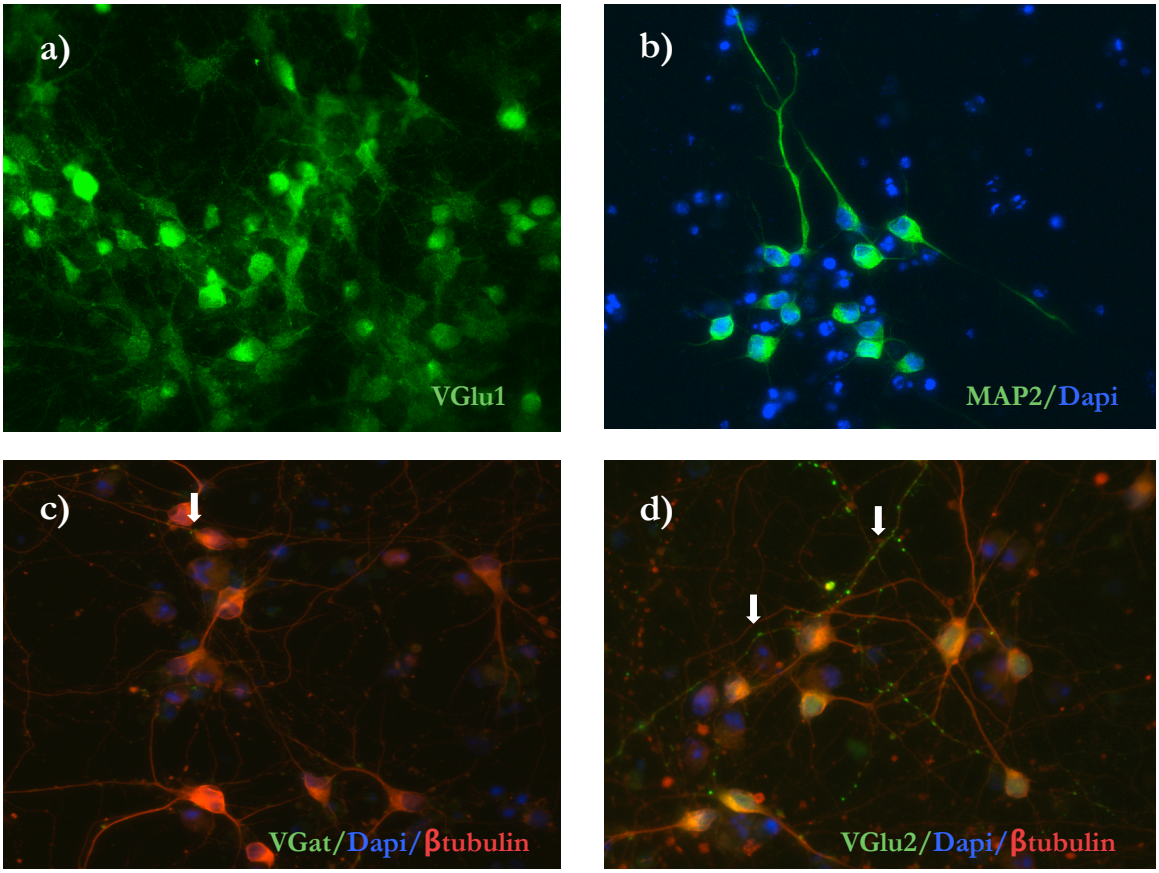

Figure 2.19 a-d. Pyramidal markers in control neurons 6 days after plating.
a. Positive staining for vesicular glutamate 1 transporter expression in control neurons; **b.** Positive staining for MAP2 expression in control neurons; **c.** Very little staining of vesicular GABA, although arrow pointing to potential synapse near soma; **d**. Positive staining for vesicular glutamate 2 transporter expression in control neurons.

2.6 Discussion

The analysis here found no differences in expression of the three pluripotency markers examined in the mESCs. However, cells lacking one copy of the *Ehmt1* gene had subtitle but consistently faster doubling rates and significantly more cells going through S-phase after a 1hr essay. These findings suggest *Ehmt1*$^{+/-}$ mutant mESC proliferate more rapidly. After 8 days of neuronal differentiation however, *Ehmt1*$^{+/-}$ mutant NPCs are found to have significantly fewer cells going through S-phase.

These findings suggest mutant NPCs had slower proliferation rates—despite similar protein expression patterns in key NPC markers. When the transcriptional profile of the 8 day-old NPCs was examined, the *Ehmt1*$^{+/-}$ mutant cells had significant higher expression of a number of genes that are typically found to have peak expression at later stages in mouse brain development. These findings suggest either a rapid increase in differentiation rates in these cells or significantly greater transcriptional noise, specifically in those genes important for neural development. In addition, *Ehmt1*$^{+/-}$ mutant cells had significant reductions in the mRNA expression of REST; which in turn corresponded to a significant increased fold-change in a number of published REST-target genes. Finally, *Ehmt1*$^{+/-}$ mutant cells did not survive the full differentiation process. Rapid cell death began occurring within 2 days of the CA-dissociation. However, this phenotype only occurred in the *Ehmt1*$^{+/-}$ mutant cells, as *Ehmt1*$^{+/flped}$ controls were successfully differentiated into Vglut1+, Vglut2+, Map2 and β-tubulin+ neurons.

2.6.1 mESC discussion

There were no differences across the 3 cells lines in mESC morphology, AP-staining or protein expression of pluripotent markers *Oct4*, *Nanog* and *SSEA-1*. The high expression of all three pluripotency makers suggests that all lines are similar populations of mESC. Any differences found amongst the cell populations henceforth cannot be directly associated with changes in pluripotency or the state of 'stemness'. *Ehmt1*$^{+/-}$ mESCs were found to have 50-60% decrease in GLP expression, indicating the lack of one copy of the gene confers a significant reduction in the production of GLP. Similarly we find a significant reduction in H3K9me2, which appears to be both highly G9a/GLP dependent and acutely responsive to G9a/GLP inhibition.

Despite the similarity in 'stemness', the cell-doubling rate of the two *Ehmt1*$^{+/-}$ mESC clones was faster. The differences in proliferation were confirmed through two independent assays, first by calculating a growth curve in the *Ehmt1*$^{+/-}$ mutant cells and *Ehmt1*$^{+/Flped}$ isogenic controls. This experiment was confirmed by examining the rate of EdU incorporation; wherein the quicker proliferation rate of *Ehmt1*$^{+/-}$ mutant mESCs was corroborated.

In addition to the proliferation phenotype of the *Ehmt1*$^{+/-}$ mESCs, we find a significant up-regulation in *Wnt2*, a known target of H3K9me2-specific repression. The 8.6-10-fold increase in *Wnt2* expression in *Ehmt1*$^{+/-}$ cells may be linked to the increased rate of proliferation of these cells. The canonical Wnt pathway activity is directly associated with self-renewal in mESCs (Sato et al., 2003) while greatly influencing the proliferation of stem cells and early progenitors in a range of tissue (Sato et al., 2003; Reya & Clevers, 2005), including the brain (Machon et al., 2007; Tang et al., 2010). In fact, Wnt2 has been identified as a risk gene associated with ASD (Lin et al., 2012; Marui et al., 2010); while the Wnt pathway is believed to be dysregulated in some forms of Schizophrena (Cotter et al., 1998; for review see Moon et al., 2004). Furthermore, the Wnt signaling pathway is often studied in its association with aberrant proliferation of cancer stem cell pools (Reya & Clevers, 2005).

While immunohistochemistry analysis does not identify changes in pluripotent transcription factors Oct4 and Nanog, our findings would benefit from further analysis. Previous reports would predict an over-expression of both Oct4 and Nanog in an *Ehmt1*$^{+/-}$ mESC (Yamamizu et al., 2012). Furthermore, the expression levels of three pluripotency markers: Oct4, Nanog and Sox2 were also examined in the NPCs RT-PCR array as well. Models of both *Ehmt1* haploinsufficiency and REST de-repression would predict prolonged expression of these pluripotency markers, even after lineage commitment (Soldati et al., 2012). Surprisingly, no differences in these markers were found in the mutant population after 6 or 8 days of NPC differentiation.

However, there is a significant difference in Bmp4 expression in the day 6 mutant NPCs, where these cells have a 2.5 fold-increase in expression. Bmp4 promotes the self-renewal and proliferation of stem cells (Qi et al., 2004); in fact Bmp4 along with LIF are essential for ESC maintenance (2004). So while there is no evidence of increased mRNA expression of Nanog or Oct4 TFs in the mutant NPCs, there are signs of increased expression in at least one pluripotency regulator. Further examination is warranted.

2.6.2 NPC discussion

Unlike what was found in the *Ehmt1*$^{+/-}$ mESCs populations, a significant reduction in the number of cells going through S-phase was found in mutant NPC populations. The dynamic change in proliferation rates corresponds with shifts in Wnt2 expression. While there was a GLP-dose dependent response in Wnt2 expression and increased proliferation in *Ehmt1*$^{+/-}$ mESCs; there was no difference in Wnt2 expression and decreased proliferation *Ehmt1*$^{+/-}$ NPCs. Thus disruption of the Wnt pathway may be linked to changes in proliferation rates during the differentiation of *Ehmt1*$^{+/-}$ mutant cells.

Radial glia cells (RGCs) give rise to the vast majority of cells in the developing cortex and have the capacity to eventually differentiate into a wide range of glia and neuronal cell types (Kowalczyk et al., 2009). These cells form essential developmental scaffolding in cortex, necessary for neuronal migration (Schmid et al., 2003) The transcription factor Paired-box protein 6 (*Pax6*) is a key regulator of RGCs and is often used as a marker of this cell type during neurogenesis (Gotz et al., 1998). In the developing cortex, cells that are basally located are known as intermediate progenitor cells (IPCs) or basal progenitors and extend up to the intermediate zone of the SVZ (Miyata et al., 2004). *Pax6*—the RGC regulator is found to activate the transcription of Neurogenin 2 (*Ngn2*) (Scardigli et al. 2003). Ngn2 is believed to promote the switch of apical progenitors to INPs or basal progenitors (Miyata et al., 2004). This switch corresponds with the expression of the T-box brain protein (*Tbr2*) gene. Tbr2 is specifically expressed in IPCs of the developing cerebral cortex and leads to the development of pyramidal-projection neurons of all six cortical layers (Sessa et al., 2008).

The positive staining for Pax6, Ngn2 and Tbr2 suggests there is a mixed population of RGCs and IPCs in the 8 day NPCs. Bibel et al. reported 84+/-12.2% Pax6+ cells, using immunocytochemtry after 4 days of RA-induction. The variation in quantification here may in fact be due to variation in immunocytochemistry protocols. The FACs sorted cells were >80% Pax6+, a percentage very close to that of the published protocol (Bibel et al., 2004).

Unfortunately, specificity of Ngn2 was problematic. Similar staining patterns were found in the E14.5 brain (data not presented), which suggests it may be the cellular location of the antigen or non-specific binding of the antibody, which limits Ngn2 quantification, and not a lack of specificity in the NPCs *per se*. However the clear expression of Tbr2, which is directly activated by the transcriptional regulator Ngn2 suggests these cells are Ngn2+. Meanwhile the expression of Tbr2 is an important indication that the protocol leads to the successful recapitulation of pyramidal differentiation.

The combined down-regulation of earlier RGC marker *Pax6* and up-regulation of the later IPC markers *Ngn2* and *Tbr2* expression in the RT-PCR experiment and in the mutant cells may suggest there is a greater shift in the number of earlier RGC compared to later IPC in the mutant population compared to controls, despite the lack of detectible differences in antigen labeling. These data might be the most reliable for detecting differences in the rate of differentiation, and suggests the *Ehmt1*$^{+/-}$ NPCs may in fact be differentiating at a more rapid pace.

An RGC and IPC-specific RT-PCR experiment was designed to examine the developmental transcriptional profile and test the hypothesis that the reduced expression of GLP leads to rapid neural induction and differentiation. By examining two separate developmental stages, changes in transcriptional profiles of these progenitor populations are captured with greater temporal resolution. There was significantly greater expression of genes, which are found to have peak expression from E18.5 up until P28 and in post-mitotic neurons in the *Ehmt1*$^{+/-}$ NPC populations, genes like *Ascl1, Srr, Ntrk3, Cux1, Ctnnd2, Dlg4, Syn1* and *Nrxn3, Fez1, L1cam.* Furthermore, the majority of these genes were found to have greater fold-change from day 6 to day 8. Overall this array provides evidence for the precocious up-regulation of later lineage markers as a result of *Ehmt1*-haploinsufficiency.

As reviewed, Glp/G9a activity is important for REST-mediated repression. Reduction of GLP expression during NPC differentiation led to the hypothesis that the regulation of REST-mediated repression may be disrupted as well. Mutant NPCs

had a significant increase in mRNA expression of three SWI/SNF chromatin remodelers *Smarce1, Smarca2* and *Smarcd3*, all of which are members of the REST complex and are in fact found to be under the transcriptional control of REST/Nrsf (Loe-Mie et al., 2010). Loe-Mie found deregulation in the six REST-complex components after REST silencing. Of the SWI/SNF members, *Smarcd3* was significantly up regulated while *Smarce1* and *Smarca2* were significantly down regulated. Meanwhile, both *Rcor1* and *Mecp2* were also significantly up regulated and *Hdac1* was significantly down regulated in their study. Thus with the significant decrease in REST expression found in the mutant NPCs in this study, the dysregulation of these SWI/SNF chromatin remodelers and the other REST-components may be expected. The specific pattern of expression changes do not match that reported by Loe-Mie et al.; however, this may be due to the fact there was only a reduction of REST expression as opposed to complete silencing. In addition, these cells had the added complexity of reduction in GLP repressor activity as well.

The mRNA levels of 14 genes that demonstrated endogenous REST occupancy at their RE1-sites *in vivo* (Bruce et al., 2004) were examined. As what might be expected with decreases in REST expression, all targets demonstrated trends for greater expression than found in control NPCs. Five genes *Ntrk3, Snap25, Syn1, Syp* and *Stmn/Scg10* were all significantly up regulated. Furthermore, with the exception of *Nefh* and *Smad2* all of these targets had between .22-117 fold enrichment from day 6 to day 8 of differentiation. Several of these genes do overlap with those reported to be precociously up-regulated in the developmental array; those that do not overlap with this array however are also generally found to have peaks during post-natal neural development.

Interestingly, *L1cam* and *Snap25,* which had 15.85 and 117.4 fold-increase from day 6 to day 8, respectively, are found to have greater REST occupancy *in vivo* than other loci examined (Bruce et al., 2004). Upon closer investigation these two genes are found to have an additional RE1 flanking sequence within 30 bp of the original sites, only with 1bp deviance from the consensus RE1. Thus the existence of the tandem

RE1 site might suggest a secondary mechanism for transcriptional regulation, which in light of the reductions in the REST may lead to an even greater fold change and increased expression of these genes during differentiation, as was found here.

The final observation from the RT-PCR experiments is that regarding the genes found to be significantly down-regulated in *Ehmt1*$^{+/-}$ mutant NPCs: *Foxg1, Gfap* and *Grm8.* All three of these genes are independently associated with a number of psychiatric disorders. *Foxg1* expression coordinates pyramidal progenitor integration into the cortical plate while helping determine laminar identify (Miyoshi & Fishell, 2012). Mutations in *Foxg1* underlie the atypical, congenital form of Retts syndrome—a syndrome typically caused by mutations in *Mecp2*. The *Foxg1* form of Retts leads to severe intellectual disabilities, language and motor dysfunction and dyskinesia (Ariani et al., 2008). Meanwhile, Foxg1 is known to play a central role regulation progenitor proliferation in the central nervous system (Hanashima et al., 2004; Martynoga et al., 2005); thus decreases in *FoxG1* could also be related to the slower proliferation rate in day 8 *Ehmt1*$^{+/-}$ NPCs.

Gfap encodes the glial fibrillary acidic protein. Gfap protein levels are altered and/or decreased in the frontal cortex in a range of psychiatric conditions from schizophrenia, bipolar disorder, and major depressive disorder (Johnston-Wilson et al., 2000). *Grm8* encodes a metabotropic glutamate receptor, and is believed to a play an important role in regulating neuronal hyperexcitability and homeostatsis (Cartmell & Schoepp, 2000). Mutations in *Grm8* have been associated with ASD (Li et al., 2008).

Even though G9a/GLP activity is primarily associated with its role in H3K9me2 repression, G9a/GLP is also found to play a role in transcriptional activation (Gupta-Agarwal et al., 2012). It is possible that G9a/GLP acts as transcriptional activators during neural development and that *Foxg1, Gfap* and *Grm8* are potential targets of G9a/GLP-specific activation. Ultimately however, these data cannot establish a mechanistic link between GLP expression and *Foxg1, Gfap* and *Grm8* transcriptional regulation.

2.6.3 Pyramidal Neuron discussion

In order to verify the successful differentiation of pyramidal projection neurons, after 8 days of differentiation, the co-expression of the vesicular glutamate transporters Vglut1 and Vglu2—both highly expressed in glutamatergic projection-neurons were analysed. The class III *ß*-tubulin protein, which is exclusively expressed in neurons, and the microtubule-associate protein 2 (Map2*),* a neuron-specific cytoskeletal protein enriched in dendrites were also analysed. In addition, vesicular GABA transporter (Vgat*)*, which is highly expressed in interneurons, not projection neurons was used as a negative control. The positive expression of Vglut1, Vglut2, Map2 and *ß*-tubulin at the post-mitotic stage along with positive expression of the earlier lineage markers for RGC and IPC strongly suggests this protocol was successful at generating cortical neurons. And the negative expression of Vgat, suggests they were indeed excitatory projection neurons or pyramidal neurons.

The *Ehmt1+/-* cells did not survive for examination into post-mitotic stages. These results are especially unsatisfying, when considering *Ehmt1*$^{+/-}$ does not lead to drastic morphological changes in the forebrain or large differences in pyramidal cell numbers *in vivo* (as discussed in Chapter 3). The increase in cell death may be due to exogenous factors, or in this case the culture conditions. The mouse transgenic line—C57BL/6N (B6) was chosen for both mice breeding and mESC work. Unfortunately in most cases the B6 cell strain is far more difficult to maintain in culture (Brook & Gardner, 1997), loses pluripotency much more rapidly and deteriorate in normal conditions (Sharova et al., 2007). Due to the instability of these cells, differentiation into a specific and homogenous cell type, like the pyramidal neurons, has proven especially difficult. Small adjustments to the protocol were made throughout the process, but perhaps ideal conditions were still not met. If the mutant cells were even slightly more sensitive to steps like the mechanical dissociation of the CAs, then the added instability of the specific strain used for *in vitro* differentiation may have led to increased cell death at neuronal stages. A logical way forward would be to test out new culture conditions, different

strategies for pyramidal differentiation and cells from different background strains. Unfortunately the timely establishment of the current protocol precluded further studies of this type.

A second explanation is that the increased cell death reported here is due to endogenous factors. In this instance, *Ehmt1* dosage may be especially important for the later stages of differentiation in the NPCs, and indeed in a cell-specific or tissue specific manner. In this case, pyramidal cells may be highly sensitive to perturbations in *Ehmt1* dosage. Thus without the support of the surrounding structures and signalling cascades of the developing brain, *Ehmt1*$^{+/-}$ pyramidal cells differentiated in a dish are particularly vulnerable. The disruption of the developmental program in these cells, but not the controls may help explain why control cells were successfully differentiated under the same conditions.

To summarise the findings, changes in *Ehmt1* dosage during pyramidal neuron development has profound effects on the rate of proliferation and differentiation. Unfortunately, how these effects manifest in the post-mitotic neuron could not be assessed. The *in vitro Ehmt1*$^{+/-}$ cells died during the later stages of pyramidal differentiation. These findings have profound implications for the importance of the GLP in the regulation of pyramidal neuronal development.

Chapter III. Development of *Ehmt1*$^{D6cre/+}$ mouse

3.1 General introduction

In this chapter a viable system for investigating the functional consequences of *Ehmt1* during mouse forebrain development is established. The aims of the chapter are to capture basic physiological or motoric function and activity level changes resulting from *Ehtmt1* forebrain-specific haploinsufficiency. First, evidence from previous models of Ehmt1 disruption is reviewed in both flies and mice. The review highlights the specific limitations of each model while framing the present goals for developing a novel mouse model. The development of a novel *Ehmt1*$^{D6Cre/+}$ mouse mutant is discussed—the transgenic breeding program, the region-specific expression patterns of the model, sex and transgenic birth ratios and adult weight data are reported. Basic motor learning, motor coordination and activity levels are then compared in the *Ehmt1*$^{D6Cre/+}$ mouse model with *Ehmt1*$^{Flp/+}$ control littermates.

3.1.1 Previous animal models of Ehmt1 haploinsufficiency

3.1.1.1 EHMT expression in drosophila development

In the literature, *EHMT* haploinsufficiency has been studied in the fruit fly, *Drosophila melanogastor*. Fruit flies possess a single ortholog of *EHMT*, unlike the two found in mammals. *Drosophila EHMT* is found to be equally similar to themammalian *EHMT1* and *EHMT2* genes. *EHMT* protein is abundantly expressed in the developing fly, specifically in the neurons, while expression levels remain high throughout adulthood. In one study, loss of *EHMT* resulted in altered dendritic development in sensory neurons—the higher-order branching led to dendritic fields of significantly reduced complexity (Kramer et al., 2011). In order to establish whether the phenotype was *EHMT*-specific, a cell autonomous recovery experiment in the developing larvae was performed, and drastic changes in dendritic morphology were rescued with *EHMT*-re-expression (Kramer et al., 2011). Interestingly, in the control line, over-expression actually led to comparable deficits

in arborisation as that found in the constitutive knockout, strongly suggesting gene dosage is also very important for normal fly development. The developing larvae of *EHMT* hemizygous mutants also demonstrated altered crawling and locomotor behaviours.

3.1.1.2 Global hemizygous Ehmt1 knockout mice

In addition to the fly work, Ehmt1 function has also been examined in two mouse models: a hemizygous knockout (KO) and a forebrain-specific condition KO. In mammals the *Ehmt1* gene is highly conserved, demonstrating 97% homology in amino acid sequence between mouse and human (Tachibana et al., 2011). The GLP enzyme is highly expressed in early development, with a 10-fold decrease in the first monthly postnatal development (Balemans et al. 2012). Nullizygous *Ehmt1* mice are embryonically lethal at day 9.5 (Tachibana et al., 2011).

In the constitutive hemizygous knockout mouse model, the loss of function of one copy of the gene led to 40-50% reduction in GLP expression (Balemans et al. 2012). *Ehmt1*$^{+/-}$ mutants had a number of developmental delays and deficits. These mice showed significant reductions in body weight throughout postnatal development (Balemans et al., 2012). Weight differences however did not continue into adulthood (Balemans et al., 2010; 2013). They also showed delays in the onset of upper incisor eruption, ear opening, and eye opening compared to wild type; and early postnatal hypotonia and motor function delays (Balemans et al., 2013).

Ehmt1$^{+/-}$ mutant mice had no gross morphological changes in their brains at 1, 3, 10, and 20 months of age, and no apparent difference in layering. However, much like the changes found in drosophila, the hemizygous mutant mice showed reductions in dendritic arborisation as well as a reduced number of mature spines in hippocampal CA1 pyramidal neurons (Balemans et al. 2012). *Ehmt1*$^{+/-}$ mice showed significant reductions in activity levels and exploration. In addition, these mice demonstrated increased anxiety when exposed to a range of novel objects or spaces.

3.1.1.3 Forebrain-specific postnatal homozygous Ehmt1 KO mice

A conditional forebrain-specific homozygous KO mouse has also been generated using a Ca2+/Calmodulin-dependent protein kinase II alpha gene promoter (Camk2a-Cre) (Schaefer et al., 2009). CamKIIα is only expressed in the postnatal periods. Consequently, ablation of the GLP enzyme in the animals occurs postnatally, thus missing many critical periods of neurodevelopment. These mice did show a significant reduction in euchromatic H3K9me2 as well as a range of behavioural and cognitive impairments. They had diminished exploratory behaviours and were also hypoactive. However, unlike the hemizygous mutants, these mice showed reduced anxiety and fear. Mutants did not demonstrate a preference for sucrose, suggesting an anhedonic response or an underlying dysfunction in motivation and reward pathways. The *Ehmt1*$^{Camk2a\text{-}Cre/Camk2a\text{-}Cre}$ mutants had twice the body weight of controls after 5-6 weeks. Despite the behavioural phenotypes, cellular integrity and architecture did not appear changed and there was no major impact on neuronal morphology.

3.1.2 Mouse model limitations

Reduced *Ehmt1* in both mouse models confer motor and hypoactivity-related phenotypes. However both models present a number of limitations. The *Ehmt1*$^{+/-}$ mice demonstrated an array of developmental delays, motor deficits, cranial mutations, hypotonia and significant hypoactivity and anxiety. The reduced activity levels, delays in motor development and significant increases in anxiety are a set of phenotypes that are confounding for interpretation of learning, memory or social behaviours. The *Ehmt1*$^{Camk2a\text{-}Cre/Camk2a\text{-}Cre}$ conditional KO mouse model avoids embryonic lethality of the constitutive nullizygous animal, while still permitting an investigation into fully GLP ablated neurons of the forebrain. Unfortunately postnatal ablation of GLP distinctively misses GLP peak expression during embryogenesis (as reported here, Figure 3.3). Meanwhile, neuronal populations completely lacking GLP are not representative of neuropsychiatric populations, as full deletions are not viable in mice or found in humans. Thus both models prove

especially limited in their ability to capture the disease relevant consequences of forebrain-specific *Ehmt1* haploinsufficiency during development.

3.1.3 A novel model of Ehmt1 haploinsufficiency

Constitutive KO models of widely expressed molecules like GLP are limited in their ability to strictly address cerebral function. For example, *Ehmt1* is expressed throughout embryonic development and in peripheral tissues like the developing retina, kidney, gut, lungs and whiskers (Kleefstra et al., 2005). So, in addition to the physiological and behavioural limitations discussed above, the hemizygous mutants may also suffer from a range of still unreported deficits. For example, sensory and perceptual deficits associate with abnormal eye and whisker development. To reduce anatomical complexity and allow a more precise focus on learning, memory, and executive function, a forebrain-specific conditional model was designed. Based on the evidence reported in this chapter, GLP peak expression occurs at E14.5 in the mouse, such evidence was used when considering the design of a novel mouse model. Unlike the postnatal *Ehmt1*$^{Camk2a\text{-}Cre/Camk2a\text{-}Cre}$ model, the aim here was to recapitulate disease relevant disruption to cortical circuits. Thus it was essential that one allele remains intact; and *Ehmt1* ablation occur at the earliest stages of cortical development. Such a model also allows greater potential overlap with the *in vitro* cell work in Chapter 2, in that the functional outcome GLP haploinsufficiency throughout cortical development may be evidenced in mouse behavior and physiology.

3.1.3.1 Conditional Mutagenesis

Conditional mutations are those in which gene function is altered under spatial-restricted and/or temporal-restricted conditions (Morozo et al., 2003). The Cre-Lox recombninase system is one form of conditional transgenic techniques. Cre recombinase is a bacteriophage PI enzyme, which is able to catalyse recombination between two 34-bp loxP recognition sites inserted in genomic DNA (Ruff & Kieffer, 2007). Another type of site-specific recombination system is the Flp-frt system where the flippase recombines DNA with 2 frt flanking regions. The 'knockout-first'

conditional allele, developed by Skarnes et al., , combines the advantages of reporter-tagged and both Cre-lox and Flp-frt conditional mutation (2011).

There are three configurations of the 'knockout-first' allele. In the first, 'tm1a' contains an IRES:lacZ trapping cassette and floxed promoter-driven neo cassette inserted into the intron, which disrupts gene function (Figure 3.1). This iteration leads to global gene disruption. When Flp recombination occurs the allele is converted into a conditional allele 'tm1c', which returns gene activity. Finally Cre-recombinase deletes the floxed exon of the tm1c allele to generate a frameshift mutation, 'tm1d', triggering nonsense mediated decay of the transcript in those regions in which the Cre-recombinase is expressed (Skarnes et al., 2011). Thus, the knockout first Ehmt1 conditional allele was used—the same allele used in the development of the Schaefer et al. model (2009).

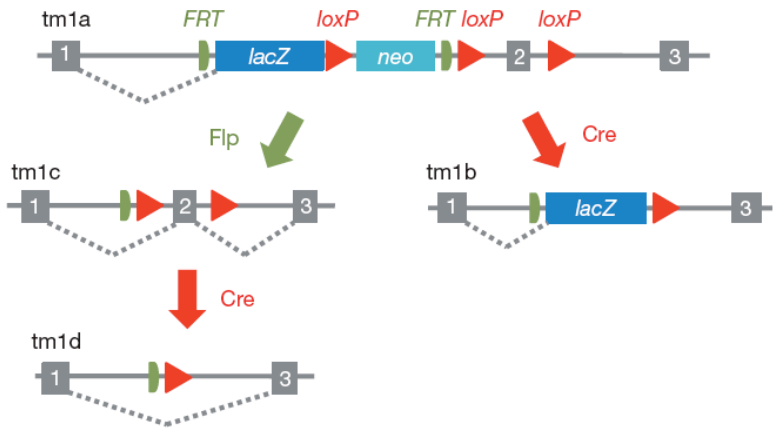

Figure 3.1 'Knockout-first' conditional allele

tm1a: IRES:LacZ trapping cassette and floxed promoter-driven neo cassette inserted at intron disrupt gene function.
tm1c: Flp-recombination converts it to a conditional allelle and gene activity is returned.
tm1d: After Flp, if Cre-recombination occurs the floxed exon of the tm1c allele generates a frameshift mutation, which triggers nonsense mediate decay of the transcript in the regions in which Cre recominase is expressed (Image borrowed from Skarnes et al., 2009).

3.1.3.2 Dach1-Cre expression pattern

The forebrain-specific D6 enhancer element is a 2.5kb region of the *Dach1* gene. The

Dach1-Cre is a transgenic mouse line that expresses Cre under the control of the D6 promoter (van de Bout et al., 2002 & Machon et al., 2002). Using reporter lines, the transgene was found to have highly specific and reproducible expression in the developing telencephalon from embryonic day 10.5 (E10.5), with high expression remaining in the neocortex and hippocampus throughout adulthood in the mouse (Figure 3.2).

In the newborn hippocampus positive staining for D6-cre activity was primarily found in the stratum pyramidale, with some in the stratum oriens and very few in the stratum radiatum. At this stage the majority of cells in the stratum oriens and radiatum are migratory interneurons born in the basal ganglia (van de Bout et al., 2002). The more sparsely stained cells in these areas at birth are likely to be pyramidal cells completing migration from the ventricular zone. In support of this, only the stratum pyramidalis is D6-Cre positive in the adult. In newborn and adult brains D6-Cre+ staining was found in layers II-VI of the cortex. Only the molecular layer (layer I) lacked D6-Cre+ cells. With the exception of cells from the dorsal wall of the lateral ventricles in neonates and adults, the majority of the D6-Cre+ were B-tubulin III+, a marker of mature neurons.

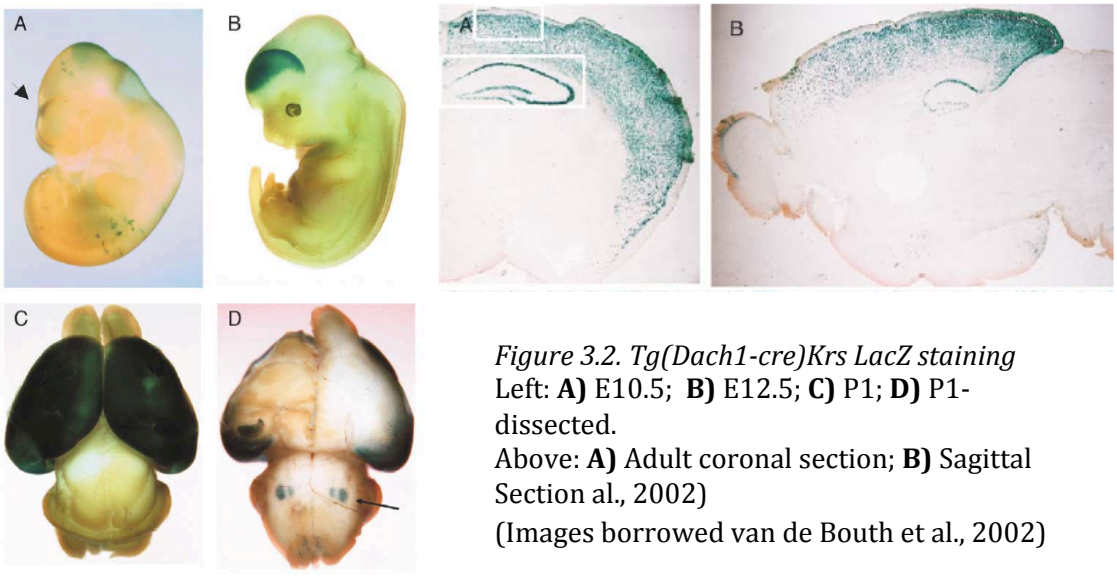

Figure 3.2. Tg(Dach1-cre)Krs LacZ staining
Left: **A)** E10.5; **B)** E12.5; **C)** P1; **D)** P1-dissected.
Above: **A)** Adult coronal section; **B)** Sagittal Section al., 2002)
(Images borrowed van de Bouth et al., 2002)

3.1.4 Chapter aims: Characterization of *Ehmt1*$^{D6Cre/+}$ mice

The aims of this chapter are three-fold. First, patterns of GLP expression throughout brain development are established. The analysis of endogenous GLP protein expression during development helps highlight the importance of studying prenatal forebrain-specific *Ehmt1* haploinsufficiency in mice. Second, the design and development of the model is described, while basic observations of breeding, development, and general health in the conditional model are assessed. Third, motoric function and activity levels in adult animals are compared.

3.2 Materials & Methods

3.2.1 Animals and housing

All mice were group-housed (3-5 per cage) in environments enriched with cardboard tubes, shred-mats and tissue paper, in temperature and humidity

controlled animal holding room (21 +/- 2°C and 50+/- 10%, respectively) with a 12 hour light-dark cycle. All cages included both mutant and control animals. Standard rodent laboratory chow and water were available *ab libitum*. Animal cages were cleaned out weekly.

3.2.2 Animal breeding

Ehmt1$^{flp/flp}$ male mice on a (C57BL/6 x CBA)F1 background were received from Rockfeller University, New York from the lab of Dr. Alexander Tarakovsky. These mice were received at sexual maturity and allowed to acclimatise to the new environment for one week before breeding began. *Ehmt1*$^{flp/flp}$ mice male studs were paired with homozygous females carrying two Cre-alleles with the *B6CBAF1-Tg(Dach1-cre)1Krs/Kctt* transgene on a (C57BL/6 x CBA)F1 background. These mice were received as cryopreserved embryos, sent from the Karolinska Institute on a transfer agreement with travel cost paid by the European Mouse Mutant Archive (EMMA); mice originally provided by Dr. Ondrej Machon. Embryos were re-derived in the barrier unit by the trained technologist at Cardiff University. In order to generate behaviour cohorts three Dach1-cre females and three controls females on a (C57BL/6 x CBA)F1 background were paired up in mixed groups of three, with each male on three different occasions. Mice from the first two breeding cohorts were used for all behavioural assays, while the third cohort were used for tissue.

3.2.3 Animal handling

All behavioural tests were performed on adult male *Ehmt1*$^{D6Cre/+}$ mice and *Ehmt1*$^{flp/+}$ controls. Two experimental cohorts were used for the behavioural experiments: there were $N = 18$ mutant and $N = 10$ control mice in the first cohort and $N = 17$ mutant and $N = 15$ control mice in second behavioural corhort. This N suffices the necessary minimal of $N = 10$ per genotype for this type of study (Crawley, 1999). Before testing, animals were handled and weighed everyday for 7 days. Animals were then continually weighed weekly throughout all behavioural testing. All apparatus were thoroughly cleaned with 1% acetic acid between subjects and in each session on all behavioural experiments. The experimenter was blinded to the genotypes of the mice for all tasks. Behavioural testing was conducted in the light

phase of the light-dark cycle in quiet animal holding room (between 07:00 hours and 19:00 hours) and run in low-level (15 lux) white light. All procedures involving animals conformed to the revised UK Animals (Scientific Procedures) Act 1986.

3.2.4 Genotyping

Mice were weaned around postnatal day 28 and either a small ear perforation was taken or a tail biopsy was collected. The tissue samples were then digested with 100-250ul of DirectPCR tail lysis buffer (Qiagen, Crawley, UK) with 0.2-0.4 mg/ml of fresh Proteinase K (Sigma, p6556) added. Tissue samples were incubated at 55°C for 5-6hrs until no tissue clumps were observed. Samples were then immediately incubated at 85°C for 45mins. Samples were spun down and stored on ice while PCR reactions were prepared. 1ul of sample was used for 25ul PCR reaction. PCR reaction consisted of 12.5ul of 2X GoTaq (Promega) with 1ul of sample and 11.5ul of H_2O. All PCR cycle programs and primer pairs are found in Appendix Chart 3.1. Amplified PCR products were then loaded on 2% agarose gels to visualized.

3.2.5 PCRs for Cre-specificity

In order to establish Cre specificity and verify the accuracy of the PCR methods for genotyping, sections from the prefrontal cortex (PFC) and the hippocampus were taken for positive verification of the deleted allele in the mutants (985-bp band in the gel). While a section of the cerebellum, a region where Dach1 is not expressed was taken to check for the non-deleted floxed allele (792-bp). A positive control for the wild type allele was included (95-bp). In addition sections from control PFC, hippocampus and cerebellum animals, which are expected to have one copy of the floxed-allele, were also examined. The PCR conditions and primers are reported in the Appendix (see Appendix Chart 3.2; Appendix Figure 3.1).

3.2.6 Western blot analysis

Whole head lysates for embryonic stage 12.5 (E12.5) and E13.5 were used; while whole brains for E14.5, E18.5, postnatal days 1 (P1) and P7 and P28 were used for the peak expression assay. Lysates from ≥4 pups from two separate litters were combined for each time point. Tissue was extracted and lysed on ice at 5mg/ml of

RIPPA buffer (100mM NaCl, 20nM Tris HCl pH 8, 0.5% deoxycholate, 0.5% NP40, 25uL SDS of 20% stock) using a glass dounce homogenizer. Tissue lyses was then agitated for 2h at 4º C. Western Blots were then ran following the 4-12% NuPage protocol.

3.2.7 Histology

Mice were terminally anaesthetized and transcardially-perfused using 4% PFA. Whole brains were extracted and left in 4% PFA at 4° overnight. The next day brains were washed twice in PBS. PBS was replaced with 70% ethanol. Whole brains were wax-embedded and sectioned in 4um sections by the histology lab at Cardiff University. For Nissl staining, sections were de-paraffined by soaking in xylene 2 x at 3-mins each. Sections were then rehydrated by soaking in 100% ethanol 2 x at 3-mins, 95% ethanol 1 x at 3-mins, 75% ethanol 1 x at 3-mins, and 50% ethanol 1 x at 3-mins. Sections were then stained by soaking in 0.1% Cresyl Violet in acetate buffer (Fronine, HH155) for 3-mins. Sections were then soaked in tap water to remove excess stain and taken through the same series of ethanol soaks, starting with 50% and going in reverse. Finally sections were taken through xylene 2 x at 3-mins and allowed to dry in the fume hood. After sections were dried slide covers were mounted with DPX and slides were dried overnight. Images were capture using 20 x resolution on an Olympus IX-71 inverted wide field fluorescent microscope with an Exfo X-cite 120 light source using the SimplePCI (Hamamatsu) software package. Images were capture using only bright field settings.

3.2.8 Rotarod task

A rotarod task (Ugo Basile, Italy) was used to assess motor learning and co-ordination. This consisted of a rotating rod 30 mm in diameter, with five separated chambers 57 mm in width, with a rod elevation of 160 mm. If the mice fell, they were continuously replaced on the rotating rod, until the 300sec-session was over. This prevented any confounds from arising from overall differences in time spent on the rotarod across sessions. Motor learning was assessed across six rotarod sessions, one morning session and one evening session on three consecutive days. The rod speed accelerated incrementally from 5-50rpm across the 300sec session.

The latency to fall was recorded for each animal and each session. In a separate session and in order to assess motor coordination the mice were given one 300-sec session at 10rpm, 20rpm, 30rpm, 40rpm and 50rpm consecutively in one morning session. Again the latency to fall was recorded for each animal at each speed.

3.2.9 Locomotor activity

Spontaneous locomotor activity (LMA) levels of control and *Ehmt1*^{D6Cre} mice were measured in custom-made activity chambers, across five consecutive days. These apparatus consist of twelve clear Perspex chambers (21cm x 36cm x 20cm) with two embedded transverse infrared beams each cage, 30mm from each end and 1cm from the floor. Beam breaks were recorded as an index of activity, by custom written software (Dr. Trevor Humby) with additional interfacing by ARACHNID (Cambridge Cognition Ltd, Cambridge, UK). Subjects were individually placed into the activity chambers and allowed to move freely for 2hrs. Data recorded were the total number of beam breaks. The measures were broken up into the number of 'runs' (scored as consecutive breaks of the two separate infrared beams), or 'breaks' (single beam break episodes) in each of the 5-min bins over the 2hr sessions. Activity levels were always measured during the early light cycle, between the hours of 08:00 and 13:00. Data from the first and final two sessions were analysed; this provided a measure of activity in a novel environment (session 1) and baseline, habituated activity (session 4 and 5)

3.2.10 Statistics

All data were analysed using SPSS 20 (SPSS, USA). The statistical differences between groups were analysed using independent samples t-tests, ANOVAs, or where appropriate Repeated Measures ANOVA (RP-ANOVAs). The main between subject factor was genotype (controls or *Ehmt1*$^{D6Cre/+}$) and the following within-subject factors were also analysed: day (day of testing: LMA and the 3 days of locomotor learning), bin (time bin: 5-min bins across day 1 LMA, 5-min bins across day 1 locomotor learning), session (locomotor learning), or RPM trial (Locomotor coordination). To check for normal distribution, Mauchly's test of sphericity of the covariance matrix or Levenes test for equality of variances were applied. The more

conservative Huynh- Feldt corrections, with adjusted degrees of freedom are reported in cases in which test assumptions were violated. Finally all error bars reported represent the standard error of the mean (SEM).

3.2.11 Power Calculations

There are numerous measurements of effect size known, many of which are based on the type of statistics used; for example in regressions and ANOVA analysis Cohens F^2 is often reported while other means test, like the Student t-test, Cohen's *d* is often reported. The desired effect size is essential for determining the ideal sample size. In cases such as the one at present, in which a new knockout model is being tested, its difficult to estimate the expected effect size (Ref). Looking for very small effect size may limit interpretation of the data. Thus, it is ideal for such experiments to minimally with have 90% power to detect a medium effect size of δ =.50/.75 with an alpha value of .05 (Wahlsten, 2006).

When considering effect size in behavioural experiments previous published reports are valuable. Among common inbred strains of mice, variation can be quite large. Meanwhile, in a review of behavioural phenotyping of transgenic and knockout mice by Crawley (1999), the number of animals for experimental designs and appropriate statistics for +/+ wild type littermate controls, -/+ heterozygotes and -/- null mutants is $N = 10$ in each case (if all the same gender is used). In order to carry out a power analysis, the standard deviation of the experimental units is required. Therefore in a case in which there are multiple experiments using numerous scales, standardised measures of effect are typical used. However, for exploratory purposes, and in order to test effect size for the smallest sample size (Control $N = 12$; *Ehmt1*$^{Dach6/+}$ $N = 16$) used in the behavioural tests reported here, the standard deviation from the amount of time spent in the central area in the Open Field test $\sigma = 13.23$; with Group 'A' mean $\mu_A = 13$; Group 'A' $\mu_B = 28$; for power .8 and $\alpha = .05$; the minimal sample size is 12 to establish a medium effect size of δ =.5.

3.3 Results

3.3.1 Peak expression of GLP in mouse embryonic development

Using wild type tissue, western blot analysis identified two peaks in GLP expression (Figure. 3.3). The first and largest peak was found at E14.5. There was a second postnatal peak in GLP protein at P7. G9a expression was similarly found to have higher prenatal expression patterns, however, there was higher expression of G9a at E18.5 specifically and more consistent postnatal expression. Thus unlike GLP, G9a did not show a distinct P7 peaks. Adults were found to have lower expression of both G9a and GLP. H3K9me2 peak expression occurs in the earlier stages, at E12.5-14.5, with significant decreases after E14.5.

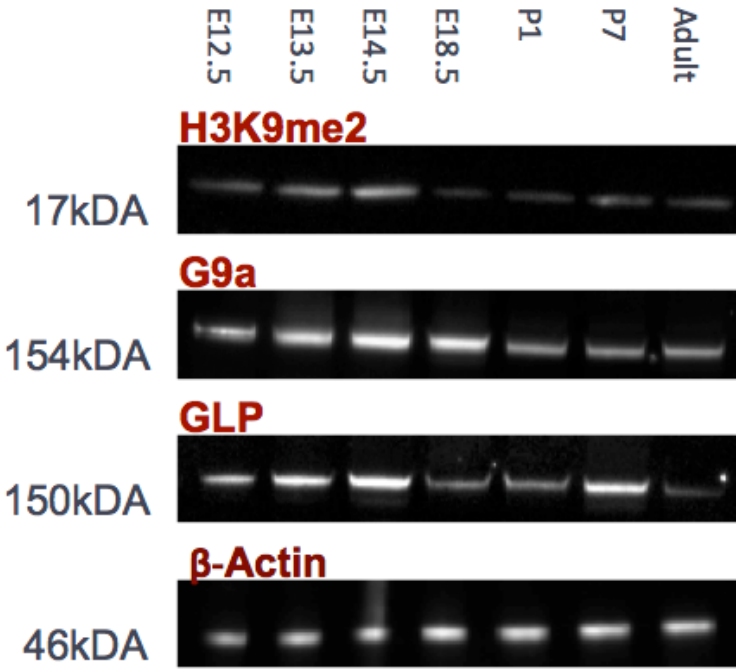

Figure 3.3 Protein expression
H3K9me2, G9a and GLP protein expression throughout brain development. β-Actin is used as internal control.

3.3.2 D6-Cre specificity in *Ehmt1*^{D6Cre} mutant mice forebrain

Verification of Cre specificity was assessed by PCR. For mutant and control mice, the hippocampus and forebrain were removed to check for the presence of the Cre deleted allele. Cerebellum tissue was used as a negative control. As expected, for those animals with positive cre expression, we find the deleted allele is found in both the hippocampus and the PFC, but not in cerebellum (for example PCR, see Appendix Chart 3.2).

3.3.3 *Ehmt1*^{D6Cre} litters display normal Mendelian ratios

Across the course of experiments reported in this thesis, 16 litters were born to 6 breeding females (3 controls and 3 *Ehmt1*$^{D6\text{-}Cre/D6\text{-}Cre}$), the average litter size was 9.67 (SEM: ± .89). There was no difference in the ratio of males to females t (2, 30) = -.106, p = .916. Nor did the proportion of mutant animals born significantly deviate from the expected 50%, t = 1.312, p = .211.

3.3.4 *Ehmt1*^{D6Cre} mutant mice display normal body weight

Weight was monitored from the week before behaviour experimentation began and throughout the experimentation period. Overall animal weights remained consistent and all animals were healthy. There was a main effect of time $\boldsymbol{F}$ **(1,59) = 4.626,** $\boldsymbol{p}$ **= .04**, the animals weight increased during the experimentation period, as they got older and as might be expected. However, there was no main effect of genotype F (1, 59) = .111, p = .741, or interaction between time x genotype, F (1, 59) = .126, p = .726.

3.3.5 *Ehmt1*^{D6Cre} mutant mice display barbering phenotype

Barbering is fur and whisker trimming associate with noticeable hair loss and bald patches. It is a behaviour not uncommon to laboratory rodents and in C57BL has been found to occur at a frequency of 27/788 (Long, 1972), or about 3% of mice. This behaviour is found at a rate of 9/28 males in behavioural cohort 1 and 9/33 males in behavioural cohort 2 or in 27-32% of the male mice. When comparing the barbing frequency in these mice with that found in a wild type C57BL population

(reported by Long, 1972), there was a significant increase in the phenotype X^2 = 57.34; $p < .001$ (see Figure 3.4).

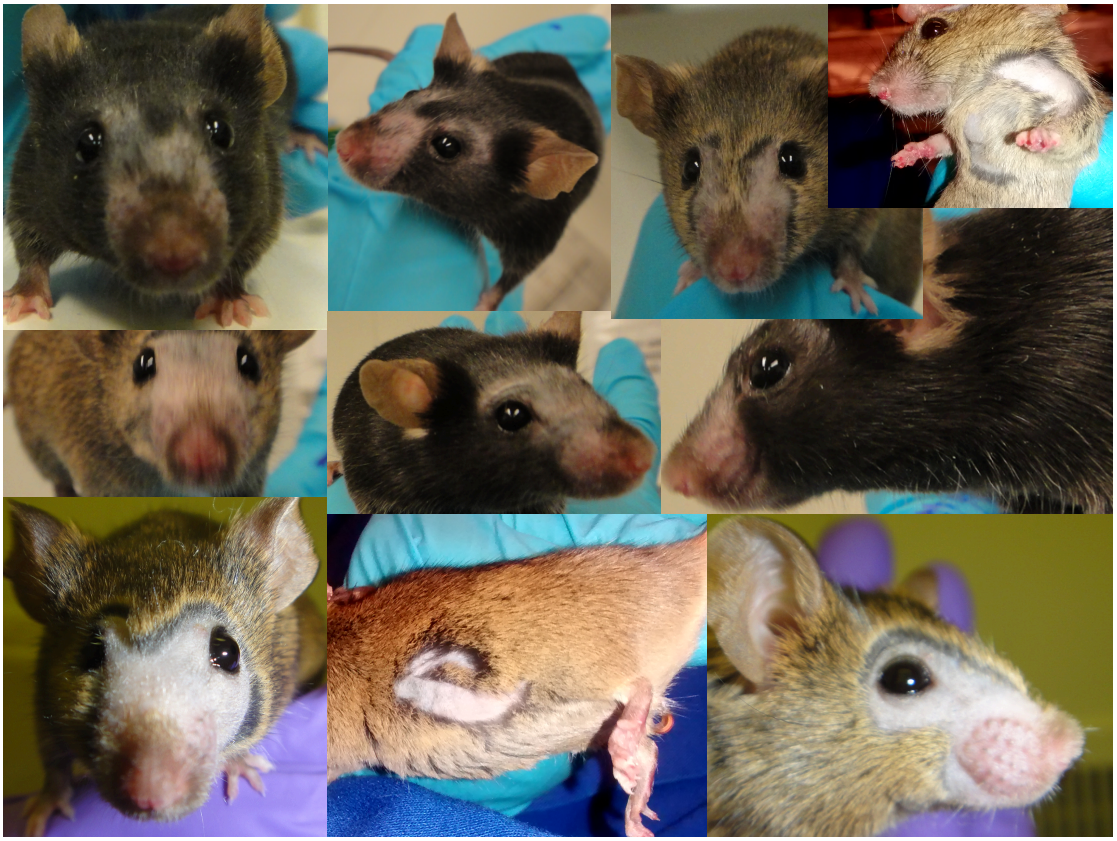

Figure 3.4 Barbering phenotype
There was a 10-fold increase in the number of mice normally observed to have undergone barbering in the mixed genotype groups.

3.3.6 *Ehmt1*^{D6Cre} mutant mice forebrain structure

Histology was performed on $N = 6$ *Ehmt1*$^{D6Cre/+}$ mutant mice and $N = 4$ control mice. Brain anatomy was visually compared, with focus specifically on cortical and limbic structures. Deficiency in GLP throughout neuronal development had no apparent impact on the gross structural organization of the affected regions. There were no apparent changes in cortical layering or in the substructures of the hippocampus. Similarly while histological techniques limited the opportunity to count cells, there did not appear to gross differences in cells numbers, however further quantification

is warranted, and further quantification is necessary especially in neuronal morphology (Figures 3.10-3.).

3.3.7 *Ehmt1*^{D6Cre} mutant mice demonstrate normal motor functions

In the locomotor learning task all animals showed motor learning across sessions, measured by an increase in the latency to fall of the rota rod. The average time spent on the rod was well over double between the first session, with an average of 91-secs and 102-secs before the first fall in controls and *Ehmt1*$^{D6Cre/+}$ mutants, respectively; and the sixth session, with 243-secs and 221-secs before first fall in controls and mutants, respectively. Thus there was a significant main effect of session, $\boldsymbol{F\ (5, 130) = 21.325, p < .001}$. However, there was neither a main effect of genotype $F(1, 26) = .121$, $p = .731$; nor an interaction effect between session and genotype, $F(5, 130) = .668$, $p = .648$, suggesting both populations of mice had similar patterns of motor learning (Figure 3.5).

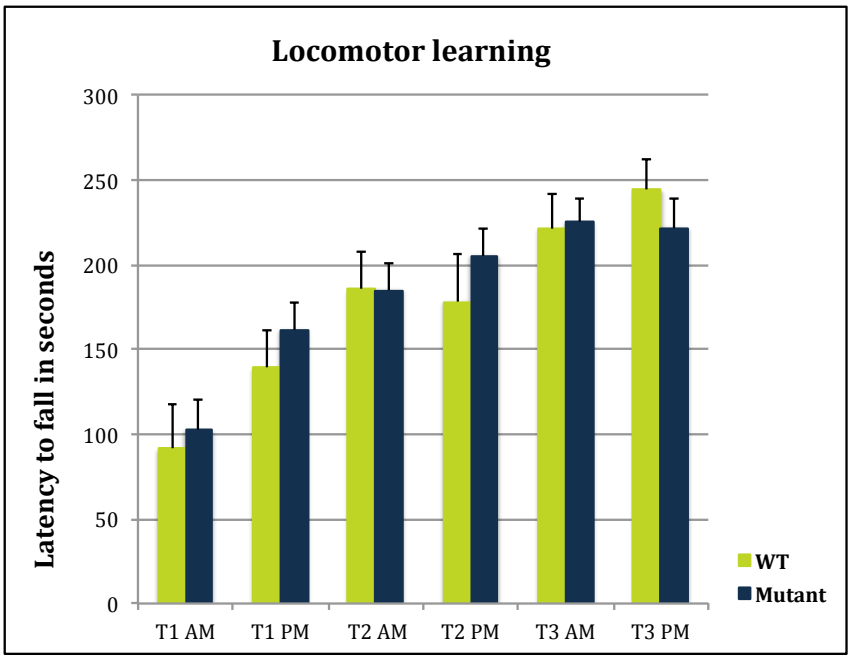

Figure 3.5 Locomotor learning—latency to fall across 6 sessions.
No differences were found in the latency to fall from the rotarod across the 6 sessions of locomotor learning.

In the locomotor coordination task there was a decrease in the latency to fall as the rod speed was increased; inasmuch there was a significant main effect of the speed of the rod rotation, ***F*(4,104) = 38.380, p < .001**. However, there was neither a main effect of genotype, $F(1, 26) = .673$, $p = .420$; nor an interaction effect between session and genotype $F(4, 104) = .649$, $p = .629$ (Figure 3.6).

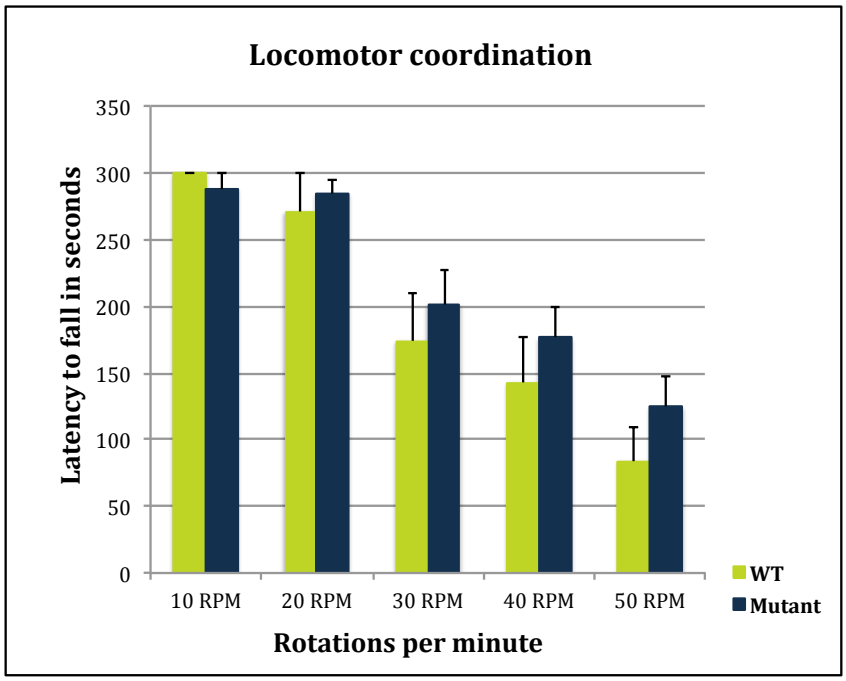

Figure 3.6 Locomotor coordination—latency to fall with increasing speed.
No differences were found in the latency to fall off the rotarod with increasing speed.

3.3.8 *Ehmt1*^{D6Cre} mutant mice are less active

Activity levels were analysed by looking at both the number of single beam breaks or 'breaks' and the number of consecutive breaks of the two separate infrared beams or 'runs' in each of the 5-min bins over the first 2hr sessions. In addition individual bin averages were compared across days 1, 4 and 5 of activity. In the first

2hr session, all mice were found to habituate to the activity chamber, as a gradual decrease in beam breaks was found throughout the session. Thus when comparing across the five-min bin data in the task using RM-ANOVA, a significant main effect of bin for the number of breaks was found, $\boldsymbol{F\ (10.46, 282.28) = 29.868, p < 0.001}$. There was a significant main effect of genotype, $\boldsymbol{F(27,1) = 5.348, p = .029}$; however, there was no interaction between bin and genotype, $F(10.46, 282.28) = 1.093$, $p = .367$ (Figure 3.7). A similar pattern was observed for the number of runs across the 5-min bins, there was a main effect of bin $\boldsymbol{F(13.532, 365.361) = 32.577, p < .001}$. There was a main effect of genotype, $\boldsymbol{F(1, 27) = 6.152, p = .020}$. However, no interaction between bin and genotype, $F(13.532, 365.361) = 1.058$, $p = .395$ (Figure 3.8).

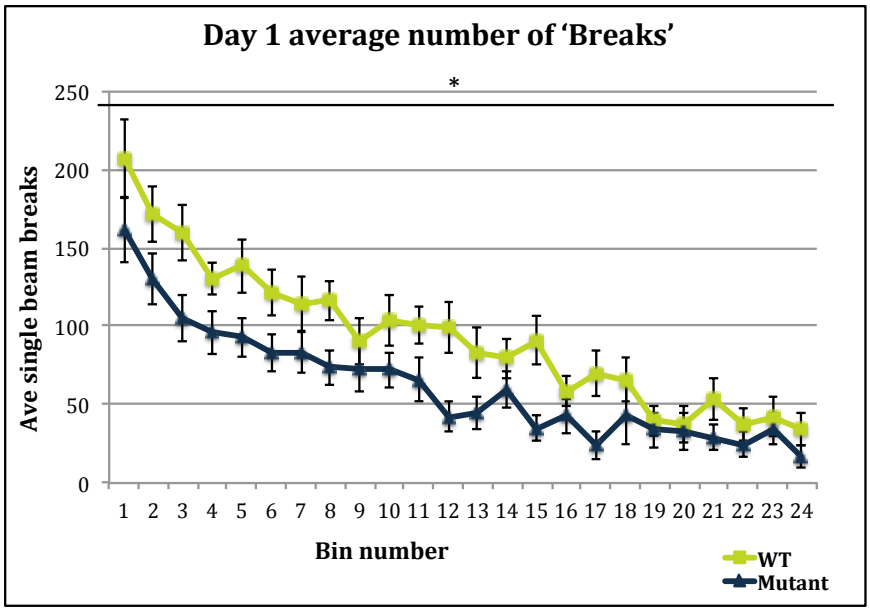

Figure 3.7 Number of single 'Breaks' across 5min time bins on day 1.
Mutant mice were significantly less active on day one across all time bins at $p = .029$. However, there was no interaction between genotype and bin, suggesting the same rate of habituation occurred across genotypes.

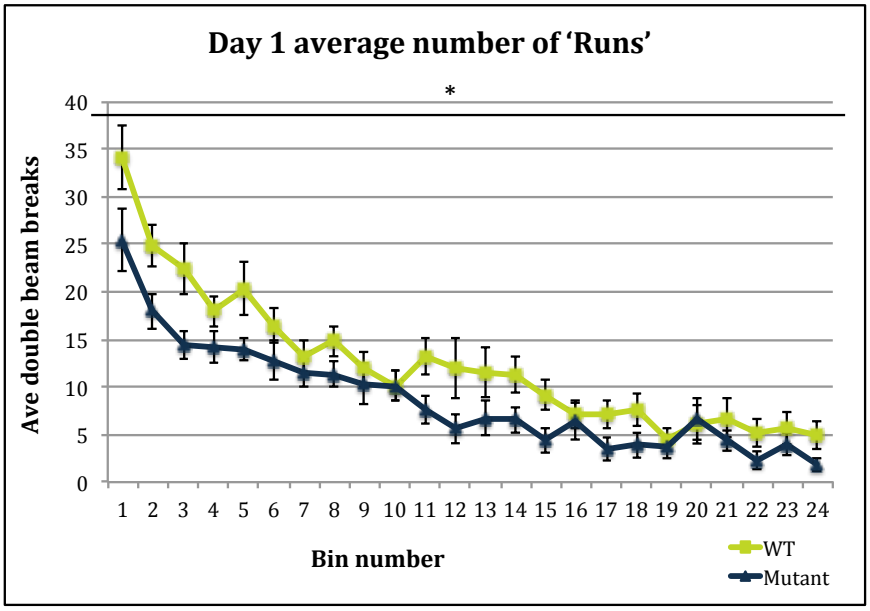

Figure 3.8 Number of 'Runs' across 5min time bins on day 1.
Mutant mice were significantly less active on day one across all time bins at $p = .020$. Again, there was no interaction between genotype and bin, suggesting the same rate of habituation occurred across genotypes.

When the total number of breaks were compared across the three days, using a RM-ANOVA, there is a significant main effect of day, ***F*(1.774, 47.911) = 59.474, *p* < .001**; and a significant main effect of genotype, ***F*(1, 27) = 6.335, *p* = .018**. However there was no interaction between the day and genotype, $F(1.774, 47.911) = .617$, $p = .512$ (Figure 3.9A). Again the same pattern can be observed for the total number of runs. There was a significant main effect of day, ***F*(1.808, 48.810) = 58.381, *p* < .001**; and a significant main effect of genotype, ***F*(1,27) = 7.027, *p* = .013**. However, there was no interaction between day and genotype, $F(1.808, 48.810) = .930$, $p = .386$. (Figure 3.9B).

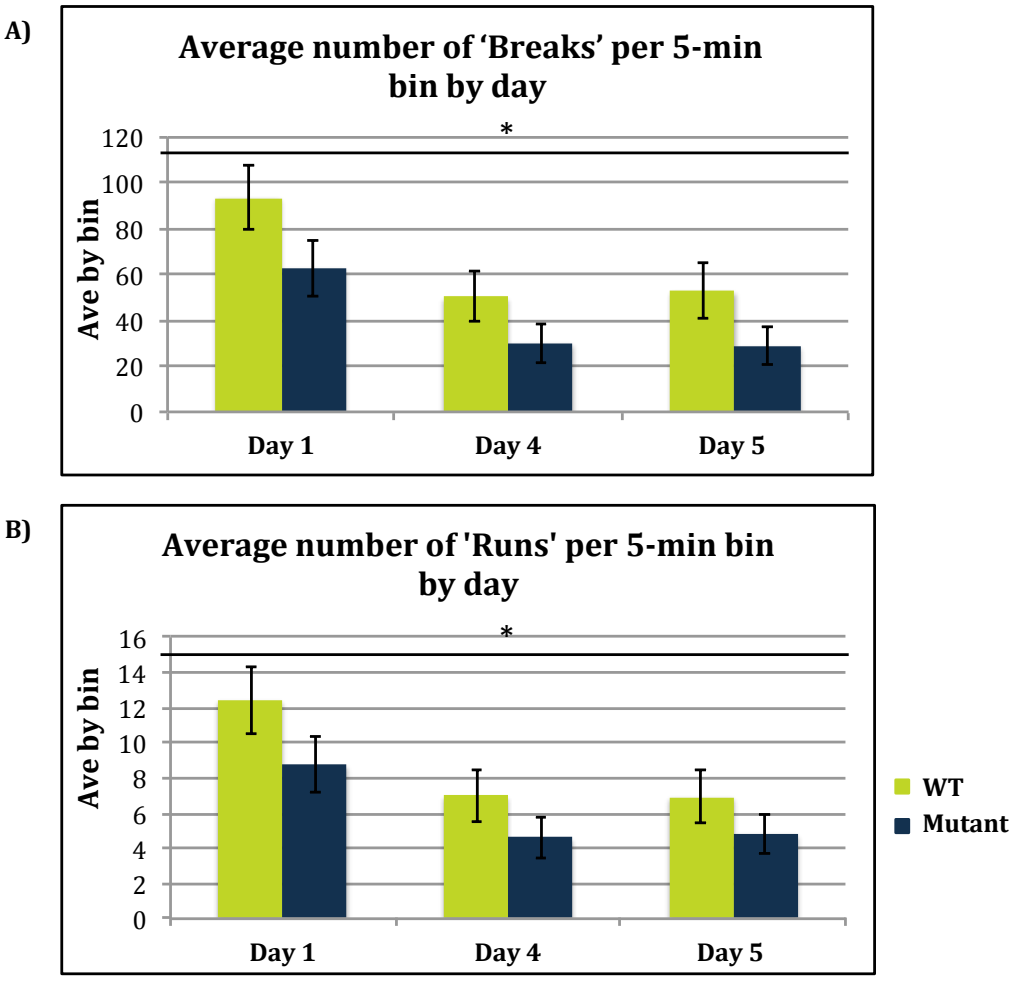

Figure 3.9 Activity across days
A) Average number of breaks by bin across the three days of activity. Mutants demonstrated a significant reduction in breaks across the 3 days, $p = .018$. **B)** Average number of runs by bin across the three days of activity. Mutants demonstrated a significant reduction in runs across the 3 days, $p = .013$.

3.4 Discussion

In this chapter the *Ehmt1*$^{D6Cre/+}$ mutant mouse was designed and the basic phenotype describe. These mice demonstrated normal breeding and weight patterns; they did not have changes in locomotor learning or coordination; and gross cortical morphology appeared normal. However, they did have a hypoactive phenotype—which is corroborated by previous models of *Ehmt1* disruption. Finally, the mixed-genotype cage groups were found to have above normal levels of whisker and hair barbering.

3.4.1 GLP peak expression in prenatal development

Western blot analysis demonstrated peak expression of the GLP enzyme occurs during prenatal and early postnatal periods of brain development. Expression of GLP in adult brain tissue was markedly reduced compared to developmental periods. The peak expression of GLP, in prenatal stages may suggest this enzyme plays an important role in neural development and differentiation. A distinct peak was found at E14.5, a stage in development, while the second peak at P7.

Unfortunately the direct role of GLP in telecephalic expansion at E14.5, or in pruning and the transitional change in receptor subtypes in the forebrain at P7 cannot be established from the analysis of whole brain protein extraction. While further examination is warranted, we do find the regional-specific expression patterns of GLP reported in the literature may align with evidence suggesting GLP may be involved in these important developmental benchmarks. For example, using in situ hybridsation, Kleestra reported the highest level of GLP expression between E14.5-E16.5 occurs in the developing telencephalon, with much less expression occurring in the midbrain or hindbrain (2005). Ultimately however, a considerable amount of work remains to establish the specific role of GLP in these activities during brain development.

The expression patterns of GLP are very similar to that of the similar methyltransferase, G9a. As reviewed these enzymes form a stable heteromeric complex and are found to have largely overlapping function, though not entirely

redundant function (Shinkai & Tachibana, 2011). The slight differences in pattern of expression levels reported here however, may in fact reflect subtle, but important differences in their activities during neural development—for example the unique GLP peak at P7, or the slightly greater expression in G9a at P1. We also find the corresponding patterns of G9a/GLP modification—H3K9me2 reflects the same gradual increase in expression during prenatal development, with a sharp decrease after P1.

3.4.2 Forebrain specificity of *Ehmt1*^{D6Cre} mutants

The extensive analysis of Dach1 cre-line reported in the literature, strongly predicts the deletion of *Ehmt1* in our model is restricted primarily to pyramidal neurons of the forebrain. Here analysis of Cre-mediated deletion of Ehmt1 appears to be specific to the forebrain structures, as reflected by the positive bands found in the mutant cortex and hippocampal structures, but not the cerebellum. However, further PCR analysis is necessary, as these data are not overwhelmingly convincing. Therefore, before any conclusions can be drawn about specificity, the PCR protocol is in need of further optimisation. Additionally, further analysis is necessary to determine cell-type specific deletion and region-specific deletion in this model. Furthermore, as consistency in Cre-deletion has not always been reported (Korets-Smith et al., 2004), it is also important to further establish consistency of deletion, within the different brain structures and across animals. In the future a more thorough analysis of GLP expression throughout cortical development in these animals is also very pertinent. However, due to a number of difficulties associated with generating these animals and the time constraints of the present work, the numbers of breeding pairs necessary for carrying out a developmental series of timed-mattings were not reached. However, such analysis is recognized as one of immediate importance.

3.4.2 Normal weight, breeding and forebrain structure in *Ehmt1*^{D6Cre} mutants

Importantly, the transgenic breeding program did not appear to affect Mendelian birth ratios or litter size. Similarly there were no differences in survival or health of the animals. Unlike the reduced body weight in early adulthood in the constitutive

hemizygous mice (Balemans et al., 2010) or the significant increase in body weight found at 5-6 weeks in the homozygous conditional KO mice (Schaefer et al., 2009), *Ehmt1*^{D6Cre} mutants did not have a weight phenotype.

There was no evidence of gross morphological changes in primary somatosensory cortical (Sup Figure 3.10 A & B), retrosplenial cortical (Sup Figure 3.10 C & D), or parietial cortical (Sup Figure 3.10 E & F) layers or structure. Neither did there appear to be any gross structural change in either rostral or caudual hippocampal structures (Sup Figure 3.10 E–I). This preliminary evidence is similar to that reported in both the global and condition *Ehmt1* KO mice. However, methods of further quantification are needed before conclusions can be drawn. Staining methods that allow focus on strictly neuronal populations would improve analysis and may allow calculation of cell populations. For example this model would especially benefit from the quantification of pyramidal neurons, as Cre-deletion targeted these cells. Golgi cox staining methods could be used to stain a percentage of neurons. Pyramidal neurons could then be identified based on their classic morphology, and quantified in different cortical regions. Such methods would provide an opportunity to assess dendritic complexity in these cells as well. In previous models, *Ehmt1* haploinsufficiency has been found to correspond with decreased complexity in dendritic branching and spine density (Kramer et al., 2011; Balemans et al., 2013). The expression and distribution of NMDA receptors would also aid in the interpretation of some of the present findings. Thus additional analysis of morphology at the cellular level is necessary.

3.4.3 Normal motoric function in *Ehmt1*^{D6Cre} mice

No differences were found in motor learning between controls and *Ehmt1*$^{D6Cre/+}$ mutant mice across the six motor learning sessions. Similarly there were no differences found in the motor coordination. In fact, there was a subtle trend for enhanced performance by the mutants in the two quickest speeds, at 40 and 50 RPM. Interestingly, a significant increase in latency to fall across rotarod sessions was also reported in the Camk2a conditional KO model as well. However, in this study the trend was non-significant. The lack of differences in motor learning and

coordination do have important implications for all further cognitive and behavioural analysis. In other words, any differences found in more complex behaviours cannot be explained by deficits in general motoric function.

3.4.4 *Ehmt1*^{D6Cre} mice demonstrate significantly reduced activity

Ehmt1^{D6Cre} mice had significantly reduced activity, on two measures (breaks and runs), in the LMA task. This difference was present from within the first 15-mins of the first session and persisted through to the final days of testing. This finding, coupled with no interaction between bin and genotype, suggests that controls and *Ehmt1*^{D6Cre} mice habituated to the locomotor boxes at the same rate and that the activity phenotype is one of general hypoactivity and not an adverse reactivity to a novel environment.

Evidence of reduced activity levels is corroborated across the three *Ehmt1* mutant mouse models. Schaefer et al., reported significant reductions in activity levels in a 60-min open field task, beginning within the first 10-mins of the task (2009). Similarly, Baleman et al., reported in two open field tests (30mins and 10mins, in two different behavioural cohorts respectively) heterozygous *Ehmt1* KO spent significantly less time walking, rearing or wall leaning and significantly more time grooming when compared to controls mice, in both groups (2010). However, these mice showed regular patterns of day and night time activity in their home cage. Thus differences found in activity levels in the open field task may suggest hypoactivity was novelty induced; and reductions in activity may be due to increased in anxiety that was also reported in these mice.

In summary, the *Ehmt1*-haploinsufficiency in the mouse forebrain throughout development did not result in gross motor or morphological dysfunctions that would be confounding to cognitive and behavioural assays. No effects were found on breeding or weight. However, the expression of GLP in the forebrain does appear to be important for normal activity levels, for as of yet unidentified reasons.

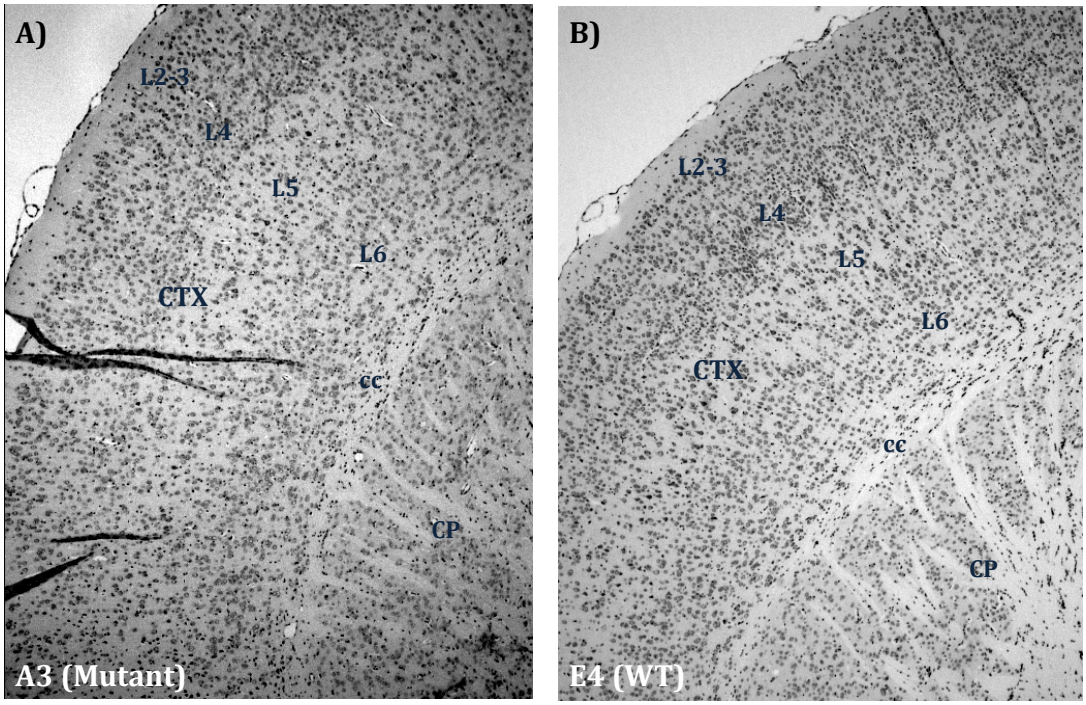

Figures 3.10 A & B) Primary somatosensory cortex.
CTX (cortex) L2-3 (layers 2-3) L4, L5, L6 (layers 4, 5, 6); cc (corpus collosum); CP (Caudoputamen).

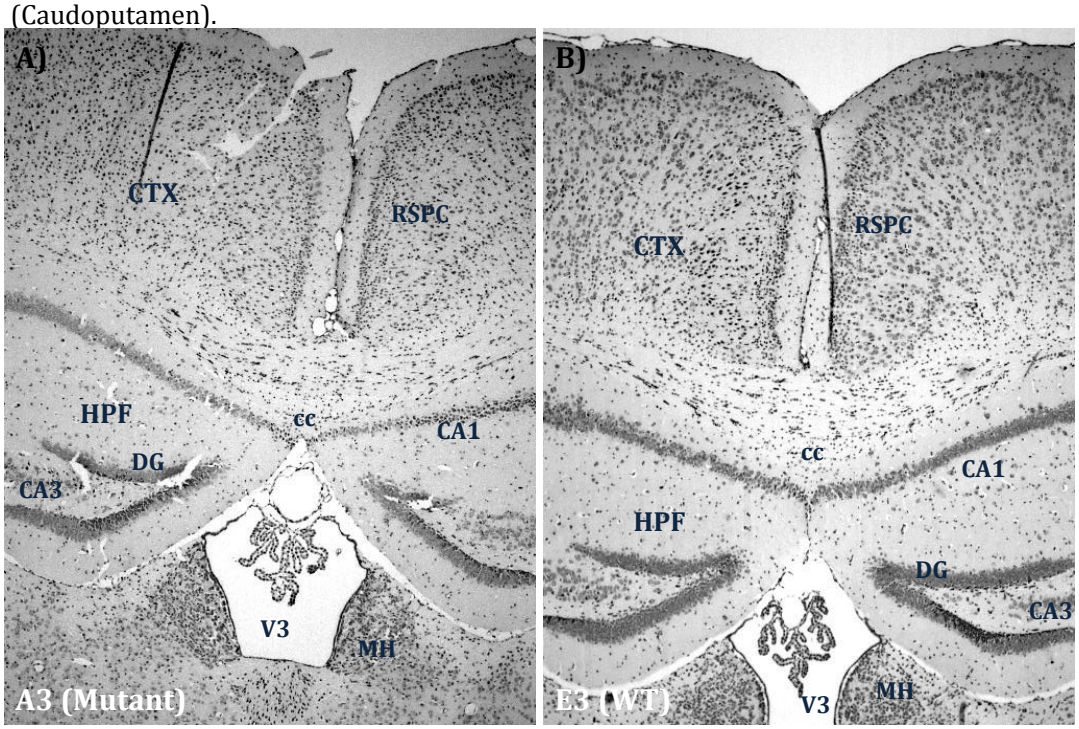

Figures 3.11 A & B Retrosplenial cortex & hippocampus:
HPF (hippocampal formation) CA1 & CA3 (cornu ammonis area 1 & 3), DG (dentate gyrus), MH (medial habenula), RSPC (retrosplenial cortex), V3 (third ventricle)

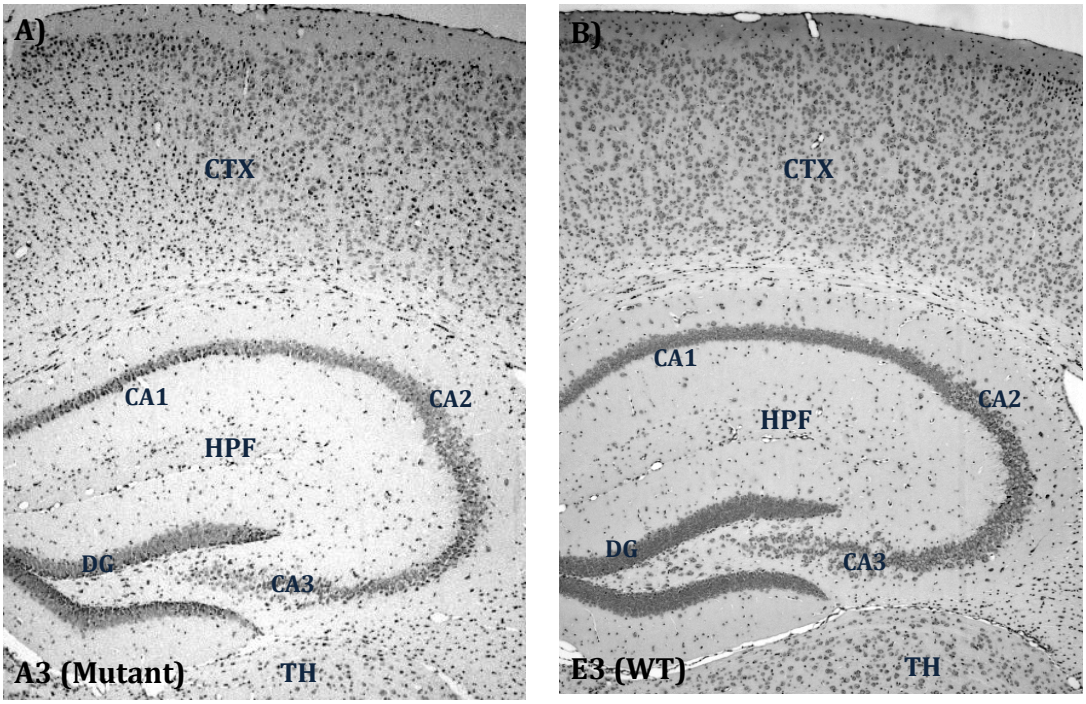

Figures 3.11 A & B Primary somatosensory cortex & hippocampus:
CA2 (cornu ammonis area 2); TH (thalamus).

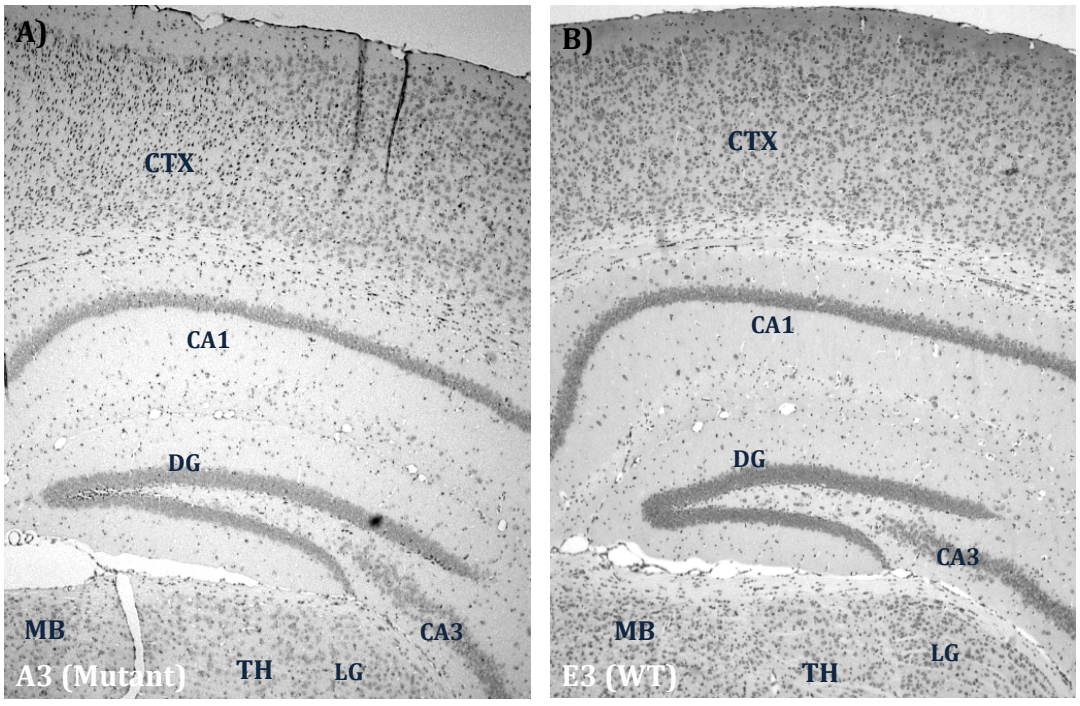

Sup. Figures 3.12 A & B Posterior parietial associated cortex & hippocampus:
LG (lateral genticulate complex of the thalamus); MB (Midbrain)

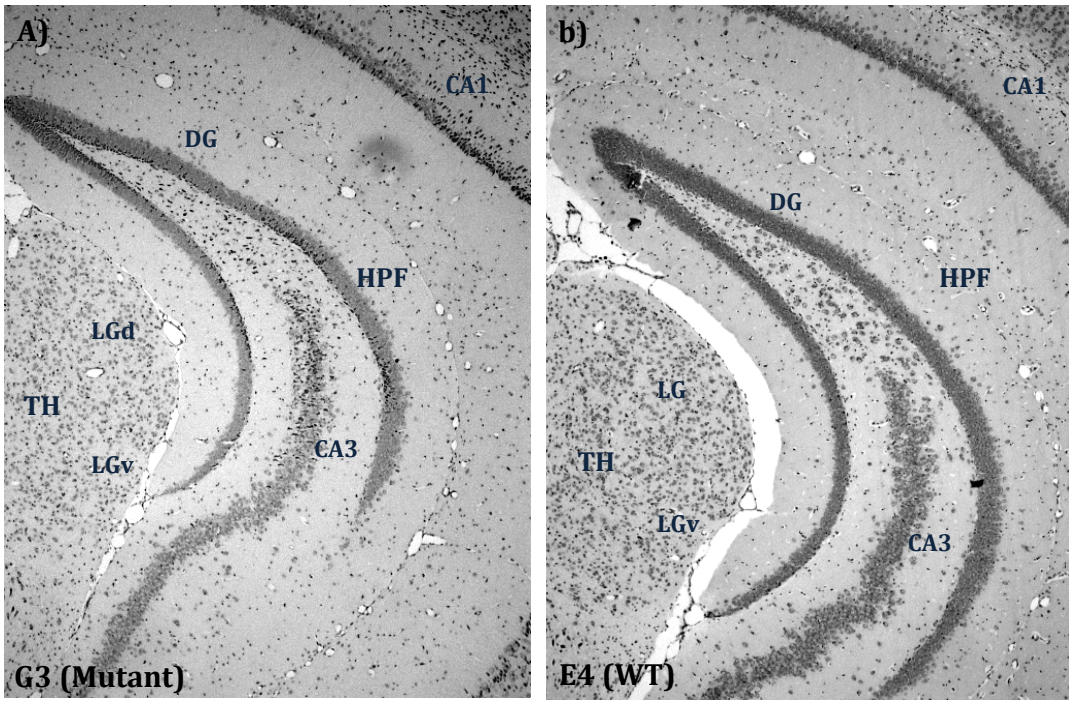

Figures 3.13 A & B Posterior hippocampal formation.

Chapter IV. Anxiety and novelty preference behaviour in *Ehmt1*$^{D6cre/+}$

4.1 General Introduction

In this chapter anxiety-related phenotypes are assessed in *Ehmt1*$^{D6cre/+}$ and *Ehmt1*$^{Flp/+}$ littermate controls mice. This work is first placed in the context of the overlap between anxiety disorders and those neurodevelopmental and psychiatric populations found to have disruptions in the *EHMT1* gene in humans. The relevant anatomical and neurochemical substrates of anxiety are briefly discussed and interspecies measurements of anxiety are reviewed. Finally three classic tests of anxiety-related behaviour in rodents are assessed—the Open Field Test (OFT), the Elevated-Plus Maze (EPM) and the Novel Place-Preference (NPP) test. Anxiety is a confounding artefact for evidence of deficits in learning, memory and social behaviour. The aims of this chapter are thus two-fold, first to establish whether there are any anxiety-related endophenotypes, which may allow us to consider the gross behavioural changes associated with *Ehmt1* disruption. Second, it is important to establish whether there are behaviour confounds, which are necessary to address prior to examining the cognitive deficits found in the NOR task in Chapter 5.

4.1.1 Anxiety in developmental disorders and intellectual disabilities

Estimates for the comorbidity of anxiety disorders in individuals with neurodevelopmental disorders, developmental delays and intellectual disabilities are often very high. However, the psychiatric literature pertaining to anxiety is extremely heterogeneous in the statistics reported, the methods of analysis and sample sizes used. In a recent meta-analysis of 52 studies looking at anxiety disorders in schizophrenia there was a mean prevalence of 38.3%; one of the highest disorder cormorbities reported being obsessive-compulsive disorder (OCD) at 12.1% (Achim et al., 2011). Estimates in children with ASD are often higher and

more varied. In a similar meta-analysis of reports published over a 10-year span, between 11% and 84% of children with ASD experience some form of anxiety disorder (White et al., 2009). In one study focusing on individuals with Pervasive Developmental Disorders (PDD) 43% of the 171 children assessed were found to have at least one anxiety disorder (Sukhodolsky et al., 2008, see also Davis et al., 2008). Interestingly, those with lower the IQ in this population, were less likely to have anxiety disorders than those with higher IQ and functional language use. Another report suggested the prevalence of anxiety is as high as 55.3% in those with PDD (de Bruin et al, 2007).

4.1.2 Anxiety as an ethologically important behaviour

Anxiety is marked by behaviour changes such at increased risk avoidance (Yates, 2013); and a rise in physiological measurements like respiratory rate, cortisol levels and increased startle, urination, defecation, freezing and heart rate (Davis, 1992). It is a behavioural and physiological response to the conflict that arises between response options (Barkus et al., 2010). Anxiety and fear may be distinguished by the concept of the 'defensive direction' (Gray & McNaughton, 2000). Where fear might lead to 'active avoidance' of a potentially dangerous situation (and may result in etiologically relevant responses like freezing or flight), anxiety instead may lead to 'passive avoidance'. In other words, fear is a response to an immediate threat and anxiety to a potential threat (Barkus et al. 2010).

4.1.3 Neuroanatomical substrates of anxiety

The underlying neurocircuitry of anxiety and fear is not entirely understood. However, both fear and anxiety are at least partially and differentially dependent on the amygdala and the ventral hippocampus, respectively (Gray & McNaughton, 2000). The central nucleus of the amygdala is found to have direct projections to both the hypothalamus and brainstem, which are areas also found important to fear response (Davis, 1992). Meanwhile, the ventral subregions of the hippocampus are believed to be important for anxiety. This region of the hippocampus is important for emotional processing, which has been suggested to mediate more anxiety-related responses; distinguishing it from the role of the amygdala (Davis, 1992).

The ventral hippocampus also projects directly to the prefrontal cortex, and shares connections with the amygdala and the hypothalamic-pituitary-adrenal axis (Bannerman et al., 2004). Finally, prefrontal cortical structures are believed to aid in interpretation of emotional stimuli and in modifying behavioural responses (Charney, 2003).

4.1.4 Measurements of anxiety in rodents

A majority of anxiety-related tasks in rodents involve conditioned fear responses (Charney, 2003). Those that are not conditioned fear related-responses often involve unconditioned exploratory behaviours or acute responses to stimulus—like freezing and startle behaviours. These types of behaviour examine the natural conflict that exists between tendencies to both explore novelty and avoid danger—also known as the approach-avoidance conflict (Ramos, 2008). The approach-avoidance conflict is ameliorated by the administration of anxiolytic drugs, for example rodents are extremely sensitive to benzodiazepine, like diazepam and chloridiazepoxide when administered (for review see Ramos, 2008). As a result exploratory behaviour in approach-avoidance conflict tasks is significantly increased, and subsequently believed to represent an anxiolytic-like phenotype.

Exploratory tests do rely on motor behaviours, which can be a confounding factor and must be assessed in the analysis. The three tests used here are all inter-related and based on "alternative indices for the same emotional construct (Ramos, 2008)." However, there do appear to be some differences in what the EPM and OF measure—as demonstrated by the dissociable effects pharmacological intervention that may suggest these test measure different psychobiological constructs (Vendruscolo et al., 2003).

4.1.4.1 Open field task

The open field test (OFT) relies on rodents' aversion to open, brightly lit spaces. The arenas are typically much larger than their home cage. Normal rodent behaviour would predict the vast majority of time spent close to the walls and away from the

centre of the arena. Therefore, measurements of exploration in the central area of the arena is considered an indicy of anxiety-related behaviours.

4.1.4.2 Elevated plus maze task

Like the OFT the elevated plus maze (EPM) indexes an innate aversion to open spaces in rodents. It is one of the most common tests of anxiety used. It measures the time spent in an unprotected, elevated and open arm (Pellow et al., 1985). Like the OFT, the EPM is found to be very sensitive to anxiolytic drugs, as administration is found to drastically increase the time a rodent spends in the open arm (Engin et al., 2009; Garcia et al., 2011; Vendruscolo et al., 2003)

4.1.4.3 Novel place preference task

The novel place preference test (NPP) explicitly tests an animal's willingness to explore a novel environment. It is conceivable that anxiety (i.e. an aversion to the novel environment) may be an influence on behaviour in this task, although experiments with anxiolytics suggest that this is not the case, and instead, that the major factor is the rewarding property of the novel environment (Klebaur & Bardo 1999). Furthermore, previous work has demonstrated how differences in these traits can be teased apart in geneticall manipulated mouse models (Plagge et al., 2005; Grailhe, et al., 1999). Nevertheless the preference for a novel environment is an important part of the overall package of examining anxiety and anxiety-related behaviours, not least of which, an altered willingness to explore a novel environment could be a confounding factor in the OF and EPM test.

4.2 Methods

4.2.1 Animals and housing

All mice were group-housed (3-5 per cage) in environments enriched with cardboard tubes, shred-mats and tissue paper, in temperature and humidity controlled animal holding room (21 +/- 2°C and 50+/- 10%, respectively) with a 12 hour light-dark cycle. All cages included both *Ehmt1*$^{D6cre/+}$ and control animals.

Standard rodent laboratory chow and water were available *ab libitum*. Animal cages were cleaned out weekly. All testing took place between 07:00 and 19:00 and at the same time of day for each task. For further details see Chapter 3, Sections 3.2.1-3.2.4.

4.2.2 EthoVision Observer system

The EPM, OFT and NPP tasks all utilized the EthoVision Observer video tracking software (version 3.0.15, Noldus Information Technology, Netherlands) and an overhead digital camera. This software tracks all movements and activity of the mice in spatially defined regions within an apparatus or open arena. Activity is summarized over a series of frames (12 frames/sec) and allow for a range of descriptors about the movement and location of the subject. Animal movement was first calibrated using non-experimental mice of the same body size and coat colour.

4.2.3 Open Field Test

The open field test indexes an innate aversion to open spaces in rodents (Simon, 1994). The OFT arena is constructed of white Perspex (75cm x 75cm x 45cm (length x width x height) walls. For analysis purposes, the arena was subdivided into three virtual zones of concentric squares: the inner zone (20 x 20cm), middle zone (40 x 40cm) and outer zone (15cm periphery). All behaviour was quantified using EthoVision software. Animals were placed in the arena facing one of the four walls, in the periphery of the arena. Placement was counterbalanced across animals. Among the variables calculated were total time spent in the two central zones, the frequency of entries into the two central zones, the latency of first entry into the Inner zone and the number of rears. Animals were placed in the arena for ten minutes and each session was broken into 1 min intervals to assess performance within a session. Entering sooner and/or spending more time in the two inner zones are considered less anxious behaviours.

4.2.4 Elevated plus maze

The elevated plus maze (EPM) is constructed of black Perspex covered in white tape. The plus shape consisted of two adjacent arms, which were enclosed on the sides

(19 x 8 x 15cm, length x width x height) and two adjacent arms, which were open (19 x 8cm, length x width). The maze was 94cm above the ground and illuminated with an even low level white light. All behaviour was quantified using EthoVision software. Animals were placed in the centre of the maze facing one of the open arms and were allowed to explore the maze for 5 min. The EPM was divided in to 3 virtual zones – open arms, closed arms, middle. Among the variables calculated were duration and entries into each zone, time spent moving and rearing frequency. Entering sooner and/or spending more time in the open arms are considered less anxious behaviours.

4.2.5 Novel Place Preference

There were two boxes each 30cm X 30cm X 30cm (height X width X length); conjoined by a small door. The door was closed until the choice trial. Like other light-dark tasks, one box had black walls and black floors. The floor was covered in sandpaper in order to increase the valence of box—the side with the sandpaper was counterbalanced across genotype and whether received in the habituation and test trial or only the test trial. The second box had white walls and white floors. Both sides were equally illuminated. However, the dark side did have less reflecting light, due to the white tape on the white side. Mice were introduced to one side, either white or black (counterbalanced across genotype) and allowed to habituate for 60min. 24hrs later mice were placed in the habituated box and the door separating the two boxes was removed. Mice were allowed to explore the two boxes for 30mins. Measurements assessed include the distance moved and the duration moved during the habituation trial; the ratio of distance moved and time spent in movement between novel and non-novel sides, reported as 5min time bins across the 30min trial. Finally intra-individual preference for black and white box exploration was assessed using paired t-tests for both duration spent in the box and distance travelled.

4.2.6 Statistics

All data were analysed using SPSS 20 (SPSS, USA). The statistical differences between groups were analysed using the independent samples t-test, ANOVA, or where appropriate Repeated Measures ANOVA (RP-ANOVAs). To check for normal distribution, Mauchly's test of sphericity of the covariance matrix or Levenes test for equality of variances were applied. Huynh- Feldt corrections were applied as necessary, and adjusted degrees of freedom are provided. Finally all error bars reported represent the standard error of the mean (SEM).

4.3 Results

4.3.1 *Ehmt1*$^{D6cre/+}$ mutants display behavioural inhibition in Open Field test

As expected in the OFT when comparing the distance travelled in the inner two zones with the outer zone, there is a main effect of zone $\boldsymbol{F(26,1) = 492.845, p < .001}$. All mice preferred traveling in the outer zone significantly more than they travelled in the inner. There was a significant main effect of genotype, $\boldsymbol{F(26,1) = 5.510, p = .027}$; and also an interaction between zone and genotype, $\boldsymbol{F(26,1) = 12.361, p = .002}$. A post hoc t-test was run to compare the distance travelled in each zone independently by genotype. The main effect of genotype appears to be driven by the *Ehmt1*$^{D6cre/+}$ mice traveling significantly further in the outer zone $\boldsymbol{t(26,1) = -2.883, p = .008}$; and not the inner zone $t(26,1) = -.323$, $p = .746$ (Figures 4.1A-C). No differences were found in the latency to enter the inner zones, $t(26,1) = .06$, $p = .953$ or in the amount of time spent rearing, $t(26,1) = -.146$, $p = .885$. However *Ehmt1*$^{D6cre/+}$ mice had significantly greater frequency of entries into the inner zone compared to the control mice, $\boldsymbol{t(26,1) = -2.922, p = .007}$; and were found to spend a significantly greater amount of time in the inner zones compared to the control mice, $\boldsymbol{t(26,1) = -2.885, p = .008}$.

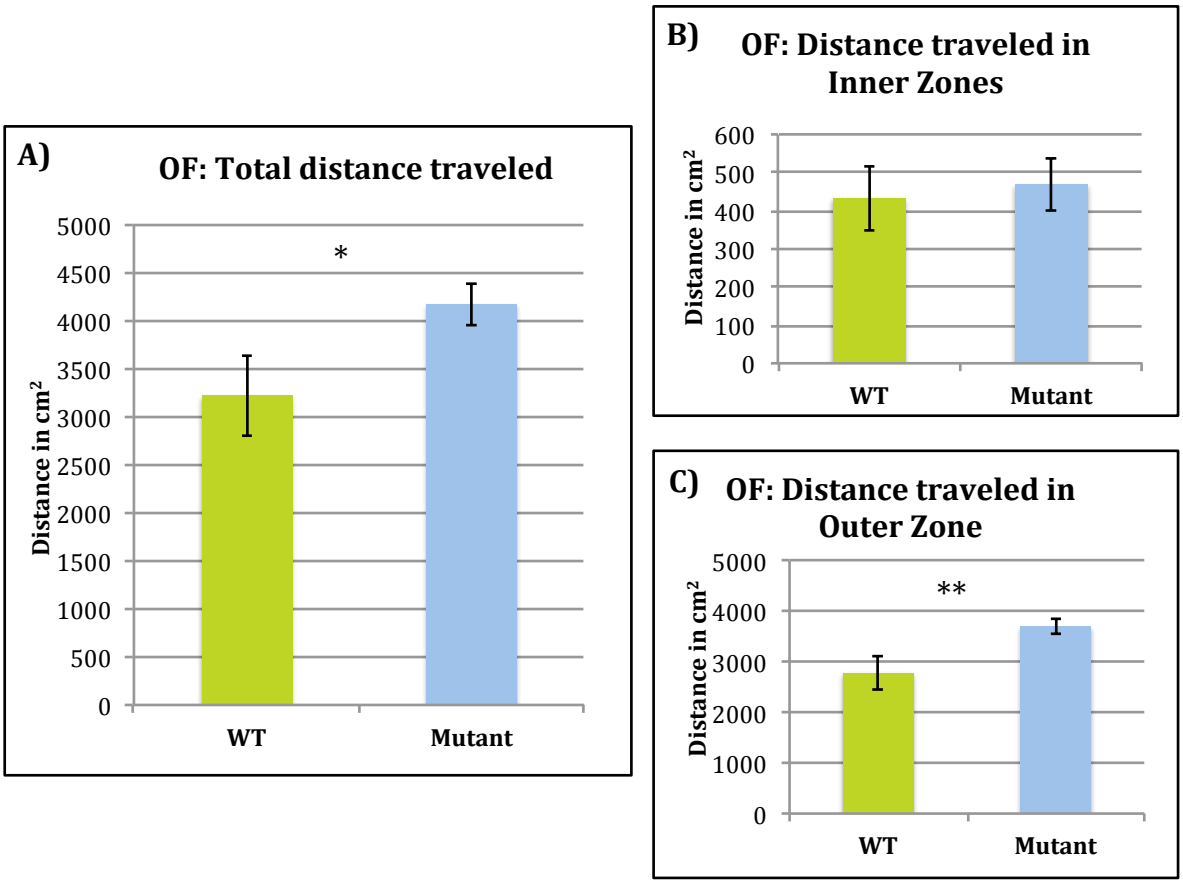

Figure 4.1 A-C Open Field Test distance travelled
A) *Ehmt1*$^{D6cre/+}$ mice travelled significantly more over the 10min OFT than control mice (p = .027); **B)** The distance travelled in the inner zones was not difference across genotype; **C)** The distance travelled in the outer zone was significantly different across genotype (p = .008), *Ehmt1*$^{D6cre/+}$ mice travelled more.

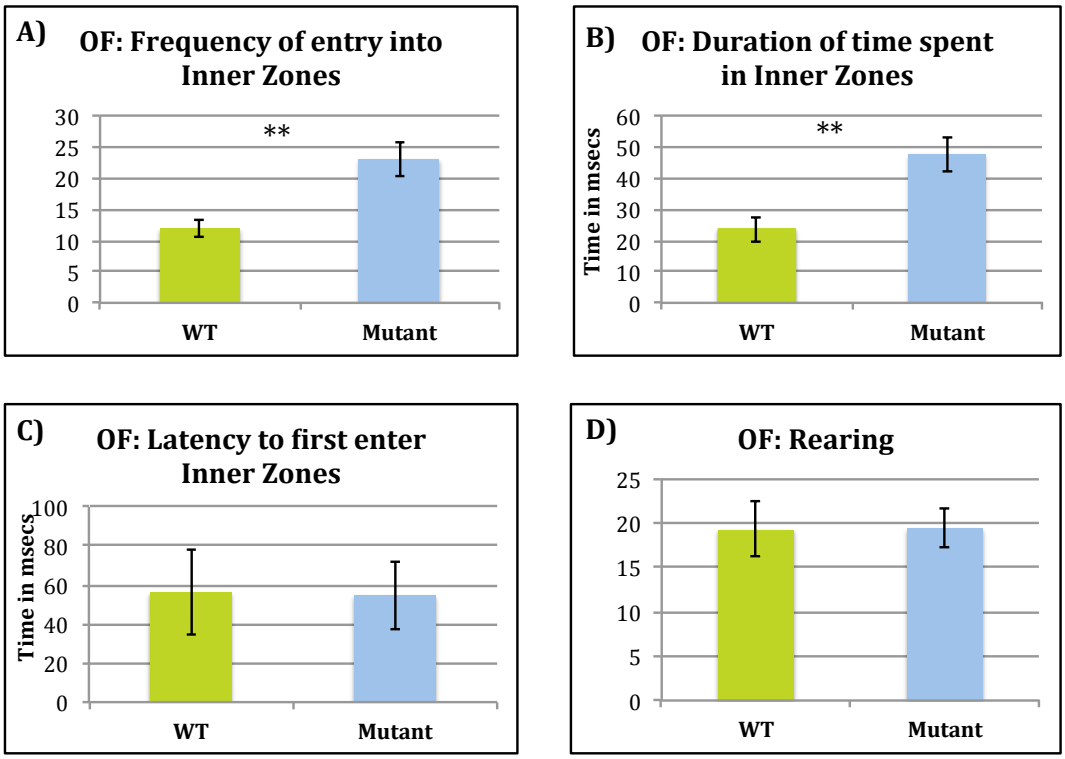

Figure 4.2 A-D Open Field Test
A) *Ehmt1*$^{D6cre/+}$ mice had significantly greater frequency of entries into the inner zone compared to the control mice *(p* = .007); **B)** *Ehmt1*$^{D6cre/+}$ mice spent a significantly greater amount of time in the inner zones compared to the control mice (*p* = .008); **C)** No differences were found in the latency to enter the inner zones (*p* =.953); **D)** No differences were found in time spent rearing *(p* = .885).

4.3.2 *Ehmt1*$^{D6cre/+}$ mutants display behavioural inhibition in Elevated Plus Maze

As expected, in the EPM we find a significant difference in the time spent in the closed-arm zone versus the central area and opened-arm zone combined. *Ehmt1*$^{D6cre/+}$ mice were found to spend significantly more time in the open arm compared to control, ***t*(26,1) = -2.076, *p* = .048**; but not in the central region *t*(26,1) = -1.303, *p* = .204, or the closed arm, *t*(26,1) = 1.857, *p* = .075. There was no difference in the total number of entries into any zone between genotype: in the closed arm, *t*(26,1) = -.356, *p* .725; central zone, *t*(26,1) = -.904, *p* = .374 or open arm *t*(26,1) = -1.522, *p* = .140. Finally, there was no difference in the latency to enter the

closed zone, $t(26,1) = -1.095$, $p = .284$ or the open arm zone, $t(26,1) = -1.522$, $p = .140$.

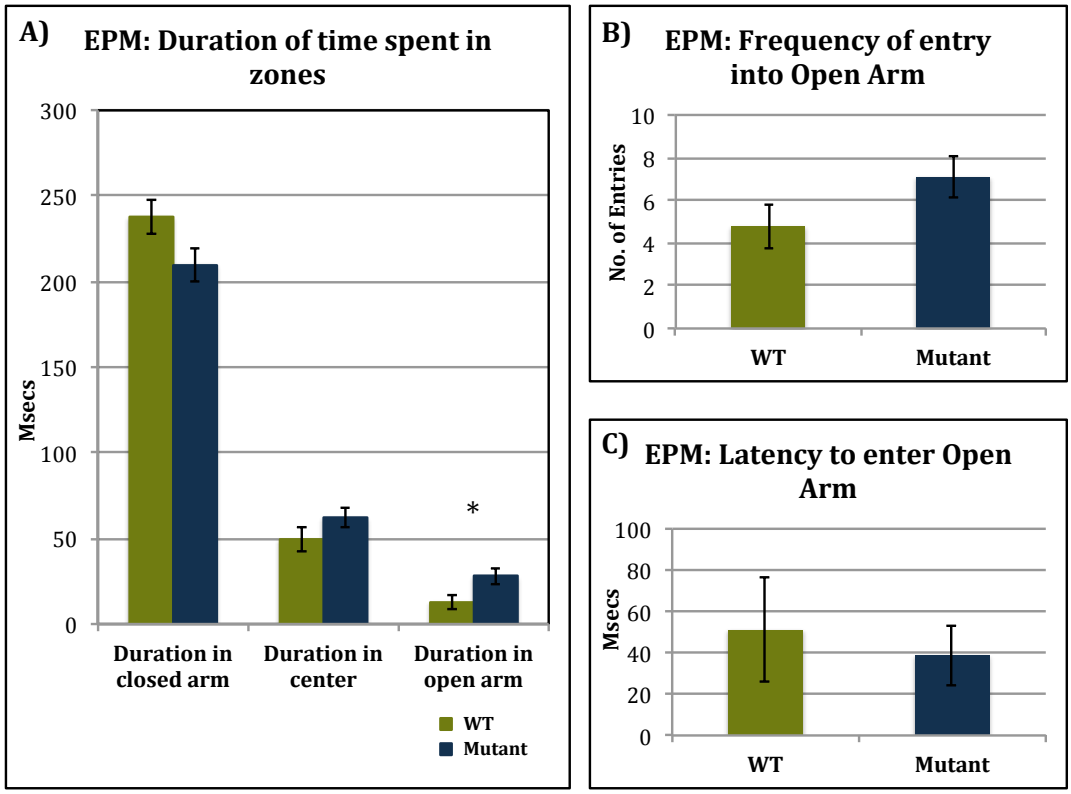

Figure 4.3 A-C Elevated Plus Maze
A) *Ehmt1*$^{D6cre/+}$ mice spent significantly more time in the open arm compared to control mice *(p =* .048); **B)** There was no differences in frequency of entering the open arm $p = .140$; C) No differences were found in the latency to enter the open arm ($p = .140$).

4.3.3 Novel place preference

Because differences were found initially in activity levels in Chapter 3, it was important to establish whether there were also differences in activity levels during the habituation trial. The distance travelled in the 60min habituation trial was compared using an RM-ANOVA. There was a significant main effect of 5min bin, ***F* (11, 324) = 12.094, *p* < .001**; however there was no main effect of genotype F (26,1) = .586, p = .451; nor an interaction effect of bin by genotype, F (11, 324) = 1.255, p = .251.The duration of time spent moving was also compared for the NPP habituation period. Again there was a main effect of bin number, ***F* (11, 324) = 18.930, *p* > .001**. However no main effect of genotype F (26,1) = .785, p = .384; nor an interaction between bin and genotype, F (11, 324) = 1.674, p = .079. Thus in this task there appears to be no differences between the genotypes in the distance travelled or the time spent moving during the habituation period.

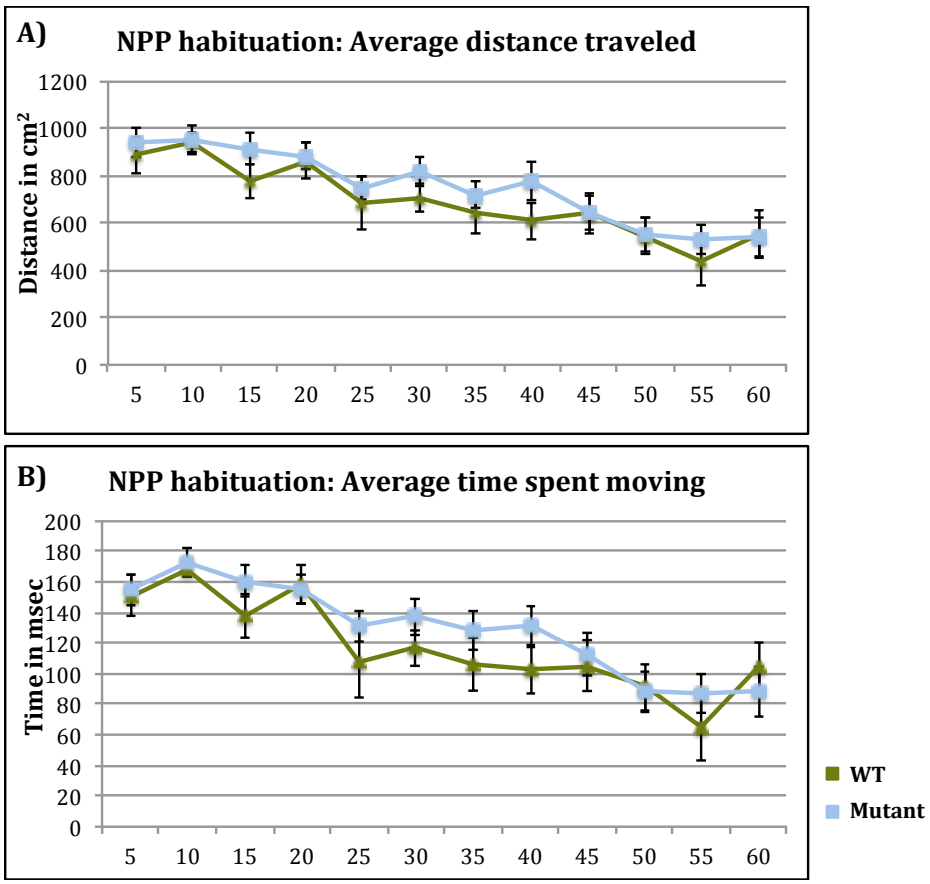

Figure 4.4 A&B Novel Place Preference habituation
A) No differences were found in distance travelled in NPP habituation**; B)** No differences were found in time spent moving.

Next we examined preferences for the light box verses the dark box in the test trial. A RM-ANOVA was run across the 4min time bins for the average duration spent in the white box and the black by genotype. There was no main effect of the box, F (26, 1) = .669, p = .421, nor of genotype, F (26,1) = .376, p = .545. There was an interaction between box and genotype, F (26, 1) = 4.680, p = .040.

Over the 30min choice trial, the differences in ratio of duration of time spent and distance travelled in the novel versus non-novel boxes were compared across 5min time bins. First, there was no significant difference across the 6 5min bins for the ratio of movement in the novel versus the non-novel, F (5, 125) = .6121, p = .684. There was no main effect of genotype F (26) = .043, p = .838; and there was no interaction between the time bin and genotype F (5, 125) = 1.834, p = .111 (Figure 4.6A).

In the analysis of the duration spent in the novel versus the non-novel condition, there was no main effect of the bin F (5, 125) = 1.439, p = 215. There was no main effect of genotype F (1, 26) = 1.016, p = .322; however there was an interaction effect between time bin and genotype was $\boldsymbol{F}$ **(5,125) = 2.712,** $\boldsymbol{p}$ **= .05** (Figure 4.5A). After running independent t-tests on each time bin, there was a difference across genotype **t (26) = -2.747, p = .011** in the first time bin. Mutant mice were found to spend in significantly more time in the novel box within the first 5mins of the test trial (Figure 4.6B).

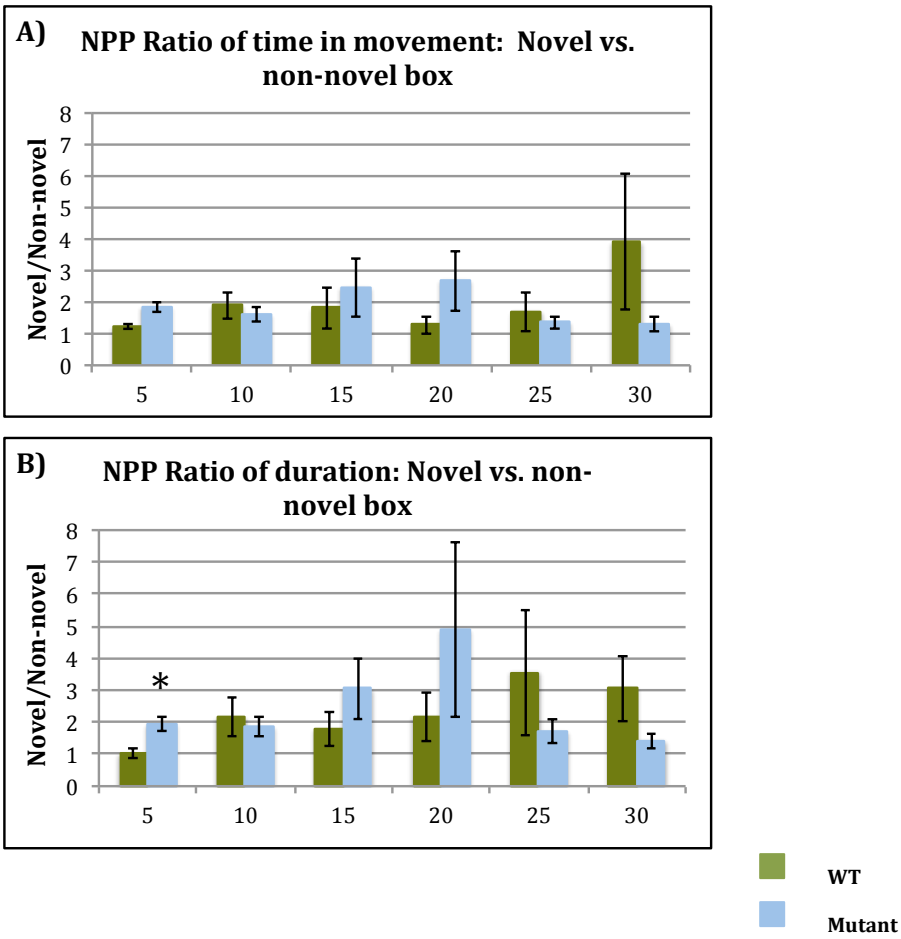

Figure 4.6 A&B Novel Place Preference: Novel vs. non-novel box preference
A) *Ehmt1*$^{D6cre/+}$ were found to travel more in the novel box in the first 5min time bin; **B)** *Ehmt1*$^{D6cre/+}$ mice spent a significantly greater amount of time in novel box in the first 5min time bin.

4.4 Discussion

The main results found in this chapter are that *Ehmt1*$^{D6cre/+}$ mutants entered the central zones more frequently and spent more time in this zone, in the OFT. They also spent significantly more time in the open arm on the EPM task. There was a trend for higher frequency of entries and decreased latency to enter the open arms in the EPM as well. In addition, *Ehmt1*$^{D6cre/+}$ mutant mice spent significantly longer and travelled more in the novel box, within the first five minutes of the NPP task. At face value, together these data suggest that *Ehmt1*$^{D6cre/+}$ mutant mice have reduced anxiety across several domains of behaviour.

4.4.1 Decreased anxiety behaviour in *Ehmt1*$^{D6cre/+}$ mice across tests

While these three test are believed to measure fairly similar indices, especially in studies of genetically modified animals; pharmacological interventions have revealed often differential effects, at least in the OFT and the EPM (Ramos, 2008). Nevertheless, consistent direction of effects in the OFT, EPM and NPP tests in *Ehmt1*$^{D6cre/+}$mutants present fairly strong support for what is often consider reduced anxiety in rodents.

The consistency in findings may be related to the fairly localised genetic lesion in this model. In studies considering the pharmacological effects on anxiety behaviours, often drugs are systemic administered instead of locally and involve numerous off-target effects (Barkus et al., 2010). For example, while Ketamine is a noncompetitive NMDA receptor antagonist it also has effects on opioid and dopaminergic transmission (White & Ryan, 1996). Thus the overlap in results across tests reported here, may be partially due to the more localised circuitry effects of the *Ehmt1*$^{D6cre/+}$ mutation.

Anxiety, emotionality and fear are multidimensional constructs that may only be accessed through several independent axes (Ramos, 2008). In rodents these axes may involve novelty, brightness, openness, pain, and loudness etc. Assays that distinguish between different environmental effects and subtle variations in the emotional constructs are essential for developing rodent models of anxiety. While the outcome of tests like the OFT in rodents are difficult to directly map onto human anxiety, clinical pathologies in humans are often triggered by specific environmental stimuli (White et al., 2009). Thus generating a portfolio of anxiety related indices in rodents like those explored here, may be the only way to draw parallels between human and rodent anxiety. That being said, further emotional testing in *Ehmt1*$^{D6cre/+}$ mutants is necessary before any conclusions can be made.

4.4.2 Novelty induced hyperactivity in Ehmt1D6cre/+ mice

In the 10min open field task *Ehmt1*$^{D6cre/+}$ mice were found to travel significantly further than control mice. However, this increased movement occurred only in the

outer zones. These data present a behavioural dissociation with those reported in the locomotor activity (LMA) task from Chapter 3. However, by looking further at the differences in time bins in the LMA, the significant reductions in activity, the *Ehmt1*$^{D6cre/+}$ mice did not occur until after the first ten minutes, on the first day of testing. Meanwhile, the OFT was only 10min in duration. Should the OFT task last longer, then a similar hypoactivity phenotype may have occurred.

Why there was not a similar trend—of increased activity levels in the *Ehmt1*$^{D6cre/+}$ mutants in the first 10min of LMA however, is unclear. It may be partially explained by differences in arena size and the conditions of the tests. The activity chambers are less than a fifth of the size of the OFT arena—so there was significantly more space to investigate in the OFT. In addition, the activity data was collected in a dark room, while the OFT arena was lit. Therefore the combination of a large well-lit space in the OFT may have resulted in greater levels of novelty induced hyperactivity in the *Ehmt1*$^{D6cre/+}$ mice, in this task. Previous work has shown illumination effects exploratory behaviour, and such behaviour is sensitive to pharmacological manipulation of different neurotransmitter systems (Garcia et al., 2011).

Furthermore, these two tests do not necessarily capture identical measurements of activity. The activity levels measured during LMA are determined by the number of times infra red beams are crossed; whereas the OF data is tracking all movements and thus the overall distance travelled. In other words, beam break measurements in the LMA task only capture movements along the longitudinal plane of the arena—or the number of times an animal transects the length of the chamber, but not the width. Therefore, beam break measurements could underestimate the overall distance travelled. Additionally, were a more fine-grained analysis of the first 10 minutes of the LMA task possible, this may have revealed an initial hyperactivity on the first day of exposure.

In support of the novelty induced hyperactivity theory, we find in the first time bin of the NPP task, *Ehmt1*$^{D6cre/+}$ mice spent significantly more time moving in the novel

box compared to the non-novel box. However, this was found despite similar levels of activity in the initial habituation trial of the NPP. Similarly, in Chapter 5 we find a significantly reduction in the latency to explore social novelty, in the social approach task. Thus, again there appears to be a greater impact of novelty on exploration and activity levels in the *Ehmt1*$^{D6cre/+}$ mutant mice.

Overall the mutant mice displayed reduced anxiety-like behaviour across two measurements in rodents, the EPM and the OFT. These mice appear to display novelty induced hyperactivity in these tests and in the first 5mins of the NPP test.

4.4.3 Limiations in anxiety phenotyping in Ehmt1D6cre/+ mice

The hypothalamic-pituitary-adrenal axis (HPA) found downstream of the ventral hippocampus and is the principal effectors of the stress response. The HPA axis is regulated by the synthesis and secretion of corticotrophin-releasing factor. The binding of CRF to pituitary corticotropes then leads to the release of adrenocorticotropic hormones, which in turn stimulates glucocorticoid synthesis. Glucocorticoids act as a feedback to the HPA axis to regulate physiological changes to stress (Sullivan & Gratton, 2002).

The HPA and stress response plays a key role in the regulation of anxiety and fear. One explanation for why the *Ehmt1*$^{Dach6/+}$ mice did not replicate the full range of anxiety-related phenotypes found in the Ehmt1$^{+/-}$ model is that normal expression of *Ehmt1* would be expected in the HPA and other subcortical structures involved in the regulation of stress and anxiety. The *Ehmt1*$^{Dach6/+}$ mice model only partially models the neurocircuitry of fear and anxiety; and indeed the phenotype reported is most similar to reports which model the effects of hippocampal dysfunction on stress, anxiety and emotional processing explicitly (Sullivan & Gratton, 2002). So while our model does not reflect the full range of potential anxiety phenotypes, it is fairly consistent with the anatomical specificity of the Dach6 genetic lesion and the expected forebrain dysfunction.

Chapter V. Neurodevelopmental endophenotypes in Ehmt1D6Cre$^{/+}$

5.1 General introduction

When modelling complex neurodevelopmental disorders like schizophrenia, autism and intellectual disabilities or those associated with *EHMT1* mutations, it is essential to evaluate more complex behaviours, especially those that share analogous mouse and human components. Furthermore, for the current model it is also important to consider behaviours and neurological function that are forebrain-dependent. In this chapter three endophenotypes relevant to neurodevelopmental disorders are assessed in *Ehmt1*$^{D6Cr/+}$ mutant mice and their control littermates. Differences in novel object recognition, sensory motor gating and sociability are evaluated.

5.1.1 Establishing *Ehmt1*$^{D6Cr/+}$ cognitive endophenotypes

Neurodevelopmental disorders, for the most part, have complex polygenetic architecture (Burmeister et al., 2008). It is unlikely the full spectrum of symptoms of any one of these complex disorders will ever be modelled in rodents, especially when the majority of rodent models involve the disruption of single locus. Furthermore, when assessing the role of an individual gene, like the *Ehmt1* model used here, it is more advantageous to consider discrete processes or endophenotypes, instead of the entire syndrome (Davis & Isles, 2014). An endophenotype is a concept that has gained considerable traction in psychiatric medicine. It's a term first coined by Gottesman and Gould (for review see, Gottesman & Gould 2003). The endophenotype approach sub-categorizes "components along the pathway between a defined risk factor (whether genetic or environmental) and the clinical syndrome (Pratt et al., 2012)." An endophenotype is a more narrow definition of disruption, which does not necessarily capture symptoms that define the clinical phenomenology of the disorder. Instead an

endophenotype may be a closer approximation of a gene-based neurobiological deficit than the illness itself (Braf et al., 2008).

The endophenotype approach is especially appealing for nonhuman research of neuropathology—where we might expect a stark contrast in illness symptomology between humans and rodents, but core processes and functions may have much greater interspecies overlap. The list of neurodevelopmental disorder-associated endophenotypes that are found to have neuroanatomical, neuropharmacological and behavioural equivalents in rodents is growing. To date the most promising models of schizophrenia and autism-related rodent models provide corroboration across a subset of endophenotypes (for reviews see, Amann et al., 2010; Kellendonk et al., 2009; Nestler & Hyman, 2010; Silverman et al., 2010). Several studies go on to demonstrate predictable pharmacological modulation or recovery, providing further evidence of homology in neural circuitry and function (e.g. Won et al., 2012). Among the strongest candidate endophenotypes for modelling neurodevelopment disorders and those evaluated here are: declarative and episodic memory deficits (this Chapter), reductions in general sociability (this Chapter), sensorimotor gating deficits (this Chapter), gamma oscillations (Chapter 6) auditory event related potential amplitude and gaiting deficits (Chapter 6), and impaired mismatch negativity (Chapter 6).

The behavioural tasks examined here were chosen, first in an effort to cover the broad domains in which we find shared endophenotypes across the neurodevelopmental and psychiatric populations with *EHMT1* disruptions: so cognitive deficits, abnormal social behaviours and sensorimotor gating deficits. Second, tasks choices were determined based on availability of apparatus and the considerable time constraints that had to be taken into account. Future studies and the additional tasks, which may be especially beneficial, are reviewed in the discussion.

5.1.2. Sensorimotor gating

The majority of overlapping phenotypes shared by schizophrenia and autism

diagnoses can be tied to gross deficits in attention and cognition. This is believed to be in part because patients are often unable to filter out intrusive stimuli (Belmonte et al., 2004; Greyer et al., 2001; Perry et al., 2007; Orekhova et al., 2008; Javitt, 2009). These disorders can be thought of as 'gating disorders' and are amongst a range of neurological and neuropsychiatric 'gating disorders', like Huntington's disease, Tourette's syndrome and obsessive-compulsive disorder (see Geyer et al., 2001). A common method of assessing sensorimotor gating deficits in both humans and rodents is examining auditory startle response (ASR) and prepulse inhibition of the startle response (PPI). In the instance of the former, habituation of the startle reactivity to a loud noise is assessed; while in the instance of the latter, a weak auditory prepulse is presented immediately prior to the loud pulse. The weaker prepulse is expected to lead to a rapid attenuation of the startle response (Braff & Geyer, 1990). The PPI is believed to measure an important adaptive function, which enables an individual to gate distracting stimuli and focus on relevant stimuli (Geyer et al., 2001).

5.1.2.1 The neurocircuitry of acoustic startle and PPI

As Swerdlow et al., reviews, PPI is regulated by sequential and parallel neural connections between the limbic cortex, the ventral striatum, the ventral pallidum, and the potine tegmentum (Geyer et al., 2001). The contribution of brain areas can be subdivided into those elements that mediate the activity and those that regulate the activity. Mediating brain areas are those that are phasically activated by the prepulse and thus respond to the prepulse the same as the startle tone (Fendt et al., 2001). Meanwhile, regulating brain areas provide tonic activity and regulate the PPI response by impinging on the mediating circuitry (for review see Swerdlow et al., 2001). For example, regulating components may impact on PPI through changes in attention states, pharmacological manipulations or neuropathological changes.

The regulating activity of PPI largely depends upon the striatum, the hippocampus, the medial prefrontal cortex, and the amygdala (Swerdlow et al., 2001)—the latter three are regions in which *Ehmt1* deletion may be expected in this mouse model. Meanwhile, manipulation of any of one of these areas results in disruption of the PPI

response. For example there is direct electrophysiological evidence of the important role of the hippocampus in sensory gating (Freedman et al., 1996). Similarly, individuals with temporal lobe epilepsy have disrupted PPI responses (Morton et al., 1994).

5.1.2.2 Pharmacological disruption of PPI

Four robust models of PPI disruption exist in rodents, those produced by DA agonists, 5-HT2 agonists, NMDA antagonists, and that which occurs after isolation rearing. These models have been developed from the strong association between neurotransmitter system dysfunction in schizophrenia (Geyer et al., 2001). All four models replicate decreases in PPI, and in some instances, enhanced startled, which mirrors those deficits found in schizophrenic populations (Braff et al., 2001) as well as individuals with ASD (Perry et al., 2007; Orekhova et al., 2008). Thus intact function of DA, 5-HT2 or NMDA neurotransmitter systems are important for normal gating functions. Furthermore, each model is found to show some improvement after antipsychotics are administered. Recovery for 5-HT2 agonists is more limited; and NMDA antagonist recovery is only apparent after atypical antipsychotic administration, like clozapine (for review see Geyer et al., 2001).

5.1.2.3 Measuring sensory gating in rodents

Measurements of sensorimotor gating in rodents rely on an innate startle response to intense stimulus, whether it is delivered in the auditory, tactile or visual modality. Such a response is adaptive and can facilitate escape from danger (Swerdlow et al., 2001). Here, auditory stimuli are delivered and the percentage of change in the magnitude of the startle response is measure. Initial startle response to stimulus, the habituation to the startling stimulus, and inhibition of the startle response when a non-startle stimulus precedes the startle stimulus (the PPI) are all measurements of sensory perception and sensory gating, which are believed to rely on low-level attention processing (2001). Importantly, measurements of startle and PPI are extremely analogous across species.

5.1.3 Object recognition memory

As discussed in the introduction, pervasive cognitive impairments are common to most neurodevelopmental disorders. Meanwhile, the diagnostic overlap between severe intellectual disabilities, developmental delays with schizophrenia and ASD in human populations with *EHMT1* mutations is a strong indication that appropriate *EHMT1* expression during development may be essential for normal cognitive function. In order to test higher order cognitive processes, the recognition of a novel object was tested in the *Ehmt1*$^{D6Cr/+}$ mutant mice.

5.1.3.1 The neurocircuitry of declarative memory

The recognition of an object—or an ability to judge the prior occurrence of an object is an integral component of declarative memory (Winters et al., 2008). Declarative memory is believed to be a conscious memory process for previous events and facts. Declarative memory processes are dependent on components of the medial temporal lobe—inclusive of the hippocampus, entrohinal cortex, perirhinal cortex and the postrhinal cortex (Akirav et al., 2006; Broadbent et al., 2010; Balderas et al., 2014;). Decades of lesion studies have established the importance of an intact perirhinal cortex, specifically for object memory (Balderas et al., 2014). While the hippocampus is critical for spatial memory (Bird & Burgess, 2008); however a consensus on the role of the hippocampus in object recognition has still not been reached (Broadbent et al., 2010; Clark & Squire, 2010).

5.1.3.2 Measuring novel object recognition in rodents

The novel object recognition task (NOR) is a simple paradigm for testing declarative memory capacities in rodents and relies on the natural tendencies of mice and rats to explore novel stimuli in preference to more familiar stimuli (Antuens & Biala 2012;). One strength of the paradigm is the fact that no reinforcement learning or pre-training is necessary. A task that does not necessitate food or water deprivation, food reward or the stressors of foot shocks and water mazes also limit complications of eliciting reward and fear circuitry during the memory event (Dere et al., 2007). The simple and direct approach to declarative memory skills in rodents is especially suited for looking at genetic interventions. The task involves both a

sample and a choice phase, which is separated by relevant retention delays. During the sample phase mice are introduced into an arena with two identical matching objects and allowed to explore for a set period of time. After retention delay the animal is re-introduced into the arena with two objects in the exact locations as before, only there is now a triplicate copy of the familiar object from the first session and a novel object. The amount of time that each object is explored is recorded. Object recognition is driven by a single exposure to the familiar object and occurs when the time spent exploring the novel object is significantly greater than the non-novel (Dere et al., 2007).

5.1.4 Pervasive social impairment in developmental disorders

Abnormal social interaction and social withdraw are common endophenotypes in a range of neurodevelopmental disorders and are hallmark characteristics of both ASD and schizophrenia (for reviews see Sasson et al., 2011; Each et al., 2013). In fact, initially SCZ and ASD were considered the same disorder as a result of the large overlap in social withdrawal and dysfunction (Sasson et al., 2011). Still today the pervasive social dysfunction shared by SCZ and ASD has led to the suggestion that these disorders exist within a single diagnostic spectrum and are not distinctive disorders (Bryan & Lord, 2011). It follows that overall sociality is perhaps not the most distinctive endophenotype in terms of disorder-specific association; however such overlap may provide important incite into the shared neurobiological substrates of both disorders.

5.1.4.1 The neurocircuitry of social behaviours

In humans, disruption in the network of brain structures corresponding to social dysfunction is found mostly in the forebrain: the fusiform gyrus, the superior temporal sulcus, the medial prefrontal cortex and the amygdala (Pinkham et al., 2003; Perlphrey et al., 2004). Mice are a highly social species (Murcia et al., 2005), displaying a variety of social behaviours, which enable fairly straightforward assessments of abnormality (e.g. Lijam et al., 1997; Kwon et al., 2006). However, even though the neural circuitry of mouse social behaviour is not as well understood; there is robust evidence that demonstrates the importance of intact

limbic and medial frontal cortical regions for normal social behaviour in mice (Perlphrey et al., 2004; Wang et al 2011 Science). Furthermore, social behaviour remains one of the most robust methods for classifying mouse models of neurodevelopmental disorders (for ASD see Silverman et al., 2010, and schizophrenia see Amann et al., 2010; Nestler & Hyman, 2010).

5.1.4.2 Measuring social behaviours in rodents

Examination of social behaviour in mice begins with observations of home cage activity, and any anecdotal evidence that there are social isolates in the cage. Nest building behaviours, and whisker trimming and barbering, are innate social behaviours often found either exaggerated or diminished in models of psychiatric disorders (Kaluff et al., 2006). The social approach assay, which is analysed here, relies on an innate preference for social versus non-social stimuli. The social approach task exposes a test mouse to a novel conspecifics, the total time spent investigating the novel target mouse verses a novel inanimate object is consider a mark of sociability. Typical mouse behaviour would predict a significant amount of time sniffing and inspecting the novel mouse.

5.2 Methods

5.2.1 Animals and housing

All mice were group-housed (3-5 per cage) in environments enriched with cardboard tubes, shred-mats and tissue paper, in temperature and humidity controlled animal holding room (21 +/- 2°C and 50+/- 10%, respectively) with a 12 hour light-dark cycle. All cages included both *Ehmt1*$^{D6Cr/+}$ mutant and control animals. Standard rodent laboratory chow and water were available *ab libitum*. Animal cages were cleaned out weekly. All testing took place between 07:00 and 19:00 and at the same time of day for each task. For further details see Chapter 3.

5.2.2 Acoustic startle and prepulse inhibition

Acoustic startle response (ASR) and prepulse inhibition (PPI) were assessed using

SR-Lab apparatus (San Diego Instruments, USA) according to published methods (Relkovic et al., 2010). The acoustic startle apparatus was a ventilated soundproof chamber. The chambers were mounted with (12cm) loud speakers and 70 dB white-noise background was continually presented when the startle pulses were not. Subjects were placed in sound attenuating champers, within a 35mm diameter, Perspex tube mounted to the Perpex plinth. Beneath the tube was a piezolelectric sensor that detects flexion in the plinth. The piezolelectric sensor measures the displacement from movement within the tube and sends a digitalized signal to a computer. The whole body startle response, which causes the displacement, is thus considered the physiological startle reactivity.

ASR and PPI were measured in a single session lasting 30 min. Both were recorded as the average startle during a 65ms window, from the onset of the startle pulse. A session consisted of a 5min habituation period of 70 dB white-noise followed by 3 blocks of acoustic stimuli. The startle amplitude was set to 120db in the first block, 105db in the second and a range (80 to 120db) in the third block. Pulse-alone trials consisted of a 40ms startle stimulus, while prepulse trials consisted of a 20ms prepulse at 4, 8, or 16db above background and a 40ms, 120db or 105db startle stimulus, 70ms after the prepulse onset. In blocks 1 and 2, following 5 pulse-alone trials, there followed five sub-blocks consisting of 2 pulse-alone trials, 1 no stimulus trial and 6 prepulse trials (2 each of 4, 8 and 16db above background). In each block, the different stimuli were presented in a pseudorandom manner every 15s. No-stimulus trials were averaged and used to normalize acoustic trials. While percentage PPI score for each trial was calculated: [$\%PPI = 100 \times (ASR_{\text{startle pulse alone}} - ASR_{\text{prepulse + startle pulse}})/ASR_{\text{startle pulse alone}}$]. Response output was adjusted for weight as described in Relkovic et al., (2010).

5.2.3 EthoVision Observer system

The NOR, object novelty, and social investigation tasks all utilized the EthoVision Observer video tracking software (version 3.0.15, Noldus Information Technology, Netherlands) and an overhead digital camera. This software tracks all movement and activity of the mice in spatially defined regions within an apparatus or open

arena. Activity is summarized over a series of frames (12 frames/sec) and allows for a range of qualitative descriptors about the movement and location of the subject. Animal movement was first calibrated using non-experimental mice of the same body size and coat colour.

5.2.4 Novel object recognition

The NOR test was used to evaluate object recognition memory, a process that requires judgement concerning prior exposure (in this instance to an object). The arena was a square 30cm x 30cm with 30cm high, white Perspex walls. Four different, non-displaceable objects were used. All objects were white and selected for their equal appeal and available in triplicate to avoid the use of olfactory cues.

In the habituation phase, 24hr prior to the task, each subject was allowed to explore the OF arena for 10min in the absence of objects. In the familiarisation phase, the subject was returned to the OF arena containing 2 identical sample objects (A, A') and given 10min to explore. After a retention phase, consisting of 15min or 90min, the subject was returned to the OF arena with two objects, one identical to the sample and the other novel (A, B). During both the familiarisation and test phase, objects were located in adjacent corners of the arena. The location of the novel object was counterbalanced. To prevent coercion to explore the objects, the subject was released in a third corner. Objects were cleaned with 70% ethanol wipes between sessions and object selection was randomised.

The *Recognition Index* (RI) is a measure of whether the animal investigated the novel object more than chance; calculated by the percentage of time spent investigating the novel object relative to the total object investigation [RI= $T_N/(T_N+T_F)$ x 100]. An RI significantly above chance or 50% indicates recognition of novelty and an RI equal to or below 50% indicates either no preference for the novelty or no recognition of novelty. Other parameters recorded were: frequency and latency to enter the zones containing an object. Data was collected in 1-min time bins across the 10-min session by a camera linked to a computer with Ethovision software (Noldus, Nottingham, UK).

5.2.5 Social Approach

A social approach task was used to measure preference for novel stimuli and social approach behaviour in control and *Ehmt1*^{D6Cre} mice. In this procedure, the subject is placed in a square OF arena (L75cm x W75cm x H45cm) with white Perspex walls, defined into 4 quadrants of equal size, each with a central circular zone of 15 cm in diameter. In one of the central zones, a wire mesh cage was present that contained a stranger mouse during test trials. The cages were cylindrical (H10cm x W10cm) with bars spaced 1cm apart to prevent full physical contact but allow sniffing. The mesh cages allowed inspection but prevented aggressive and sexual interactions, thus providing a more accurate and simple measure of social interest and approach (Silverman et al., 2010)

In the habituation phase, the mouse was allowed to explore the arena containing an empty cage for 10min. The level of investigation of the empty cage provided a measure for interest in a novel stimulus with no social valence. The subject was then briefly removed whilst an anaesthetised (10mg/kg pentobarbital) stranger mouse was placed into the cage. In the test trial, the subject was re-introduced to the arena for 10min. Sociability was defined as the tendency to approach and remain in close proximity to a stranger mouse (Moy, 2004). Thus sociability was measured using the *Sociability index* (SI). SI was calculated by the ratio of time spent investigating the empty cage relative to the time spent investigating stranger mouse ($SI= T_H/T_S$). An SI above 1 indicates a preference for exploring the stranger mouse compared to a novel object and an SI equal to, or below 1 indicates no preference for exploring the stranger mouse over the novel object.

The release of the mice and relative position of the cage was counterbalanced. For each subject mouse, the cage location was maintained during habituation and test trials. The parameters used to measure investigation of the cage (+/- stranger mouse) were: time spent in the zone containing the cage, entries into the zone containing the cage, latency and rearing in the zone containing the cage. Data was acquired in 1-min bins by a camera linked to a computer with Ethovision software

(Noldus, Nottingham, UK). One mouse (control) failed to move during the task; it was therefore excluded from analysis.

5.2.6 Statistical analysis

All data were analysed using SPSS 20 (SPSS, USA). The statistical differences between groups were analysed using the independent samples t-test and Repeated Measures ANOVA (RM-ANOVA). The main between subject factor was genotype (Control or *Ehmt1*^{D6Cre}) and the following within-subject factors were also analysed: in the ASR—across trials for 105dB and 120dB; and in the PPI—trial type (whether 4, 8 or 16dB). To check for normal distribution, Mauchly's test of sphericity of the covariance matrix or Levenes test for equality of variances were applied. Huynh-Feldt corrections were applied as necessary, and adjusted degrees of freedom are provided. The binomial distribution one sample Kolmongolov Smirnov (KS) test was applied to determine whether average RIs or SIs were significantly above chance (above 50% and 1, in the NOR and social approach task, respectively). For all comparisons, alpha value was set at $p < .05$. Finally all error bars reported represent the standard error of the mean (SEM).

5.3 Results

5.3.1 Acoustic startle reactivity & habituation deficits in *Ehmt1*$^{D6Cr/+}$ mice

Values across the two behavioural cohorts were collapsed in order to increase statistical power (Controls $N = 25$; *Ehmt1*$^{D6Cr/+}$ *Ehmt1*$^{D6Cr/+}$ mutant $N = 35$). After the 120dB stimuli, *Ehmt1*$^{D6Cr/+}$ mice demonstrated markedly different patterns of overall startle reactivity and habituation relative to controls. There was a significant difference in the average startle response to the 13 trials at 120dB. There was a main effect of trials, $\boldsymbol{F(12,1) = 8.309, p < .001}$ as well as by genotype, $\boldsymbol{F(64, 1) = 7.597, p = .008}$. Finally there was a significant interaction between trial and genotype $\boldsymbol{F\ (648, 1) = 2.797, p = .006}$. Follow-up *t*-tests comparing mean startle reactivity trial-by-trial revealed five trials to be significantly different at the Bonferroni adjusted *p*-value ($p = .005$): trial three, $\boldsymbol{t(64,1) = -3.755\ , p < .001}$; trial

four ***t*(64,1) = -3.981, *p* < .001**, trial five **t(64,1) = -2.960**, ***p* = .005**, trial six ***t*(64,1) = -2.911, *p* = .005** and trial seven ***t*(64,1) = 3.234, *p* = .002** (Figure 5.1).

However across the 13 trials at 105dB pulse trials there was no difference by trial, $F(5.415, 1) = .636$, $p = .811$, by genotype $F(64,1) = .455$, $p = .506$, nor an interaction between genotype and trial $F(435.384, 1) = .739$, $p = .398$.

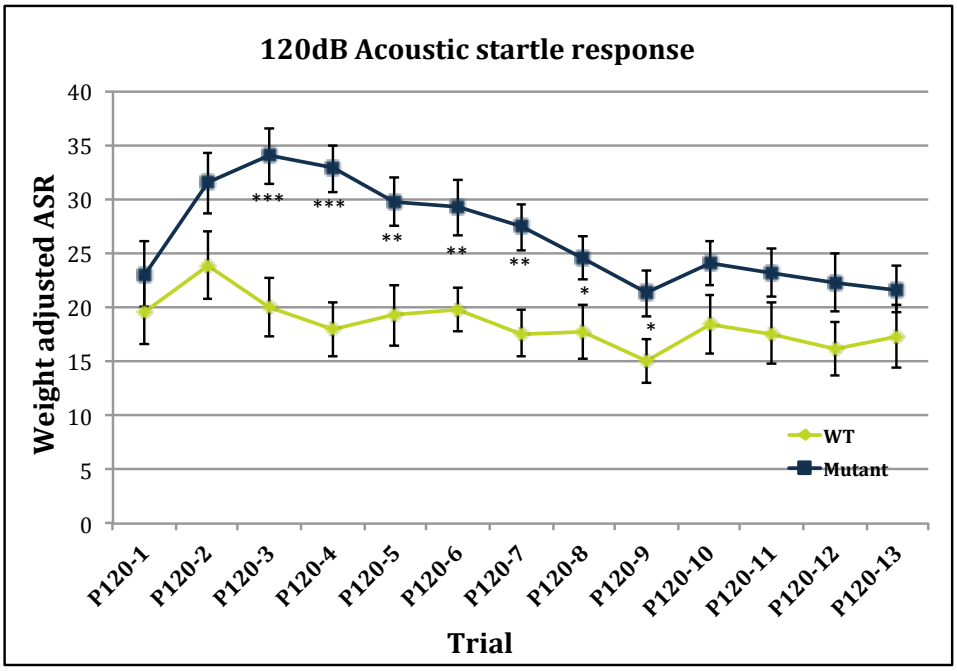

Figure 5.1 ASR habituation.
In the ASR there was a significant difference by trial ***F*(12,1) = 8.309, p < .001;** by genotype, ***F*(64, 1) = 7.597, p = .008**; and a significant interaction between trial and genotype ***F* (648, 1) = 2.797, p = .006**. *(* p < .05; ** p < .01; *** p < .001)*

5.3.2 Prepulse Inhibition deficits in *Ehmt1*$^{D6Cr/+}$ mice

Prepulse trials were preceded by three types of pulses, at 4dB, 8dB and 16dB. Using a RM-ANOVA there was a significant main effect for the trial type (whether 4, 8 or 16dB), ***F*(2,1) = 115.382, *p* < .001**. There was also a significant main effect of

genotype, ***F*(64,1) = 5.369, *p* = .024**. However, there was no interaction between genotype and trial type, $F(108, 1) = .154$, $p = .857$.

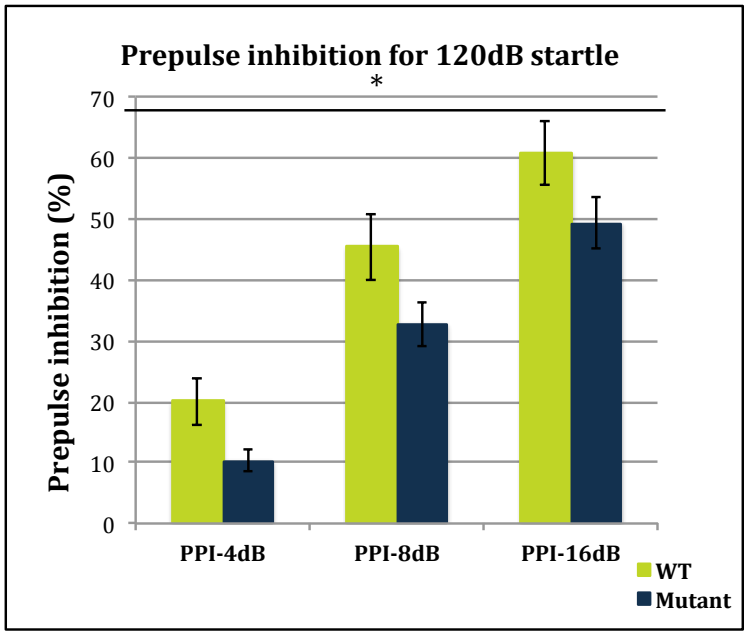

Figure 5.2 PPI by trial type.
There was a significant difference in the PPI response by trial type (whether 4, 8, 16dB) ***F*(2,1) = 115.382, *p* < .001**; a main effect of genotype, ***F*(64,1) = 5.369, *p* = .024**.

5.3.3 *Ehmt1*^{D6Cre} mice have impaired object recognition memory

Ehmt1^{D6Cre} and control mice were tested on their abilities to distinguish a novel object from a familiar object following a 15min or 90min retention period. The average Recognition Index (RI) for control mice were significantly above chance, as determined by the Kolmongolov Smirnov (KS) after both the 15min retention trial ($N = 7$), **(*p* = .022)** and the 90min retention trial ($N = 9$) **(*p* = .002)**. In contrast, the KS test demonstrated that the average RIs for *Ehmt1*^{D6Cre} mice after the 15min retention trial ($N = 7$) ($p = .971$), and 90min retention trial ($N = 6$) ($p = .44$) were not

significantly above chance. *Ehmt1*$^{D6Cr/+}$ mutant mice therefore did not demonstrate novelty detection or object memory (Figure 5.3).

Two important control measures were considered in the NOR task. First, during the familiarisation phase, the KS test showed the time spent investigating sample object *A* relative to sample object *A'* was not different in either genotype. In other words none of the objects were investigated significantly above chance: control mice in 15min retention trial (p =. 948) control mice in 90min retention trial (p = .628); *Ehmt1*^{D6Cre} in 15min retention trial (p = .659) or *Ehmt1*^{D6Cre} in 90min retention trial (p = .493).

Second, the absolute time mice spent in the two zones with objects (one where familiar object (A_F) is and one where the familiar object is replaced by the novel object (A_N) in the test trial) was considered. A RM-ANOVA test revealed there was no main effect of genotype for total time spent in A_F relative to A_N F (29,1) = 0.31, p = 0.862, no main effect of test time (15m/90m) for the total time spent in A_F relative to A_N F(29,1) = 0.31, p=0.319, or interaction between genotype and test time for total time spent in A_F relative to A_N F(1, 29)= 0.31, p=0.487.

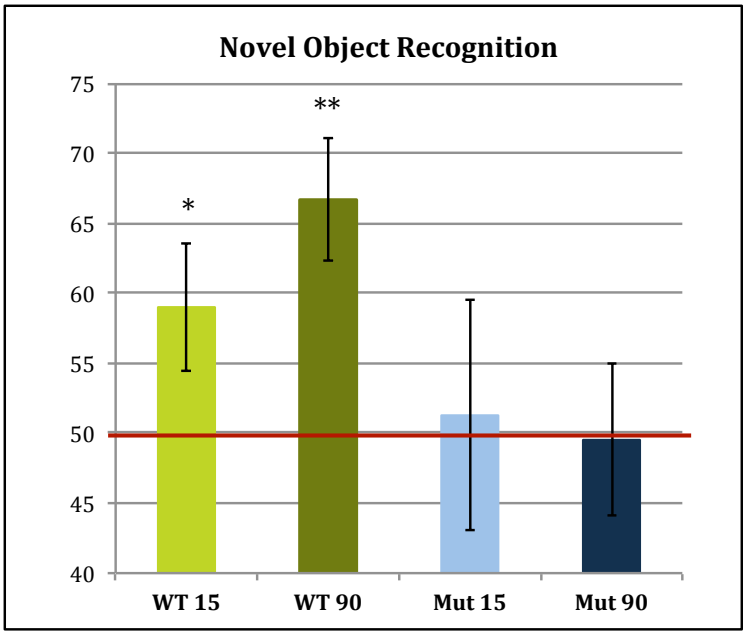

Figure 5.3 Novel object recognition.
After the 15-min and 90-min retention period wt mice spent significantly more time investigating novel objects (***p* = .022** and ***p* = .002**, respectively); however, mutant mice did not investigate the novel object above chance after either retention period (p = .440; p = .971, respectively).

5.3.4 *Ehmt1*^{D6Cre} mice show a normal sociability response

There was no difference between control and *Ehmt1*$^{D6Cre/+}$ mice in the sociability response. The Kolmongolov Smirnov test demonstrated the average SIs were significantly above chance for both control (p = 0.040) and *Ehmt1*$^{D6Cre/+}$ mice (p = 0.021). Similarly both genotypes displayed similar responses to the novel cage alone. A series of t-tests revealed no significant differences between the parameters recorded in the habituation trial, in which the novel object (empty cage) and social trial (Table 5.1), but for two exceptions. First, *Ehmt1*^{D6Cre} mice reared significantly less at the empty cage than controls $t(1,28) = 5.058$, $p<0.05$). Second, *Ehmt1*^{D6Cre} had a marginally reduced latency to investigate the social individual compared to control mice (Table 5.1).

Measure	CONTROL	*Ehmt1*^{D6Cre}	*t* -value	*P*-value
Entries into zone				
Habituation	52.3 ± 6	50.9 ± 5.3	-0.681	NS
Test (Social novelty)	42.4 ± 3.6	48.4 ± 5.1	-0.681	NS
Duration in zone				
Habituation	*128.7* ± 21.8	124.5 ± 19.2	0.441	NS
Test (Social novelty)	156.6 ± 18.1	184.2 ± 19.2	-0.756	NS
Latency in zone				
Habituation	2504.6± 181.5	2484.5 ± 79.7	1.695	NS
Test (Social novelty)	2504.1± 150.7	2306.8 ±136.5	-2.66	=0.04
Rearing in the zone				
Habituation	59.7± 6.6	20 ± 3.6	5.506	<0.05
Test (Social novelty)	46.2 ± 3.5	52.5 ± 4.9	-0.653 (18)	NS

Table 5.1: Behavioural measures in the social novelty task.

5.4 Discussion

In summary, the *Ehmt1*$^{D6Cre/+}$ mutant mice showed sensory habituation deficits and sensory-motor gating deficits, as explored using the auditory startle and prepulse inhibition test. The *Ehmt1*$^{D6Cre/+}$ mutant mice did not show an evidence of novel object recognition, despite what appears to be novelty induced hyperactivity in previous tasks and Chapter 4. This latter result is suggestive of impaired memory. Finally, there were no observable differences in the amount of time spent

investigating an anaesthetised novel social individual; however, the mutant mice did have a decreased latency to approach the novel individual.

5.4.1 Enhance ASR and reduced ASR habituation in *Ehmt1*$^{D6Cre/+}$ mutants

In the ASR task *Ehmt1*$^{D6Cre/+}$ mice showed significantly greater startle than controls. In addition, the habituation of startle was slower in mutants. For example control mice demonstrated marked reductions in reactivity in the third and forth trials of 120dB pulses compared to trial one and two; however *Ehmt1*$^{D6Cr/+}$ mutants demonstrated greater activity still in their third, fourth and fifth trials. This evidence corroborates that found in the *Ehmt1*$^{+/-}$ mice. Like *Ehmt1*$^{D6Cre/+}$ mice, the *Ehmt1*$^{+/-}$ mutants showed 60% increase in their startle response levels to acoustic stimulation (Balemans et al., 2013). Meanwhile, *Ehmt1*$^{+/-}$ mutants showed significant freezing levels during acquisition and context testing in context and cued fear conditioning paradigms, as well as significant reductions in fear extinction compared to control mice. Thus the consistent finding here may suggest that forebrain-specific *Ehmt1* dosage is important for both electrical-shock and acoustic-mediated reactivity in mice.

5.4.2 Reductions in PPI in *Ehmt1*$^{D6Cre/+}$ mutants

Ehmt1$^{D6Cre/+}$ mice showed a significant reduction PPI, especially at the two lowest prepulse tones. These findings suggest GLP deficiency in the forebrain leads to sensorimotor gating deficits similar to those reported in a range of neurodevelopmental disorders, like ASD and SCZ. PPI has not been investigated in the other models of *Ehmt1*-haploinsufficiency. Therefore, evidence reported here is the first of its kind.

In humans, PPI deficits are found to be highly reproducible, heritable and fairly easily measured—which may explain why it is currently one of the most robust endophenotypes found in neurodevelopment and neuropsychiatric populations (Braf et al., 2001). That being said, a completely homologous relationship between neurocircuitry in mice and humans for the regulation of PPI cannot be assumed (Geyer et al., 2001). While the medial prefrontal cortex is found to be very important

for PPI regulation in rodents (Ellenbroek et al., 1996, Zavitsanou et al., 1999); the exact role of the different medial temporal lobe structures is still not entirely known (Geyer et al., 2001). Caution is especially warranted, as the greatest phylogenetically divergent brain area in mammals are those that have undergone the most recent and greatest evolutionary change—i.e. more rostral regions of the cortex, like the medial prefrontal cortex (Swerdlow et al., 2001). Thus before complete homology is assumed between mouse and human *Ehmt1*-related PPI deficits, a greater understanding of PPI neurocircuitry may be necessary.

The pharmacological manipulations of PPI may present a promising avenue for future work on the *Ehmt1*$^{D6Cre/+}$ mice. For example the manipulation of PPI via different neurotransmitter systems may reveal more region-specific and cell-specific information about the PPI disruption found in these mice. Furthermore, differential responses to either typical or atypical antipsychotics may have important implications regarding the deficit and associate neuropsychiatric populations as well.

5.4.2.1 Complications of startle interpretation

Measurements of startle magnitude provide several conceptually important forms of plasticity, including habituation and fear potentiation, which are importantly, regulated by the forebrain structures (Swerdlow et al., 2000). Genetic manipulations that lead to significant changes in the pulse-alone magnitude can be challenging for the interpretation of the PPI. As Swerdlow et al. points out: "changes in PPI that reflect a change in startle 'pulse-alone' magnitude cannot be unequivocally ascribed to a change in sensorimotor gating.(2000)." In other words it is difficult to determine on these data alone, whether the increases in startle magnitude in the prepulse + pulse trials is the result of sensorimotor gating deficits or instead 'ceiling effects' of the startle magnitude.

As suggested, perhaps an unequivocal reduction in sensorimotor gating can only be inferred when there is a reduction in the startle-inhibiting impact of prepulses (not due to an elevation of sensory thresholds), in the absence of changes in pulse-alone

magnitude (Swerdlow et al., 2000). This occurs when startle magnitude in prepulse + pulse trials increases, while startle magnitude in pulse-alone does not change. While these conditions may not have been met in our study, a few important observations can be made. First, we do find a consistent reduction in inhibition, in the mutants, across the PPI trials, throughout the duration of the experiment. This is where the strength of the experimental design can aid our interpretation. The PPI trials were randomly, but evenly distributed across pulse-alone trials in the three-block session. Thus while we find a substantial habituation in the mutants in their startle magnitude to pulse-alone trials—Ehmt1$^{Dach6/+}$ mutants had significantly higher startle magnitude in the first 6 trials of the block but not in the second 6; we do not see a similar decrement in the PPI magnitude startle (i.e. an increase in inhibition). This suggests the prepulse does not produce the same gating effects we find in the control group and subsequently, which suggests these animals do have a sensorimotor gating deficit.

5.4.3. H3K9me2 modification mediate changes in learning and memory

Significant changes in the GLP mediated H3K9me2 modification have been connected to both contextual memory and associative memory processes. H3K9me2 was significantly increased in CA1 area of the hippocampus 1 h after both 'novel context learning' and 'associative contextual learning of fear' (Gupta et al., 2010). Gupta et al. suggested active repression of transcription plays a role in the consolidation of contextual memories; however, the direct role of H3K9me2 in gene transcription was not confirmed (2010). Surprisingly, 24 h later the dimethylation was significantly decreased after fear conditioning and context alone when compared to naïve controls (Gupta et al., 2010), which mirrors the dynamic activity reported in previous studies (Vakoc et al., 2005).

In a follow up study Gupta-Agrawal et al., re-examined their findings using a G9a/GLP-specific inhibitor (2012). They also examined a second region involved in memory consolidation, the entorhinal cortex (EC). After exposure to the G9a/GLP

inhibitor in the CA1 region, animals froze significantly less 24h after fear conditioning. This finding suggesting the reduction in G9a/GLP in the hippocampus had a negative role in associative learning. However, the opposite affect was found in the EC, instead freezing was increased. These findings suggest that not only was the H3K9me2 modification G9a/GLP-specific, but that subtle changes in regional-specific expression led to gross behavioural differences (Gupta et al., 2012). What these studies demonstrate is the important regulatory activity of the G9a/GLP complex in on-going memory processes. Thus we might expect decreased expression of GLP leads to memory deficits in the *Ehmt1*$^{D6Cre/+}$ mutant mice.

5.4.3.1 Ehmt1$^{D6Cre/+}$ *mutants demonstrate NOR deficits*

Control mice spent a a significantly greater amount of time investigating the novel objected compared to the non-novel object. These findings suggest that methods of testing were successful at capture novelty detection after two delay periods. The *Ehmt1*$^{D6Cre/+}$ mutants however, did not have above chance NOR after either a 15min or 90min retention period. Importantly however, these animals also did not display overall differences in exploration rates nor reduced levels of activity during the task. Additionally, there were no biases of object or object location. These findings suggest there is a robust memory deficit in the mutant mice.

These data are similar to those previously reported in the *Ehmt1*$^{+/-}$ mutant mice. *Ehmt1*$^{+/-}$ mutants displayed deficits after the 10mins and 80mins. However, Balemans et al. did not find NOR in the control after the 80-min inter-trial interval either, thus making their longer retention delay data incomparable to the findings we report (2013). Methodological differences in the NOR task may partially explain these differences. There was a longer initial exploration time administered in this task. *Ehmt1*$^{D6Cre/+}$ and *Ehmt1*$^{Flp/+}$ control mice were allowed to habituate to the two identical objects for 10mins compared to 5mins in the Balemans et al. (2013) report. A second explanation may be that *Ehmt1*$^{D6Cre/+}$ and control littermates had either 10min or the 90min retention trials, but not both. This was unlike Balemans et al. where each mouse received three different habituation and retention test trials (2013).

Balemans et al., also reported significant deficits in *Ehmt1*$^{+/-}$ mice in a spatial variant of the task. *Ehmt1*$^{+/-}$ mice did not appear to recognise a difference in novel object location after a 60-min inter-trial interval, whereas control did. Ultimately however, the interpretation of the novel object and location memory deficits in Ehmt1$^{+/-}$ mutant mice is somewhat limited. These data are confounded by the significant reductions in novelty preference found in the earlier reports of *Ehmt1*$^{+/-}$ mutants, as well as the significant increases in general anxiety these mice display (Balemans et al., 2010). Thus, findings reported in these mice may be due less to learning and memory-related cognitive deficits and more to anxiety and hypoactivity. Therefore our data provide invaluable evidence for the importance of *Ehmt1* expression in normal cognition and medial temporal lobe-related function.

5.4.3.2 Methyltransferase mediated cognitive deficit-related recovery

Ehmt mutant flies have been tested in a non-associative learning paradigm—the light-off reflex habituation assay in both hemizygous and transheterozygous mutations in *Ehmt*. Both mutants showed significantly slower response decrement during the habituation procedure as compared to controls. In an attempted to analyse more demanding cognitive behaviours, a courtship-conditioning paradigm was used (Kramer et al., 2011). Male flies were exposed to a non-receptive female, which in control results in suppression of courtship. Heterozygous males performance was 50% that of controls after a short delay, with greater affects after longer delays. Thus learning and memory deficits are associated with decreased *Ehmt* expression in non-mammalian species as well, suggesting the role of this enzyme may be highly conserved in brain function.

Perhaps the most interesting aspect of the Kramer et al. fly work however, is that the cognitive deficit phenotype *Ehmt* mutant flies demonstrate appears to be recoverable. After re-expression of the *Ehmt* enzyme they found performance in the courtship memory task returned to control levels (2011). This work has important implications. It may suggest that the decreases in cognitive performance found in *Ehmt1*$^{D6Cre/+}$ mutant mice, and perhaps even humans with *EHMT1*-related IDs, may not be the consequence of previous development deficiencies in the protein, but

instead due to the general haploinsufficiency of GLP during active memory processes. Furthermore, what this may suggest is that *EHMT1*-related neurodevelopmental deficits are recoverable in adulthood, as has been shown in models of other disorders such as Rett (Guy J et al 2007, Science) and Angelman's syndromes (Huang HS et al 2011, Nature).

The potential plasticity and recoverability of GLP/G9a-mediate H3K9me2 events is hinted at further in work relating the reward circuitry of the brain and cocaine addiction. GLP/G9a-mediated H3K9me2 has been linked to the long-term effects of cocaine. Both GLP and G9a are significantly down-regulated 24 hours after exposure to cocaine in the nucleus acumens, corresponding to the global decrease in H3K9me2 (Maze et al., 2010). These data were supported further by the use of a selective small molecule inhibitor (siRNA). Of those genes explored, the repression by the methyltransferase complex was found to be responsible for 50% of the genes that showed enhanced expressions (2010). These authors concluded that the repression of the GLP/G9a-mediated H3K9me2 led to the de-repression and transcriptional activation of genes that regulate aberrant dendrite plasticity and mediated cocaine preference (2009). Thus the global activity of GLP-repression exhibits a type of plasticity, which may be ideal for potential drug discovery.

5.4.4 No difference in sociality index

There was a marginally significant reduction in the latency to first investigate the social individual in the mutant mice, as well as reduced rearing in the novel object exploration. But it is difficult to interpret either one of these findings without further investigation. Reductions in the latency to investigate may be suggestive of a novelty induced excitability or a reduced anxiety-like phenotype, and may not reflect differences in general sociability.

Heterozygous *Ehmt1*$^{+/-}$ mice have previously shown diminished social play and delayed or absent response to social novelty in the presence of an unfamiliar mouse (Balemans et al., 2012). This phenotype was directly associated with the autistic-like social deficits often found in connection with Kleefstra syndrome patients

(Balemans et al., 2012). Similarly, as mentioned above, Kramer used a courtship-conditioning paradigm to test more complex cognitive behaviour in flies. The *Ehmt* mutant flies displayed severe deficits at recognising non-receptive females, which may reflect not only general cognitive deficits, but perhaps more specific social memory deficits as well. Unfortunately comparing general sociality in flies and mice is fairly limited. Despite the deficits reported previously, $Ehmt1^{D6Cre/+}$ mutants did not display a difference in the SI measurements reported here.

While social approach and interest in social novelty is believed to be a good indicator of overall sociality in mice, ultimately further investigation is necessary. For example, deficits in the NOR task may suggest social novelty recognition and general social memory are phenotypes which may prove to be different in these mutants. In addition, the social approach task used here did not involve direct social interaction, thus investigation of reciprocal social behaviours, like nose-to-nose and nose-to-anogenital sniffing, following, chasing, mounting, grooming, etc. may allow more accurate detection of social abnormalities.

In conclusion, the mutant mice demonstrated both sensory processing and sensory gating deficits, in the auditory startle and prepulse inhibition experiments. They display no evidence of novel object recognition after either a 15-minute or 90-minute retention periods. Finally, the mutants did not display differences in novel social conspecific investigation, although the latency to approach the novel individual was significantly shorter in the mutants compared to the controls.

Preliminary results reported in this chapter are promising. However future exploration of these endophenotypes is necessary. There are several behavioural tasks, which may be of particular interest to further illucidate the deficits found here. In particular, in addition to NOR task, the attention, impulsitivty and working memory-related task: the 5 serial reaction time taks would be informative. Different forms of memory, which involve fear—like cue and contextual fear learning as well as those that involve food rewards—like reversal learning and spatial T-maze tasks,

or different sensory modalities—like novel odor tasks would provide a greater understanding of cognitive deficits in these animals.

Chapter VI. *In vivo* Electrophysiological Characterisation

6.1 General Introduction

In this chapter evidence of the neurophysiologic dysfunctions found in the *Ehmt1*$^{D6cre/+}$ forebrain knockout mice is reported. A combination of both cortical surface electrodes and in-depth local field potential (LFP) electrodes in the hippocampus are the source for all signals reported. Two auditory event-related experiments were carried out using paired pulse and the mismatch negativity paradigms. In addition, the NMDA-antagonist ketamine was administered in order to gauge NMDA-related task modulation in mismatch negativity. Measurements of gamma and theta oscillations are compared across all experiments. A review of neurophysiological literature and relevant measurements are followed by an outline of the chapter aims. Finally, disruptions in the ERP time-related components and time-frequency changes are reported.

6.1.1 Electrophysiology as psychiatric endophenotype

Electroencephalography (EEG) is a method of recording the brain's electrical activity from the surface of the skull; while Magnetoencephalography (MEG) measures the reciprocal magnetic field produced by the electrical currents. Both methods are widely used to study basic human sensory processes and corresponding motor and cognitive behaviour. They provide indispensable tools for noninvasively investigating neurophysiologic deficits and what are increasingly considered biomarkers, for a number of psychiatric populations (Bomba et al., 2004; Ferri et al., 2003; Haenschel et al., 2009; Kemner et al., 1995; Krishnan et al., 2009; Luck et al., 2011; Marco et al., 2011; Roberts et al., 2008; Shin et al., 2009). Such biomarkers provide opportunities for further elucidating neural and cellular substrates of underlying disease pathology, while also presenting potential targets for drug discovery with the aid of translational animal research.

In a meta-analysis of the twin studies in schizophrenia, the heritability of schizophrenia as a complex trait was estimated to be 81% (Sullivan et al., 2003). In comparison, in a study looking at the electrophysiological measurments: P50, P300 (or the P1, P2) and MMN in 40 healthy monozygotic twin pairs and 30 dizygotic pairs of healthy individuals, these measurements were also found to be highly heritable. For example, the MMN peak amplitude and mean amplitude were found to be 63 and 68% heritable; P1 was 68% heritable and P2 was 69% (Hall et al., 2006). In a study that evaluated the heritability of the power and phase locking of the gamma-band response as an endophenotype in schizophrenia, authors again found fairly high heritability. The study sample which included 15 monozygotic twin pairs concordant for schizophrenia, 9 MZ pairs discordant for schizophrenia, and 42 MZ and 31 DZ control pairs found a 65% heritability in evoked gamma power and 63% in phase locking. The patients with schizophrenia and unaffected siblings were found to significantly reduce gamma power and phase locking (Hall et al., 2009). In a study that looked specifically at gamma-band oscillatory gating in response to paired-clicks, in patients with schizophrenia (N = 102), unaffected family members (N = 74), and controls (N= 70) estimates of heritability were between 49-83% (Hong et al., 2008). So while schizophrenia as a complex trait may be more heritable than any one of the electrophysiological endophenotypes reviewed here, there is still a strong genetic component to these measurements, which in turn may be helpful in identifying the underlying pathology associated with the genetic mutation.

The neural origins of EEG and MEG signals are the summation of activity from groups of parallel-oriented neurons, which receive similar repetitive synaptic input and/or are generating similar repetitive output (Roach & Mathalon, 2008). The synchronisation of such cellular networks produce 'extracellular rhythmic field potentials'. These field potentials are then volume conducted or propagated throughout the brain allowing for recordings to take place on the scalp surface in the case of EEG and MEG in humans, or more locally using microelectrodes and generating local field potentials (LFPs) in mice. Thus, even before spectral decomposition EEG, MEG and LFP recordings represent evidence of synchronous activity (Roach & Mathalon, 2008).

Electrophysiological activity is typically measured in either the 'time domain' or in the 'frequency domain'. Both types of measurements produce unique datasets, which in turn, provide insight into specific aspects of brain activity. For example, event related potentials (ERPs) are believed to amplify sensory stimulation processes and are captured in the time domain (Shah et al., 2004). While measurements like gamma synchrony or cross-frequency coupling are associated with a range of cognitive processes, like feature binding or working memory and are captured in the 'frequency domain' (Roach & Mathalon, 2008). Although 'time' and 'frequency' domains are not mutually exclusive (and in fact a source of ERP activity is on-going oscillations (Shah et al., 2004), because these measurements involve different methods of analysis, they are discussed separately here.

6.1.2 Measurements in the 'time domain'

6.1.2.1. Event related potentials

Event related potentials (ERPs) are voltage fluctuations time locked to an event, such as an auditory stimulus, a decision process or somatosensory response (Luck et al., 2010). These events are usually isolated by signal averaging across time epochs, locked to stimulus onset in the EEG trace. A result of averaging across a large number of trials is the removal of 'random' activity in the electrical signal, which allows for the background to approach zero with increasing trial numbers (Roach & Mathalon, 2008). What remains after signal averaging is the ERP waveform (Figure 6.1). These waveforms represent the combined amplitude of the response across frequencies, and therefore do not provide information regarding the contribution of independent frequency band to the signal.

Auditory ERPS or AEPs are the most robust and well-studied sensory ERPs (Amann et al., 2010). The initial signal generated by an AEP is believed to be a pre-attentive, pre-conscious response to changes in auditory stimulation and thus can be identified in a range of behavioural states (Escera et al., 1998; Rissling et al., 2013). Meanwhile, AEPs capture auditory processing deficits, which have been indexed in a number of clinical

populations: e.g. epilepsy, autism, schizophrenia, dyslexia, stroke, and multiple sclerosis, despite gross differences in symptomatology across these populations (for review see Näätänen et al., 2012).

6.1.2.1.1 ERP components

The sequence and latency of ERP components allow us to capture neural processing activity in millisecond time resolution (Shah et al., 2004). The amplitude of the response, whether it involves a negative or positive inflection, is generally regarded as evidence of the allocation of the neuronal resources and the strength of the signal (Amann et al., 2010). However, variations in the electrical impedance and the quality of the recording may also contribute to differences in amplitude response (Luck et al., 2011).

There are three primary ERP components consistently evaluated in the literature, though the latency of these components may vary from study-to-study. In humans the P50 is a positive deflection in amplitude that occurs around 50-ms post-stimulus onset. This component is believed to represent an automatic response to the presence of a stimulus and is not found to vary substantially in response to changes in attention processes or stimulus features (Amann et al., 2010). The N100 closely follows and is a negative deflection occurring around 100ms post-stimulus onset, while the P300 is a positive deflection occurring around 300ms post-stimulus onset.

The N100 is a component sensitive to qualitative features of the stimulus, while the P300 is believed to encode high-order processing demands (Amann et al., 2010). Differences in these two components are the most frequent measurements reported in the literature. In addition, these components are selectively modulated by pharmacological manipulations (Ehrlichman et al., 2008; Phillips et al., 2007) while also being differentially affected in psychiatric populations (Bomba et al., 2004; Ferri et al., 2003; Nagai et al., 2013; Kujala et al., 2007; Todd et al., 2012; Wei et al., 2010; Yordanova et al., 2001).

6.1.2.1.2 Non-human ERPs

A growing body of evidence suggests rodents share the same ERP components (for review see Amann et al., 2010). However these components are found at a 40% latency of that in humans. The mouse P50 peak latency is instead around 20-ms post-stimulus onset; the mouse N100 is around 40-ms post-stimulus onset and the P300 peaks around 120-ms post-stimulus onset (for example see Figure 6.1). Monkey ERP components are found at a 70% latency to those of humans, leading some to suggest that changes in a components peak time may reflect differences in brain size and thus changes in the rate of signal propagation (Bickel & Javitt, 2009). For ease, the human P50 and mouse P20 will be referred to as the P1, the human N100 and mouse N40 as the N1 and the human P300 and mouse P120 as the P2 from now on.

Critically, nonhuman ERP components, similar to human components are modulated by the same pharmacological manipulations, like Ketamine and nicotine (Connolly et al., 2004; Metzger et al., 2007; Phillips et al., 2003). In addition, disorder-specific genetic modifications in rodents replicated many of the deficits found in the human populations (Featherstone et al., 2012; Gandal et al., 2012).

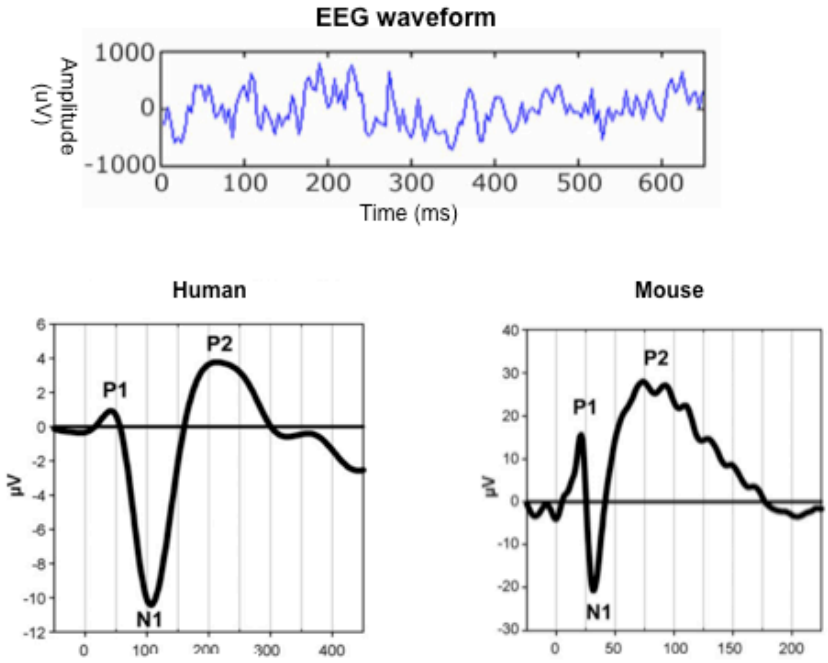

Figure 6.1 Example of the ERP waveform in human and mice

The top panel demonstrates a continuous EEG signal for which ERP waveform is extracted by averaging the signals time-locked to the onset of a stimulus event. The bottom left panel demonstrates the human ERP waveform with the three classic ERP components labelled: the first positive deflection as the P1, the first negative deflection as the N1 and the second positive deflection as the P2. The bottom right panel demonstrates the mouse ERP waveform equivalent with 40% latency in the three components found in the humans (Amann et al., 2009).

6.1.2.1.3 Paired pulse AEPs

In the paired pulse paradigm two auditory stimulus, often clicks, pulses or tones, are delivered back-to-back with a short delay between the first stimulus (S1) and the second stimulus (S2) (see Image 6.1). It has been studied extensively in both normative

human populations and individuals with schizophrenia (Brockhaus-Dumke, Mueller, Gaigle, Klosterkoetter, 2008; for review see, Sun et al., 2011). In normative populations the amplitude of S1 inhibits response to S2, thus reducing S2 amplitude components—a phenomenon that is referred to as 'sensory gating'. Individuals diagnosed with schizophrenia and other developmental disorders are found to have deficits in sensory gating: thus the ratio between S1 and S2 amplitude response is much closer to zero (Sun et al., 2011). The paired pulse paradigm is considered a neurophysiologic parallel to the sensorimotor gating measurements extracted from prepulse inhibition (PPI) paradigm (Amann et al., 2010). As discussed in Chapter 5, PPI deficits are a highly replicable and common endophenotype associated with several psychiatric populations.

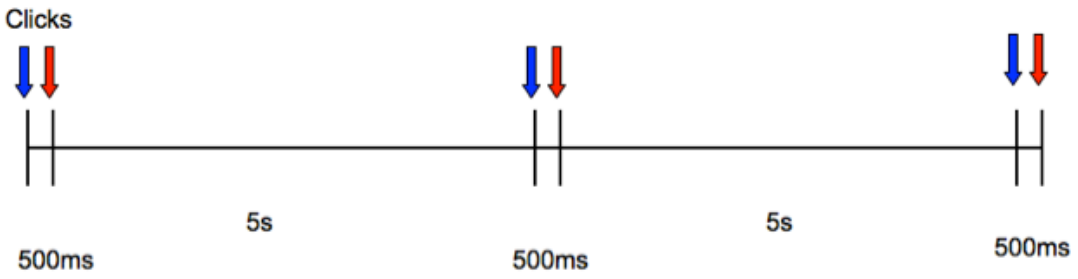

Image 6.1 Depiction of the Paired Pulse stimulus delivery

There was a 500ms delay between the S1 click (in blue) and the S2 click (red). Inter-trial intervals lasted for 5s. The inter-pulse interval between the two tones was 9-s. Each mouse received 1250 paired-pulse trials per recording session

6.1.2.1.4 Mismatch negativity AEP

The mismatch negativity paradigm (MMN) is perhaps the most reported measurement of neurophysiologic deficits in auditory processing found in psychiatric medicine (Näätänen et al., 2012; 2014). MMN is an electrophysiological response elicited when a certain qualitative difference in a sound, whether it is a change in pitch or duration, fails

to match the patterns of the previous series of sounds (Ehrlichman et al., 2009) (See Image 6.2). The unique stimulus is often referred to as the oddball or 'deviant' tone while the repetitive stimulus, the 'standard' tone. MMN is a pre-attentive and pre-consciousness process and thus, observable in a range of attentional states, during sleeping, under general anaesthesia, and during the wake state (Bickel & Javitt, 2009).

Like the classic AEPs the onset of the MMN in humans occurs within 50ms of stimulus deviance, and peaks after an additional 100-150ms, largely overlapping with the N1 component (Light & Swerlow, 2014) Therefore, in order to identify specific changes associated with the MMN, data is divided into epoch time bins and analysed for where the greatest change in the amplitude occurs. Thus, the MMN and recognition of the deviant tone is associated with a second, slightly later N1 amplitude peak (or double peak) (Näätänen et al., 2014).

In clinical populations, often a diminished amplitude and prolonged peak latency around the N1 component is found. This is believed to be the result of general deficits in auditory discrimination (Näätänen et al., 2012). MMN recognition have been directly linked to N-methyl-D-aspartate receptor function with disruptions often-reported in psychiatric populations with NMDA hypofunction (for review, Näätänen et al., 2014). For example, some have argued that deficits associated with MMN processing are the most robust and promising biomarkers reported in the schizophrenia literature to date (Light & Swerdlow, 2014). Meanwhile, because MMN is a pre-attentive process, involving passive stimulus, it is a paradigm especially conducive to translational studies in animals (Bickel & Javit, 2009).

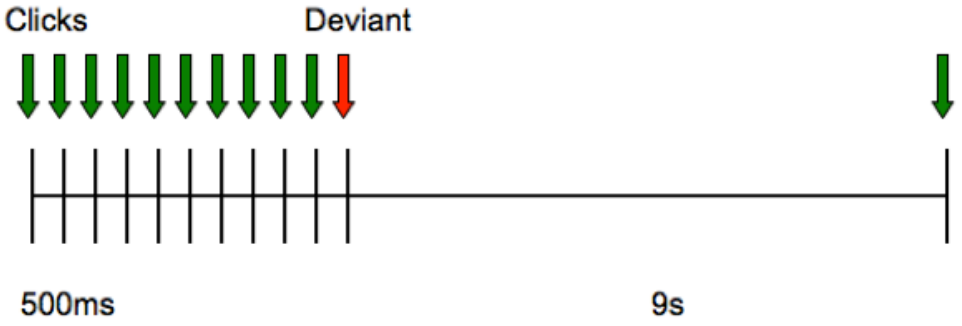

Image 6.2 Depiction of the Mismatch negativity stimulus delivery

One deviant tone was delivered at some stage in between the 24 'standard' tones. The standard tones were at 70dB and 1500Hz and the 'deviant' tone was70dB and 2000Hz. Each mouse received 1 session with saline with 360 trials and 1 session with ketamine with 360 trials.

6.1.3 Measurements in the 'frequency domain'

6.1.3.1 Cortical oscillation synchrony

Synchronised oscillation patterns are the result of coordinated neural activity, which allow for communication across anatomically distinct areas and the binding of stimulus features (Amann et al., 2010). Such oscillations can be the result of long-range networks, reflecting inter-regional activity and across-area communication or the property of local cortical networks and task-specific (Swettenham et al., 2009). Thus oscillatory activity may be essential to our understanding of cognitive and sensory processes of the brain. There is some variation in the number of bands reported and their exact thresholds. However, the five frequency bands most generally considered are delta (1-4 Hz), theta (4-8 Hz), alpha (8-13 Hz), beta (13-30), and gamma (30-80 Hz).

In recent years, there has been a rapid increase in the number of EEG and MEG studies in both normative and psychiatric populations (Basar & Guntekin, 2008; Hall et al., 2011; Klimesch et al., 1999; Lenz et al., 2011; Pentev et al., 1995; Sun et al., 2011; Uhlhass & Singer, 2013; Varela et al., 2001; Ward, 2003). Such data provide valuable information and have a number of strengths, such as good temporal resolution with measurements occurring at millisecond resolution. Unfortunately there are also a

number of limitations. For example, recording at the surface of the skull leads to poor spatial resolution and compromises in identifying the source location of on-going activity are required (Gevins et al., 1993). Meanwhile, electrical activity measured solely from the skull surface is limited—only select populations of cell can contribute to this type of signal. In fact, only cortical pyramidal neurons radially adjacent to the surface propagate activity that is measurable from the cortical surface (Roach & Mathalon, 2008). Finally, the skull also present problems with volume conductance in EEG and noise filtering in MEG (Ward, 2003)

Local field potentials or LFPs, on the other hand, are signals from a volume of tissue within the brain, and are usually recorded using extracellular microelectrodes. The signal is then low-pass filtered. Low electrical impedance and the position of the electrode can allow the activity of large number of cells to be recorded. LFP recordings allow for greater precision in anatomical localisation of the signal, while also limiting complications associated with volume conductance from the surface, and the limitations associated with cell orientation. One benefit of using rodent models to investigate psychiatric-related risk genes is the opportunity to use LFPs to probe AEP deficits (Amann et al., 2010).

6.1.3.2 Disrupted synchrony in psychiatric populations

Support for the importance of measurements in the frequency domain arise not only from strong functional correlations of certain frequency band patterns for specific tasks, but also from the range of disruptions in oscillatory patterns found in psychiatric populations. In fact, patterns of frequency oscillations represent a highly heritable trait which some have argued, may be more proximal to gene function than classic diagnostics or complex behavioural measurements (Porjesz et al., 2005). Inasmuch, focus on the spectral properties of neurophysiologic measurements have produced a number of strong biomarkers of potential dysfunction for patients with schizophrenia, bipolar disorder, autism spectrum disorders, Alzheimer's disease, attention-deficit disorder, mild cognitive impairments and alcoholism, along with a range of genetic disorders.

6.1.3.3 Gamma oscillations

There has been a surge of interest in the gamma band activity of neuropsychiatric illness in the past few decades. This may be due in part to the consistent correlation between gamma band activity and cognitive function (Engel et al., 2001); as well as claims for both high intra-individual stability and inter-individual variability (Frund et al., 2007) and direct correlations with brain structure (Zaehle and Herrmann, 2011). The importance of gamma band oscillations should not be underestimated, as one basic assumption follows from the idea that the more interconnected different brain areas are, the faster the frequency oscillations will be (Klimesch, 1999).

Frequency oscillations in the gamma range (30-80Hz) have been associated with a large range of sensory and cognitive processes: perception (Tallon-Baudry et al., 1996; Tallon-Baudry & Bertrand, 1999), motor response (Farmer, 1993), language (Pulvermuller, 1999), attention, (Cardin et al., 2009) memory (Herrmann et al., 2004), working memory (Tallon-Baudry et al., 1998), hallucinations (Behrendt and Young, 2004) and consciousness (Llinas et al., 1998). Furthermore, a direct association between evoked gamma and task performance has been identified (Lenz et al., 2008). The broad range of associations between gamma activity and cognition have lead some to suggest gamma activity acts as a "temporal coding scheme through which distributed neuronal groups are able to become synchronous—allowing communication between areas and binding of stimulus features." (Swettenham & Muthukumaraswamy, 2009).

In addition to general function, gamma activity is perhaps the most studied frequency band in terms of pathophysiology. Individuals with Alzheimer's disease are found to have an overall reduction in gamma power as well as asymmetries in gamma activity associated with lateralization of problem solving tasks (Loring et al., 1985), and with auditory and visual stimulus processing (Politoff et al., 1995; Ribary et al., 1991). Individuals with Attention Deficit Hyperactive Disorder (ADHD) have also been found to have lateral disturbances in gamma frequency (Yordanova et al., 2001) and

correlations with impaired early visual process (Lenz et al., 2010). Spontaneous increases in gamma have been reported in cases of epilepsy (Le Van Quyen et al. 1997).

Perhaps the most well studied association between neuropathology and gamma activity are those in relation to schizophrenia. Individuals with schizophrenia have been found to have an increased spontaneous or basal gamma synchrony (Bandyopadhyaya et al., 2011); but reductions in evoked and induced gamma power and phase locking as well as delayed onset of evoked response to auditory stimulation (Hall et al., 2009; Kwon et al., 1999). They are also found to have impaired cognitive-control related gamma activity (Minzenberg et al., 2010) and significant reductions in evoked gamma (Lenz et al., 2011). Positive symptoms, for example, auditory hallucinations have been significantly positively correlated with phase synchronization between primary auditory cortices, however interhemispheric phase locking was actually significantly reduced in schizophrenia patients (Mulert et al., 2011).

While there are gamma-related disruptions in a large number of neuropsychiatric and neurological conditions, at least some of these deficits seem specific to the disorder. A study by Lenz et al., 2011 attempted to look at evoked gamma band rhythms in an auditory oddball or NNM task in several different clinical groups, but found early evoked gamma activity was altered in schizophrenics only. These findings led the authors to suggest this may be a specific endophenotype of Schizophrenia (Lenz et al., 2011).

6.1.3.3.1 Types of Gamma synchrony

Several different types of synchrony can be measured. These differences arise from the source or location of the measurement and whether it is across event related trials or in spontaneous behaviour. Synchronous activity within a single cell can be measured using intercellular recordings (Herrmann & Demirlap, 2005). Local gamma activity at the cellular level is often, though inconsistently, referred to as gamma oscillations and the result of the magnitude of gamma activity (Lee et al., 2003). Synchrony can also be measured and compared across anatomically distinct locations, such activity encompasses the contribution of numerous cells using non-invasively surface

electrodes or extracellular recordings, like LFPs. Measurements across areas or within an area but across discrete event trials are often, though inconsistently, referred to as gamma synchrony. These measurements involve not only the magnitude information, but also phase information from the gamma signal (Lee et al., 2003). Unfortunately gamma oscillations and gamma synchrony are often used interchangeably in the literature. For the purposes of this study, all gamma-related measurements are derived from the assemblage of, what is assumed to be, a large volume of cells surrounding the surface of the microelectrode 100um in diameter and across two different cortical areas.

6.1.3.3.2 Basal power

Basal gamma is extracted from the baseline EEG activity or spontaneous EEG power. It is general extracted from either a period of time prior to the presentation of a stimulus or during a period of time in which activity is believed stable and does not reflect a specific cognitive event. Abnormalities in basal gamma activity has been reported in neurodevelopmental disorders (Gonzalez-Burgos & Lewis, 2012; Gogolla et al., 2009; Uhlhaas et al., 2008), and is believed to reflect a reduction in the signal to noise ratio for activity at this frequency. When capturing event-related changes, it is important to correct for pre-stimulus activity using a baseline correction method. However, as mentioned, disruptions in certain frequency bands in the baseline power, can effectively bias such methods. Therefore, basal gamma activity is important to consider along side changes in activity-related power.

6.1.3.3.3 Evoked Power

Across-trial gamma synchrony can be a result of evoked power, which reflects sensory driven activity (Uhlhaas & Singer, 2010). Evoked power refers to changes in power that are phase-locked to the onset of the trial. This type of measurement is extracted by averaging ERP trials across the time domain. Frequencies in phase synchrony at the same temporal onset will survive the averaging, while those that are out of phase with respect to the event will be lost. Thus evoked power is then extracted after squaring the magnitude associated with each point on the time-frequency matrix. As discussed above, differences in evoked power and frequency are directly associated with task

performance and a range of cognitive processes, whilst specific deficits are found in numerous psychiatric populations.

6.1.4 Chapter aims

This chapter aims to examine whether sensorimotor gating deficits identified in the *Ehmt1*$^{D6cre/+}$ mutant in Chapter 5, share neurophysiological correlates with AEP components. I aim to examine general processing deficits in the AEP components, the P1, N2 and P2, across two experiments. I look at whether mutant mice are similar to control mice in their inhibition to a repeated stimulus and their ability to detect a change in auditory stimulus pitch. In addition I examine whether there are differences in high frequency band oscillations. Specifically, I examine basal gamma; as well as both total power and evoked power of the beta and gamma frequencies after auditory stimulus. Finally, I use a low dose of the NMDA antagonist, ketamine. The pharmacological manipulation provides an opportunity to verify our methods and surgery with those models, which consistently report NMDA hypofunction induced auditory processing deficits. Such a model also provides a comparison for any deficits found in the mutants. And finally, taxing the NMDA system may allow more precise assessment of NMDA functional integrity in the *Ehmt1*$^{D6cre/+}$ mutants.

6.2 Materials and Methods

6.2.1 Animals

Adult male *Ehmt1*$^{D6cre/+}$ mice (N=7) and *Ehmt1*$^{Flp/+}$ control littermates (N=7) described previously, between 8-10 months of age were used for electrophysiology experiments reported. Mice were kept on a 12-hour light/dark cycle. All testing took place during the dark cycle, unless otherwise stated. For sample sizes all experiments were modelled on those previously reported in the literature (e.g. Ehrlichman et al., 2008), in which samples sizes are between N =7 and N = 10. Due to the data size and computational demands for the analysis, in vivo electrophysiological experiments have relatively small N. Furthermore, in order to run permutation testing on the frequency analysis, only

relatively small Ns can be used (otherwise the potential number of permutations drastically limits computational limits).

6.2.2 Electrode implantation

Mice were anesthetized with 1% isoflurane and underwent stereotaxic surgery for the implantation of five recording electrodes: two bilateral frontal electrodes, one monopolar and one bipolar (2.7-mm anterior, 1.5-mm lateral, 1.2-deep relative to bregma); two bilateral hippocampal electrodes, one monopolar and one bipolar (2.7 mm posterior, 3-mm lateral, 2.2-mm deep relative to bregma); and one bipolar electrode in the auditory cortex (2.7-mm posterior, 4-mm lateral, 1.1-deep relative to bregma) (Figure 6.2). The two-monopolar electrodes were implanted on the right hemisphere and differential signals between these two electrodes were recorded. Bipolar electrodes were implanted in the left hemisphere and referenced to two surface screw electrodes placed above the cerebellum. Electrodes were secured with the use of superglue and dental cement (Sun Medical Co., Japan). Animals were allowed 7 days recovery before recordings took place.

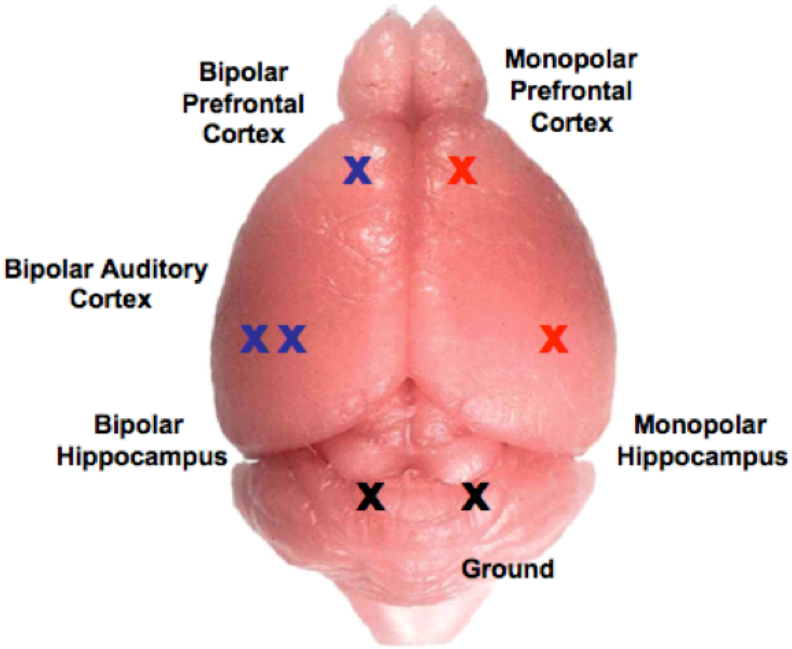

Figure 6.2 Illustration of the stereotaxic placement.
Five wire electrodes: three subdural electrodes were placed in the left auditory cortex auditory, and right and left hippocampi and two supradural, one in the right and left neocortex. Two screw electrodes were placed in the cerebellum for ground.

6.2.3 EEG recordings

Auditory stimuli were generated using Spike2, version 7.2 and were delivered through a Power1401 interface (CED, UK). Auditory stimulus was delivered with speakers positioned directly in front of each recording cage. Mice were given 30mins to acclimate for the first 2 recording trials and 15-mins thereafter. Mice were recorded in the dark, and during the dark cycle in order to record during their normal active state. The sound pressure was calibrated by using a sound meter based on the approximate height of the animal's head within the plexiglass cage.

All mice were recorded using two auditory stimulus paradigms across several sessions. Following Halene et al. (2009), each mouse received an auditory, paired-pulse session in which a single tone was presented at 1500Hz and 70dB (S1) followed by a 500ms

intra-trial interval and a second tone at 1500Hz and 70dB (S2). The tones were sinusoidal and 10ms in duration. The inter-pulse interval between the two tones was 9-s. Each mouse received 1250 paired-pulse trials per recording session.

The mice also received two sessions of the mismatch negativity (MMN) protocol. Similar to Ehrlichman et al. (2008), the mice received 24 'standard' tones at 70dB and 1500Hz and one 'deviant' tone at 70dB and 2000Hz. All tones were sinusoidal and 10ms in duration and the intra-pulse interval between the 25 tones was 500-ms, while the inter-trial interval was 5-s. Each mouse was recorded for 360 trials in each of two sessions. In one session 10mg/kg of Ketamine was administered and in the second session an equal volume of saline was administered. The dosage of ketamine was chosen based on previous work (Maxwell et al., 2006; Siegel et al., 2003; Ehrlichman et al., 2008). The within group design was counterbalanced by genotype and the order in which ketamine or saline sessions were administered. All recordings took place 5-mins after intraperitoneal injections of either 10mg/kg ketamine or the volume equivalent dose of saline. The waveform channels were filtered between 1 and 500Hz.

6.2.4 Analysis

All data reported is generated from the differentiation signal between the right frontal and right hippocampal monopolar electrodes. Previous studies demonstrate that this electrode configuration produces ERP components most characteristically similar to human EEG central cortical scalp recordings (Siegel et al., 2003; Ehrlichman et al., 2008). Data analysis was preformed using MatLab (MathWorks, Natick, MA) software. Due to an elevation in artefacts in later recording sessions, several mice were excluded from the analysis. Three mice were rejected from the saline MMN analysis (final $N = 6$ *Ehmt1*$^{D6cre/+}$ mutant mice and $N = 5$ *Ehmt1*$^{Flp/+}$ control mice). Four mice were rejected from the MMN ketamine session (final $N = 5$ *Ehmt1*$^{D6cre/+}$ mutant mice and $N = 5$ *Ehmt1*$^{Flp/+}$ control mice). All mice were included in the paired-pulse analysis ($N = 7$ *Ehmt1*$^{D6cre/+}$ mutant mice and $N = 7$ *Ehmt1*$^{Flp/+}$control mice).

6.2.5 AEP waveform and wavelet transform generation

ERPs were obtained by averaging epochs centred at Time 0 and 500msec to 0uV, respectively. For each epoch, power was calculated using either an fft or wavelet transform. For the wavelet transform, EEG signals were transformed using the complex Morlet's wavelets $w(t, f_0)$ (Kronland-Martinet et al., 1987). The script used was is the wt.m found at https://www.physics.lancs.ac.uk/research/nbmphysics/diats/tfr/. The wavelets have a Gaussian shape in the time domain (SD σ_t) and in the frequency domain (SD σ_t) around its central frequency *f0:* $w(t, f_0) = A * exp(-t^2/2\ \sigma_t^2) * exp(2i\pi f_0 t)$ with $\sigma_f = 1/\pi\sigma_t$ (Tallon-Baudry et al., 1996). The wavelet family we used was defined by $f_0/\sigma_f = 1$, with f_0 ranging from 0 to 100Hz in logarithmically distributed frequency steps. With Morlet's wavelet transformation time resolution increases with frequency, while frequency resolution decreases (Tallon-Baudry et al., 1996). At 20Hz and below the duration of the wavelet requires hundreds of milliseconds. Therefore for 20Hz and lower, only phase-locked (or evoked power and PLF) low-frequency components can be analysed. The primary focus of this study is on beta (13-30), and gamma (30-80 Hz) oscillatory activity.

The wavelet transform produces a time-frequency representation of power (TF energy). Measurements can be applied to either the averaged evoke potential or to the individual trials, thus generating either evoked power or total power, respectively. For total power, the noise remains in the signal, which may mask any activity that does not have a high signal-to-noise ratio. Thus for total power a baseline correction is applied. The baseline pre-stimulus period from –600 to –200 was subtracted from the post-stimulus period and applied to the frequency bands independently.

In order to extract the phase-locking factor of the oscillatory burst the normalized complex time-varying power of each trial $P_i(t, , f_0) = w(t, , f_0) * s_i(t)/|w(t, , f_0)*s_i(t)|$ was averaged (Tallon-Baudry et al., 1996). By averaging, complex values are produced, which includes phase information at each time-frequency region around t and f_0. The phase-locking factor is the calculated by unit normalising or transforming the

magnitude information of the complex value. The value remaining represents phase information and is an integer from 0 to 1, which ranges from non-phase-locked or 0, to strictly phase locked or 1. Such methods are found to be robust against artefacts (Tallon-Baudry et al., 1996).

6.2.6 Paired pulse components

6.2.6.1 P1 Amplitude and Latency

The P1 was considered the maximum positive deflection 10-30ms post-stimulus (Halene et al., 2009). Values for the peak latency and peak amplitude were compared using repeated measures ANOVA, with genotype as the independent variable and stimulus condition (S1 and S2) as dependent variable.

6.2.6.2 N1 Amplitude and Latency

The N1 was considered the maximum negative deflection 30-80ms post-stimulus. (Halene et al., 2009). Values for the peak latency and peak amplitude were compared using repeated measures ANOVA, with genotype as the independent variable and stimulus condition (S1 and S2) as dependent variable.

6.2.6.3 P2 Amplitude and Latency

The P2 was considered the maximum positive deflection 80-150ms post-stimulus. Values for the peak latency and peak amplitude were compared using repeated measures ANOVA, with genotype as the independent variable and stimulus.

6.2.6.4 S1 & S2 Response

For the P1, N1 and P2 the ratio in the peak amplitude response between S1 and S2 were calculated and compared across genotype using repeated measures ANOVA.

6.2.7 MMN components

6.2.7.1 Baseline Behaviour

After administration of ketamine, mice were observed for changes in motor behaviour. However, no changes were observed in behaviour that distinguished animals receiving saline from ketamine.

6.2.7.2 P1 Amplitude and Latency

The P1 was considered the maximum positive deflection 10-30ms post-stimulus (Halene et al., 2009). Values for the P1 peak amplitude in both the 'standard' tone and the 'deviant' tone condition were each compared separately using one-way ANOVAs. In addition difference waveforms between the deviant and standard conditions were generated and the P1 peak area difference was calculated. Average area values were compared between genotype and within the tone condition using repeated measures ANOVA.

6.2.7.3 N1 Amplitude and Latency

The N1 was considered the maximum negative deflection 30-80ms post-stimulus. (Halene et al., 2009). Values for the N1 peak amplitude for the 'standard' tone and the 'deviant' tone were each compared using one-way ANOVAs. In addition difference waveforms between the two stimulus conditions were generated and the N1 peak area was calculated. Average area values were compared between genotype and within the tone condition using repeated measures ANOVA.

6.2.7.4 P2 Amplitude and Latency

The P2 was considered the maximum positive deflection 80-150ms post-stimulus. Values for the P2 peak amplitude for the 'standard' tone and the 'deviant' tone were each compared using one-way ANOVAs. In addition difference waveforms between the two stimulus conditions were generated and the P2 peak area was calculated. Average area values were compared between genotype and within the tone condition using repeated measures ANOVA.

6.2.7.5 Epoch analysis

Following Ubricht et al. (2005; see also Ehrlichman et al., 2008), averaged-ERPs were divided into 25-ms time bins from 0-300-ms post stimulus onset. The area of the difference wavelets was then calculated for the 'deviant' minus the 'standard' waves for each of the time bins. A value of 0 would indicate there is no difference between the epochs analysed. Each of the 25-ms time bins was compared against a value of zero using a one-sample t-test. T-tests were carried out on ketamine and saline sessions. The

time bins created from the difference wave forms for both sessions were then compared using repeated measures ANOVA in order to determine whether there was a disruption in deviance-elicited changes as a result of the ketamine administration.

6.2.8 Permutation testing

Statistical tests on the frequency data was performed using the permutation method (Westfall & Youn, 1993), with <3,000 iterations. The number of iterations was dependent on the total number of possible permutations (which varied with the number of animals included in analysis). In the paired-pulse analysis, t-tests were calculated in between controls and mutants around the first pulse. In the MMN analysis, t-tests were calculated in the mutant between 24th pulse and the deviant pulse; and in the control between 24th pulse and the deviant pulse. Separate permutation plots were generated for the saline and ketamine condition. In addition, t-tests were calculated between mutant and controls for the ketamine condition and for the saline condition. Statistical permutation plots were generated in all of the above conditions for total power and evoked power.

6.3 Results

6.3.1 Paired Pulse

6.3.1.1 Paired pulse P1

No differences were found in the peak latency of the P1 (i.e. peak inflection ~15-30 ms post-stimulus) for either S1 condition $F(1,13) = .1.342$; $p > .05$ or the S2 conditions $F(1,13) = .988$; $p > .05$, between *Ehmt1*$^{D6cre/+}$ mutant and controls. Similarly no differences were found in the amplitude of the P1 response for S1 or S2 conditions. Finally the ratio between S1 peak and S2 peak amplitude were not different between *Ehmt1*$^{D6cre/+}$ mutants and controls $F(1,13) = .212$; $p > .05$.

6.3.1.2 Paired pulse N1

No differences in peak latency were found for the N1 component (i.e. peak inflection ~40-60ms post-stimulus) for either the S1 condition $F(1,13) = .679$; $p > .05$; or the S2

condition $F(1,13) = 2.367$; $p > .05$. There was a significant difference in the peak amplitude of the N1 component for the S1 condition**, $F(1,13) = 24.07$; $p < .001$** (Figure 6.3A). *Ehmt1*$^{D6cre/+}$ mutants were found to have a nearly two-fold lower average amplitude response in this condition: control average peak amplitude was at 59uV while *Ehmt1*$^{D6cre/+}$ mutants was 28mV. However, a difference for the S2 peak amplitude was not found $F(1,13) = 1.437$; $p > .05$. There was a significant difference in the ratio between the S1 and the S2 response **$F(1,13) = 16.731$; $p = .001$**, the ratio for the *Ehmt1*$^{D6cre/+}$ mutant mouse S1:S2 N1 amplitude being smaller.

6.3.1.3 Paired pulse P2

No differences were found in the peak latency of the P2 (i.e. peak inflection ~120-200ms post-stimulus) for either S1 condition $F(1,13) = .932$; $p > .05$ or the S2 conditions $F(1,13) = 2.971$; $p > .05$, between *Ehmt1*$^{D6cre/+}$ mutant and controls. Similarly no differences were found in the amplitude of the P1 response for S1 or S2 conditions. Finally the ratio between S1 peak and S2 peak amplitude were not different between *Ehmt1*$^{D6cre/+}$ mutants and controls $F(1,13) = .613$; $p > .05$ (Figure 6.3B).

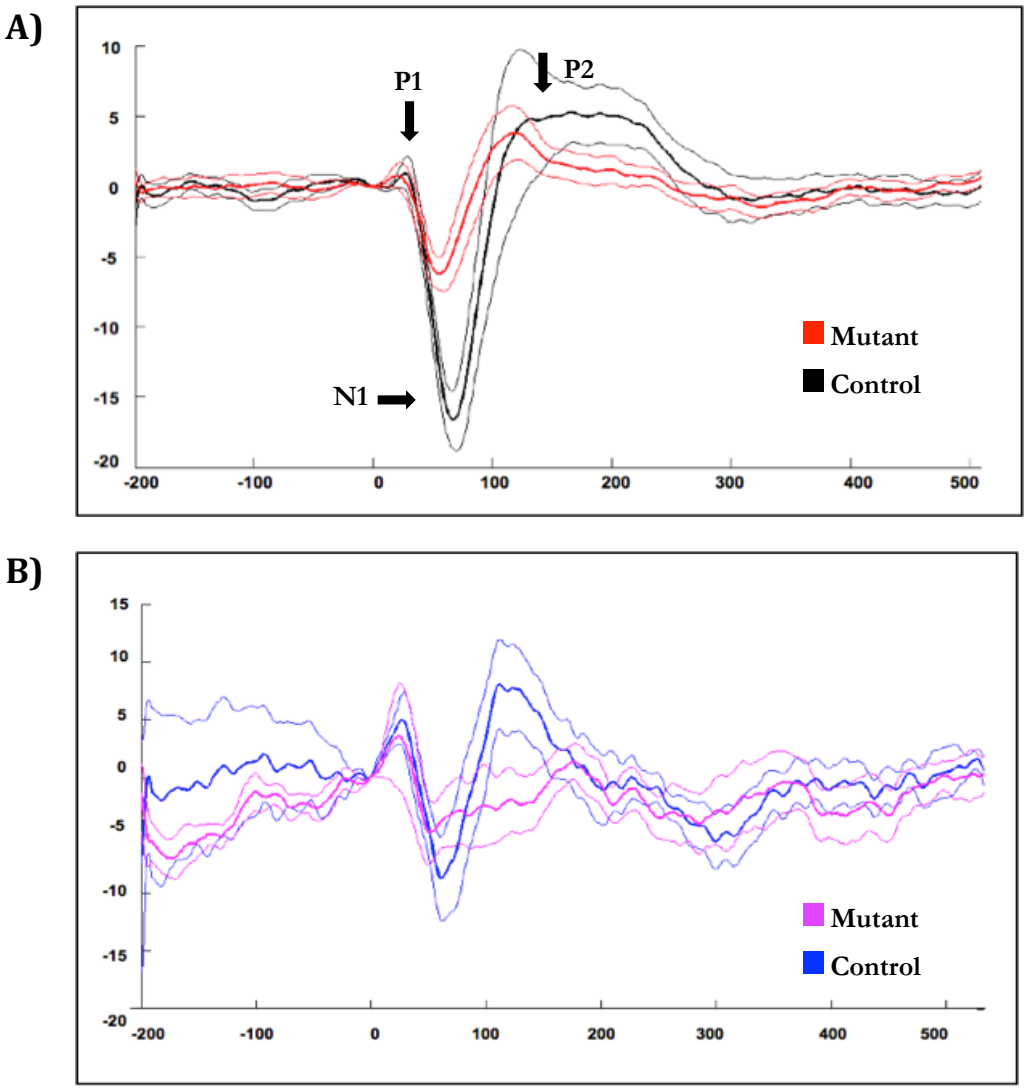

Figures 6.3 A&B Paired pulse waveforms.
A) Illustrates the AEP after the first pulse (S1) in the paired pulse experiment, thicker lines represent the mean amplitude response to the pulse, thinner lines represent the SEM. Control mice show a significantly larger N1 peak than found in the *Ehmt1*$^{D6cre/+}$ mutants as the black negative going inflection shows. **B.** Illustrates the AEP after the second pulse (S2). No differences were found in any S2 components. The mutants show a similar response to that found in the S1, while controls are found to have a significantly small N1 peak after the firs pulse.

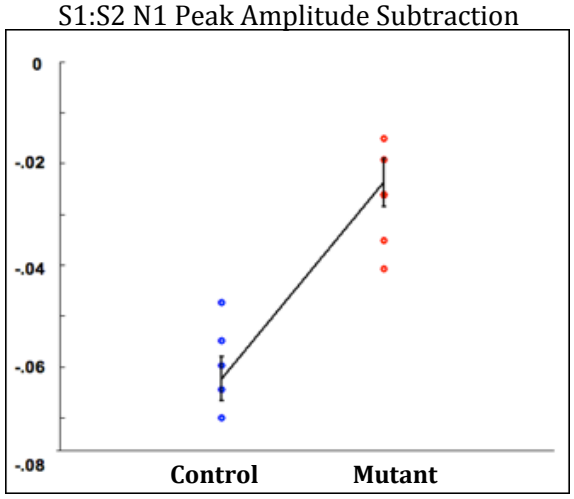

Figure 6.4 S1:S2 N1 peak amplitude subtraction.
The subtraction of the peak amplitudes in the N1 component between the S1 and S2 stimulus in the paired pulse paradigm. In response to the S1 and S2 pulses *Ehmt1*$^{D6cre/+}$ mutants ratio was consistently closer to zero—demonstrating similar peak responses to both stimulus.

6.3.1.4 Paired pulse frequency analysis

The time-frequency plots for the paired pulse experiment demonstrate evoked power from -50ms pre-stimulus onset to 300ms post-stimulus onset, from 1-100Hz after S1 (Figures 6.5 A-D). *Ehmt1*$^{D6cre/+}$ mutant mice display marked reductions in overall evoked power across the high frequency bands (Figure 6.5A). In the control mice we find a large distributed peak in evoked power at ~40ms post-stimulus from ~25-40Hz and a second smaller peak in high game a ~85Hz. Control mice are found to have significantly higher evoked power broadly across the beta and gamma frequency bands beginning ~15ms post-stimulus onset and continuing until ~100ms post-stimulus onset (Figure 6.5D).

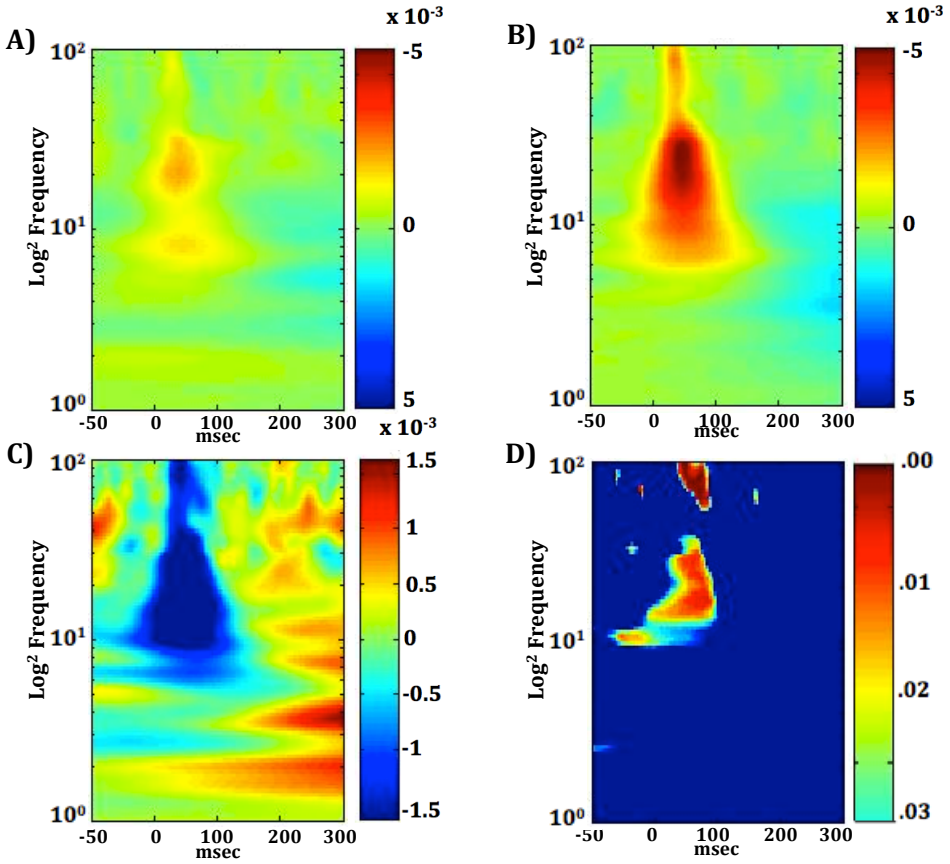

Figures 6.5 A-D Paired pulse evoked power
A) *Ehmt1*$^{D6cre/+}$ mutant evoke power in Time-Frequency plot, the left axis represents frequency from 0-100; the colour represents power which is phase locked to the stimulus, 0 on the y axis represents stimulus onset**, B)** *Ehmt1*$^{Flp/+}$ control evoked power in Time-Frequency plot **C)** The difference between mutant and control mice power (mutant – control) **D)** Is a heatmap showing the permutation test, with p-values depicted in colours other than dark blue, from light green to red.

6.3.2 Mismatch Negativity

6.3.2.1 MMN P1 component after saline

There was no main effect of tone (between standard or deviant conditions) on P1 area amplitude F (9,1) = .021; p = .887; there was no effect of genotype F (9,1) = .415; p = .535; nor a significant interaction between tone and genotype F(9,1)= 1.180; p = .306 (6.6A).

6.3.2.2 MMN P1 component after ketamine

After the administration of ketamine, there was no main effect of tone on the P1 area amplitude (in the standard or deviant conditions) F (8,1) = .053; p = .823; there was no effect of genotype F (8,1) = 2.179; p =.178; nor a significant interaction between tone and genotype F (8,1)= 2.466; p = .155 (Figure 6.6B).

6.3.2.3 MMN N1 component after saline

There was no significant main effect of tone on the N1 area amplitude F(9,1) = 3.090; p =.113; and no main effect of genotype F(9,1) = .763; p = .405. However, there was a significant interaction between tone and genotype $\boldsymbol{F}$ **(9,1) = 6.484;** $\boldsymbol{p}$ **= .031**. This interaction is driven primarily by a significantly greater N1 amplitude area specifically in the deviant condition for control mice peak average compared to the *Ehmt1*$^{D6cre/+}$ mutants (Figure 6.6A).

6.3.2.4 MMN N1 component after ketamine

Following ketamine administration, no differences between control and *Ehmt1*$^{D6cre/+}$ mutant mice for either deviant or standard tone conditions were found. In other words there was no main effect tone on the peak N1 area amplitude F(8,1) = .105; p =.755; nor a main effect of genotype F(8,1) = 1.256; p = .295 and there was no significant interaction between tone and genotype F (8,1) = .833; p = .388 (Figure 6.6B).

6.3.2.5 MMN P2 component after saline

There was not a significant main effect of tone on the P2 area amplitude F(9,1) = 2.247; p =.168; no main effect of genotype F(9,1) = .987; p = .346; nor and interaction effect between tone and genotype F (9,1) = 054; p = .821 (Figure 6.6A).

6.3.2.6 MMN P2 component after ketamine

After ketamine administration there was no differences between control and *Ehmt1*$^{D6cre/+}$ mutant mice for either deviant or standard tone conditions were found. In other words there was no main effect tone on the peak P2 area amplitude F(8,1) = .085; p =.778; nor a main effect of genotype F(8,1) = .941; p = .361 and there was no significant interaction between tone and genotype F (8,1) = .039; p = .848 (Figure 6.6B).

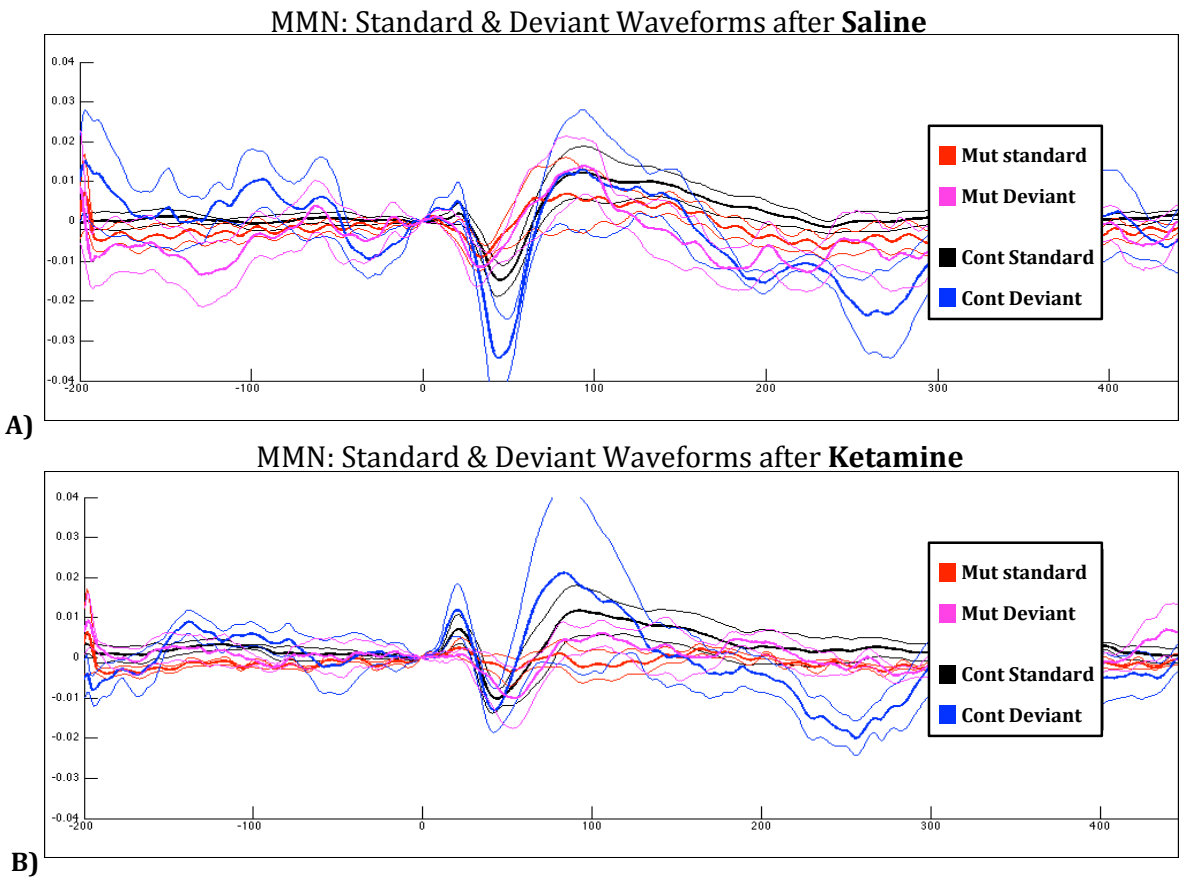

Figures 6.6 A & B. AEP waveforms in the MMN experiment
A) The top figure shows waveforms for the saline condition. The standard and deviant waveforms for both the Ehmt1$^{D6cre/+}$ mutant and controls are reported. The thin lines surrounding the bold line are the SEM for each of the waveforms**. B)** The bottom figure shows the same four waveforms for the ketamine condition.

6.3.2.7 MMN epoch analysis

For the epoch analysis 10 time bins were used starting from 0-25ms and ending with 275-300ms, in 25ms time bins. The area of the difference wavelets was then calculated for the 'deviant' minus the 'standard' for each of the time bins. A value of 0 would indicate there is no difference between the epochs analysed. A one-sample t-test was run for both sessions. In saline sessions, control mice values for the N1 time epoch from 25-50ms was non-significant *t*= -2.354, p = .070; while the epoch from 50-75ms was

significantly different ***t*= 5.91, *p* = .004**; and epochs 175-200 ***t*= -7.198, *p* = .002** , 200-225 ***t* = -4.271, *p* = .013** and 225-250 ***t*= -3.098, *p* = .036** were also significantly different. After ketamine administration in the control animals, the only time epoch to demonstrate a difference between standard and deviant tones was 225-250; ***t* = -4.733; *p* = .009.**

In saline sessions for the *Ehmt1*$^{D6cre/+}$ mutant mice, no differences were found in any of the epochs; although a marginally non-significant value was found for the 75-100ms epoch, T = 2.695; p = .054. Similarly, none of the difference wavelets for any of the epochs after ketamine in the mutants were found to be significantly different. Because there were no differences between deviant and standard detection for the *Ehmt1*$^{D6cre/+}$ mutant mice in either saline or ketamine conditions, no further testing was warranted.

Next in a repeated measures ANOVA comparing difference values between standard and deviant conditions in the control mice, following saline verse ketamine, we find there is a significant main effect of the temporal epoch, ***F* = 5.365, *p* = .014** (Greenhouse Geisser adjusted value); there is a significant main effect of the drug condition, ***F* = 7.685, *p* = .024**. However, there was no interaction between the drug and temporal epoch**,** *F* = 1.032, *p* = .339.

6.3.2.8 MMN frequency analysis

6.3.2.8.1 MMN saline condition: Evoked power

Evoked power in the 24P condition was compared with the DvP condition from -50ms pre-stimulus onset to 100ms post-stimulus onset, in the higher frequency bands (10-100Hz). For all permutation results only effects lasting 10ms or longer are reported (Lazarewicz et al., 2010). In the saline condition, *Ehmt1*$^{D6cre/+}$ mutant mice time-frequency plot for 24P and DvP conditions displayed the same overall pattern (Figure 6.7A-C). Subsequently, there were no significant differences in power at any time-frequency combination between the pulse conditions (Figure 6.8A). Control mice however demonstrated very different patterns of activity

between pulse conditions (Figure 6.7D-F). There was a significant increase in low beta frequency after the DvP (10-14Hz) surrounding stimulus onset until ~50ms post-stimulus compared to the 24P. There were two significant peaks after DvP in high gamma, one surrounding stimulus-onset and a second, from ~20ms until ~50ms. There were also two smaller overlapping periods in low gamma between 50ms and 100ms stimulus onset in the same condition (Figure 6.8B).

A prominent distinction is found between *Ehmt1*$^{D6cre/+}$ mutant mice and *Ehmt1*$^{Flp/+}$ controls after the DvP. There was a significant increase in the controls compared to the mutants in the high beta and low gamma frequencies starting ~30ms post-stimulus and lasting > 100ms. There was also a significant increase in high gamma starting ~20ms post-stimulus and lasting ~50ms post-stimulus (Figure 6.8 C). This brief peak in high gamma is similar to that found in the DvP evoked gamma reported above.

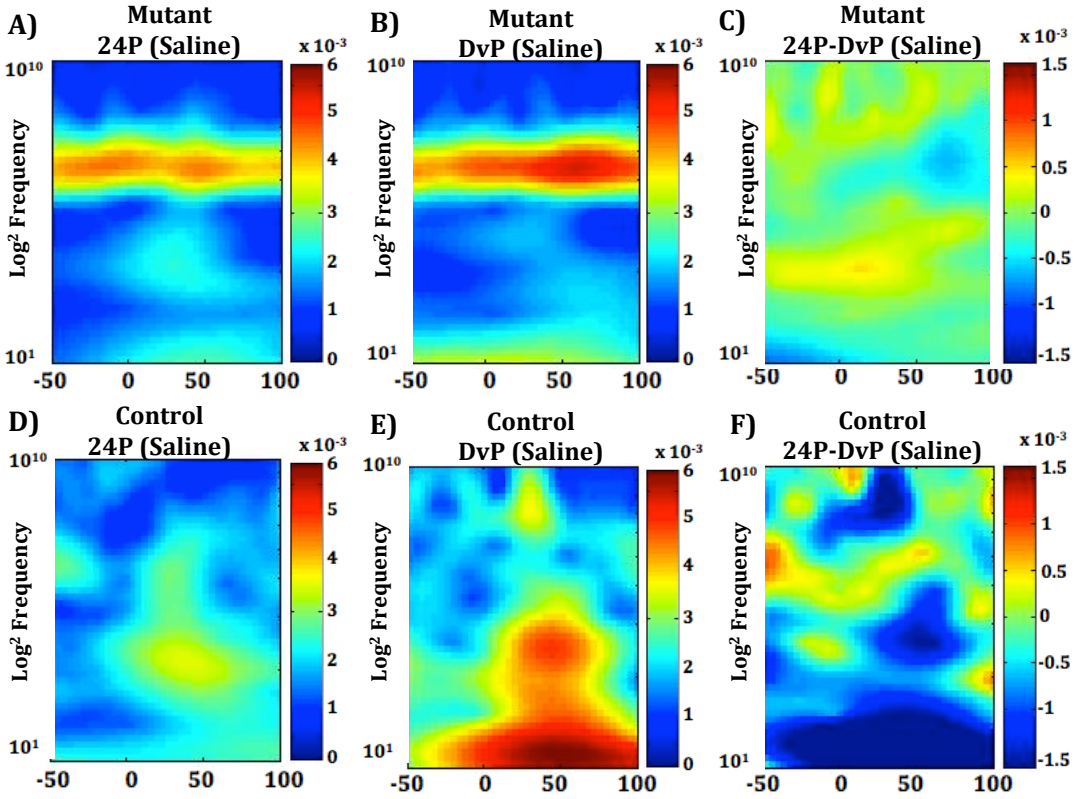

Figures 6.7 Time-Frequency plots for MMN experiment: The 24th & Deviant pulses after ***SALINE***
Top row is the time-frequency plots for *Ehmt1*$^{D6cre/+}$ mutant mice after saline: **A)** mutant evoked power after the 24th pulse (24P); **B)** mutant evoked power after the deviant pulse (DvP); **C)** mutant power of 24P – DvP. Bottom row is the time-frequency plots for control mice after saline: **D)** control evoked power after the 24th pulse (24P); **E)** control evoked power after the deviant pulse—which represents a substantial change in power from ~10Hz to 30 and a smaller change in the high gamma ~80Hz (DvP); **F)** control power of 24P – DvP

..

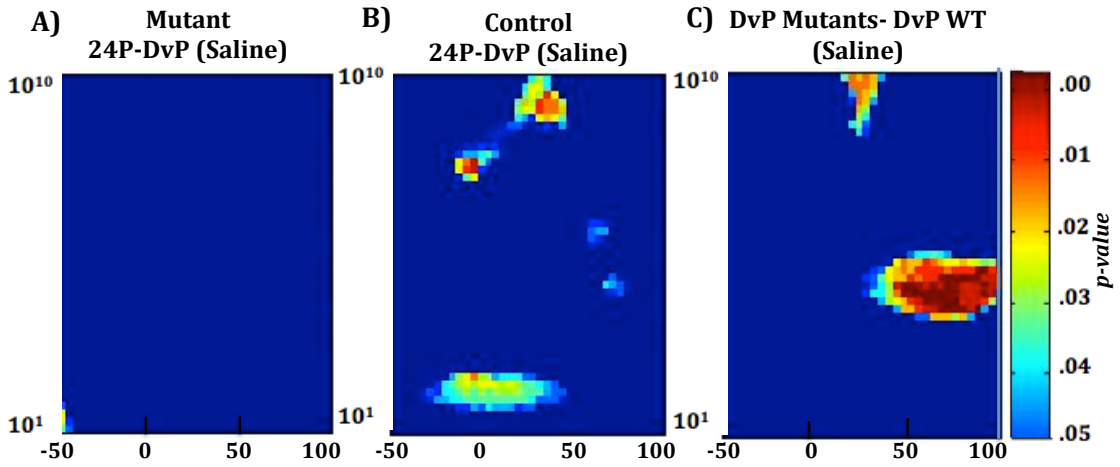

Figure 6.8 Permutation t-test of MMN EVOKED power after SALINE.
A) Permutation *p*-values for comparison of evoked power between 24P and DvP in mutants after saline. **B)** Permutation *p*-values for comparison of evoked power between 24P and DvP in control after saline. **C)** Permutation *p*-values for comparison of evoked power between mutant DvP and control DvP after saline.

6.3.2.8.2 MMN saline condition: Total power

Total power after the 24P was compared with total power after DvP, from -50ms pre-stimulus to 100ms post-stimulus on, in the higher frequency bands. In the saline conditions, *Ehmt1*$^{D6cre/+}$ did not display significant differences in the total power between these two conditions for any time-frequency combination. While a few pixels display higher *p*-values, none lasted >10ms (Figure 6.9A). Control mice display significantly higher total power after the DvP in the lower beta frequency band from stimulus onset until >100ms; as well as increases in the lower gamma frequency for the same time period (Figure 6.9B). When compared, control mice are found to have a significantly increased lower gamma at ~30-40Hz between ~25-80ms (Figure 6.9C). This peak increase in control mice is fairly consistent with that found in evoked power.

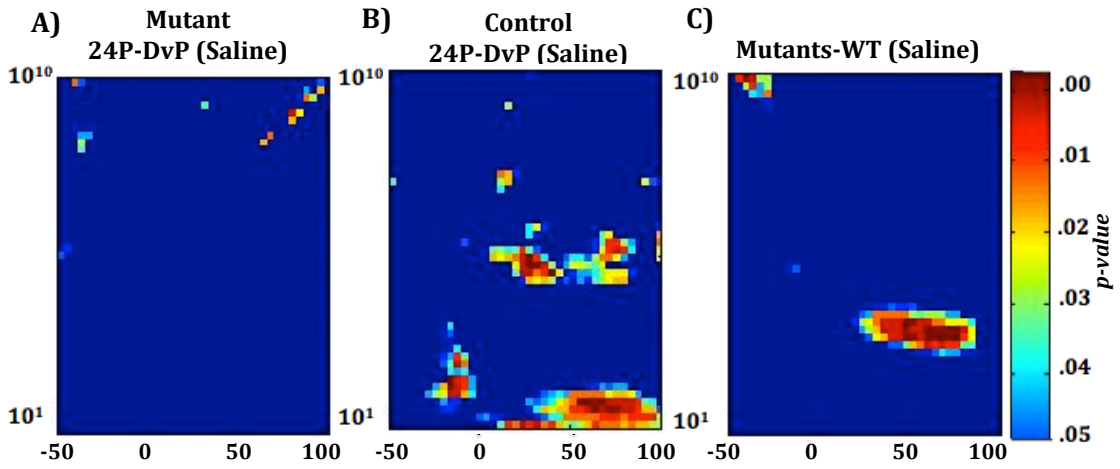

Figure 6.9 Permutation t-test of MMN TOTAL power after SALINE.
A) Permutation *p*-values for comparison of total power between 24P and DvP in mutants after saline. **B)** Permutation *p*-values for comparison of total power between 24P and DvP in control after saline. **C)** Permutation *p*-values for comparison of total power between mutant DvP and control DvP after saline.

6.3.2.8.3 MMN ketamine condition: Evoked Power

There was an overall decrease in amplitude of the time-frequency plots after the administration of ketamine in both mice populations. Meanwhile, administration of ketamine resulted in time-frequency plots, which show remarkable similarity across group and condition (Figure 6.10A-F). *Ehmt1*$^{D6cre/+}$ mutant mice however, displayed significantly higher gamma after the DvP, the largest peak started around stimulus-onset and last ~50ms in the 30-40Hz gamma range (Figure 6.11A). Control mice had significantly higher beta after DvP, from ~80ms until >100ms. (6.11B). This peak did not overlap with any of those reported in the control mice administered saline. Despite the significant differences in pulse conditions, there were no differences between the mutants and controls in evoked power (after stimulus-onset) in the DvP Ketamine condition (Figure 6.11C).

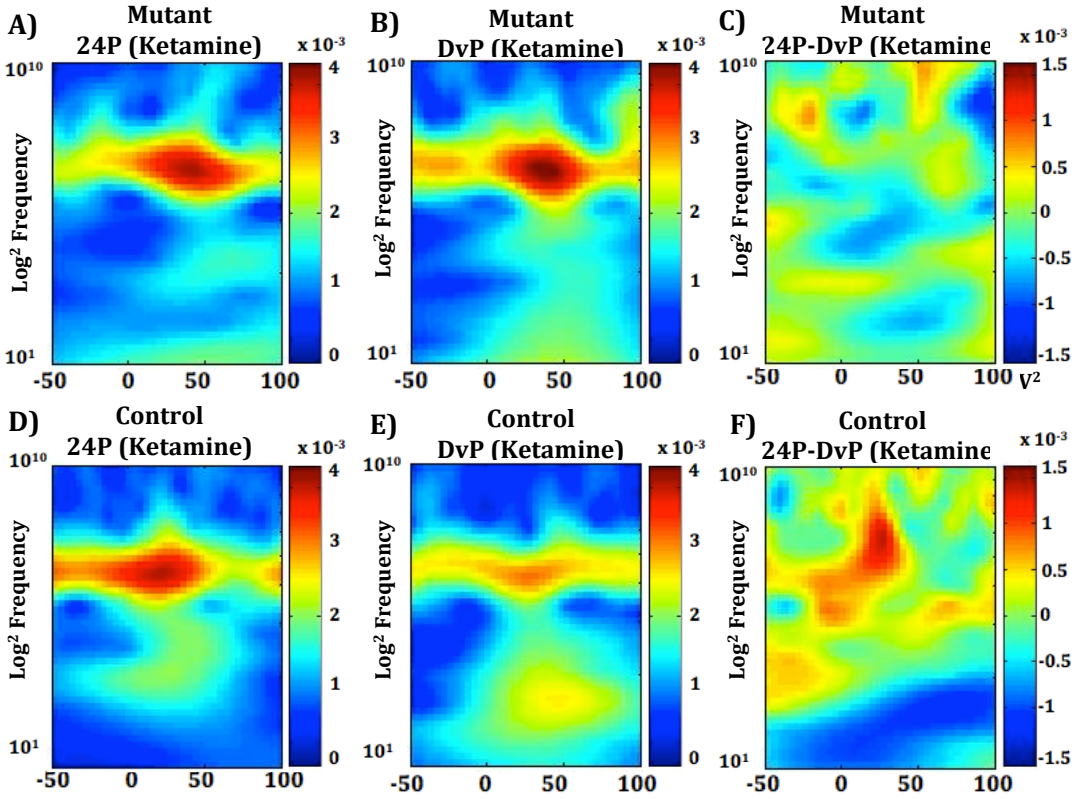

Figures 6.10 Time-Frequency plots for MMN experiment: The 24th & Deviant pulses after ***KETAMINE***
Top row is the time-frequency plots for *Ehmt1*$^{D6cre/+}$ mutant mice after ketamine: **A)** mutant evoked power after the 24P; **B)** mutant evoked power after DvP; **C)** mutant power of 24P – DvP. Bottom row is the time-frequency plots for control mice after saline: **D)** control evoked power after 24P; **E)** control evoked power after DvP; **F)** control power of 24P – DvP.

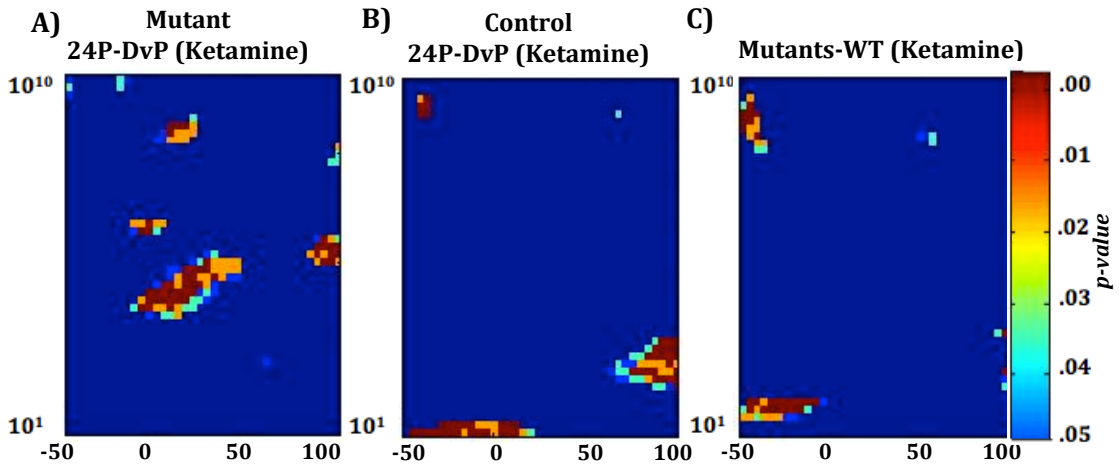

Figure 6.11 Permutation t-test of MMN EVOKED power after KETAMINE.
A) Permutation *p*-values for comparison of evoked power between 24P and DvP in mutants after ketamine. **B)** Permutation *p*-values for comparison of evoked power between 24P and DvP in control after ketmine. **C)** Permutation *p*-values for comparison of evoked power between mutant DvP and control DvP after ketamine.

6.3.2.8.4 MMN ketamine condition: Total Power

In the ketamine condition, *Ehmt1*$^{D6cre/+}$ did not display significant differences in the total power between these two conditions for any time-frequency combination. While several pixels display higher *p*-values, many occurred pre-stimulus and appear fairly randomly distributed, with few lasted >10ms (Figure 6.12A). A similar condition is found for the total power in the control mice—there were numerous randomly distributed pixels that reached a *p*-value of <.05, however, those that lasted >10ms displayed single pixel widths. (Figure 6.12B). There was a significant increase in total power in the beta and low gamma frequency, in mutant mice after DvP when compared with controls however. This increase occurred ~40ms post-stimulus until ~90ms (Figure 6.12C)

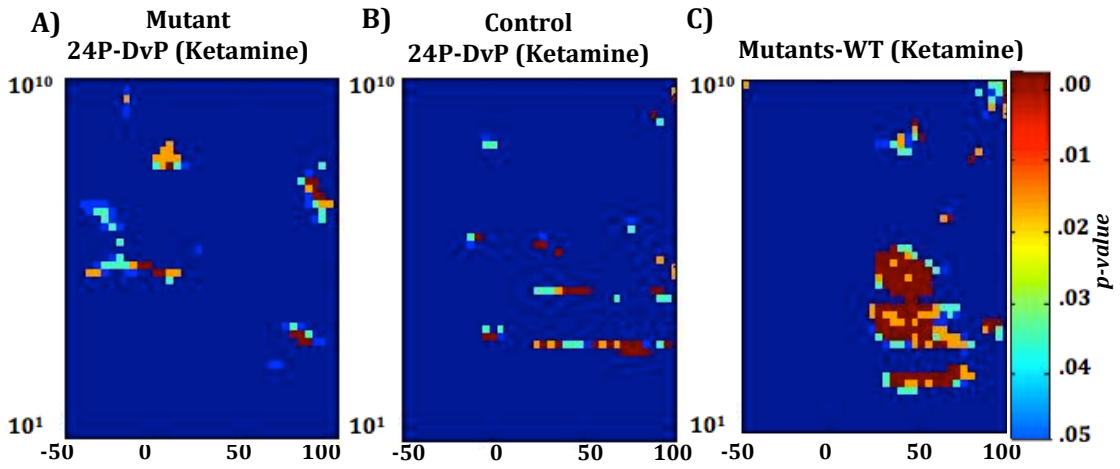

Figure 6.12 Permutation t-test of MMN TOTAL Power after ketamine.
A) Permutation *p*-values for comparison of total power between the 24P to the deviant pulse DvP in mutants after ketamine. **B)** Permutation *p*-values for comparison of total power between 24P and DvP in mutants after ketamine. **C)** Permutation *p*-values for comparison of total power between mutant DvP and wt DvP mutants after ketamine.

6.4 Discussion

The *Ehmt1*$^{D6cre/+}$mutants mice displayed substantial differences in several electrophysiological measures. These included reduced AEP amplitude response in the N1 component, in both the paired-pulse and MMN experiments. They demonstrated reductions in the S1:S2 ratio and MMN detection. Significant differences were identified in high frequency oscillation patterns. *Ehmt1*$^{D6cre/+}$ mutant mice had significantly less evoked power in the beta and gamma frequency bands from the S1 onset until ~90ms post-stimulus in the paired pulse experiment. Similarly, they displayed significantly less evoked and total power in the beta and gamma frequency bands in the MMN task after saline administration.

Ketamine administration in the control mice led to very similar patterns of deficit in electrophysiological response as that found in the *Ehmt1*$^{D6cre/+}$ mutant mice at baseline (saline). After ketamine, control mice showed significant decreases in N1 peak amplitude and deficits in the MMN detection, consistent with that found in the mutants administered only saline. Furthermore, control mice in the ketamine condition did not show the same increased oscillatory power after the deviant pulse that they showed in the saline condition.

Unexpectedly, ketamine administration in *Ehmt1*$^{D6cre/+}$ mutants led to a marginal enhancement in AEP processing. Mutants displayed a trend for increased N1 amplitudes after the deviant pulse in the MMN experiment—and although this increase was not significant, they did display a significant increase in evoked and total power, in the gamma frequency band, at the same time course. However, despite increased beta and gamma oscillations after a dose of ketamine, mutants still did not display greater evoked power than what was observed in control mice administered ketamine.

6.4.1 N1 amplitude attenuation and gating deficits in *Ehmt1*$^{D6cre/+}$ mutant mice

The significant reduction in N1 amplitude in the *Ehmt1*$^{D6cre/+}$ mutant mice replicates a robust endophenotype consistently reported in schizophrenia (for review see, Näätänen et al., 2014) and children with ASD (for review see, Javitt et al., 2012).

However, there were no significant changes in latency for the N1 component, as previously reported (Ehlrichman et al., 2008). The deficit in N1 peak amplitude measured in the time domain, is associated with significant reductions in high frequency oscillatory activity across both beta and gamma bands at the N1 temporal peak. In the paired-pulse experiment, differences in evoked gamma were found from ~20ms-100ms after the S1. In the DvP-saline condition there were significant reduction specifically in the high beta/low gamma ~30ms post-stimulus and lasting until ~90ms in both evoked and total power; and a very specific significant increase in high gamma starting ~20ms post-stimulus and lasting ~50ms post-stimulus in only evoked power after DvP. The consistent decreases in the peak change after the DvP found in both evoked power and total power measurements, in the *Ehmt1*$^{D6cre/+}$ mutant mice is the result of reduced oscillatory network activity and sensory detection. Thus these findings are an indication of robust deficits in sensory processing in these animals.

Similarly the significantly smaller S1:S2 ratios in the N1 peak amplitude, in the *Ehmt1*$^{D6cre/+}$ mutants, suggest reductions in sensory inhibition. The paired pulse paradigm is an electrophysiological measurement that is believed equivalent to the prepulse inhibition paradigm from Chapter 5. Therefore deficits in the higher order processing of sensory information—reflected here with decreased inhibition after the first pulse, corroborate the behavioural measurements in the PPI experiment.

The smaller ratio may reflect either reduced inhibition after S1, and thus a greater S2; or a general decrease in the S1 response (Clementz & Blumenfeld, 2001; Jin & Potkin, 1996; Jin et al., 1997*;* Lazarewicz et al., 2010). Mutant mice did have a significantly smaller response to the S1, which may largely account for the smaller ratio. However, ultimately the response to S1 and S2 were very similar, suggesting there was not the reciprocal inhibition to the auditory pulse in mutant mice either.

In the MMN experiment, there were no differences the AEP components in the standard-pulse, saline condition. This is likely due to pulse averaging. Each 'standard' waveform represents the averaged response across all 24 standard pulses in a trial,

with only 500ms separating each pulse in the trial. Thus, the 'standard' AEP waveforms were substantially smaller than those of the paired-pulse S1 AEP waveform.

6.4.2 No Autism-like P2 deficits in AEP

The attenuation in the P2 peak is the most consistently reported deficit in the ASD literature (for reviews see, Bomba & Pang, 2004; Marco et al., 2011). Differences in the P2 component were not significant. However a trend is observed for the reduction of the P2 peak amplitude in the *Ehmt1*$^{D6cre/+}$mutant mice. That there was a consistent trend across experiments and conditions does elicit interest. The P2 peak is found to have a longer temporal range. Thus individual variations in the temporal peak and/or prolonged peaks may increase variability of this measurement. Further examination of the component would greatly benefit from larger sample sizes.

6.4.4 *Ehmt1*$^{D6cre/+}$mutant mice deviant-detection deficits in the MMN task

There are several theories for what the MMN represents. At one extreme, the MMN is thought to be a higher-order process that involves the short-term memory of the qualitative features of the standard tone. These features are used to compare to the qualitative features of the deviant tone, and result in the detection of difference (Garrido et al., 2009). At the other extreme, it is suggested to simply represent the response elicited by different population of neurons, attuned to specific qualitative features (Garrido et al., 2009). Regardless of the level of complexity evoked by the processing demands, ultimately the mutant mice showed no evidence of auditory deviance detection or an increase in the electrical activity. These mice had identical N1 waveforms between standard or deviant tones, no differences in the 50-75ms epoch and no changes in evoked or total power at any frequency band in the saline condition. Thus evidence suggests mutant mice have deficits in auditory discrimination.

Meanwhile, the control mice demonstrated a significant difference in the N1 peak after the deviant tone in the MMN experiment. As expected, the largest difference between standard and deviant conditions in the epoch analysis was for the later 50-75ms epoch, just after the 40ms post-stimulus N1 peak. The source for this difference, and whether this protocol indeed captures the human-like MMN effect is unclear. However the MMN

effect was immediately preceded by a significant increase in evoked power in high gamma frequency, specifically in the control mice, and only when the 24P was compared with the DvP. There were two smaller peak differences in in evoked power in lower gamma; and much broader changes in total power in the lower gamma and beta frequency bands across the epoch as well. These findings suggest there was a marked increase in the allocation of resources and/or additional processing demands after DvP compared to the 24P, but in the control mice only.

One explanation for the difference between mutant and control mice could be general hearing deficits, in other words the mutant mice may not detect the 500Hz variation in the click frequency for the deviant tones. However, as we saw with the PPI experiment in Chapter 5, mutant mice display exaggerated motor responses to auditory stimulus at frequency and dB ranges below that tested here, suggesting deficits found in MMN do not arise from general deafness. That said, I cannot entirely rule out the fact the repetitive nature of the stimulus in these experiments led to frequency-specific hearing loss in the mutant mice, only. However, of note, the MMN differences reported here are found from trial one onwards, which suggests if there is a frequency-specific hearing deficit in these mice, it existed *a priori* to the MMN experiment.

6.4.5 NMDA hypofunction as a model of psychosis

Acute subanaesthetic doses of ketamine are often used to model both positive and negative symptoms of schizophrenia in humans (Kreitschmann-Andermahr et al., 2001; Malhotra et al., 1997; Newcomer et al., 1999; Umbrict et al., 2000*)* and animals (Amman et al., 2009; Ehrlichman et al., 2008; Featherstone et al., 2013; for reviews, Engin et al., 2009; Lazarewicz et al., 2010). Ketamine acts as a non-competitive antagonist of N-methyl-D-aspartate (NMDA) receptors, binding to the phencyclidine site within the ion channel of the NMDAR complex, while also altering dopaminergic neurotransmission (Becker et al., 2003; Lazarewicz et al., 2010). Thus, subanaesthetics doses are found to replicate symptoms associated with both hyperdopaminergic and hypoglutamaterigic mechanisms of the disorder (Gunduz-Bruce, 2009).

Administration of ketamine in humans leads to significant reductions in the mean peak amplitude of the N1 in the MMN-to-pitch and duration deviants (Kreitschmann-Andermahr et al., 2001). Mice administered ketamine demonstrated similar reductions in N1 amplitude, in a dose-dependent response (Lazarewicz et al., 2010). Ketamine was also reported in Ehrlichman et al. to lead to significant increase in basal gamma power and significant decreases in evoked gamma power in mice (Lazarewicz et al., 2010). Thus, ketamine administration in mice replicates the deficits reported in humans administered ketamine and individuals diagnosed with schizophrenia.

After the administration of ketamine we find deviance detection is completely attenuated in the control mice. In fact in the ketamine trials, mutant and control animals have very similar waveforms (Figure 6.6B) and very similar evoked time-frequency plots (Figure 6.10A-F.) between standard and deviant conditions. In other words, the deficits identified in the mutant mice in general are very similar to those found in the control mice, after they were administered ketamine. As discussed above, in the literature, the non-competitive NMDA-antagonist, ketamine, led to significant decreases in the N1 peak amplitude and MMN deviant detection. Furthermore, this study supports the integral role of NMDA function in these electrophysiological measurements, while suggesting *Ehmt1* haploinsufficiency in the forebrain may lead to general NMDA-hypofunction.

One notable similarity in the ketamine condition is the increase in ~50Hz oscillatory activity. This activity is found across the mean time-frequency plots and occurs regardless of the pulse (i.e. it is found before and after stimulus). 50Hz noise often occurs as a result of ambient electrical interference (Luck et al., 2011). However, the same pre-stimulus 50Hz activity is not found in the saline condition for control mice. Therefore the increase in ~50Hz oscillatory activity in the mutant mice and in the ketamine condition may reflect a global increase in basal gamma activity.

The mutant response to the DvP after ketamine condition somewhat complicates the story. While the ketamine administration was not found to have a significant effect on any of the AEP components, there was a trend for greater N1 amplitude in the DvP

condition. This trend was further supported by increases in higher frequency band activity. That being said, the permutation tests on the ketamine condition, produce a large number of randomly distributed, single-pixel p-values of <.05 (Figure 6.11A; 6.12A-C). This may suggest that either the ketamine recordings were of poorer quality or that ketamine induced random oscillatory activity, specifically in the gamma band. While the ketamine and saline trials were recorded concomitantly and the order of ketamine and saline administration was counterbalanced across genotypes, whether or not there was a systematic difference in recording quality has not been assessed. Furthermore, it is unclear whether the increase in gamma after the DvP in mutants does in fact represent increases in stimulus evoked processing activity or just noise.

In summary, *Ehmt1* forebrain-specific haploinsufficiency leads to similar electrophysiological deficits found in neurodevelopment disorders, across several measurements. Preliminary data suggests these deficits may in fact share similar mechanistic explanations. In other words, the NMDA-hypofunction associated with the human neurodevelopment deficits appears to be replicated in the *Ehmt1*$^{D6cre/+}$mutant mice. These findings are not only novel but also very pertinent. The *Ehmt1*$^{D6cre/+}$mutant model may provide an essential link between epigenetic dysregulation and NMDA hypofunction in the disturbance of normal oscillatory activity. Further investigation is warranted and may prove especially useful in the development of drug targets for the shared pathophysiology in neurodevelopment disorders.

Chapter VII. General Discussion

7.1 Summary of findings

The human brain is comprised of billions of neurons, which form complex networks. These networks interact with unimaginably precise spatial and temporal acuity to preform highly diverse functions. When considering the vast heterogeneity in cell type, the limited opportunities for isolating specific population of cells or the technological demands of capturing change that occurs at millisecond time resolutions, we find the field of epigenetics has a formidable challenge when it comes to the brain. It is perhaps no wonder that there is a lag in understanding the epigenetic regulation of such a complex organ (Shin et al., 2014).

From a much broader perspective the study of *EHMT1*-haploinsufficiency is a test bed for examining the guiding principles of epigenetics, for uncovering homologous mechanisms of cellular differentiation and memory. Such research may lead to a greater understanding of cellular plasticity and reprograming. From a more narrow perspective the outcomes of this research may benefit a specific population of people, those with neurodevelopmental disorders and *EHMT1* lesions.

Below I summarise the findings of my data and put forward two hypotheses. I offer a brief overview of some of the limitations with the research and what might be beneficial for both the immediate and more distant future. Finally I attempt to places the value of this work into the broad context of psychiatric medicine.

7.1.1 *Ehmt1*$^{+/-}$ leads to precocious neuronal differentiation

Ehmt1-haploinsufficient NPCs had significant decreases in the proliferation rates in the vitro pyramidal differentiation experiment. Whether this is due to there being greater numbers of cells in stages of terminal differentiation in the population, or to disruptions in the cell cycle, with likely increased G1 length is unclear. Ultimately, these explanations may be inextricably connected, as prolonged G1 phase is linked with a critical phase in

cell-cycle progression, were extracellular cues may direct cell cycle withdrawal or further rounds of cell division (Pilaz et al., 2009). Thus quiescence may suggest that a greater number of cells are falling out of the cell cycle as well. In support of this finding, there was a trend for the up-regulation of the transcription factor Tbr1 in the *Ehmt1*$^{+/-}$ cells at this stage in NPCs differentiation. Tbr1 is a characteristic marker of post-mitotic neurons in the developing cortex (Kowalczyk et al., 2006).

The *Ehmt1*-haploinsufficient cells demonstrated a different transcriptional profile at two stages of *in vitro* differentiation. Overall there was a significant increase in the fold-change in a number of neuronal-specific genes, many of which are typically expressed at later stages in development. There was a significant decrease in REST/NRSF mRNA, which corresponded with the up-regulation of a number of known target genes of REST/NRSF -repression. Thus evidence of the decreased proliferation in couple with the significant up-regulation in later neuronal markers suggests *Ehmt1*$^{+/-}$ cells are undergoing precocious differentiation. Furthermore, this phenotype appears partially mediated by decreases in REST/NRSF expression. However, whether the transcriptional changes in the REST-network represent actual disruption or the appropriate stage-specific expression in cells further along the differentiation timeline, is unclear. Based on previous findings and the role of G9a/GLP in REST-mediate repression, one could speculate that the precocious differentiation is indeed a symptom of REST-complex dysregulation (Gao et al., 2011).

The *Ehmt1*$^{+/-}$ NPCs ultimately did not survive the differentiation process. How precocious differentiation relates to cell death at later stages of differentiation is unknown. And indeed, reasons for the lack of pyramidal neuron survive in *Ehmt1*$^{+/-}$ cells is also unknown. One suggestion is that these cells had disruptions in their ability to handle oxidative stress. A similar explanation may be that precocious differentiation led to premature up-regulation in a number of glutamate receptor subunit genes, and a hyperglutamaturgic state. In turn cells died of excitotoxicity. Ultimately these hypotheses are only speculation at this stage.

7.1.2 *Ehmt1*$^{D6Cre/+}$ mice display neurodevelopmental endophenotypes

The functional consequences of Ehmt1 haploinsufficiency in the mouse forebrain, throughout development were profound. Importantly, no deficits were found in motor coordination and motor-learning—thus subsequent phenotypes could not be accounted for by impaired motoric function. However, the *Ehmt1*$^{D6Cre/+}$ mutant mice were hypoactive when activity levels were examined specifically, albeit during the light cycle. However, they demonstrated novelty-induced hyperactivity, especially in the earlier stages of the novelty investigation experiments. They displayed decreased latency to investigate a novel social conspecific, but similar amounts of time spent in overall inspection of the novel individual. Mixed genotype cages displayed unexpectedly high levels of whisker, facial hair and in some instances, whole body barbering.

Perhaps the most interesting outcomes were those relating to translational psychiatric endophenotypes. *Ehmt1*$^{D6Cre/+}$ mice did not display novel object recognition (NOR), even after short (15min) retention periods. These data are especially weighty considering the increased activity in response to novelty in general, in environment and social novelty exploration tasks. Thus the equal exploration times spent investigating the non-novel and novel objects during the test phase suggest these mice have severe memory deficits. *Ehmt1*$^{D6Cre/+}$ mice displayed deficits in sensory processing—demonstrated by the enhanced auditory startle response, decreased startle habituation and decreased N1 amplitude in auditory event related potentials (AEP). They also displayed sensorimotor gating deficits in the prepulse inhibition (PPI) experiment and in the paired pulse AEP experiment. Finally the deficits identified in the AEP experiments were associated with physiological deficits. The mice had significant reductions in the evoked and total power in gamma and beta frequency oscillations—which contribute to an imbalance between excitatory and inhibitory neurotransmitter systems.

In summary, *Ehmt1* regulates neuronal-specific gene expression throughout differentiation, in a model of pyramidal NPC development. *Ehmt1* gene dosage does appear to be important for stability and survival of neurons *in vitro*. The functional outcome of forebrain-specific *Ehmt1*-haploinsufficiency during development, suggests that *Ehmt1* dosage is important for a range of electrophysiological and behavioural

responses in the adult mouse. The deficits in the electrophysiological and behavioural responses reported here are very similar to those found in *Ehmt1*-associated neurodevelopmental disorders in humans.

7.2 Hypothesis of findings

7.2.1 GLP plays a important role in forebrain development and function

In previous research, one *Ehmt1*-null model demonstrated the up-regulation of mostly non-neuronal genes in the mouse brain. These findings led to the hypothesis that *Ehmt1*/Glp acts as a regulator of transcriptional homeostasis and may not have a direct a role in essential cellular processes in the brain (Schaefer et al., 2009). This animal model did show subtle differences in cell morphology—or reduced dendrite complexity in the hippocampus. But on the whole *Ehmt1*-haploinsufficiency did not lead to gross structural changes. One of the primary goals of the work in this thesis was to establish whether *Ehmt1*/Glp does in fact play a role in the regulation of neuronal specific genes and development. The data reported here not only supports the hypothesis that GLP is a key epigenetic regulator in neuronal development, it also suggests peak activity may occur in prenatal stages of development and NPC differentiation. An important difference between these data and that previously reported in Schaefer et al. may have been the stage at which genetic ablation took place (2009). I investigated differentiation from the ground state to the neuronal state, whereas in $Ehmt1^{flp/flp;camkIIα/camkIIα}$, loss of Glp occurs postnatal.

Similar to previous observations, gross morphological changes were not identified. However, forebrain development appears to be especially sensitive to GLP dosage. In an attempt to replicate disease-relevant cortical disruptions, only one allele was disrupted in this mouse. However, disruption still led to robust electrophysiological and behavioural changes, reminiscent of those reported in *Ehmt1*-associated neurodevelopmental disorders. That a spatial-restricted model was able to recapitulate many of the translational endophenotypes found in patient populations, may suggest a

predominant role for this enzyme in forebrain-specific development. This finding has profound implications for future work. First, *Ehmt1*/Glp -regulation is likely a part of a complex pathway—thus identifying interacting partners in this pathway could greatly contribute to our general understanding of forebrain development and neurodevelopmental disorders. And second, targeting the forebrain for pharmacological intervention in these patients may be sufficient for marked improvements in the functional outcome.

7.2.2 Ehmt1-haploinsufficiency shows NMDA receptor hypofuntion

There are several lines of evidence that point to the involvement of a dysfunctional glutamate system in neurodevelopment disorders. The evidence ranges from the huge overlap in susceptibility of disorder and genetic risk in glutamate system-related genes (Crespi et al., 2010; Harrison & Weinberger, 2005; Reichelt et al., 2012; Walsh et al., 2008; Zoghbi & Bear, 2012); to the acute and chronic pharmacological manipulation of the NMDA receptors (Amann et al., 2009; Bubenikova-Valesova et al., 2008; Grayson et al., 2007; Jentsch & Roth, 1999; Paoletti & Neyton, 2007; Umbricht et al., 2000). Studies of general glutamate receptor function have also been useful for identified parallels between neurochemical changes and behavioural dysfunction (for reviews of glutamate models see, Inta et al., 2010; see also, Bickel & Javitt, 2009; Inta et al., 2012; Javitt et al., 2011; Moghaddam & Javitt, 2012). Perhaps unsurprisingly the majority of the phenotypes identified in *Ehmt1*$^{D6Cre/+}$ are remarkably similar to models of NMDA hypofunction—the mouse phenotypes reported here are reviewed in the context of this hypothesis.

7.2.2.1 NMDA in neurodevelopment

Perhaps one model which is particular relevant to the work here is the perinatal NMDA antagonism model. Mice treated throughout embryonic development with an NMDA antagonist continue to display behavioural change similar to that of schizophrenia, long after the cessation of the drugs (Bubenikova-Valesova et al., 2008; Marie du Bois & Huang, 2006;). This may be due in part to the fact developing neurons depend on NMDA stimulation for survival, as antagonism of the NMDA

system during synaptogenesis leads to significant increases in apoptotic degeneration (Olney et al., 1999). While during periods of heighten growth, cells with NMDA receptors are extremely sensitive to NMDA, both over-stimulation (Ikonomidou et al., 1989) and under-stimulation (Ikonomidou et al., 1999). It is hypothesised that imbalances in glutamate or glycine production during development and either over-stimulation or under-stimulation of NMDA receptors may have greatly contributed to the phenotype that we find in the *Ehmt1*$^{D6Cre/+}$ mice. Similarly, and while it is purely speculation, cell death in our *in vitro* cell model may have arisen as a consequence of NMDA over or under-stimulation.

7.2.2.2 NMDA in sensorimotor gating

Numerous rodent models with disruptions in the glutamate system demonstrate PPI deficits. For example, mice hypomorphic for NR1 receptor, an NMDA subunit, showed increased acoustic startle response deficits in PPI (Belforte et al., 2010; Duncan et al., 2004; Halene et al., 2009). Mice with *homer1*—an NMDA interacting protein were found to have increased levels of glutamate in prefrontal cortex and PPI deficits (Szumlinski et al., 2005); as well as mice with Neuregulin 1 mutations (*Nrg1*) (Stefansson et al., 2002). Nrg1 activity is associated with the suppression of NMDA receptor activation, and is believed to contribute to NMDA hypofunction especially in the prefrontal cortex (Hahn et al., 2006). Furthermore, the direct administration of NMDA to different regions of the limbic cortex resulted in disruptions in PPI as well (Swerdlow et al., 2001), which may suggest glutamate dysregulation, regardless of whether it involves increases or decreases in function confer sensorimotor gating deficits.

7.2.2.3 NMDA in electrophysiological measurements

Mismatch negativity (MMN) deficits are associated with numerous neurodevelopmental disorders (Naantanen et al., 2014). Ketamine is often used to model the MMN deficit. *S*-ketamine is found to lead to significant blunting of the MMN, especially in frontal source electrodes in humans (Heekeren et al., 2008). Similar effects have been found in non-humans as well (Csepe et al., 1987; Ehrlichman et al., 2009; Javitt et al., 1996; Witten et al., 2014). In fact, "MMN-

generation appears to index the functional state of NMDAR-mediated neurotransmission even in subjects who do not demonstrate psychopathology (Umbricht et al., 2002)". Gamma and beta frequency oscillations are often significantly reduced in a range of psychiatric populations (Kwon et al., 1999; Ulhass & Singer 2010). Again NMDA antagonism is found to produce changes in global oscillation patterns found in neurodevelopmental disorders. And again, ketamine administration leads to increases in basal gamma frequency oscillations and decreases in behaviourally relevant—evoked gamma frequency oscillations.

The findings that best match my data are that from models of chronic ketamine administration in mice, where there was a decrease in the S1 amplitude (Amann et al., 2009; Lazarewicz et al., 2010). Mice administered ketamine were also found to attenuate the increased N1 amplitude and latency in the MMN (Ehrlichman et al., 2008). While patterns in gamma frequency oscillations were similar as well (Lazarewicz et al., 2010).

7.2.2.4 NMDA cognitive deficits

Compounds that enhance NMDA receptor activity have long been associated with cognitive enhancing effects (Karasawa et al., 2008; Javitt et al., 2012). NMDA receptors are essential for certain types of long-term synaptic plasticity events and the consolidation of memory (Martin & Morris, 2002) and appear essential for one-trial object recognition trials (for review see Dere et al., 2007). MK-801 NMDA receptor antagonist is associated with deficits in NOR; such deficits are recoverable with glycine and D-serine transporter inhibitors. The NMDA antagonist APV (D,L-2-amino-5-phosphonovaleric acid) administered into the prefrontal cortex leads to long term (24hrs+) memory deficits (Akirav & Maroun, 1991). While ketamine administration is found to induce even further cognitive impairments in schizophrenia (Malhotra et al., 1997) it is also found to replicate those found in schizophrenia, in healthy individuals (Umbricht et al., 2000; Newcomer et al., 1999).

7.2.2.5 NMDA in anxiety

The OFT, EPM and NPP tasks from Chapter 4 are often used as measurements of anxiety in rodents. A range of neurotransmitter systems is found to mediate anxiety-related behaviours, including: peptidergic neurotransmitters, corticotropin-releasing hormones, monoaminergic transmitters—norepinephrine, serotonin (5-HT), dopamine, and the amino acid transmitters—gamma-aminobutryric acid (GABA) and glutamate (Bermudo-Soriano et al., 2012). While the monoaminergic systems (serotonergic, noradrenergic and dopaminergic) have received perhaps the most attention in mood and anxiety disorders, there is an increasing interest in the role in the glutamatergic system. A growing body of evidence suggesting the glutamatergic NMDA-receptors are important for the mediation of anxiety, specifically. Numerous competitive NMDA antagonists demonstrate anxiolytic effects—these include (CPP) (3-(2-carboxy piperazine-4yl)-propyl-1-phosphonic-acid) which leads to increases in time spent in open arm and in social interactions and AP5 (2-amino-5-phosphonoheptanoate) and AP7 (2-amino-7-phosphonoheptanoate) which leads to increased time spent in novel social interactions and time spent on the open arm (for review see Bermudo-Soriano, et al., 2012). Genetic mutations in both NMDA subunits: NR1 (Niewoehner et al., 2007) and NR2B (Fraser et al., 1996) lead to significant reductions in anxiety-related behaviours.

The non-competitive NMDA antagonist MK-801, PCP and ketamine have also demonstrated a range of anxiolytic effects. Ketamine has been found to decrease behavioural despair in a forced swim test (Maeng et al, 2008), while also producing anxiolytic-like effects in the EPM and OFT measurements without affecting general locomotor behaviour (Engin, Treit & Dickson, 2009). However, the anxiolytic effects of ketamine may be especially complex, as interspecies differences have been reported while conflicting reports exist within species (for review, Bermudo-Soriano, et al., 2012). One explanation for these differences may be variation on the dosages administered across reports—as lower doses of ketamine are found to decrease anxiety, while higher doses increases anxiety (Krystal et al., 1994).

At this stage, *Ehmt1*$^{D6cre/+}$ mice appear to display a range of very similar phenotypes with models of NMDA-receptor hypofunction. While such a hypothesis is speculative, the D6-Cre model targets the pyramidal neurons of the forebrain—cells that are primarily glutamatergic. Therefore, it is not inconceivable that we find the greatest disruptions in those behaviours mediated by the glutamatergic system. A considerable amount of work remains to establish whether or not there is indeed NMDA-receptor hypofunction in the *Ehmt1*$^{D6cre/+}$ mice; however, preliminary evidence is promising.

7.3 Limitations of findings and areas for improvement

7.3.1 Limitations

Unfortunately the data from the *in vitro* cell differentiation is current not directly relatable to the deficits identified in the *Ehmt1* animal model. This is due to problems with the end point in the cells, and the death of mutant neurons on the one hand; and the strict focus on adult function in the mouse, on the other. In the future, assessing potential roles of oxidative stress and glutamateric toxicity in the NPCs during differentiation might be a next step for investigating decreased cell survival. Corroboration of the cell phenotypes with additional cell models, using different background strains and differentiation protocols, as well examining different types of cells, would be beneficial. And culturing embryonic pyramidal cells from the mutant animals would provide useful models for comparison. Once cells survival is established, ideally connection between these two models will be made through electrophysiological properties.

Characterisation of embryonic brain development and GLP expression in the haploinsufficient mouse model is necessary. Verifying potential changes in proliferation rates and the precocious differentiation in the cortex may provide

useful overlaps between cell phenotype to the animal behaviour and physiology. In addition, analysis of REST-regulation and target genes in the animal brain at different stages of development may provide a mechanistic explanation.

Finally, substantial work is still needed for the assessment of histology in the adult brains—in quantifying structural change, microstructural and cytoarchitecture change, differences in cell number and cell complexity. In addition, despite the initial interest for designing a forebrain-specific animal model, due to time constraints only one cognitive endophenotype was assessed. Future work needs to include a battery of cognitive tasks, potentially utilising touchscreens to assess reversal learning, spatial memory, working memory, and dentate gyrus-dependent pattern separation tasks.

7.3.2 Future outlook

The long-term goals would involve manipulating and addressing the deficits found in the mouse model by attempting both stress and recovery models. At this stage I can only speculate about what type of recovery model would be most beneficial—however they might include things like increasing methyl-donors during prenatal development. Increasing methyl-donors may potentially enhance the methylation activity, in the methyltransferase deficient model. One method may be supplementing maternal diet with high protein levels—throughout pregnancy. Another model of potential recovery would be to modulated the glutamate system during early postnatal development, potentially testing outcomes of the administration of various agonists and antagonist of the NMDA and AMPA receptors. A third model of recovery would be to manipulation adult neurogenesis—either directly through molecular targeting or indirect through environmental stimulation, like exercise. Finally a re-expression model could also be hugely informative for firmly distinguishing the consequences of developmental neuropathology and on-going deficiencies in GLP regulation.

Similar to the recovery models, for a stress model maternal diets low in methyl-donors may lead to more exaggerated phenotypes. Manipulation of the glutamate

system throughout development could also lead to further stress. Finally, social isolation raring could be an intervention that leads to more exaggerated phenotypes in this model.

In addition to aiding in the general characterisation of GLP regulation, stress and recovery models may provide more rapid conclusions to be drawn about potentials for cellular plasticity and recovery of the epigenetic program. Ultimately, recovery and stress models of Ehmt1 haploinsufficiency would provide an opportunity to assess to what degree we might expect functional recovery in patients with disruption in epigenetic regulators and increased psychiatric risk factors. They may aid in predicting to what degree cognitive deficits in the patient populations can be overcome, and thus whether deficits are in large part due to on-going deficiency in GLP as opposed to irreversible neuropathologies associated with developmental disruptions.

7.4 Contributions to the field and future outlook

Despite limitations outline above, the work presented here is novel and I believe it has provided important contributions to the field. First, prior to my research the field lacked precise tools for investigating the role of *Ehmt1* in cognitive function—the $Ehmt1^{D6Cre}$ model is promising in this regard. Second, this model recapitulates many endophenotypes associated with neurodevelopmental disorders, which may point to the forebrain being a particular area of vulnerability and, from the wider perspective, may be especially advantageous for drug development studies. It is the first model to identify cell-specific and region-specific responses to *Ehmt1*-haploinsufficiency, in a disease relevant context. It is the first model to find *Ehmt1*-dosage greatly influences sensory processing, sensorimotor gating, and high frequency oscillations in the cortex. Finally, the cell model is the first to hint at the important interaction between the REST-repressor complex, gene regulation and GLP expression, specifically in pyramidal NPC differentiation and development.

Appendix

Appendix Chart 2.1 mESC PCR protocol for determine non-floxed or floxed allele and wild type allele, used to generate control cell line

PCR Primers	Forward	Reverse- R1	Reverse- R2
Ehmt1$^{Flp/-}$	gcctggtgaattttagtgggc	gtttggggcaagtgtggag	ttgtacaagaaagctgggtct

PCR profile

94°, 5min

94°, 40s

60°, 45s

72°, 1min 35 cycles

72°, 10min

10°, ∞

Appendix Chart 2.2 Primary Antibody chart

Type	Gene	Product	Company
Primary	Nanog	(Cat. No. 09-0020)	Stemgent
Primary	Oct4	(Cat. No. 09-0023)	Stemgent
Primary	SSEA-1	(Cat. No. 09-0005)	Stemgent
Primary	Tbr2	Cat No. AB2283	Millipore
Primary	Pax6	Cat No. AB2237	Millipore

Primary	Nrg2	Cat No. AB15812	Millipore
Primary	RC2	Cat No. MAB5740	Millipore
Primary	Vglut1	Cat No. 135 304	Synaptic Systems
Primary	Vglut2	Cat No. 135 404	Synaptic Systems
Primary	Vgat	Cat No. 131 011	Synaptic Systems
Primary	B3-Tubulin	Cat No. 302 302	Synaptic Systems
Primary	Map2	Cat No. MAB3418A5	Millipore

Appendix Chart 2.3 Secondary Antibody chart

Type	**Name**	**Product**	**Company**
Secondary	DyLight 488	Cat No. 130-95-641	
Secondary	Alexa Fluor 568	Cat No. A11011	Invitrogen
Secondary	Alexa Fluor 546	Cat No. A11010	Life Technologies
Secondary	Alexa Fluor 488	Cat No. A11008	Life Technologies
Secondary	Alexa Fluor 488	Cat No. A11029	Life Technologies
Secondary	Alexa Fluor 568	Cat No. A11011	Invitrogen
Secondary	NL557	NL001	R&D

Secondary	NL637	NL017	R&D

Appendix Chart 2.4 qPCR mESC Primers

q-PCR Primers	Forward	Reverse
Wnt2	5'-AGCTGGAAGGAAGGCTGTAA-3'	5'-GTCGCCTGTT-TTCCTGAAGT-3'
Bpil	5'-GAGAACAGCCAACGAGATGC-3'	5'-AGGG-GTTGGGAAGAGGAA AT-3'
Grm8	5'-CTCGCGCAGTGATTATGTTT-3'	5'-GAAAATGCC CACTCTGGTTT-3'

Appendix Chart 2.5 NPC qPCR gene array results

Gene	D6 Fold-Change	D8 Fold-Change	Genotype *F-value*	Genotype *p-value*	Interaction *F-value*	Interaction *p-value*
Ascl1	20.303	31.607	**23.933**	**0.008**	**32.350**	**0.005**
Bdnf	0.984	1.222	0.851	0.408	4.671	0.097
Bmp4	2.504	0.899	3.730	0.126	**33.952**	**0.004**
Cdh2	22.950	7.137	**35.363**	**0.004**	6.853	0.059
Ctnnd2	3.115	5.040	**19.124**	**0.012**	14.089	0.020
Cux1	1.936	1.792	**18.627**	**0.012**	3.366	0.140
Dkk1	3.300	0.911	3.088	0.154	9.237	0.038
Dkk3	1.155	1.155	1.105	0.353	0.359	0.581

Dlg4	1.361	2.171	**17.701**	**0.014**	**19.872**	**0.011**
Dlx2	0.702	1.443	2.111	0.220	**23.882**	**0.008**
Dnmt3a	1.527	1.041	4.992	0.089	6.287	0.066
Emx2	10.876	2.896	**42.743**	**0.003**	10.768	0.030
Tbr2	1.614	1.676	1.126	0.348	0.033	0.864
Fez1	1.666	9.847	**143.496**	**>0.001**	**74.434**	**>0.001**
Foxg1	0.518	0.271	**19.938**	**0.011**	11.347	0.028
Gfap	0.434	0.383	**39.174**	**0.003**	7.481	0.052
Grin1	3.492	2.724	6.295	0.066	0.967	0.381
Grin2a	1.456	6.872	8.546	0.043	13.609	0.021
Grin3a	0.936	0.971	0.464	0.533	0.003	0.961
Grm8	0.944	0.469	8.235	0.045	**29.530**	**0.006**
L1cam	0.779	15.210	**17.361**	**0.014**	**21.430**	**0.010**
Lhx2	0.716	0.676	8.713	0.042	4.616	0.098
Nanog	1.096	1.538	.524	.509	.751	.435
Nes	7.923	3.670	8.956	0.040	3.074	0.154
Neurod1	44.643	56.000	**83.770**	**0.001**	**92.929**	**0.001**
Neurog1	50.106	60.816	13.449	0.021	**22.389**	**0.009**
Neurog2	40.789	153.900	5.053	0.088	6.654	0.061

Nr2f1	15.068	3.702	**39.009**	**0.003**	5.961	0.071
Nrg1	1.118	1.515	1.268	0.323	4.123	0.112
Nrg2	0.926	0.537	0.897	0.387	2.814	0.169
Nrxn3	9.454	22.547	**17.695**	**0.014**	**17.443**	**0.014**
Ntrk3	1.211	3.244	15.254	0.017	**43.215**	**0.003**
Pax6	19.170	10.706	**33.559**	**0.004**	0.280	0.625
Oct4	0.493	0.898	2.743	0.173	5.524	0.078
Pten	0.930	0.599	15.410	0.017	**38.109**	**0.003**
Shh	4.949	6.557	11.920	0.026	6.158	0.068
Slc1a3	5.409	4.791	12.892	0.023	5.364	0.081
Smarce1	1.684	1.460	**61.465**	**0.001**	0.067	0.809
Sox2	1.148	2.798	12.514	0.024	2.510	0.188
Sox6	1.149	0.991	0.029	0.874	0.104	0.763
Srr	2.051	1.639	**66.211**	**0.001**	1.931	0.237
Syn1	1.204	5.412	**33.920**	**0.004**	**20.108**	**0.011**
Tbr1	0.567	1.998	0.084	0.786	**19.123**	**0.012**

Appendix Chart 2.6 NPC NRSF/REST-complex qPCR results

Gene	D6 Fold-Change	D8 Fold-Change	Genotype *F-value*	Genotype *p-value*	Interaction *F-value*	Interaction *p-value*
Ehmt2	1.125	1.300	5.053	0.088	2.734	0.174
Hdac1	1.251	0.855	0.378	0.572	10.028	0.034
Mecp2	1.005	1.305	3.657	0.128	6.031	0.070
Rcor1	1.483	1.065	11.377	0.028	4.198	0.110
Smarca2	2.316	1.459	**23.038**	**0.009**	0.000	0.985
Smarcd3	1.811	1.281	**22.852**	**0.009**	0.005	0.945
Smarce1	1.684	1.460	**61.465**	**0.001**	0.067	0.809
Nrsf	0.264	0.161	**92.912**	**0.001**	0.455	0.537

Appendix Chart 2.7 NPC NRSF/REST-target genes qPCR results

Gene	D6 Fold-Change	D8 Fold-Change	Genotype *F-value*	Genotype *p-value*	Interaction *F-value*	Interaction *p-value*
Bdnf	0.984	1.222	0.851	0.408	4.671	0.097
Ctnnd2	3.115	5.040	**19.124**	**0.012**	14.089	0.020
Grin2a	1.456	6.872	8.546	0.043	13.609	0.021
L1cam	0.779	15.210	**17.361**	**0.014**	**21.430**	**0.010**
Nefh	1.018	1.315	2.023	0.228	0.244	0.647

Neurog2	40.789	153.900	5.053	0.088	6.654	0.061
Notch4	2.490	5.605	10.099	0.034	8.596	0.043
Nrxn3	9.454	22.547	**17.695**	**0.014**	**17.443**	**0.014**
Ntrk3	1.211	3.244	15.254	0.017	**43.215**	**0.003**
Smad2	1.299	1.043	4.105	0.113	6.139	0.068
Snap25	5.512	122.908	**58.090**	**0.002**	**54.739**	**0.002**
Syn1	1.204	5.412	**33.920**	**0.004**	**20.108**	**0.011**
Syp	2.092	13.010	**44.391**	**0.003**	**64.385**	**0.001**
Stmn/Scg10	1.174	98.946	**299.444**	**>0.001**	**213.036**	**>0.001**

Appendix Chart 2.8 NPC published H3K9me2-targets qPCR results

Gene	D6 Fold-Change	D8 Fold-Change	Genotype *F-value*	Genotype *p-value*	Interaction *F-value*	Interaction *p-value*
Slc6a7	0.432	0.271	**19.042**	**0.012**	0.051	0.833
Bmp5	76.388	0.773	0.190	0.685	6.085	0.069
Bmper	2.279	1.714	7.864	0.049	1.731	0.259
Casp1	3.390	4.110	3.070	0.155	0.521	0.510
Dppa5a	0.383	0.761	10.957	0.030	10.645	0.031
Eif4ebp1	0.616	0.651	**45.162**	**0.003**	0.799	0.422

Appendix Chart 2.9 ***NPC results of genes misregulated in mESC qPCR results***

Gene	D6 Fold-Change	D8 Fold-Change	Genotype *F-value*	Genotype *p-value*	Interaction *F-value*	Interaction *p-value*
Sfrp2	4.640	12.632	**17.075**	**0.014**	7.731	0.050
Nes	7.923	3.670	8.956	0.040	3.074	0.154
Nog	2.215	2.988	6.376	0.065	0.556	0.497
Pten	0.930	0.599	15.410	0.017	**38.109**	**0.003**
Wnt2	0.782	1.024	1.071	0.359	2.289	0.205
Blk	0.717	0.832	2.845	0.167	1.677	0.265

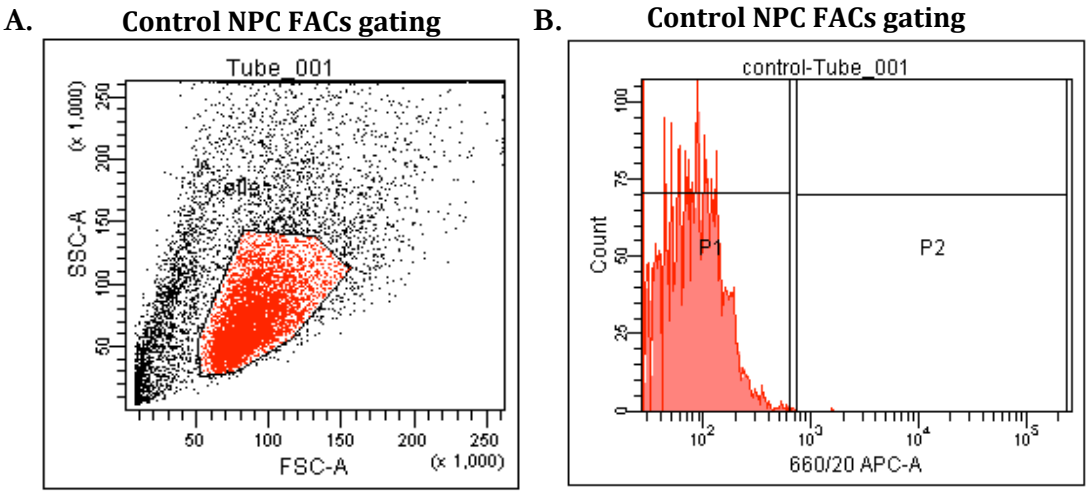

Appendix Figure 2.1 FACs Gating and Control.
A) Plot demonstrating the gating used to determine cell population and to eliminate clumps and debris. Cell population gated based on size using Forward scatter (FSC) and Side scatter (SSC. **B)** Histogram of secondary antibody control for NPCs, demonstrating no florescent positive cells.

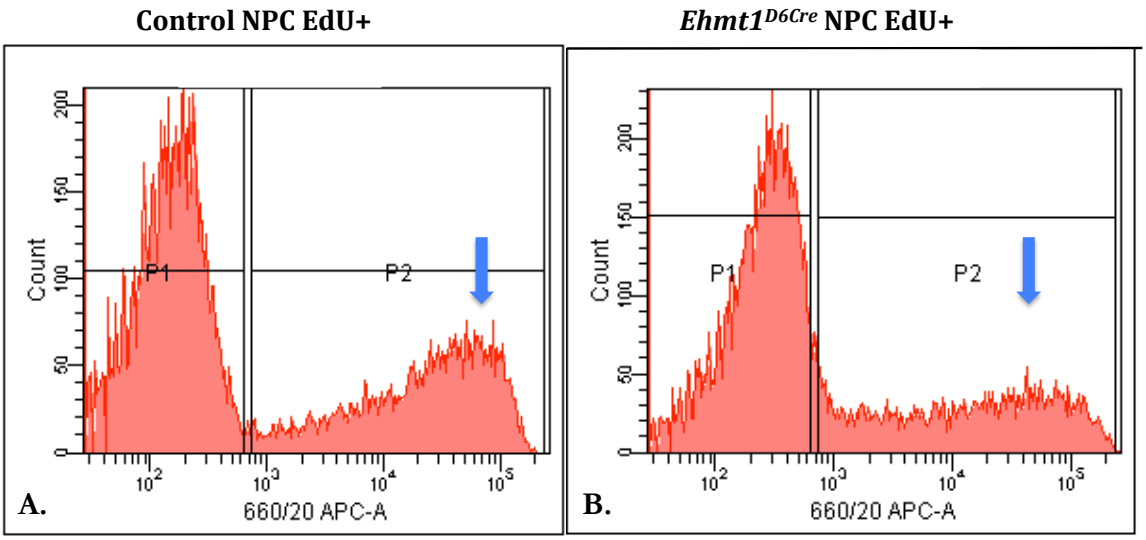

Appendix Figure 2.2 EdU labeled NPC cells.
A) *Ehmt1*$^{+/Flped}$ control NPCs, P2 shows histogram of the florescent positive EdU labeled NPC **B)** *Ehmt1*$^{+/-}$NPCs, blue arrow pointing to the positive cells.

Appendix Chart 3.1 Mouse PCR protocol for determining deleted allele; floxed allele and wild type allele

PCR Primers	Forward	Reverse- R1	Reverse- R2
Ehmt1$^{Flp/+}$	ctcagtcatttactaaaggtg	ccgtgtatttgcagtgcaag	tgcctggcacagaagccatag

PCR profile

94°, 3min

94°, 20s

60°, 45s

72°, 1min 29 cycles

72°, 10min

10°, ∞

Appendix Chart 3.2 Mouse PCR protocol for determine Cre+ expression

PCR Primers	Forward	Reverse
D6-Cre	gtcccattactgaccgtaca	tgaagcatgtttagctggcc

PCR profile

95°, 6min

94°, 45s

58°, 45s

72°, 1min 35 cycles

72°, 10min

10°, ∞

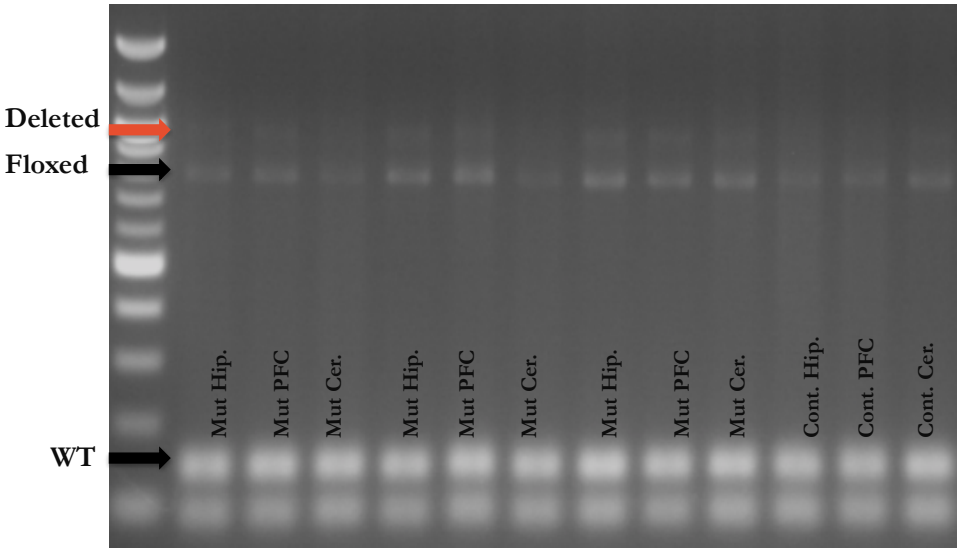

Appendix Figure 3.1 Forebrain & Cerebellum mice PCRs.
Hip—hippocampus; PFC—prefrontal cortex; Cer—Cerebellum. Example PCR gel of 3 brain areas in 3 mutant brains and 1 control brain.

Bibliography

Abrajano, J. J., Qureshi, I. a, Gokhan, S., Zheng, D., Bergman, A., & Mehler, M. F. (2009). REST and CoREST modulate neuronal subtype specification, maturation and maintenance. *PloS One*, *4*(12), e7936. doi:10.1371/journal.pone.0007936

Achim, A. M., Maziade, M., Raymond, E., Olivier, D., Mérette, C., & Roy, M.-A. (2011). How prevalent are anxiety disorders in schizophrenia? A meta-analysis and critical review on a significant association. *Schizophrenia Bulletin*, *37*(4), 811–21. doi:10.1093/schbul/sbp148

Akbarian, S., & Huang, H.-S. (2009). Epigenetic regulation in human brain-focus on histone lysine methylation. *Biological Psychiatry*, *65*(3), 198–203. doi:10.1016/j.biopsych.2008.08.015

Akbarian, S., Ruehl, M. G., Bliven, E., Luiz, L. a, Peranelli, A. C., Baker, S. P., … Guo, Y. (2005). Chromatin alterations associated with down-regulated metabolic gene expression in the prefrontal cortex of subjects with schizophrenia. *Archives of General Psychiatry*, *62*(8), 829–40. doi:10.1001/archpsyc.62.8.829

Akirav, I., & Maroun, M. (2006). Ventromedial prefrontal cortex is obligatory for consolidation and reconsolidation of object recognition memory. *Cerebral Cortex (New York, N.Y. : 1991)*, *16*(12), 1759–65. doi:10.1093/cercor/bhj114

Amann, L. C., Gandal, M. J., Halene, T. B., Ehrlichman, R. S., White, S. L., McCarren, H. S., & Siegel, S. J. (2010). Mouse behavioral endophenotypes for schizophrenia. *Brain Research Bulletin*, *83*(3-4), 147–61. doi:10.1016/j.brainresbull.2010.04.008

Amann, L. C., Halene, T. B., Ehrlichman, R. S., Luminais, S. N., Ma, N., Abel, T., & Siegel, S. J. (2009). Chronic ketamine impairs fear conditioning and produces long-lasting reductions in auditory evoked potentials. *Neurobiology of Disease*, *35*(2), 311–7. doi:10.1016/j.nbd.2009.05.012

Amiet, C., Gourfinkel-An, I., Bouzamondo, A., Tordjman, S., Baulac, M., Lechat, P., … Cohen, D. (2008). Epilepsy in autism is associated with intellectual disability and gender: evidence from a meta-analysis. *Biological Psychiatry*, *64*(7), 577–82. doi:10.1016/j.biopsych.2008.04.030

Anderson, S. a, Kaznowski, C. E., Horn, C., Rubenstein, J. L. R., & McConnell, S. K. (2002). Distinct origins of neocortical projection neurons and interneurons in vivo. *Cerebral Cortex (New York, N.Y. : 1991)*, *12*(7), 702–9. Retrieved from http://www.ncbi.nlm.nih.gov/pubmed/12050082

Angevine, J. B., & Sidman, R. L. (1961). Autoradiographic study of cell migration during histogenesis of cerebral cortex in the mouse.

Antunes, M., & Biala, G. (2012). The novel object recognition memory: neurobiology, test procedure, and its modifications. *Cognitive Processing*, *13*(2), 93–110. doi:10.1007/s10339-011-0430-z

Arguello, P. A., & Gogos, J. a. (2012). Genetic and cognitive windows into circuit mechanisms of psychiatric disease. *Trends in Neurosciences*, *35*(1), 3–13. doi:10.1016/j.tins.2011.11.007

Ariani, F., Hayek, G., Rondinella, D., Artuso, R., Mencarelli, M. A., Spanhol-Rosseto, A., ... & Renieri, A. (2008). *FOXG1* Is Responsible for the Congenital Variant of Rett Syndrome. *The American Journal of Human Genetics*, *83*(1), 89-93.

Atkins, C. M., Selcher, J. C., Petraitis, J. J., Trzaskos, J. M., & Sweatt, J. D. (1998). The MAPK cascade is required for mammalian associative learning. *Nature Neuroscience*, *1*(7), 602–9. doi:10.1038/2836

Balderas, I., Rodriguez-Ortiz, C. J., & Bermudez-Rattoni, F. (2014). Consolidation and reconsolidation of object recognition memory. *Behavioural Brain Research*. doi:10.1016/j.bbr.2014.08.049

Balemans, M. C. M., Ansar, M., Oudakker, A. R., van Caam, A. P. M., Bakker, B., Vitters, E. L., … van Bokhoven, H. (2014). Reduced Euchromatin histone methyltransferase 1 causes developmental delay, hypotonia, and cranial abnormalities associated with increased bone gene expression in Kleefstra syndrome mice. *Developmental Biology*, *386*(2), 395–407. doi:10.1016/j.ydbio.2013.12.016

Balemans, M. C. M., Huibers, M. M. H., Eikelenboom, N. W. D., Kuipers, A. J., van Summeren, R. C. J., Pijpers, M. M. C. a, … Van der Zee, C. E. E. M. (2010). Reduced exploration, increased anxiety, and altered social behavior: Autistic-like features of euchromatin histone methyltransferase 1 heterozygous knockout mice. *Behavioural Brain Research*, *208*(1), 47–55. doi:10.1016/j.bbr.2009.11.008

Balemans, M. C. M., Kasri, N. N., Kopanitsa, M. V, Afinowi, N. O., Ramakers, G., Peters, T. a, … Van der Zee, C. E. E. M. (2013). Hippocampal dysfunction in the Euchromatin histone methyltransferase 1 heterozygous knockout mouse model for Kleefstra syndrome. *Human Molecular Genetics*, *22*(5), 852–66. doi:10.1093/hmg/dds490

Ballas, N., Grunseich, C., Lu, D. D., Speh, J. C., & Mandel, G. (2005). REST and its corepressors mediate plasticity of neuronal gene chromatin throughout neurogenesis. *Cell*, *121*(4), 645-657.

Bandyopadhyaya, D., Nizamie, S. H., Pradhan, N., & Bandyopadhyaya, A. (2011). Spontaneous gamma coherence as a possible trait marker of schizophrenia-An explorative study. *Asian Journal of Psychiatry*, *4*(3), 172–7. doi:10.1016/j.ajp.2011.06.006

Bannerman, D. M., Rawlins, J. N. P., McHugh, S. B., Deacon, R. M. J., Yee, B. K., Bast, T., … Feldon, J. (2004). Regional dissociations within the hippocampus--memory and anxiety. *Neuroscience and Biobehavioral Reviews*, *28*(3), 273–83. doi:10.1016/j.neubiorev.2004.03.004

Barkus, C., McHugh, S. B., Sprengel, R., Seeburg, P. H., Rawlins, J. N. P., & Bannerman, D. M. (2010). Hippocampal NMDA receptors and anxiety: at the interface between cognition and emotion. *European Journal of Pharmacology*, *626*(1), 49–56. doi:10.1016/j.ejphar.2009.10.014

Başar, E., & Güntekin, B. (2008). A review of brain oscillations in cognitive disorders and the role of neurotransmitters. *Brain Research*, *1235*, 172–93. doi:10.1016/j.brainres.2008.06.103

Behrendt, R.-P., & Young, C. (2004). Hallucinations in schizophrenia, sensory impairment, and brain disease: a unifying model. *The Behavioral and Brain Sciences*, *27*(6), 771–87; discussion 787–830. Retrieved from http://www.ncbi.nlm.nih.gov/pubmed/16035402

Belforte, J. E., Zsiros, V., Sklar, E. R., Jiang, Z., Yu, G., Quinlan, E. M., & Nakazawa, K. (2010). Postnatal NMDA receptor ablation in corticolimbic interneurons confers schizophrenia-like phenotypes, *13*(1), 76–83. doi:10.1038/nn.2447.

Belmonte, M. K., Cook, E. H., Anderson, G. M., Rubenstein, J. L. R., Greenough, W. T., Beckel-Mitchener, a, … Tierney, E. (2004). Autism as a disorder of neural information processing: directions for research and targets for therapy. *Molecular Psychiatry*, *9*(7), 646–63. doi:10.1038/sj.mp.4001499

Betancur, C. (2011). Etiological heterogeneity in autism spectrum disorders: more than 100 genetic and genomic disorders and still counting. *Brain Research*, *1380*, 42–77. doi:10.1016/j.brainres.2010.11.078

Bibel, M., Richter, J., Lacroix, E., & Barde, Y. A. (2007). Generation of a defined and uniform population of CNS progenitors and neurons from mouse embryonic stem cells. *Nature protocols*, *2*(5), 1034-1043.

Bibel, M., Richter, J., Schrenk, K., Tucker, K. L., Staiger, V., Korte, M., ... & Barde, Y. A. (2004). Differentiation of mouse embryonic stem cells into a defined neuronal lineage. *Nature neuroscience*, *7*(9), 1003-1009.

Bickel, S., & Javitt, D. C. (2009). Neurophysiological and neurochemical animal models of schizophrenia: focus on glutamate. *Behavioural Brain Research*, *204*(2), 352–62. doi:10.1016/j.bbr.2009.05.005

Bird, C. M., & Burgess, N. (2008). The hippocampus and memory: insights from spatial processing. *Nature Reviews. Neuroscience*, *9*(3), 182–94. doi:10.1038/nrn2335

Black, J. C., & Whetstine, J. R. (2011). Chromatin landscape: methylation beyond transcription. *Epigenetics : Official Journal of the DNA Methylation Society*, *6*(1), 9–15. doi:10.4161/epi.6.1.13331

Bomba, M. D., & Pang, E. W. (2004). Cortical auditory evoked potentials in autism: a review. *International Journal of Psychophysiology : Official Journal of the International Organization of Psychophysiology*, *53*(3), 161–9. doi:10.1016/j.ijpsycho.2004.04.001

Braf, D.L. & Geyer, M. A. (1990). Sensorimotor gating and schizophrenia: Human and animal model studies. *Arch Gen Psychiatry.* (Vol. 47(2) pp. 181–188).

Braff, D. L., Geyer, M. a., & Swerdlow, N. R. (2001). Human studies of prepulse inhibition of startle: normal subjects, patient groups, and pharmacological studies. *Psychopharmacology*, *156*(2-3), 234–258. doi:10.1007/s002130100810

Braff, D., & Greenwood, T. (2008). Advances in endophenotyping schizophrenia. *World Psychiatry*, (12), 11–18. Retrieved from http://onlinelibrary.wiley.com/doi/10.1002/j.2051-5545.2008.tb00140.x/full

Brenner, C. A., Kieffaber, P. D., Clementz, B. A., Johannesen, J. K., Shekhar, A., O'Donnell, B. F., & Hetrick, W. P. (2009). Event-related potential abnormalities in schizophrenia: a failure to "gate in" salient information?. *Schizophrenia research*, *113*(2), 332-338.

Broadbent, N. J., Gaskin, S., Squire, L. R., & Clark, R. E. (2010). Object recognition memory and the rodent hippocampus. *Learning & Memory (Cold Spring Harbor, N.Y.)*, *17*(1), 5–11. doi:10.1101/lm.1650110

Brockhaus-Dumke, A., Mueller, R., Faigle, U. & Klosterkoetter, J. (2008). Sensory gating revisited: Relation between brain oscillations and auditory evoked potentials in schizophrenia *Schizophrenia Research.* 99(1) 238 – 249.

Brook, F. A., & Gardner, R. L. (1997). The origin and efficient derivation of embryonic stem cells in the mouse. *Proceedings of the National Academy of Sciences*, *94*(11), 5709-5712.

Brown, A. S. (2006). Prenatal infection as a risk factor for schizophrenia. *Schizophrenia Bulletin*, *32*(2), 200–2. doi:10.1093/schbul/sbj052

Brown, A. S., & Susser, E. S. (2008). Prenatal nutritional deficiency and risk of adult schizophrenia. *Schizophrenia Bulletin*, *34*(6), 1054–63. doi:10.1093/schbul/sbn096

Bruce, A. W., Donaldson, I. J., Wood, I. C., Yerbury, S. A., Sadowski, M. I., Chapman, M., ... & Buckley, N. J. (2004). Genome-wide analysis of repressor element 1 silencing transcription factor/neuron-restrictive silencing factor (REST/NRSF) target genes. *Proceedings of the National Academy of Sciences of the United States of America*, *101*(28), 10458-10463.

Bubeníková-Valesová, V., Horácek, J., Vrajová, M., & Höschl, C. (2008). Models of schizophrenia in humans and animals based on inhibition of NMDA receptors. *Neuroscience and Biobehavioral Reviews*, *32*(5), 1014–23. doi:10.1016/j.neubiorev.2008.03.012

Burmeister, M., McInnis, M. G., & Zöllner, S. (2008). Psychiatric genetics: progress amid controversy. *Nature Reviews. Genetics*, *9*(7), 527–40. doi:10.1038/nrg2381

Butler, T., Weisholtz, D., Isenberg, N., Harding, E., Epstein, J., Stern, E., & Silbersweig, D. (2012). Neuroimaging of frontal-limbic dysfunction in schizophrenia and epilepsy-related psychosis: toward a convergent neurobiology. *Epilepsy & Behavior : E&B*, *23*(2), 113–22. doi:10.1016/j.yebeh.2011.11.004

Cardin, J. a, Carlén, M., Meletis, K., Knoblich, U., Zhang, F., Deisseroth, K., … Moore, C. I. (2009). Driving fast-spiking cells induces gamma rhythm and controls sensory responses. *Nature*, *459*(7247), 663–7. doi:10.1038/nature08002

Cartmell, J., & Schoepp, D. D. (2000). Regulation of neurotransmitter release by metabotropic glutamate receptors. *Journal of neurochemistry*, *75*(3), 889-907.

Cascella, N. G., Schretlen, D. J., & Sawa, A. (2009). Schizophrenia and epilepsy: Is there a shared susceptibility? *Neuroscience Research*, *63*(4), 227–235. doi:10.1016/j.neures.2009.01.002

Cavalli, G. (2006). Chromatin and epigenetics in development: blending cellular memory with cell fate plasticity. *Development (Cambridge, England)*, *133*(11), 2089–94. doi:10.1242/dev.02402

Chao, H.-T., Chen, H., Samaco, R. C., Xue, M., Chahrour, M., Yoo, J., … Zoghbi, H. Y. (2010). Dysfunction in GABA signalling mediates autism-like stereotypies and Rett syndrome phenotypes. *Nature*, *468*(7321), 263–9. doi:10.1038/nature09582

Charney, D. S. (2003). Neuroanatomical circuits modulating fear and anxiety behaviors. *Acta Psychiatrica Scandinavica. Supplementum*, *108*(417), 38–50. Retrieved from http://www.ncbi.nlm.nih.gov/pubmed/12950435

Chen, J., Lipska, B. K., & Weinberger, D. R. (2006). Genetic mouse models of schizophrenia: from hypothesis-based to susceptibility gene-based models. *Biological Psychiatry*, *59*(12), 1180–8. doi:10.1016/j.biopsych.2006.02.024

Chen, R. Z., Akbarian, S., Tudor, M., & Jaenisch, R. (2001). Deficiency of methyl-CpG binding protein-2 in CNS neurons results in a Rett-like phenotype in mice. *Nature Genetics*, *27*(3), 327–31. doi:10.1038/85906

Clark, R. E., & Squire, L. R. (2010). An animal model of recognition memory and medial temporal lobe amnesia: history and current issues. *Neuropsychologia*, *48*(8), 2234–44. doi:10.1016/j.neuropsychologia.2010.02.004

Clarke, M. C., Tanskanen, A., Huttunen, M. O., Clancy, M., Cotter, D. R., & Cannon, M. (2012). Evidence for shared susceptibility to epilepsy and psychosis: a population-based family study. *Biological Psychiatry*, *71*(9), 836–9. doi:10.1016/j.biopsych.2012.01.011

Clementz, B. A., & Blumenfeld, L. D. (2001). Multichannel electroencephalographic assessment of auditory evoked response suppression in schizophrenia. *Experimental Brain Research*, *139*(4), 377-390.

Connolly, P. M., Maxwell, C. R., Kanes, S. J., Abel, T., Liang, Y., Tokarczyk, J., … Siegel, S. J. (2003). Inhibition of auditory evoked potentials and prepulse inhibition of startle in DBA/2J and DBA/2Hsd inbred mouse substrains. *Brain Research*, *992*(1), 85–95. doi:10.1016/j.brainres.2003.08.035

Cooper, G. M., Coe, B. P., Girirajan, S., Rosenfeld, J. a, Vu, T. H., Baker, C., … Eichler, E. E. (2011). A copy number variation morbidity map of developmental delay. *Nature Genetics*, *43*(9), 838–46. doi:10.1038/ng.909

Costall, B., Jones, B. J., Kelly, M. E., & Naylor, R. J. (1989). Exploration of mice in black and white test box: validation as a model of anxiety. *Pharmacology, Biochemistry, and Behavior*, *32*, 777–785.

Cotter, D., Kerwin, R., Al-Sarraji, S., Brion, J. P., Chadwich, A., Lovestone, S., ... & Everall, I. (1998). Abnormalities of Wnt signalling in schizophrenia-evidence for neurodevelopmental abnormality. *Neuroreport*, *9*(7), 1379-1383.

Crawley, J. & Goodwin, F. K. (1980). Preliminary report of a simple animal behavior model for the anxiolytic effects of benzodiazepines. *Pharmacol Biochem Behav* 13, 167-70 (1980).

Crawley, J. N. (1999). Behavioral phenotyping of transgenic and knockout mice: experimental design and evaluation of general health, sensory functions, motor abilities, and specific behavioral tests. *Brain Research*, *835*(1), 18–26. Retrieved from http://www.ncbi.nlm.nih.gov/pubmed/10448192

Crespi, B., Stead, P., & Elliot, M. (2010). Evolution in health and medicine Sackler colloquium: Comparative genomics of autism and schizophrenia. *Proceedings of the National Academy of Sciences of the United States of America*, *107 Suppl 1*, 1736–41. doi:10.1073/pnas.0906080106

Csépe, V., Karmos, G., & Molnár, M. (1987). Evoked potential correlates of stimulus deviance during wakefulness and sleep in cat--animal model of mismatch negativity. *Electroencephalography and Clinical Neurophysiology*, *66*(6), 571–8. Retrieved from http://www.ncbi.nlm.nih.gov/pubmed/2438122

Davis, E., Saeed, S. A., & Antonacci, D. J. (2008). Anxiety disorders in persons with developmental disabilities: empirically informed diagnosis and treatment. Reviews literature on anxiety disorders in DD population with practical take-home messages for the clinician. *The Psychiatric Quarterly*, *79*(3), 249–63. doi:10.1007/s11126-008-9081-3

Davis, M. (1992). The role of the amygdala in fear and anxiety. *Annual Review of Neuroscience*, *15*, 353–75. Retrieved from http://www.annualreviews.org/doi/pdf/10.1146/annurev.ne.15.030192.002033

Dawson, a J., Putnam, S., Schultz, J., Riordan, D., Prasad, C., Greenberg, C. R., … Chudley, a E. (2002). Cryptic chromosome rearrangements detected by subtelomere assay in patients with mental retardation and dysmorphic features. *Clinical Genetics*, *62*(6), 488–94. Retrieved from http://www.ncbi.nlm.nih.gov/pubmed/12515261

Day, J. J., & Sweatt, J. D. (2011). Epigenetic mechanisms in cognition. *Neuron*, *70*(5), 813–29. doi:10.1016/j.neuron.2011.05.019

De Bruin, E. I., Ferdinand, R. F., Meester, S., de Nijs, P. F. a, & Verheij, F. (2007). High rates of psychiatric co-morbidity in PDD-NOS. *Journal of Autism and Developmental Disorders*, *37*(5), 877–86. doi:10.1007/s10803-006-0215-x

Dere, E., Huston, J. P., & De Souza Silva, M. a. (2007). The pharmacology, neuroanatomy and neurogenetics of one-trial object recognition in rodents. *Neuroscience and Biobehavioral Reviews*, *31*(5), 673–704. doi:10.1016/j.neubiorev.2007.01.005

Di Cristo, G. (2007). Development of cortical GABAergic circuits and its implications for neurodevelopmental disorders. *Clinical Genetics*, *72*(1), 1–8. doi:10.1111/j.1399-0004.2007.00822.x

Dong, K. B., Maksakova, I. a, Mohn, F., Leung, D., Appanah, R., Lee, S., … Lorincz, M. C. (2008). DNA methylation in ES cells requires the lysine methyltransferase G9a but not its catalytic activity. *The EMBO Journal*, *27*(20), 2691–701. doi:10.1038/emboj.2008.193

Donohoe, M. E., Silva, S. S., Pinter, S. F., Xu, N., & Lee, J. T. (2009). The pluripotency factor Oct4 interacts with Ctcf and also controls X-chromosome pairing and counting. *Nature*, *460*(7251), 128-132.

Du Bois, T. M., & Huang, X.-F. (2007). Early brain development disruption from NMDA receptor hypofunction: relevance to schizophrenia. *Brain Research Reviews*, *53*(2), 260–70. doi:10.1016/j.brainresrev.2006.09.001

Duncan, G. E., Moy, S. S., Perez, A., Eddy, D. M., Zinzow, W. M., Lieberman, J. a, … Koller, B. H. (2004). Deficits in sensorimotor gating and tests of social behavior in a genetic model of reduced NMDA receptor function. *Behavioural Brain Research*, *153*(2), 507–19. doi:10.1016/j.bbr.2004.01.008

Eack, S. M., Bahorik, A. L., McKnight, S. a F., Hogarty, S. S., Greenwald, D. P., Newhill, C. E., … Minshew, N. J. (2013). Commonalities in social and non-social cognitive impairments in adults with autism spectrum disorder and schizophrenia. *Schizophrenia Research*, *148*(1-3), 24–8. doi:10.1016/j.schres.2013.05.013

Efroni, S., Duttagupta, R., Cheng, J., Dehghani, H., Hoeppner, D. J., Dash, C., ... & Meshorer, E. (2008). Global transcription in pluripotent embryonic stem cells. *Cell stem cell*, *2*(5), 437-447.

Egan, M. F., Goldberg, T. E., Gscheidle, T., Weirich, M., Rawlings, R., Hyde, T. M., … Weinberger, D. R. (2001). Relative risk for cognitive impairments in siblings of patients with schizophrenia. *Biological Psychiatry*, *50*(2), 98–107. Retrieved from http://www.ncbi.nlm.nih.gov/pubmed/11527000

Ehrlichman, R. S., Gandal, M. J., Maxwell, C. R., Lazarewicz, M. T., Finkel, L. H., Contreras, D., … Siegel, S. J. (2009). N-methyl-d-aspartic acid receptor antagonist-induced frequency oscillations in mice recreate pattern of electrophysiological deficits in schizophrenia. *Neuroscience*, *158*(2), 705–12. doi:10.1016/j.neuroscience.2008.10.031

Ehrlichman, R. S., Maxwell, C. R., Majumdar, S., & Siegel, S. J. (2008). Deviance-elicited changes in event-related potentials are attenuated by ketamine in mice. *Journal of Cognitive Neuroscience*, *20*(8), 1403–14. doi:10.1162/jocn.2008.20097

Ellenbroek, B. a, Budde, S., & Cools, a R. (1996). Prepulse inhibition and latent inhibition: the role of dopamine in the medial prefrontal cortex. *Neuroscience*, *75*(2), 535–42. Retrieved from http://www.ncbi.nlm.nih.gov/pubmed/8931016

Engel, a K., Fries, P., & Singer, W. (2001). Dynamic predictions: oscillations and synchrony in top-down processing. *Nature Reviews. Neuroscience*, *2*(10), 704–16. doi:10.1038/35094565

Engin, E., Treit, D., & Dickson, C. T. (2009). Anxiolytic- and antidepressant-like properties of ketamine in behavioral and neurophysiological animal models. *Neuroscience*, *161*(2), 359–69. doi:10.1016/j.neuroscience.2009.03.038

English, J. D., & Sweatt, J. D. (1996). Activation of p42 Mitogen-activated Protein Kinase in Hippocampal Long Term Potentiation. *Journal of Biological Chemistry*, *271*(40), 24329–24332. doi:10.1074/jbc.271.40.24329

Epsztejn-Litman, S., Feldman, N., Abu-Remaileh, M., Shufaro, Y., Gerson, A., Ueda, J., … Bergman, Y. (2008). De novo DNA methylation promoted by G9a prevents reprogramming of embryonically silenced genes. *Nature Structural & Molecular Biology*, *15*(11), 1176–83. doi:10.1038/nsmb.1476

Escera, C., Alho, K., Winkler, I., & Näätänen, R. (1998). Neural Mechanisms of Involuntary Attention to acoustic novelty and change. *Journal of Cognitive …*, 590–604. Retrieved from http://www.mitpressjournals.org/doi/abs/10.1162/089892998562997

Espósito, M. S., Piatti, V. C., Laplagne, D. A., Morgenstern, N. A., Ferrari, C. C., Pitossi, F. J., & Schinder, A. F. (2005). Neuronal differentiation in the adult hippocampus recapitulates embryonic development. *The Journal of neuroscience*, *25*(44), 10074-10086.

Estève, P.-O., Chin, H. G., Smallwood, A., Feehery, G. R., Gangisetty, O., Karpf, A. R., … Pradhan, S. (2006). Direct interaction between DNMT1 and G9a coordinates DNA and histone methylation during replication. *Genes & Development*, *20*(22), 3089–103. doi:10.1101/gad.1463706

Etherton, M. R., Blaiss, C. A., Powell, C. M., & Su, T. C. (2009). Mouse neurexin-1 ␣ deletion causes correlated electrophysiological and behavioral changes.

Evans, M. (2011). Discovering pluripotency: 30 years of mouse embryonic stem cells. *Nature Reviews. Molecular Cell Biology*, *12*(10), 680–6. doi:10.1038/nrm3190

Evans, M. J., & Kaufman, M. H. (1981). Establishment in culture of pluripotential cells from mouse embryos. *nature*, *292*(5819), 154-156.

Farmer, S. F. (1998). Topical Review Rhythmicity , synchronization and binding in human and primate motor systems, 3–14.

Fass, D. M., Reis, S. a, Ghosh, B., Hennig, K. M., Joseph, N. F., Zhao, W.-N., … Haggarty, S. J. (2013). Crebinostat: a novel cognitive enhancer that inhibits histone deacetylase activity and modulates chromatin-mediated neuroplasticity. *Neuropharmacology*, *64*, 81–96. doi:10.1016/j.neuropharm.2012.06.043

Featherstone, R. E., M Tatard-Leitman, V., Suh, J. D., Lin, R., Lucki, I., & Siegel, S. J. (2013). Electrophysiological and behavioral responses to ketamine in mice with reduced Akt1 expression. *Psychopharmacology*, *227*(4), 639–49. doi:10.1007/s00213-013-2997-9

Feil, R., & Fraga, M. F. (2011). Epigenetics and the environment: emerging patterns and implications. *Nature Reviews. Genetics*, *13*(2), 97–109. doi:10.1038/nrg3142

Feinberg, A. P., & Irizarry, R. a. (2010). Evolution in health and medicine Sackler colloquium: Stochastic epigenetic variation as a driving force of development, evolutionary adaptation, and disease. *Proceedings of the National Academy of Sciences of the United States of America*, *107 Suppl* , 1757–64. doi:10.1073/pnas.0906183107

Fendt, M., Li, L., & Yeomans, J. S. (2001). Brain stem circuits mediating prepulse inhibition of the startle reflex. *Psychopharmacology*, *156*(2-3), 216–224. doi:10.1007/s002130100794

Ferri, R., Elia, M., Agarwal, N., Lanuzza, B., Musumeci, S. a, & Pennisi, G. (2003). The mismatch negativity and the P3a components of the auditory event-related potentials in autistic low-functioning subjects. *Clinical Neurophysiology*, *114*(9), 1671–1680. doi:10.1016/S1388-2457(03)00153-6

Fierz, B., & Muir, T. W. (2012). Chromatin as an expansive canvas for chemical biology. *Nature chemical biology*, *8*(5), 417-427.

Finlay, B. L., & Darlington, R. B. (1995). Linked regularities in the development and evolution of mammalian brains. *Science*, *268*(5217), 1578-1584.

Fisahn, A., Neddens, J., Yan, L., & Buonanno, A. (2009). Neuregulin-1 modulates hippocampal gamma oscillations: implications for schizophrenia. *Cerebral Cortex (New York, N.Y. : 1991)*, *19*(3), 612–8. doi:10.1093/cercor/bhn107

Fraser, C. M., Cooke, M. J., Fisher, a, Thompson, I. D., & Stone, T. W. (1996). Interactions between ifenprodil and dizocilpine on mouse behaviour in models of anxiety and working memory. *European Neuropsychopharmacology : The*

Journal of the European College of Neuropsychopharmacology, *6*(4), 311–6. Retrieved from http://www.ncbi.nlm.nih.gov/pubmed/8985715

Freeman, R., Adler, L.E., Myles-Worsley, M., Nagamoto, H. T. Miller, C., Kisley, M., McRae, K, Cawthra, E, Waldo, M. (1996). Inhibitory gating of an evoked response to repeated auditory stimuli in schizophrenia and normal subjects: Human recordings, computer stimulation, and an animal model. *Arch Gen Psychiatry*. 53(12), 1114–1121.

Fritsch, L., Robin, P., Mathieu, J. R. R., Souidi, M., Hinaux, H., Rougeulle, C., … Ait-Si-Ali, S. (2010). A subset of the histone H3 lysine 9 methyltransferases Suv39h1, G9a, GLP, and SETDB1 participate in a multimeric complex. *Molecular Cell*, *37*(1), 46–56. doi:10.1016/j.molcel.2009.12.017

Fromer M., Pockllington, A.J., Kavanagh, DH., Williams, H.J, Dwyer, S., Gormley P., et al. (2014). De novo mutations in schizophrenia implicat synaptic networks. *Nature*. 506: 179-184.

Fründ, I., Schadow, J., Busch, N. a, Körner, U., & Herrmann, C. S. (2007). Evoked gamma oscillations in human scalp EEG are test-retest reliable. *Clinical Neurophysiology : Official Journal of the International Federation of Clinical Neurophysiology*, *118*(1), 221–7. doi:10.1016/j.clinph.2006.09.013

Fuks, F., Burgers, W. a, Brehm, a, Hughes-Davies, L., & Kouzarides, T. (2000). DNA methyltransferase Dnmt1 associates with histone deacetylase activity. *Nature Genetics*, *24*(1), 88–91. doi:10.1038/71750

Gandal, M. J., Edgar, J. C., Klook, K., & Siegel, S. J. (2012). Gamma synchrony: towards a translational biomarker for the treatment-resistant symptoms of schizophrenia. *Neuropharmacology*, *62*(3), 1504–18. doi:10.1016/j.neuropharm.2011.02.007

Gao, Z., Ure, K., Ding, P., Nashaat, M., Yuan, L., Ma, J., … Hsieh, J. (2011). The master negative regulator REST/NRSF controls adult neurogenesis by restraining the neurogenic program in quiescent stem cells. *The Journal of Neuroscience : The Official Journal of the Society for Neuroscience*, *31*(26), 9772–86. doi:10.1523/JNEUROSCI.1604-11.2011

Garcia, A. M. B., Cardenas, F. P., & Morato, S. (2011). The effects of pentylenetetrazol, chlordiazepoxide and caffeine in rats tested in the elevated plus-maze depend on the experimental illumination. *Behavioural Brain Research*, *217*(1), 171–7. doi:10.1016/j.bbr.2010.09.032

Garrido, M. I., Kilner, J. M., Stephan, K. E., & Friston, K. J. (2009). The mismatch negativity: a review of underlying mechanisms. *Clinical Neurophysiology :*

Official Journal of the International Federation of Clinical Neurophysiology, *120*(3), 453–63. doi:10.1016/j.clinph.2008.11.029

Gaspar-Maia, A., Alajem, A., Meshorer, E., & Ramalho-Santos, M. (2010). Open chromatin in pluripotency and reprogramming. *Nature reviews Molecular cell biology*, *12*(1), 36-47.

Gavériaux-Ruff, C., & Kieffer, B. L. (2007). Conditional gene targeting in the mouse nervous system: Insights into brain function and diseases. *Pharmacology & Therapeutics*, *113*(3), 619–34. doi:10.1016/j.pharmthera.2006.12.003

Geyer, M. A., Krebs-Thomson, K., Braff, D. L., & Swerdlow, N. R. (2001). Pharmacological studies of prepulse inhibition models of sensorimotor gating deficits in schizophrenia: a decade in review. *Psychopharmacology* (Vol. 156, pp. 117–154). doi:10.1007/s002130100811

Gibson, J. R., Bartley, A. F., Hays, S. a, & Huber, K. M. (2008). Imbalance of neocortical excitation and inhibition and altered UP states reflect network hyperexcitability in the mouse model of fragile X syndrome. *Journal of Neurophysiology*, *100*(5), 2615–26. doi:10.1152/jn.90752.2008

Gogolla, N., LeBlanc, J. J., Quast, K. B., Südhof, T. C., Fagiolini, M., & Hensch, T. K. (2009). Common circuit defect of excitatory-inhibitory balance in mouse models of autism. *Journal of neurodevelopmental disorders*, *1*(2), 172-181.

Gogtay, N., Giedd, J. N., Lusk, L., Hayashi, K. M., Greenstein, D., Vaituzis, a C., … Thompson, P. M. (2004). Dynamic mapping of human cortical development during childhood through early adulthood. *Proceedings of the National Academy of Sciences of the United States of America*, *101*(21), 8174–9. doi:10.1073/pnas.0402680101

Gonzalez-Burgos, G., & Lewis, D. A. (2012). NMDA receptor hypofunction, parvalbumin-positive neurons and cortical gamma oscillations in schizophrenia. *Schizophrenia bulletin*, sbs010.

Gottesman, I. I., Ph, D., & Gould, T. D. (2003). Reviews and Overviews The Endophenotype Concept in Psychiatry : Etymology and Strategic Intentions, (April), 636–645.

Götz, M., & Barde, Y. A. (2005). Radial Glial Cells: Defined and MajorIntermediates between EmbryonicStem Cells and CNS Neurons. *Neuron*, *46*(3), 369-372.

Götz, M., Stoykova, A., & Gruss, P. (1998). Pax6 Controls Radial Glia Differentiation in the Cerebral Cortex. *Neuron*, *21*(5), 1031-1044.

Graff, J & Tsai, L. (2013). The potential of HDAC Inhibitors as cognitive enhancers. *Annual Review of Pharmacology and Toxicology* Vol. 53: 311-330 (Volume publication date January 2013) doi: 10.1146/annurev-pharmtox-011112-140216

Gray, J.A., & McNaughton. (2000). *The Neuropsychology of Anxiety: An enquiry into the functions of the septo-hippocampal system.* Oxford University Press.

Grayson, B., Idris, N. F., & Neill, J. C. (2007). Atypical antipsychotics attenuate a sub-chronic PCP-induced cognitive deficit in the novel object recognition task in the rat. *Behavioural Brain Research*, *184*(1), 31–8. doi:10.1016/j.bbr.2007.06.012

Grayson, B., Idris, N. F., & Neill, J. C. (2007). Atypical antipsychotics attenuate a sub-chronic PCP-induced cognitive deficit in the novel object recognition task in the rat. *Behavioural Brain Research*, *184*(1), 31–8. doi:10.1016/j.bbr.2007.06.012

Green, M. F., Kern, R. S., Braff, D. L., & Mintz, J. (2000). Neurocognitive deficits and functional outcome in schizophrenia. *Schizophrenia bulletin*, *26*(1), 119-136.

Greenway, D. J., Street, M., Jeffries, A., & Buckley, N. J. (2007). RE1 silencing transcription factor maintains a repressive chromatin environment in embryonic hippocampal neural stem cells. *Stem cells*, *25*(2), 354-363.

Greig, L. C., Woodworth, M. B., Galazo, M. J., Padmanabhan, H., & Macklis, J. D. (2013). Molecular logic of neocortical projection neuron specification, development and diversity. *Nature Reviews Neuroscience*, *14*(11), 755-769.

Gyory, I., Wu, J., Fejér, G., Seto, E., & Wright, K. L. (2004). PRDI-BF1 recruits the histone H3 methyltransferase G9a in transcriptional silencing. *Nature Immunology*, *5*(3), 299–308. doi:10.1038/ni1046

Haenschel, C., Bittner, R. a, Waltz, J., Haertling, F., Wibral, M., Singer, W., … Rodriguez, E. (2009). Cortical oscillatory activity is critical for working memory as revealed by deficits in early-onset schizophrenia. *The Journal of Neuroscience : The Official Journal of the Society for Neuroscience*, *29*(30), 9481–9. doi:10.1523/JNEUROSCI.1428-09.2009

Hahn, C.G., Wang, H.-Y., Cho, D.-S., Talbot, K., Gur, R. E., Berrettini, W. H., … Arnold, S. E. (2006). Altered neuregulin 1-erbB4 signaling contributes to NMDA receptor hypofunction in schizophrenia. *Nature Medicine*, *12*(7), 824–8. doi:10.1038/nm1418

Halene, T. B., Ehrlichman, R. S., Liang, Y., Christian, E. P., Jonak, G. J., Gur, T. L., … Siegel, S. J. (2009). Assessment of NMDA receptor NR1 subunit hypofunction in mice as a model for schizophrenia. *Genes, Brain, and Behavior*, *8*(7), 661–75. doi:10.1111/j.1601-183X.2009.00504.x

Hall, D. A., & Plack, C. J. (2009). Pitch processing sites in the human auditory brain. *Cerebral Cortex*, *19*(3), 576-585.

Hall, M.H., Taylor, G., Sham, P., Schulze, K., Rijsdijk, F., Picchioni, M., … Salisbury, D. F. (2011). The early auditory gamma-band response is heritable and a putative endophenotype of schizophrenia. *Schizophrenia Bulletin*, *37*(4), 778–87. doi:10.1093/schbul/sbp134.

Hall, M., Schulze, K., Rijsijk, F., Picchioni, M., Ettinger, U., Bramon, E., Freedman, R., Murray, R.M., Sham, P. (2006). Heritability and reliability of the P300, P50 and duration mismatch negativity. *Behav Genet* 36: 845-857.

Hanashima, C., Li, S. C., Shen, L., Lai, E., & Fishell, G. (2004). Foxg1 suppresses early cortical cell fate. *Science*, *303*(5654), 56-59.

Harrison, P. J., & Weinberger, D. R. (2005). Schizophrenia genes, gene expression, and neuropathology: on the matter of their convergence. *Molecular Psychiatry*, *10*(1), 40–68; image 5. doi:10.1038/sj.mp.4001558

He, W., Chai, H., Zheng, L., Yu, W., Chen, W., Li, J., … Wang, W. (2010). Mismatch negativity in treatment-resistant depression and borderline personality disorder. *Progress in Neuro-Psychopharmacology & Biological Psychiatry*, *34*(2), 366–71. doi:10.1016/j.pnpbp.2009.12.021

Heekeren, K., Daumann, J., Neukirch, A., Stock, C., Kawohl, W., Norra, C., … Gouzoulis-Mayfrank, E. (2008). Mismatch negativity generation in the human 5HT2A agonist and NMDA antagonist model of psychosis. *Psychopharmacology*, *199*(1), 77–88. doi:10.1007/s00213-008-1129-4

Heldt, S. a, & Ressler, K. J. (2009). The Use of Lentiviral Vectors and Cre/loxP to Investigate the Function of Genes in Complex Behaviors. *Frontiers in Molecular Neuroscience*, *2*(November), 22. doi:10.3389/neuro.02.022.2009

Herrmann, C. S., & Demiralp, T. (2005). Human EEG gamma oscillations in neuropsychiatric disorders. *Clinical Neurophysiology : Official Journal of the International Federation of Clinical Neurophysiology*, *116*(12), 2719–33. doi:10.1016/j.clinph.2005.07.007

Hevner, R. F., Hodge, R. D., Daza, R. A., & Englund, C. (2006). Transcription factors in glutamatergic neurogenesis: conserved programs in neocortex, cerebellum, and adult hippocampus. *Neuroscience research*, *55*(3), 223-233.

Hong, E.L., Summerflelt, A., Mitchel, B.D., McMahon, R P., Wonodi, I., Buchanan, R.W., Thaker, G.K. (2008). Sensory gating endophenotypes based on its neural oscillatory pattern and heritability estimate. *Arch Gen Psychiatry.* 65(9): 1008-1016.

Horvath, J. E., Bailey, J. a, Locke, D. P., & Eichler, E. E. (2001). Lessons from the human genome: transitions between euchromatin and heterochromatin. *Human Molecular Genetics*, *10*(20), 2215–23. Retrieved from http://www.ncbi.nlm.nih.gov/pubmed/11673404

Huang, H.-S., & Akbarian, S. (2007). GAD1 mRNA expression and DNA methylation in prefrontal cortex of subjects with schizophrenia. *PloS One*, *2*(8), e809. doi:10.1371/journal.pone.0000809

Huang, H.-S., Matevossian, A., Whittle, C., Kim, S. Y., Schumacher, A., Baker, S. P., & Akbarian, S. (2007). Prefrontal dysfunction in schizophrenia involves mixed-lineage leukemia 1-regulated histone methylation at GABAergic gene promoters. *The Journal of Neuroscience : The Official Journal of the Society for Neuroscience*, *27*(42), 11254–62. doi:10.1523/JNEUROSCI.3272-07.2007

Huang, J., Dorsey, J., Chuikov, S., Zhang, X., Jenuwein, T., Reinberg, D., & Berger, S. L. (2010). G9a and Glp methylate lysine 373 in the tumor suppressor p53. *Journal of Biological Chemistry*, *285*(13), 9636-9641.

Iguchi-Ariga, S. M., & Schaffner, W. (1989). CpG methylation of the cAMP-responsive enhancer/promoter sequence TGACGTCA abolishes specific factor binding as well as transcriptional activation. *Genes & Development*, *3*(5), 612–619. doi:10.1101/gad.3.5.612

Ikegami, K., Iwatani, M., Suzuki, M., Tachibana, M., Shinkai, Y., Tanaka, S., … Shiota, K. (2007). Genome-wide and locus-specific DNA hypomethylation in G9a deficient mouse embryonic stem cells. *Genes to Cells : Devoted to Molecular & Cellular Mechanisms*, *12*(1), 1–11. doi:10.1111/j.1365-2443.2006.01029.x

Ikonomidou, C. (1999). Blockade of NMDA Receptors and Apoptotic Neurodegeneration in the Developing Brain. *Science*, *283*(5398), 70–74. doi:10.1126/science.283.5398.70

Ikonomidou, C., Price, M. T., Mosinger, J. L., & Shahid, K. (1989). Hypobaric-lschemic Conditions Produce Cytopathology in Infant Rat Brain Glutamate-like, (May 1969).

Inta, D., Monyer, H., Sprengel, R., Meyer-Lindenberg, A., & Gass, P. (2010). Mice with genetically altered glutamate receptors as models of schizophrenia: a comprehensive review. *Neuroscience and Biobehavioral Reviews*, *34*(3), 285–94. doi:10.1016/j.neubiorev.2009.07.010

Inta, D., Vogt, M. a, Perreau-Lenz, S., Schneider, M., Pfeiffer, N., Wojcik, S. M., … Gass, P. (2012). Sensorimotor gating, working and social memory deficits in mice with reduced expression of the vesicular glutamate transporter VGLUT1. *Behavioural Brain Research*, *228*(2), 328–32. doi:10.1016/j.bbr.2011.12.012

Iwakoshi, M., Okamoto, N., Harada, N., Nakamura, T., Yamamori, S., Fujita, H., … Matsumoto, N. (2004). 9Q34.3 Deletion Syndrome in Three Unrelated Children. *American Journal of Medical Genetics. Part A*, *126A*(3), 278–83. doi:10.1002/ajmg.a.20602

Jaaro-Peled, H., Hayashi-Takagi, A., Seshadri, S., Kamiya, A., Brandon, N. J., & Sawa, A. (2009). Neurodevelopmental mechanisms of schizophrenia: understanding disturbed postnatal brain maturation through neuregulin-1-ErbB4 and DISC1. *Trends in Neurosciences*, *32*(9), 485–95. doi:10.1016/j.tins.2009.05.007

Javitt, D. C. (2009). Sensory processing in schizophrenia: neither simple nor intact. *Schizophrenia Bulletin*, *35*(6), 1059–64. doi:10.1093/schbul/sbp110

Javitt, D. C. (2009). Sensory processing in schizophrenia: neither simple nor intact. *Schizophrenia Bulletin*, *35*(6), 1059–64. doi:10.1093/schbul/sbp110

Javitt, D. C., Schoepp, D., Kalivas, P. W., Volkow, N. D., Zarate, C., Merchant, K., … Potter, W. Z. (2012). Translating Glutamate : From Pathophysiology to Treatment, *3*(102). doi:10.1126/scitranslmed.3002804.Translating

Javitt, D. C., Steinschneider, M., Schroeder, C. E., & Arezzo, J. C. (1996). Role of cortical N-methyl-D-aspartate receptors in auditory sensory memory and mismatch negativity generation: implications for schizophrenia. *Proceedings of the National Academy of Sciences of the United States of America*, *93*(21), 11962–7. Retrieved from http://www.pubmedcentral.nih.gov/articlerender.fcgi?artid=38166&tool=pmcentrez&rendertype=abstract

Jentsch, J. D., & Roth, R. H. (1999). The neuropsychopharmacology of phencyclidine: from NMDA receptor hypofunction to the dopamine hypothesis of schizophrenia. *Neuropsychopharmacology : Official Publication of the American College of Neuropsychopharmacology*, *20*(3), 201–25. doi:10.1016/S0893-133X(98)00060-8

Jiang, Y.-H., Pan, Y., Zhu, L., Landa, L., Yoo, J., Spencer, C., … Beaudet, A. L. (2010). Altered ultrasonic vocalization and impaired learning and memory in Angelman syndrome mouse model with a large maternal deletion from Ube3a to Gabrb3. *PloS One*, *5*(8), e12278. doi:10.1371/journal.pone.0012278

Jin, Y., & Potkin, S. G. (1996). P50 changes with visual interference in normal subjects: a sensory distraction model for schizophrenia. *Clinical EEG (electroencephalography)*, *27*(3), 151-154.

Jin, Y., Potkin, S. G., Patterson, J. V., Sandman, C. A., Hetrick, W. P., & Bunney Jr, W. E. (1997). Effects of P50 temporal variability on sensory gating in schizophrenia. *Psychiatry Research*, *70*(2), 71-81.

Johnston-Wilson, N. L., Sims, C. D., Hofmann, J. P., Anderson, L., Shore, A. D., Torrey, E. F., & Yolken, R. H. (2000). Disease-specific alterations in frontal cortex brain proteins in schizophrenia, bipolar disorder, and major depressive disorder. *Molecular psychiatry*, *5*(2), 142-149.

Kalueff, a V, Minasyan, a, Keisala, T., Shah, Z. H., & Tuohimaa, P. (2006). Hair barbering in mice: implications for neurobehavioural research. *Behavioural Processes*, *71*(1), 8–15. doi:10.1016/j.beproc.2005.09.004

Karasawa, J.-I., Hashimoto, K., & Chaki, S. (2008). D-Serine and a glycine transporter inhibitor improve MK-801-induced cognitive deficits in a novel object recognition test in rats. *Behavioural Brain Research*, *186*(1), 78–83. doi:10.1016/j.bbr.2007.07.033

Kavanagh, D.H., Tansey, K.E., O'Donovan M.C., & Owne M.J. (2015). Schizophrenia genetics emerging themes for a complex disorder. *Molecular Psychiatry*. 20, 72-76.

Kellendonk, C., Simpson, E. H., & Kandel, E. R. (2009). Modeling cognitive endophenotypes of schizophrenia in mice. *Trends in Neurosciences*, *32*(6), 347–58. doi:10.1016/j.tins.2009.02.003

Kemner, C., Verbaten, M. N., Cuperus, J. M., Camfferman, G., & van Engeland, H. (1995). Auditory event-related brain potentials in autistic children and three different control groups. *Biological Psychiatry*, *38*(3), 150–65. doi:10.1016/0006-3223(94)00247-Z

Kendler, K. S., Mohs, R. C., & Davis, K. L. (1983). The effects of diet and physical activity on plasma homovanillic acid in normal human subjects. *Psychiatry research*, *8*(3), 215-223.

Khare, T., Pai, S., Koncevicius, K., Pal, M., Kriukiene, E., Liutkeviciute, Z., … Petronis, A. (2012). 5-hmC in the brain is abundant in synaptic genes and shows differences at the exon-intron boundary. *Nature Structural & Molecular Biology*, *19*(10), 1037–43. doi:10.1038/nsmb.2372

King, B. H., & Lord, C. (2011). Is schizophrenia on the autism spectrum? *Brain Research*, *1380*, 34–41. doi:10.1016/j.brainres.2010.11.031

Kirov, G., Pocklington, a J., Holmans, P., Ivanov, D., Ikeda, M., Ruderfer, D., … Owen, M. J. (2012). De novo CNV analysis implicates specific abnormalities of postsynaptic signalling complexes in the pathogenesis of schizophrenia. *Molecular Psychiatry*, *17*(2), 142–53. doi:10.1038/mp.2011.154

Kleefstra, T., Kramer, J. M., Neveling, K., Willemsen, M. H., Koemans, T. S., Vissers, L. E. L. M., … van Bokhoven, H. (2012). Disruption of an EHMT1-associated

chromatin-modification module causes intellectual disability. *American Journal of Human Genetics*, *91*(1), 73–82. doi:10.1016/j.ajhg.2012.05.003

Kleefstra, T., Schenck, A., Kramer, J. M., & van Bokhoven, H. (2014). The genetics of cognitive epigenetics. *Neuropharmacology*, *80*, 83–94. doi:10.1016/j.neuropharm.2013.12.025

Kleefstra, T., Smidt, M., Banning, M. J. G., Oudakker, a R., Van Esch, H., de Brouwer, a P. M., … van Bokhoven, H. (2005). Disruption of the gene Euchromatin Histone Methyl Transferase1 (Eu-HMTase1) is associated with the 9q34 subtelomeric deletion syndrome. *Journal of Medical Genetics*, *42*(4), 299–306. doi:10.1136/jmg.2004.028464

Kleefstra, T., van Zelst-Stams, W. a, Nillesen, W. M., Cormier-Daire, V., Houge, G., Foulds, N., … Brunner, H. G. (2009). Further clinical and molecular delineation of the 9q subtelomeric deletion syndrome supports a major contribution of EHMT1 haploinsufficiency to the core phenotype. *Journal of Medical Genetics*, *46*(9), 598–606. doi:10.1136/jmg.2008.062950

Kleschevnikov, A. M., Belichenko, P. V, Villar, A. J., Epstein, C. J., Malenka, R. C., & Mobley, W. C. (2004). Hippocampal long-term potentiation suppressed by increased inhibition in the Ts65Dn mouse, a genetic model of Down syndrome. *The Journal of Neuroscience : The Official Journal of the Society for Neuroscience*, *24*(37), 8153–60. doi:10.1523/JNEUROSCI.1766-04.2004

Klimesch, W. (1999). EEG alpha and theta oscillations reflect cognitive and memory performance: a review and analysis. *Brain Research. Brain Research Reviews*, *29*(2-3), 169–95. Retrieved from http://www.ncbi.nlm.nih.gov/pubmed/10209231

Koh, K. P., Yabuuchi, A., Rao, S., Huang, Y., Cunniff, K., Nardone, J., … Rao, A. (2011). Tet1 and Tet2 regulate 5-hydroxymethylcytosine production and cell lineage specification in mouse embryonic stem cells. *Cell Stem Cell*, *8*(2), 200–13. doi:10.1016/j.stem.2011.01.008

Korets-Smith, E., Lindemann, L., Tucker, K. L., Jiang, C., Kabacs, N., Belteki, G., … Nagy, A. (2004). Cre recombinase specificity defined by the tau locus. *Genesis (New York, N.Y. : 2000)*, *40*(3), 131–8. doi:10.1002/gene.20074

Kouzarides, T. (2007). Chromatin modifications and their function. *Cell*, *128*(4), 693–705. doi:10.1016/j.cell.2007.02.005

Kowalczyk, T., Pontious, A., Englund, C., Daza, R. a M., Bedogni, F., Hodge, R., … Hevner, R. F. (2009). Intermediate neuronal progenitors (basal progenitors) produce pyramidal-projection neurons for all layers of cerebral cortex. *Cerebral Cortex (New York, N.Y. : 1991)*, *19*(10), 2439–50. doi:10.1093/cercor/bhn260

Kramer, J. M., Kochinke, K., Oortveld, M. a W., Marks, H., Kramer, D., de Jong, E. K., … Schenck, A. (2011). Epigenetic regulation of learning and memory by Drosophila EHMT/G9a. *PLoS Biology*, *9*(1), e1000569. doi:10.1371/journal.pbio.1000569

Kramer, J. M., Kochinke, K., Oortveld, M. A. W., Marks, H., Kramer, D., Eiko, K., … Schenck, A. (2011). Epigenetic Regulation of Learning and Memory by, *9*(1). doi:10.1371/journal.pbio.1000569

Kreitschmann-Andermahr, I., Rosburg, T., Demme, U., Gaser, E., Nowak, H., & Sauer, H. (2001). Effect of ketamine on the neuromagnetic mismatch field in healthy humans. *Brain Research. Cognitive Brain Research*, *12*(1), 109–16. Retrieved from http://www.ncbi.nlm.nih.gov/pubmed/11489614

Kriegstein, A. R., & Götz, M. (2003). Radial glia diversity: a matter of cell fate. *Glia*, *43*(1), 37-43.

Krishnan, G. P., Hetrick, W. P., Brenner, C. a, Shekhar, a, Steffen, a N., & O'Donnell, B. F. (2009). Steady state and induced auditory gamma deficits in schizophrenia. *NeuroImage*, *47*(4), 1711–9. doi:10.1016/j.neuroimage.2009.03.085

Krystal JH, Karper LP, Seibyl JP, et al. Subanesthetic Effects of the Noncompetitive NMDA Antagonist, Ketamine, in Humans: Psychotomimetic, Perceptual, Cognitive, and Neuroendocrine Responses. *Arch Gen Psychiatry.* 1994;51(3):199-214. doi:10.1001/archpsyc.1994.03950030035004

Kujala, T., Tervaniemi, M., & Schröger, E. (2007). The mismatch negativity in cognitive and clinical neuroscience: theoretical and methodological considerations. *Biological Psychology*, *74*(1), 1–19. doi:10.1016/j.biopsycho.2006.06.001

Kwon, C.-H., Luikart, B. W., Powell, C. M., Zhou, J., Matheny, S. a, Zhang, W., … Parada, L. F. (2006). Pten regulates neuronal arborization and social interaction in mice. *Neuron*, *50*(3), 377–88. doi:10.1016/j.neuron.2006.03.023

Kwon, J. S., O'Donnell, B. F., Wallenstein, G. V, Greene, R. W., Hirayasu, Y., Nestor, P. G., … McCarley, R. W. (1999). Gamma frequency-range abnormalities to auditory stimulation in schizophrenia. *Archives of General Psychiatry*, *56*(11), 1001–5. Retrieved from http://www.pubmedcentral.nih.gov/articlerender.fcgi?artid=2863027&tool=pmcentrez&rendertype=abstract

Kwon, S. H., & Workman, J. L. (2011). The changing faces of HP1: From heterochromatin formation and gene silencing to euchromatic gene expression: HP1 acts as a positive regulator of transcription. *BioEssays : News and Reviews*

in Molecular, Cellular and Developmental Biology, *33*(4), 280–9. doi:10.1002/bies.201000138

Lazarewicz, M. T., Ehrlichman, R. S., Maxwell, C. R., Gandal, M. J., Finkel, L. H., & Siegel, S. J. (2010). Ketamine modulates theta and gamma oscillations. *Journal of Cognitive Neuroscience*, *22*(7), 1452–64. doi:10.1162/jocn.2009.21305

Le Van Quyen, M., Adam, C., Lachaux, J. P., Martinerie, J., Baulac, M., Renault, B., & Varela, F. J. (1997). Temporal patterns in human epileptic activity are modulated by perceptual discriminations. *Neuroreport*, *8*(7), 1703–10. Retrieved from http://www.ncbi.nlm.nih.gov/pubmed/9189918

Lee, J. S., Kim, Y., Kim, I. S., Kim, B., Choi, H. J., Lee, J. M., ... & Baek, S. H. (2010). Negative regulation of hypoxic responses via induced Reptin methylation. *Molecular cell*, *39*(1), 71-85.

Lee, K.-H., Williams, L. M., Breakspear, M., & Gordon, E. (2003). Synchronous gamma activity: a review and contribution to an integrative neuroscience model of schizophrenia. *Brain Research. Brain Research Reviews*, *41*(1), 57–78. Retrieved from http://www.ncbi.nlm.nih.gov/pubmed/12505648

Lenz, D., Fischer, S., Schadow, J., Bogerts, B., & Herrmann, C. S. (2011). Altered evoked γ-band responses as a neurophysiological marker of schizophrenia? *International Journal of Psychophysiology : Official Journal of the International Organization of Psychophysiology*, *79*(1), 25–31. doi:10.1016/j.ijpsycho.2010.08.002

Lenz, D., Krauel, K., Flechtner, H.-H., Schadow, J., Hinrichs, H., & Herrmann, C. S. (2010). Altered evoked gamma-band responses reveal impaired early visual processing in ADHD children. *Neuropsychologia*, *48*(7), 1985–93. doi:10.1016/j.neuropsychologia.2010.03.019

Lenz, D., Krauel, K., Schadow, J., Baving, L., Duzel, E., & Herrmann, C. S. (2008). Enhanced gamma-band activity in ADHD patients lacks correlation with memory performance found in healthy children. *Brain Research*, *1235*, 117–32. doi:10.1016/j.brainres.2008.06.023

Li, E., Bestor, T. H., & Jaenisch, R. (1992). Targeted mutation of the DNA methyltransferase gene results in embryonic lethality. *Cell*, *69*(6), 915–26. Retrieved from http://www.ncbi.nlm.nih.gov/pubmed/1606615

Li, H., Li, Y., Shao, J., Li, R., Qin, Y., Xie, C., & Zhao, Z. (2008). The association analysis of RELN and GRM8 genes with autistic spectrum disorder in Chinese Han population. *American Journal of Medical Genetics Part B: Neuropsychiatric Genetics*, *147*(2), 194-200.

Li, M., Liu, G. H., & Belmonte, J. C. I. (2012). Navigating the epigenetic landscape of pluripotent stem cells. *Nature Reviews Molecular Cell Biology*, *13*(8), 524-535.

Lienert, F., Mohn, F., Tiwari, V. K., Baubec, T., Roloff, T. C., Gaidatzis, D., … Schübeler, D. (2011). Genomic prevalence of heterochromatic H3K9me2 and transcription do not discriminate pluripotent from terminally differentiated cells. *PLoS Genetics*, *7*(6), e1002090. doi:10.1371/journal.pgen.1002090

Lienert, F., Mohn, F., Tiwari, V. K., Baubec, T., Roloff, T. C., Gaidatzis, D., … Schübeler, D. (2011). Genomic prevalence of heterochromatic H3K9me2 and transcription do not discriminate pluripotent from terminally differentiated cells. *PLoS Genetics*, *7*(6), e1002090. doi:10.1371/journal.pgen.1002090

Light, G.A., Swerdlow, N.R. (2014) Neurophysiological biomarkers informing the clinical neuroscience of schizophrenia: Mismatch Negativity and Prepulse Inhibition of Startle*. Curr Topics Behav. Neurosci.* Springer-Verlag Berlin. doi:10.1007/7854_2014_316

Lijam, N., Paylor, R., McDonald, M. P., Crawley, J. N., Deng, C. X., Herrup, K., … Wynshaw-Boris, a. (1997). Social interaction and sensorimotor gating abnormalities in mice lacking Dvl1. *Cell*, *90*(5), 895–905. Retrieved from http://www.ncbi.nlm.nih.gov/pubmed/9298901

Lin, P. I., Chien, Y. L., Wu, Y. Y., Chen, C. H., Gau, S. S. F., Huang, Y. S., ... & Chiu, Y. N. (2012). The WNT2 gene polymorphism associated with speech delay inherent to autism. *Research in developmental disabilities*, *33*(5), 1533-1540.

Llinás, R., Ribary, U., Contreras, D., & Pedroarena, C. (1998). The neuronal basis for consciousness. *Philosophical Transactions of the Royal Society of London. Series B, Biological Sciences*, *353*(1377), 1841–9. doi:10.1098/rstb.1998.0336

Loe-Mie, Y., Lepagnol-Bestel, A. M., Maussion, G., Doron-Faigenboim, A., Imbeaud, S., Delacroix, H., ... & Moalic, J. M. (2010). SMARCA2 and other genome-wide supported schizophrenia-associated genes: regulation by REST/NRSF, network organization and primate-specific evolution. *Human molecular genetics*, ddq184.

Loh, Y. H., Zhang, W., Chen, X., George, J., & Ng, H. H. (2007). Jmjd1a and Jmjd2c histone H3 Lys 9 demethylases regulate self-renewal in embryonic stem cells. *Genes & development*, *21*(20), 2545-2557.

Loh, Y.-H., Wu, Q., Chew, J.-L., Vega, V. B., Zhang, W., Chen, X., … Ng, H.-H. (2006). The Oct4 and Nanog transcription network regulates pluripotency in mouse embryonic stem cells. *Nature Genetics*, *38*(4), 431–40. doi:10.1038/ng1760

Loring, D. W., Sheer, D. E., & Largen, J. W. (1985). Forty Hertz EEG Activity in Dementia of the Alzheimer Type and Multi-Infarct Dementia. *Psychophysiology*, *22*(1), 116-121.

Luck, S. J., Mathalon, D. H., O'Donnell, B. F., Hämäläinen, M. S., Spencer, K. M., Javitt, D. C., & Uhlhaas, P. J. (2011). A roadmap for the development and validation of event-related potential biomarkers in schizophrenia research. *Biological Psychiatry*, *70*(1), 28–34. doi:10.1016/j.biopsych.2010.09.021

Machon, O., Backman, M., Machonova, O., Kozmik, Z., Vacik, T., Andersen, L., & Krauss, S. (2007). A dynamic gradient of Wnt signaling controls initiation of neurogenesis in the mammalian cortex and cellular specification in the hippocampus. *Developmental biology*, *311*(1), 223-237.

Machon, O., van den Bout, C. J., Backman, M., Røsok, Ø., Caubit, X., Fromm, S. H., … Krauss, S. (2002). Forebrain-specific promoter/enhancer D6 derived from the mouse Dach1 gene controls expression in neural stem cells. *Neuroscience*, *112*(4), 951–66. Retrieved from http://www.ncbi.nlm.nih.gov/pubmed/12088753

Maeng, S., Zarate, C. a, Du, J., Schloesser, R. J., McCammon, J., Chen, G., & Manji, H. K. (2008). Cellular mechanisms underlying the antidepressant effects of ketamine: role of alpha-amino-3-hydroxy-5-methylisoxazole-4-propionic acid receptors. *Biological Psychiatry*, *63*(4), 349–52. doi:10.1016/j.biopsych.2007.05.028

Maeng, S., Zarate, C. a, Du, J., Schloesser, R. J., McCammon, J., Chen, G., & Manji, H. K. (2008). Cellular mechanisms underlying the antidepressant effects of ketamine: role of alpha-amino-3-hydroxy-5-methylisoxazole-4-propionic acid receptors. *Biological Psychiatry*, *63*(4), 349–52. doi:10.1016/j.biopsych.2007.05.028

Malhotra, a K., Pinals, D. a, Adler, C. M., Elman, I., Clifton, a, Pickar, D., & Breier, a. (1997). Ketamine-induced exacerbation of psychotic symptoms and cognitive impairment in neuroleptic-free schizophrenics. *Neuropsychopharmacology : Official Publication of the American College of Neuropsychopharmacology*, *17*(3), 141–50. doi:10.1016/S0893-133X(97)00036-5

Mahotra, D., Sebat, J., (2012). CNVs: harbingers of rare variant revolution in psychiatric genetics. *Cell.* 148: 1223-1241.

Mandel, G., Fiondella, C. G., Covey, M. V., Lu, D. D., LoTurco, J. J., & Ballas, N. (2011). Repressor element 1 silencing transcription factor (REST) controls radial migration and temporal neuronal specification during neocortical development. *Proceedings of the National Academy of Sciences*, *108*(40), 16789-16794.

Marco, E. J., Hinkley, L. B. N., Hill, S. S., & Nagarajan, S. S. (2011). Sensory processing in autism: a review of neurophysiologic findings. *Pediatric Research*, *69*(5 Pt 2), 48R–54R. doi:10.1203/PDR.0b013e3182130c54

Marcus, E. A., Emptage, N. J., Marois, R. & Carew, T.J. (1994). Chapter 23: A comparison of mechanistic relationships between development and learning in Aplysia. Neuroscience: From the Molecular to the Cognitive. Elsevier. 179-88.

Marín, O. (2012). Interneuron dysfunction in psychiatric disorders. *Nature Reviews. Neuroscience*, *13*(2), 107–20. doi:10.1038/nrn3155

Martin, S. J., & Morris, R. G. M. (2002). New life in an old idea: the synaptic plasticity and memory hypothesis revisited. *Hippocampus*, *12*(5), 609–36. doi:10.1002/hipo.10107

Martynoga, B., Morrison, H., Price, D. J., & Mason, J. O. (2005). Foxg1 is required for specification of ventral telencephalon and region-specific regulation of dorsal telencephalic precursor proliferation and apoptosis. *Developmental Biology*, *283*(1), 113–27. doi:10.1016/j.ydbio.2005.04.005

Marui, T., Funatogawa, I., Koishi, S., Yamamoto, K., Matsumoto, H., Hashimoto, O., ... & Kato, N. (2010). Association between autism and variants in the wingless-type MMTV integration site family member 2 (WNT2) gene. *The International Journal of Neuropsychopharmacology*, *13*(04), 443-449.

Maze, I., Covington, H. E., Dietz, D. M., LaPlant, Q., Renthal, W., Russo, S. J., … Nestler, E. J. (2010). Essential role of the histone methyltransferase G9a in cocaine-induced plasticity. *Science (New York, N.Y.)*, *327*(5962), 213–6. doi:10.1126/science.1179438

Meshorer, E., & Misteli, T. (2006). Chromatin in pluripotent embryonic stem cells and differentiation. *Nature reviews Molecular cell biology*, *7*(7), 540-546.

Metzger, K. L., Maxwell, C. R., Liang, Y., & Siegel, S. J. (2007). Effects of nicotine vary across two auditory evoked potentials in the mouse. *Biological Psychiatry*, *61*(1), 23–30. doi:10.1016/j.biopsych.2005.12.011

Minzenberg, M. J., Firl, A. J., Yoon, J. H., Gomes, G. C., Reinking, C., & Carter, C. S. (2010). Gamma oscillatory power is impaired during cognitive control independent of medication status in first-episode schizophrenia. *Neuropsychopharmacology : Official Publication of the American College of Neuropsychopharmacology*, *35*(13), 2590–9. doi:10.1038/npp.2010.150

Mittal, V. a, Ellman, L. M., & Cannon, T. D. (2008). Gene-environment interaction and covariation in schizophrenia: the role of obstetric complications. *Schizophrenia Bulletin*, *34*(6), 1083–94. doi:10.1093/schbul/sbn080

Miyata, T., Kawaguchi, A., Saito, K., Kawano, M., Muto, T., & Ogawa, M. (2004). Asymmetric production of surface-dividing and non-surface-dividing cortical progenitor cells. *Development*, *131*(13), 3133-3145.

Miyoshi, G., & Fishell, G. (2012). Dynamic *FoxG1* Expression Coordinates the Integration of Multipolar Pyramidal Neuron Precursors into the Cortical Plate. *Neuron*, *74*(6), 1045-1058.

Moghaddam, B., & Javitt, D. (2012). From revolution to evolution: the glutamate hypothesis of schizophrenia and its implication for treatment. *Neuropsychopharmacology : Official Publication of the American College of Neuropsychopharmacology*, *37*(1), 4–15. doi:10.1038/npp.2011.181

Molyneaux, B. J., Arlotta, P., Menezes, J. R. L., & Macklis, J. D. (2007). Neuronal subtype specification in the cerebral cortex. *Nature Reviews. Neuroscience*, *8*(6), 427–37. doi:10.1038/nrn2151

Moon, R. T., Kohn, A. D., De Ferrari, G. V., & Kaykas, A. (2004). WNT and β-catenin signalling: diseases and therapies. *Nature Reviews Genetics*, *5*(9), 691-701.

Morgan, V. a, Croft, M. L., Valuri, G. M., Zubrick, S. R., Bower, C., McNeil, T. F., & Jablensky, A. V. (2012). Intellectual disability and other neuropsychiatric outcomes in high-risk children of mothers with schizophrenia, bipolar disorder and unipolar major depression. *The British Journal of Psychiatry : The Journal of Mental Science*, *200*(4), 282–9. doi:10.1192/bjp.bp.111.093070

Morozov, A., Kellendonk, C., Simpson, E., & Tronche, F. (2003). Using conditional mutagenesis to study the brain. *Biological Psychiatry*, *54*(11), 1125–1133. doi:10.1016/S0006-3223(03)00467-0

Morton, N., Gray, N.S., Mellers, J., Toone, B., Lishman, W.A., & Gray, J.A. (1994). Prepulse inhibition in temporal lobe epilepsy. Proceedings, EBPS, p191.

Mulert, C., Kirsch, V., Pascual-Marqui, R., McCarley, R. W., & Spencer, K. M. (2011). Long-range synchrony of γ oscillations and auditory hallucination symptoms in schizophrenia. *International Journal of Psychophysiology : Official Journal of the International Organization of Psychophysiology*, *79*(1), 55–63. doi:10.1016/j.ijpsycho.2010.08.004

Murcia, C. L., Gulden, F., & Herrup, K. (2005). A question of balance: a proposal for new mouse models of autism. *International Journal of Developmental Neuroscience : The Official Journal of the International Society for Developmental Neuroscience*, *23*(2-3), 265–75. doi:10.1016/j.ijdevneu.2004.07.001

Murphy, K. J., Ter Horst, J. P. F., Cassidy, A. W., DeSouza, I. E. J., Morgunova, M., Li, C., … Regan, C. M. (2010). Temporal dysregulation of cortical gene expression in

the isolation reared Wistar rat. *Journal of Neurochemistry*, *113*(3), 601–14. doi:10.1111/j.1471-4159.2010.06617.x

Näätänen, R., & Kähkönen, S. (2009). Central auditory dysfunction in schizophrenia as revealed by the mismatch negativity (MMN) and its magnetic equivalent MMNm: a review. *The International Journal of Neuropsychopharmacology / Official Scientific Journal of the Collegium Internationale Neuropsychopharmacologicum (CINP)*, *12*(1), 125–35. doi:10.1017/S1461145708009322

Näätänen, R., Kujala, T., Escera, C., Baldeweg, T., Kreegipuu, K., Carlson, S., & Ponton, C. (2012). The mismatch negativity (MMN)--a unique window to disturbed central auditory processing in ageing and different clinical conditions. *Clinical Neurophysiology : Official Journal of the International Federation of Clinical Neurophysiology*, *123*(3), 424–58. doi:10.1016/j.clinph.2011.09.020

Näätänen, R., Kujala, T., Kreegipuu, K., Carlson, S., Escera, C., Baldeweg, T., & Ponton, C. (2011). The mismatch negativity: an index of cognitive decline in neuropsychiatric and neurological diseases and in ageing. *Brain : A Journal of Neurology*, *134*(Pt 12), 3435–53. doi:10.1093/brain/awr064

Näätänen, R., S Sussman, E., Salisbury, D., & L Shafer, V. (2014). Mismatch Negativity (MMN) as an Index of Cognitive Dysfunction. *Brain Topography*. doi:10.1007/s10548-014-0374-6

Nagai, T., Tada, M., Kirihara, K., Araki, T., Jinde, S., & Kasai, K. (2013). Mismatch Negativity as a "Translatable" Brain Marker Toward Early Intervention for Psychosis: A Review. *Frontiers in Psychiatry*, *4*(September), 115. doi:10.3389/fpsyt.2013.00115

Nakamura, T., Liu, Y. J., Nakashima, H., Umehara, H., Inoue, K., Matoba, S., ... & Nakano, T. (2012). PGC7 binds histone H3K9me2 to protect against conversion of 5mC to 5hmC in early embryos. *Nature*, *486*(7403), 415-419.

Nan, X., Ng, H. H., Johnson, C. a, Laherty, C. D., Turner, B. M., Eisenman, R. N., & Bird, a. (1998). Transcriptional repression by the methyl-CpG-binding protein MeCP2 involves a histone deacetylase complex. *Nature*, *393*(6683), 386–9. doi:10.1038/30764

Nestler, E. J., & Hyman, S. E. (2010). Animal models of neuropsychiatric disorders. *Nature Neuroscience*, *13*(10), 1161–9. doi:10.1038/nn.2647

Newcomer, J. W., Farber, N. B., Jevtovic-Todorovic, V., Selke, G., Melson, a K., Hershey, T., … Olney, J. W. (1999). Ketamine-induced NMDA receptor hypofunction as a model of memory impairment and psychosis. *Neuropsychopharmacology :*

Official Publication of the American College of Neuropsychopharmacology, *20*(2), 106–18. doi:10.1016/S0893-133X(98)00067-0

Niewoehner, B., Single, F. N., Hvalby, Ø., Jensen, V., Meyer zum Alten Borgloh, S., Seeburg, P. H., … Bannerman, D. M. (2007). Impaired spatial working memory but spared spatial reference memory following functional loss of NMDA receptors in the dentate gyrus. *The European Journal of Neuroscience*, *25*(3), 837–46. doi:10.1111/j.1460-9568.2007.05312.x

Nishio, H., & Walsh, M. J. (2004). CCAAT displacement protein/cut homolog recruits G9a histone lysine methyltransferase to repress transcription. *Proceedings of the National Academy of Sciences of the United States of America*, *101*(31), 11257–62. doi:10.1073/pnas.0401343101

Niwa, H. (2007). Open conformation chromatin and pluripotency. *Genes & development*, *21*(21), 2671-2676.

Nozawa, R.-S., Nagao, K., Masuda, H.-T., Iwasaki, O., Hirota, T., Nozaki, N., … Obuse, C. (2010). Human POGZ modulates dissociation of HP1alpha from mitotic chromosome arms through Aurora B activation. *Nature Cell Biology*, *12*(7), 719–27. doi:10.1038/ncb2075

O'Roak, B. J., Deriziotis, P., Lee, C., Vives, L., Schwartz, J. J., Girirajan, S., … Eichler, E. E. (2011). Exome sequencing in sporadic autism spectrum disorders identifies severe de novo mutations. *Nature Genetics*, *43*(6), 585–9. doi:10.1038/ng.835

Ogawa, H., Ishiguro, K.-I., Gaubatz, S., Livingston, D. M., & Nakatani, Y. (2002). A complex with chromatin modifiers that occupies E2F- and Myc-responsive genes in G0 cells. *Science (New York, N.Y.)*, *296*(5570), 1132–6. doi:10.1126/science.1069861

Okano, M., Bell, D. W., Haber, D. a, & Li, E. (1999). DNA methyltransferases Dnmt3a and Dnmt3b are essential for de novo methylation and mammalian development. *Cell*, *99*(3), 247–57. Retrieved from http://www.ncbi.nlm.nih.gov/pubmed/10555141

Olmos-Serrano, J. L., Paluszkiewicz, S. M., Martin, B. S., Kaufmann, W. E., Corbin, J. G., & Huntsman, M. M. (2010). Defective GABAergic neurotransmission and pharmacological rescue of neuronal hyperexcitability in the amygdala in a mouse model of fragile X syndrome. *The Journal of Neuroscience : The Official Journal of the Society for Neuroscience*, *30*(29), 9929–38. doi:10.1523/JNEUROSCI.1714-10.2010

Olney, J. W., Newcomer, J. W., & Farber, N. B. (1999). NMDA receptor hypofunction model of schizophrenia. *Journal of Psychiatric Research*, *33*(6), 523–33. Retrieved from http://www.ncbi.nlm.nih.gov/pubmed/10628529

Orekhova, E. V, Stroganova, T. a, Prokofyev, A. O., Nygren, G., Gillberg, C., & Elam, M. (2008). Sensory gating in young children with autism: relation to age, IQ, and EEG gamma oscillations. *Neuroscience Letters*, *434*(2), 218–23. doi:10.1016/j.neulet.2008.01.066

Owen, M. J., O'Donovan, M. C., Thapar, A., & Craddock, N. (2011). Neurodevelopmental hypothesis of schizophrenia. *The British Journal of Psychiatry : The Journal of Mental Science*, *198*(3), 173–5. doi:10.1192/bjp.bp.110.084384

Pantev, C. (1995). Evoked and Induced Gamma-Band Activity of the Human Cortex. *Brain Topography*, *7*(4), 321–330. Retrieved from http://link.springer.com/article/10.1007/BF01195258

Paoletti, P., & Neyton, J. (2007). NMDA receptor subunits: function and pharmacology. *Current Opinion in Pharmacology*, *7*(1), 39–47. doi:10.1016/j.coph.2006.08.011

Parkel, S., Lopez-Atalaya, J. P., & Barco, A. (2013). Histone H3 lysine methylation in cognition and intellectual disability disorders. *Learning & Memory (Cold Spring Harbor, N.Y.)*, *20*(10), 570–9. doi:10.1101/lm.029363.112

Pauler, F. M., Koerner, M. V, & Barlow, D. P. (2007). Silencing by imprinted noncoding RNAs: is transcription the answer? *Trends in Genetics : TIG*, *23*(6), 284–92. doi:10.1016/j.tig.2007.03.018

Peça, J., Feliciano, C., Ting, J. T., Wang, W., Wells, M. F., Venkatraman, T. N., … Feng, G. (2011). Shank3 mutant mice display autistic-like behaviours and striatal dysfunction. *Nature*, *472*(7344), 437–42. doi:10.1038/nature09965

Pellow, S., Chopin, P., File, S. E., & Briley, M. (1985). Validation of open:closed arm entries in an elevated plus-maze as a measure of anxiety in the rat. *Journal of Neuroscience Methods*, *14*(3), 149–67. Retrieved from http://www.ncbi.nlm.nih.gov/pubmed/2864480

Pelphrey, K., Adolphs, R., & Morris, J. P. (2004). Neuroanatomical substrates of social cognition dysfunction in autism. *Mental Retardation and Developmental Disabilities Research Reviews*, *10*(4), 259–71. doi:10.1002/mrdd.20040

Perry, W., Minassian, A., Lopez, B., Maron, L., & Lincoln, A. (2007). Sensorimotor gating deficits in adults with autism. *Biological Psychiatry*, *61*(4), 482–6. doi:10.1016/j.biopsych.2005.09.025

Peter, C. J., & Akbarian, S. (2011). Balancing histone methylation activities in psychiatric disorders. *Trends in Molecular Medicine*, *17*(7), 372–9. doi:10.1016/j.molmed.2011.02.003

Peters, A. H. F. M., Kubicek, S., Mechtler, K., O'Sullivan, R. J., Derijck, A. a H. a, Perez-Burgos, L., … Jenuwein, T. (2003). Partitioning and plasticity of repressive histone methylation states in mammalian chromatin. *Molecular Cell*, *12*(6), 1577–89. Retrieved from http://www.ncbi.nlm.nih.gov/pubmed/14690609

Phillips, J. M., Ehrlichman, R. S., & Siegel, S. J. (2007). Mecamylamine blocks nicotine-induced enhancement of the P20 auditory event-related potential and evoked gamma. *Neuroscience*, *144*(4), 1314–23. doi:10.1016/j.neuroscience.2006.11.003

Pilaz, L.-J., Patti, D., Marcy, G., Ollier, E., Pfister, S., Douglas, R. J., … Dehay, C. (2009). Forced G1-phase reduction alters mode of division, neuron number, and laminar phenotype in the cerebral cortex. *Proceedings of the National Academy of Sciences of the United States of America*, *106*(51), 21924–9. doi:10.1073/pnas.0909894106

Pinkham, A., & Penn, D. (2003). Implications for the neural basis of social cognition for the study of schizophrenia. *American Journal of …*, *160*, 815–824. Retrieved from http://journals.psychiatryonline.org/article.aspx?articleid=176198

Politoff, A. L., Monson, N., Stadter, R. P., & Hass, P. (1995). Severity of dementia correlates with loss of broad-band visual cortical responses. *Dementia and Geriatric Cognitive Disorders*, *6*(3), 169-173.

Porjesz, B., Rangaswamy, M., Kamarajan, C., Jones, K.A., Padmanabhapilllai, A., & Begleiter, H. (2004) The utility of neurophysiological markers in the study of alcoholism. *Clin Neurophysiology*. 116(5), 993-1018.

Pratt, J., Winchester, C., Dawson, N., & Morris, B. (2012). Advancing schizophrenia drug discovery: optimizing rodent models to bridge the translational gap. *Nature Reviews. Drug Discovery*, *11*(7), 560–79. doi:10.1038/nrd3649

Pulvermüller, F. (1999). Words in the brain's language. *Behavioral and Brain Sciences*, *22*, 253–336.

Purcell, S.M., Moran, J., Former M., Ruderfer, D., Solovieff, N., Roussos, P., e al. (2014). A polygenic burden of rare disruptive mutations in schizophrenia. *Nature*. 706: 185-190.

Qi, X., Li, T.-G., Hao, J., Hu, J., Wang, J., Simmons, H., … Zhao, G.-Q. (2004). BMP4 supports self-renewal of embryonic stem cells by inhibiting mitogen-activated protein kinase pathways. *Proceedings of the National Academy of Sciences of the United States of America*, *101*(16), 6027–32. doi:10.1073/pnas.0401367101

Qureshi, I. A., Mehler, M. F., & B, P. T. R. S. (2014). An evolving view of epigenetic complexity in the brain An evolving view of epigenetic complexity in the brain, (August).

Ramos, A. (2008). Animal models of anxiety: do I need multiple tests? *Trends in Pharmacological Sciences*, *29*(10), 493–8. doi:10.1016/j.tips.2008.07.005

Rathert, P., Dhayalan, A., Murakami, M., Zhang, X., Tamas, R., Jurkowska, R., ... & Jeltsch, A. (2008). Protein lysine methyltransferase G9a acts on non-histone targets. *Nature chemical biology*, *4*(6), 344-346.

Rea, S., Eisenhaber, F., O'Carroll, D., Strahl, B. D., Sun, Z. W., Schmid, M., … Jenuwein, T. (2000). Regulation of chromatin structure by site-specific histone H3 methyltransferases. *Nature*, *406*(6796), 593–9. doi:10.1038/35020506

Rees, E., Kirov, G., Sanders A., Walters, J.T., Chambert K.D. et al., (2014) Evience that duplications in 22.q11.2 protect against schizophrenia. *Mol psychiatry*. 19(1): 37-40.

Reichelt, a C., Rodgers, R. J., & Clapcote, S. J. (2012). The role of neurexins in schizophrenia and autistic spectrum disorder. *Neuropharmacology*, *62*(3), 1519–26. doi:10.1016/j.neuropharm.2011.01.024

Relkovic, D., Doe, C. M., Humby, T., Johnstone, K. a, Resnick, J. L., Holland, A. J., … Isles, A. R. (2010). Behavioural and cognitive abnormalities in an imprinting centre deletion mouse model for Prader-Willi syndrome. *The European Journal of Neuroscience*, *31*(1), 156–64. doi:10.1111/j.1460-9568.2009.07048.x

Reya, T., & Clevers, H. (2005). Wnt signalling in stem cells and cancer. *Nature*, *434*(7035), 843-850.

Rhee, I., Bachman, K. E., Park, B. H., Jair, K.-W., Yen, R.-W. C., Schuebel, K. E., … Vogelstein, B. (2002). DNMT1 and DNMT3b cooperate to silence genes in human cancer cells. *Nature*, *416*(6880), 552–6. doi:10.1038/416552a

Riaza Bermudo-Soriano, C., Perez-Rodriguez, M. M., Vaquero-Lorenzo, C., & Baca-Garcia, E. (2012). New perspectives in glutamate and anxiety. *Pharmacology, Biochemistry, and Behavior*, *100*(4), 752–74. doi:10.1016/j.pbb.2011.04.010

Ribary, U., Lado, F., & Mogilner, A. (1991). Magnetic field tomography of coherent thalamocortical 40-Hzoscillations in humans, *88*(December), 11037–11041.

Rice, J. C., Briggs, S. D., Ueberheide, B., Barber, C. M., Shabanowitz, J., Hunt, D. F., … Allis, C. D. (2003). Different Degrees of Methylation to Define Distinct Chromatin Domains, *12*, 1591–1598.

Rissling, A. J., Park, S.-H., Young, J. W., Rissling, M. B., Sugar, C. a, Sprock, J., … Light, G. a. (2013). Demand and modality of directed attention modulate "pre-attentive" sensory processes in schizophrenia patients and nonpsychiatric controls. *Schizophrenia Research*, *146*(1-3), 326–35. doi:10.1016/j.schres.2013.01.035

Roach, B. J., & Mathalon, D. H. (2008). Event-related EEG time-frequency analysis: an overview of measures and an analysis of early gamma band phase locking in schizophrenia. *Schizophrenia Bulletin*, *34*(5), 907–26. doi:10.1093/schbul/sbn093

Roberts, T. P. L., Schmidt, G. L., Egeth, M., Blaskey, L., Rey, M. M., Edgar, J. C., & Levy, S. E. (2008). Electrophysiological signatures: magnetoencephalographic studies of the neural correlates of language impairment in autism spectrum disorders. *International Journal of Psychophysiology : Official Journal of the International Organization of Psychophysiology*, *68*(2), 149–60. doi:10.1016/j.ijpsycho.2008.01.012

Rodenas-Ruano, A., Chávez, A. E., Cossio, M. J., Castillo, P. E., & Zukin, R. S. (2012). REST-dependent epigenetic remodeling promotes the developmental switch in synaptic NMDA receptors. *Nature neuroscience*, *15*(10), 1382-1390.

Roopra, A., Qazi, R., Schoenike, B., Daley, T. J., & Morrison, J. F. (2004). Localized domains of G9a-mediated histone methylation are required for silencing of neuronal genes. *Molecular Cell*, *14*(6), 727–38. doi:10.1016/j.molcel.2004.05.026

Rump, A., Hildebrand, L., Tzschach, A., Ullmann, R., Schrock, E., & Mitter, D. (2013). A mosaic maternal splice donor mutation in the EHMT1 gene leads to aberrant transcripts and to Kleefstra syndrome in the offspring. *European Journal of Human Genetics : EJHG*, *21*(8), 887–90. doi:10.1038/ejhg.2012.267

Sampath, S. C., Marazzi, I., Yap, K. L., Sampath, S. C., Krutchinsky, A. N., Mecklenbräuker, I., … Tarakhovsky, A. (2007). Methylation of a histone mimic within the histone methyltransferase G9a regulates protein complex assembly. *Molecular Cell*, *27*(4), 596–608. doi:10.1016/j.molcel.2007.06.026

Sasson, N. J., Pinkham, A. E., Carpenter, K. L. H., & Belger, A. (2011). The benefit of directly comparing autism and schizophrenia for revealing mechanisms of social cognitive impairment. *Journal of Neurodevelopmental Disorders*, *3*(2), 87–100. doi:10.1007/s11689-010-9068-x

Sato, N., Meijer, L., Skaltsounis, L., Greengard, P., & Brivanlou, A. H. (2003). Maintenance of pluripotency in human and mouse embryonic stem cells through activation of Wnt signaling by a pharmacological GSK-3-specific inhibitor. *Nature medicine*, *10*(1), 55-63.

Scardigli, R., Bäumer, N., Gruss, P., Guillemot, F., & Le Roux, I. (2003). Direct and concentration-dependent regulation of the proneural gene Neurogenin2 by Pax6. *Development*, *130*(14), 3269-3281.

Schaefer, A., Sampath, S. C., Intrator, A., Min, A., Gertler, T. S., Surmeier, D. J., … Greengard, P. (2009). Control of cognition and adaptive behavior by the GLP/G9a epigenetic suppressor complex. *Neuron*, *64*(5), 678–91. doi:10.1016/j.neuron.2009.11.019

Schizophrenia Working Group of the Psychiatic Genomics Cosortium. (2014) Biological insights rom 108 schizophrenia-assocaiated genetic loci. *Nature*. 511: 421-427.

Schmid, R. S., & Anton, E. S. (2003). Role of integrins in the development of the cerebral cortex. *Cerebral Cortex*, *13*(3), 219-224.

Schmiedt, C., Brand, a, Hildebrandt, H., & Basar-Eroglu, C. (2005). Event-related theta oscillations during working memory tasks in patients with schizophrenia and healthy controls. *Brain Research. Cognitive Brain Research*, *25*(3), 936–47. doi:10.1016/j.cogbrainres.2005.09.015

Schwaibold, E.M., Smogavec, M., Hobbiebrunken, E., Winter, L., Zoll, B., Burfeind, P, Brockmann, K., & Pauli, S. (2014). Intragenic duplication of EHMT1 gene results in Kleefstra syndrome. *Molecular Cytogenetics*. 7:74.

Sessa, A., Mao, C. A., Hadjantonakis, A. K., Klein, W. H., & Broccoli, V. (2008). Tbr2 directs conversion of radial glia into basal precursors and guides neuronal amplification by indirect neurogenesis in the developing neocortex. *Neuron*, *60*(1), 56-69.

Shah, A. S., Bressler, S. L., Knuth, K. H., Ding, M., Mehta, A. D., Ulbert, I., & Schroeder, C. E. (2004). Neural dynamics and the fundamental mechanisms of event-related brain potentials. *Cerebral Cortex (New York, N.Y. : 1991)*, *14*(5), 476–83. doi:10.1093/cercor/bhh009

Sharova, L. V., Sharov, A. A., Piao, Y., Shaik, N., Sullivan, T., Stewart, C. L., ... & Ko, M. S. (2007). Global gene expression profiling reveals similarities and differences among mouse pluripotent stem cells of different origins and strains. *Developmental biology*, *307*(2), 446-459.

Shih, R. A., Belmonte, P. L., & Zandi, P. P. (2004). A review of the evidence from family, twin and adoption studies for a genetic contribution to adult psychiatric disorders. *International Review of Psychiatry*, *16*(4), 260-283.

Shin, J., Ming, G.-L., & Song, H. (2014). DNA modifications in the mammalian brain. *Philosophical Transactions of the Royal Society of London. Series B, Biological Sciences*, *369*(1652). doi:10.1098/rstb.2013.0512

Shin, K. S., Kim, J. S., Kang, D.-H., Koh, Y., Choi, J.-S., O'Donnell, B. F., … Kwon, J. S. (2009). Pre-attentive auditory processing in ultra-high-risk for schizophrenia with magnetoencephalography. *Biological Psychiatry*, *65*(12), 1071–8. doi:10.1016/j.biopsych.2008.12.024

Shinkai, Y., & Tachibana, M. (2011). H3K9 methyltransferase G9a and the related molecule GLP. *Genes & Development*, *25*(8), 781–8. doi:10.1101/gad.2027411

Sims, R. J., Nishioka, K., & Reinberg, D. (2003). Histone lysine methylation: a signature for chromatin function. *Trends in Genetics : TIG*, *19*(11), 629–39. doi:10.1016/j.tig.2003.09.007

Skarnes, W. C., Rosen, B., West, A. P., Koutsourakis, M., Bushell, W., Iyer, V., … Bradley, A. (2011). A conditional knockout resource for the genome-wide study of mouse gene function. *Nature*, *474*(7351), 337–42. doi:10.1038/nature10163

Slack, J. M. W. (2002). Conrad Hal Waddington: the last Renaissance biologist? *Nature Reviews. Genetics*, *3*(11), 889–95. doi:10.1038/nrg933

Smith, S.S., Vale, W.W. (2006). The role of the hypothalamic-pituitary-adrenal axis in neuroendocrine responses to stress. *Dialogues Clin Neurosci*. 8(4): 383-395.

Soldati, C., Bithell, A., Johnston, C., Wong, K. Y., Teng, S. W., Beglopoulos, V., ... & Buckley, N. J. (2012). Repressor element 1 silencing transcription factor couples loss of pluripotency with neural induction and neural differentiation. *Stem Cells*, *30*(3), 425-434.

Spruston, N. (2008). Pyramidal neurons: dendritic structure and synaptic integration. *Nature Reviews. Neuroscience*, *9*(3), 206–21. doi:10.1038/nrn2286

Stefansson, H., Sigurdsson, E., Steinthorsdottir, V., Bjornsdottir, S., Sigmundsson, T., Ghosh, S., … Stefansson, K. (2002). Neuregulin 1 and Susceptibility to Schizophrenia, 877–892.

Sukhodolsky, D. G., Scahill, L., Gadow, K. D., Arnold, L. E., Aman, M. G., McDougle, C. J., … Vitiello, B. (2008). Parent-rated anxiety symptoms in children with pervasive developmental disorders: frequency and association with core autism symptoms and cognitive functioning. *Journal of Abnormal Child Psychology*, *36*(1), 117–28. doi:10.1007/s10802-007-9165-9

Sullivan, R.M., Gratton, A. (2002). Prefrontal cortical regulation of hypothalamic-pituitary-adrenal function in the rate and implications for psychopathology: side matters. *Psychoneuroendocrinology*. 27: 99-114.

Sullivan, P.F., Kendler, K.S. & Neale, M.C. (2003). Schizophrenia as a complex trait. *Arch Gen Psychiatry*. 60: 1187-1192.

Sullivan, P.F., Daly, M.J, Donovan, M. (2012). Genetic architectures of psychiatric disorders: the emerging picture and its implications. *Nat. Rev Genet*: 13: 537-551.

Sun, Y., Farzan, F., Barr, M. S., Kirihara, K., Fitzgerald, P. B., Light, G. a, & Daskalakis, Z. J. (2011). Γ Oscillations in Schizophrenia: Mechanisms and Clinical Significance. *Brain Research*, *1413*, 98–114. doi:10.1016/j.brainres.2011.06.065

Sweatt, J. D. (2001). The neuronal MAP kinase cascade: a biochemical signal integration system subserving synaptic plasticity and memory. *Journal of Neurochemistry*, *76*(1), 1–10. Retrieved from http://www.ncbi.nlm.nih.gov/pubmed/11145972

Swerdlow, N., Geyer, M., & Braff, D. (2001). Neural circuit regulation of prepulse inhibition of startle in the rat: current knowledge and future challenges. *Psychopharmacology*, *156*(2-3), 194–215. doi:10.1007/s002130100799

Swettenham, J. B., Muthukumaraswamy, S. D., & Singh, K. D. (2009). Spectral properties of induced and evoked gamma oscillations in human early visual cortex to moving and stationary stimuli. *Journal of Neurophysiology*, *102*(2), 1241–53. doi:10.1152/jn.91044.2008

Szumlinski, K. K., Lominac, K. D., Kleschen, M. J., Oleson, E. B., Dehoff, M. H., Schwarz, M. K., … Kalivas, P. W. (2005). Behavioral and neurochemical phenotyping of Homer1 mutant mice: possible relevance to schizophrenia. *Genes, Brain, and Behavior*, *4*(5), 273–88. doi:10.1111/j.1601-183X.2005.00120.x

Tachibana, M., Sugimoto, K., Fukushima, T., & Shinkai, Y. (2001). Set domain-containing protein, G9a, is a novel lysine-preferring mammalian histone methyltransferase with hyperactivity and specific selectivity to lysines 9 and 27 of histone H3. *The Journal of Biological Chemistry*, *276*(27), 25309–17. doi:10.1074/jbc.M101914200

Tachibana, M., Ueda, J., Fukuda, M., Takeda, N., Ohta, T., Iwanari, H., … Shinkai, Y. (2005). Histone methyltransferases G9a and GLP form heteromeric complexes and are both crucial for methylation of euchromatin at H3-K9. *Genes & Development*, *19*(7), 815–26. doi:10.1101/gad.1284005

Takahashi, K., & Yamanaka, S. (2006). Induction of pluripotent stem cells from mouse embryonic and adult fibroblast cultures by defined factors. *cell*, *126*(4), 663-676.

Talamini, L. M., Koch, T., Luiten, P. G., Koolhaas, J. M., & Korf, J. (1999). Interruptions of early cortical development affect limbic association areas and social behaviour in rats; possible relevance for neurodevelopmental disorders. *Brain Research*, *847*(1), 105–20. Retrieved from http://www.ncbi.nlm.nih.gov/pubmed/10564742

Talkowski, M. E., Mullegama, S. V, Rosenfeld, J. a, van Bon, B. W. M., Shen, Y., Repnikova, E. a, … Elsea, S. H. (2011). Assessment of 2q23.1 microdeletion syndrome implicates MBD5 as a single causal locus of intellectual disability, epilepsy, and autism spectrum disorder. *American Journal of Human Genetics*, *89*(4), 551–63. doi:10.1016/j.ajhg.2011.09.011

Talkowski, Michael E., Jill A. Rosenfeld, Ian Blumenthal, Vamsee Pillalamarri, Colby Chiang, Adrian Heilbut, Carl Ernst et al. "Sequencing chromosomal abnormalities reveals neurodevelopmental loci that confer risk across diagnostic boundaries." *Cell* 149, no. 3 (2012): 525-537.

Tallon-Baudry, C., & Bertrand, O. (1999). Oscillatory gamma activity in humans and its role in object representation. *Trends in Cognitive Sciences*, *3*(4), 151–162. Retrieved from http://www.ncbi.nlm.nih.gov/pubmed/11102663

Tallon-Baudry, C., Bertrand, O., Delpuech, C., & Pernier, J. (1996). Stimulus specificity of phase-locked and non-phase-locked 40 Hz visual responses in human. *The Journal of Neuroscience : The Official Journal of the Society for Neuroscience*, *16*(13), 4240–9. Retrieved from http://www.ncbi.nlm.nih.gov/pubmed/8753885

Tallon-Baudry, C., Bertrand, O., Peronnet, F., & Pernier, J. (1998). Induced gamma-band activity during the delay of a visual short-term memory task in humans. *The Journal of Neuroscience : The Official Journal of the Society for Neuroscience*, *18*(11), 4244–54. Retrieved from http://www.ncbi.nlm.nih.gov/pubmed/9592102

Tang, M., Villaescusa, J. C., Luo, S. X., Guitarte, C., Lei, S., Miyamoto, Y., ... & Huang, E. J. (2010). Interactions of Wnt/β-catenin signaling and sonic hedgehog regulate the neurogenesis of ventral midbrain dopamine neurons. *The Journal of Neuroscience*, *30*(27), 9280-9291.

Tang, Y. P., Shimizu, E., Dube, G. R., Rampon, C., Kerchner, G. a, Zhuo, M., … Tsien, J. Z. (1999). Genetic enhancement of learning and memory in mice. *Nature*, *401*(6748), 63–9. doi:10.1038/43432

Todd, J., Michie, P. T., Schall, U., Ward, P. B., & Catts, S. V. (2012). Mismatch negativity (MMN) reduction in schizophrenia-impaired prediction--error generation, estimation or salience? *International Journal of Psychophysiology : Official Journal of the International Organization of Psychophysiology*, *83*(2), 222–31. doi:10.1016/j.ijpsycho.2011.10.003

Tsankova, N., Renthal, W., Kumar, A., & Nestler, E. J. (2007). Epigenetic regulation in psychiatric disorders. *Nature Reviews. Neuroscience*, *8*(5), 355–67. doi:10.1038/nrn2132

Tyssowski, K., Kishi, Y., & Gotoh, Y. (2014). Chromatin regulators of neural development. *Neuroscience*, *264*, 4–16. doi:10.1016/j.neuroscience.2013.10.008

Uhlhaas, P. J., & Singer, W. (2010). Abnormal neural oscillations and synchrony in schizophrenia. *Nature Reviews. Neuroscience*, *11*(2), 100–13. doi:10.1038/nrn2774

Uhlhaas, P. J., & Singer, W. (2013). High-frequency oscillations and the neurobiology of schizphrenia. *Dialouges Clin Neurosci*, *15*(3), 301–313.

Uhlhaas, P. J., Haenschel, C., Nikolić, D., & Singer, W. (2008). The role of oscillations and synchrony in cortical networks and their putative relevance for the pathophysiology of schizophrenia. *Schizophrenia bulletin*, *34*(5), 927-943.

Umbricht, D., Koller, R., Vollenweider, F. X., & Schmid, L. (2002). Induced by NMDA Receptor Antagonist in Healthy Volunteers, *3223*(01).

Umbricht, D., Schmid, L., Koller, R., Vollenweider, F. X., Hell, D., & Javitt, D. C. (2000). Ketamine-Induced Deficits in Auditory and Visual Context-Dependent Processing in Healthy Volunteers. *Archives of General Psychiatry*, *57*(12), 1139. doi:10.1001/archpsyc.57.12.1139

Vakoc, C. R., Mandat, S. a, Olenchock, B. a, & Blobel, G. a. (2005). Histone H3 lysine 9 methylation and HP1gamma are associated with transcription elongation through mammalian chromatin. *Molecular Cell*, *19*(3), 381–91. doi:10.1016/j.molcel.2005.06.011

Van Bokhoven, H., & Kramer, J. M. (2010). Disruption of the epigenetic code: an emerging mechanism in mental retardation. *Neurobiology of Disease*, *39*(1), 3–12. doi:10.1016/j.nbd.2010.03.010

Van den Bout, C. J., Machon, O., Røsok, Ø., Backman, M., & Krauss, S. (2002). The mouse enhancer element D6 directs Cre recombinase activity in the neocortex and the hippocampus. *Mechanisms of Development*, *110*(1-2), 179–82. Retrieved from http://www.ncbi.nlm.nih.gov/pubmed/11744379

Varela, F., Lachaux, J., Rodriguez, E., & Martinerie, J. (2001). The brainweb: Phase synchronization and large-scale integration. *Nature Neuroscience*, *2*(April), 220–39.

Vastenhouw, N. L., & Schier, A. F. (2012). Bivalent histone modifications in early embryogenesis. *Current opinion in cell biology*, *24*(3), 374-386.

Vendruscolo, L. F., Takahashi, R. N., Brüske, G. R., & Ramos, A. (2003). Evaluation of the anxiolytic-like effect of NKP608, a NK1-receptor antagonist, in two rat strains that differ in anxiety-related behaviors. *Psychopharmacology*, *170*(3), 287–93. doi:10.1007/s00213-003-1545-4

Vogel-Ciernia, A., & Wood, M. a. (2014). Neuron-specific chromatin remodeling: A missing link in epigenetic mechanisms underlying synaptic plasticity, memory, and intellectual disability disorders. *Neuropharmacology*, *80*, 18–27. doi:10.1016/j.neuropharm.2013.10.002

Wahlsten, D. (2006). Sample Size Requirements for Experiments in Laboratory Animals. In: Neurobehavioural Genetics: Methods and Applications, Second Edition. Ed. Jones, B.C. & Mormede, P. CRC Press. Pg. 149-167.

Walsh, T, McClellan, J. McCarthy, S.E., Addington, A.M., Pierce, S.B., Cooper G.M., et al., (2008). Rare structural variants disrupt multiple genes in neurodevelopmental pathways in schizophrenia. *Science*. 320; 539-543.

Ward, L. M. (2003). Synchronous neural oscillations and cognitive processes. *Trends in Cognitive Sciences*, *7*(12), 553–559. doi:10.1016/j.tics.2003.10.012

Wen, B., Wu, H., Shinkai, Y., Irizarry, R. a, & Feinberg, A. P. (2009). Large histone H3 lysine 9 dimethylated chromatin blocks distinguish differentiated from embryonic stem cells. *Nature Genetics*, *41*(2), 246–50. doi:10.1038/ng.297

White, S. W., Oswald, D., Ollendick, T., & Scahill, L. (2009). Anxiety in children and adolescents with autism spectrum disorders. *Clinical Psychology Review*, *29*(3), 216–29. doi:10.1016/j.cpr.2009.01.003

Wilczynski, G. M. (2014). Significance of higher-order chromatin architecture for neuronal function and dysfunction. *Neuropharmacology*, *80*, 28–33. doi:10.1016/j.neuropharm.2014.01.016

Winters, B. D., Saksida, L. M., & Bussey, T. J. (2008). Object recognition memory: neurobiological mechanisms of encoding, consolidation and retrieval. *Neuroscience and Biobehavioral Reviews*, *32*(5), 1055–70. doi:10.1016/j.neubiorev.2008.04.004

Won, H., Lee, H.-R., Gee, H. Y., Mah, W., Kim, J.-I., Lee, J., … Kim, E. (2012). Autistic-like social behaviour in Shank2-mutant mice improved by restoring NMDA receptor function. *Nature*, *486*(7402), 261–5. doi:10.1038/nature11208

Wotton, C. J., & Goldacre, M. J. (2012). Coexistence of schizophrenia and epilepsy: record-linkage studies. *Epilepsia*, *53*(4), e71–4. doi:10.1111/j.1528-1167.2011.03390.x

Xin, Z., Tachibana, M., Guggiari, M., Heard, E., Shinkai, Y., & Wagstaff, J. (2003). Role of histone methyltransferase G9a in CpG methylation of the Prader-Willi syndrome imprinting center. *The Journal of Biological Chemistry*, *278*(17), 14996–5000. doi:10.1074/jbc.M211753200

Yamamizu, K., Fujihara, M., Tachibana, M., Katayama, S., Takahashi, A., Hara, E., ... & Yamashita, J. K. (2012). Protein kinase A determines timing of early differentiation through epigenetic regulation with G9a. *Cell stem cell*, *10*(6), 759-770.

Yates, D. (2013). Neuronal circuits: piecing together anxiety. *Nature Reviews. Neuroscience*, *14*(5), 305. doi:10.1038/nrn3500

Ying, Q.-L., Wray, J., Nichols, J., Batlle-Morera, L., Doble, B., Woodgett, J., … Smith, A. (2008). The ground state of embryonic stem cell self-renewal. *Nature*, *453*(7194), 519–23. doi:10.1038/nature06968

Yokochi, T., Poduch, K., Ryba, T., Lu, J., Hiratani, I., Tachibana, M., … Gilbert, D. M. (2009). G9a selectively represses a class of late-replicating genes at the nuclear periphery. *Proceedings of the National Academy of Sciences of the United States of America*, *106*(46), 19363–8. doi:10.1073/pnas.0906142106

Yordanova, J., Banaschewski, T., Kolev, V., Woerner, W., & Rothenberger, a. (2001). Abnormal early stages of task stimulus processing in children with attention-deficit hyperactivity disorder--evidence from event-related gamma oscillations. *Clinical Neurophysiology : Official Journal of the International Federation of Clinical Neurophysiology*, *112*(6), 1096–108. Retrieved from http://www.ncbi.nlm.nih.gov/pubmed/11377270

Zaehle, T., & Herrmann, C. S. (2011). Neural synchrony and white matter variations in the human brain--relation between evoked γ frequency and corpus callosum morphology. *International Journal of Psychophysiology : Official Journal of the International Organization of Psychophysiology*, *79*(1), 49–54. doi:10.1016/j.ijpsycho.2010.06.029

Zavitsanou, K., Cranney, J., & Richardson, R. (1999). Dopamine antagonists in the orbital prefrontal cortex reduce prepulse inhibition of the acoustic startle reflex

in the rat. *Pharmacology, Biochemistry, and Behavior*, *63*(1), 55–61. Retrieved from http://www.ncbi.nlm.nih.gov/pubmed/10340524

Zhou, V. W., Goren, A., & Bernstein, B. E. (2011). Charting histone modifications and the functional organization of mammalian genomes. *Nature Reviews. Genetics*, *12*(1), 7–18. doi:10.1038/nrg2905